

Universität
Rostock



Traditio et Innovatio

Characterization of Time-Dependent Quantum Phenomena

Kumulative Dissertation
zur Erlangung des akademischen Grades

doctor rerum naturalium (Dr. rer. nat.)

der Mathematisch-Naturwissenschaftlichen Fakultät
der Universität Rostock

vorgelegt von

Fabian Wolfgang Krumm, geb. am 11. Juni 1990 in Siegen

Betreuer: Prof. Dr. Werner Vogel , Universität Rostock

eingereicht am 23. November 2018

verteidigt am 17. Mai 2019

https://doi.org/10.18453/rosdok_id00002483

Gutachter:

Prof. Dr. Werner Vogel
Universität Rostock
Universitätsplatz 3
18051 Rostock
Germany

Prof. Dr. Radim Filip
Palacký University Olomouc
17. Listopadu
77146 Olomouc
Czech Republic

Abstract

A fundamental question of quantum optics is whether a physical state can be described by using solely classical electrodynamics or, conversely, whether the state is *nonclassical*. Over the last decades an enormous amount of effort was spent to investigate this issue by use of different strategies. A widely accepted definition of nonclassicality is related to the phase-space P representation, which was introduced by Glauber and Sudarshan in 1963. The developed criterion can be used to verify nonclassicality of a state at one particular point in time. However, it cannot be applied to multiple points in time. Such a scenario is important, for example in the description of photon antibunching. In this thesis, based on a multi-time-dependent generalization of the P function, the so-called P functional, which was introduced in 2008, a technique is developed to reveal nonclassicality with respect to multiple points in time. In this multi-time scenario novel effects occur, which are not present in the single-time case. Those effects and their impact are extensively discussed. The criteria eventually derived can be applied to arbitrary dynamics and any number of points in time. In the course of the investigation of explicitly time-dependent Hamiltonians, the detuned nonlinear Jaynes-Cummings model is considered. It is shown that its dynamics can be solved exactly if the Hilbert space is extended. The resulting evolution reveals many interesting effects, such as anomalous quantum correlations. It turns out that the model is especially suitable to study non-equal-time commutators of the corresponding Hamiltonian, since they can be obtained from a measurement of the excited electronic-state occupation probability.

Zusammenfassung

Eine fundamentale Frage der Quantenoptik ist, ob ein physikalischer Zustand ausschließlich mittels klassischer Elektrodynamik beschrieben werden kann oder ob er *nichtklassisch* ist. Während der letzten Jahrzehnte wurde enormer Aufwand betrieben, um diese Frage mittels verschiedener Strategien zu beantworten. Eine weithin akzeptierte Definition von Nichtklassizität bezieht sich auf die Phasenraum P Darstellung, welche 1963 von Glauber und Sudarshan eingeführt wurde. Das entwickelte Kriterium kann genutzt werden, um Nichtklassizität eines Zustands für einen bestimmten Zeitpunkt nachzuweisen. Allerdings kann es nicht für mehrere Zeitpunkte angewendet werden. Solch ein Szenario ist beispielsweise bei der Beschreibung von Photon Antibunching wichtig. Basierend auf einer mehrzeitlichen Verallgemeinerung der P Funktion, dem so genannten P Funktional, das 2008 eingeführt wurde, wird in dieser Arbeit eine Technik entwickelt, um Nichtklassizität im Hinblick auf mehrere Zeitpunkte aufzuzeigen. In diesem Mehrzeitszenario treten neue Effekte auf, die im einzeitlichen Fall nicht vorhanden sind. Diese Effekte und deren Einflüsse werden detailliert diskutiert. Die schlussendlich hergeleiteten Kriterien können auf beliebige Dynamiken und Zeitpunkte angewendet werden. Im Zuge der Untersuchung von explizit zeitabhängigen Hamiltonoperatoren wird das bestimmte nichtlineare Jaynes-Cummings Modell betrachtet. Es wird gezeigt, dass die entsprechende Dynamik exakt gelöst werden kann, wenn der Hilbertraum erweitert wird und dass die resultierende Entwicklung viele interessante Effekte aufzeigt, wie zum Beispiel anomale Quantenkorrelationen. Es zeigt sich, dass das Modell insbesondere für die Untersuchung von nichtgleichzeitigen Kommutatoren des zugehörigen Hamiltonoperators geeignet ist, da diese Kommutatoren direkt aus einer Messung der Besetzungswahrscheinlichkeit des angeregten elektronischen Zustands ermittelt werden können.

Contents

1	Introduction	1
2	Fundamentals	5
2.1	Phase-space formalism	5
2.2	Time evolution and time ordering	7
2.3	Nonclassicality in terms of the P function	9
2.4	Normal- and time-ordered quantum correlations	10
2.5	Summary of Chapter 2	11
3	Multi-time nonclassicality via characteristic functions	13
3.1	Multi-time-dependent nonclassicality criteria	13
3.2	Application to degenerate parametric down-conversion	15
3.2.1	Time-ordering corrections	16
3.2.2	Multi-time scenario	18
3.3	Summary of Chapter 3	18
4	Multi-time nonclassicality via generalized quasiprobabilities	19
4.1	Universal multi-time filters	19
4.2	Application to degenerate parametric down-conversion	21
4.3	Stronger divergences in the multi-time scenario	22
4.4	Summary of Chapter 4	22
5	Off-resonantly driven nonlinear Jaynes-Cummings model	25
5.1	Solution of the dynamics	25
5.2	Nonclassicality	28
5.3	Quantum-pump dynamics	30
5.4	Measurement of the trapped ion's total quantum state	31
5.5	Non-commuting Hamiltonians	33
5.6	Summary of Chapter 5	35
6	Conclusion	37
	Bibliography	41
	Manuscripts	54

1. Introduction

In the wide-ranging field of quantum optics, physical states of quantized light fields can be subdivided into classical and nonclassical states. The notion *nonclassical state* means that the state under study reveals features, which cannot be described by using classical electrodynamics and physical statistics alone. These features can be expressed via field correlation functions, which describe the full statistical properties of the state. If the outcome of a measurement of such correlation functions cannot be explained by using only classical physics—i.e., classical electrodynamics and mechanics—the state is called nonclassical. Prominent examples of these nonclassical effects are squeezing [1–6], sub-Poisson photon statistics [7–10], and antibunching [11–15]. Since the development of quantum mechanics, it was, and currently still is, an important question, how nonclassicality can be algebraically defined and how it can be verified for general quantum states.

A first problem arises due to the transition from the classical to the quantum regime, i.e., when the classical field variables (like position and momentum) are replaced by operators over Hilbert spaces. Such operators do, in general, not commute and hence, field correlation functions are subjected to a specific operator ordering. The most famous ordering prescriptions are normal, anti-normal, and symmetric ordering which will be discussed within the first chapter of this thesis. But which one of them is suitable in order to reveal nonclassical properties? In 1963, Glauber and Sudarshan introduced the P function representation [16, 17], by which general normal-ordered correlation functions can formally be expressed as a classical stochastic process. Furthermore, any quantum state—i.e., its density operator—can be expressed as a pseudo-mixture of coherent states with the P function as weighting factor. Coherent states are, to put it simply, the quantum states, whose expectation value of the electromagnetic field operator attains the form of a classical electromagnetic wave. Thus, they can be seen as reference states, dividing the classical and the nonclassical regime. On the basis of this finding, Titulaer and Glauber [18] formulated an universal classification of nonclassicality: If the Glauber-Sudarshan P function [16, 17] does not fulfill the properties of a classical probability density, especially positive semi-definiteness, the corresponding state is referred to as nonclassical. Remarkably, based on the theory of photocounting detection by Kelley and Kleiner [19], the outcome of a photocounting measurement can be explained in terms of normal ordered expectation values. Some further comments on the P function will follow in the first chapter of this thesis.

Why not simply measure the P function and probe for its negativities? Unfortunately, the P function is highly singular for many states and thus, cannot be directly observed in experiments. To overcome this circumstance, several approaches were introduced, which are collectively referred to as *nonclassicality*

criteria. Criteria, which are closely related to P , can be based on the Fourier transform of P [20–24], determinants of normal-ordered moments [25, 26] or unifications [27] of both. Disadvantageously, such criteria are in general no necessary statements as only a finite number of orders can be considered. In 2010, a method was developed for a negativity-preserving regularization of the Glauber-Sudarshan P function [28], which is in general still a complete representation of the state under study. This method was extensively investigated, extended, and applied to experiments [29–37]. However, the mentioned approaches are restricted to a single point in time, i.e., correlation functions, which are evaluated at one time only. Yet, it is well known that some quantum effects can only be understood if multiple points in time are considered. Prominent examples are photon antibunching [11–15], which, from the algebraic point of view, is the violation of an inequality involving two-time-dependent correlation functions of the field operators, and higher-order correlation measurements [38]. In 2008, a generalization of the Glauber-Sudarshan P function was introduced, called the P functional [39], with which it is possible to express the expectation values of general normal- and time-ordered correlation functions formally as a classical stochastic process. Thus, the P functional allows for a treatment of normal- and time-ordered multi-time effects in terms of a quasiprobability representation. Unfortunately, the former may be highly singular as well and, until now, it was not clear whether a regularization procedure, as in the single-time case (Ref. [28]), could be employed. Similar to the single-time considerations, a correlation measurement of multiple photodetectors includes, as a natural extension, both normal- and time-ordering prescriptions.

Another fundamental topic, which arises from the non-commutativity of field operators, or Hamiltonians, at different points in time is the time ordering. This particular effect is present in all quantum interaction problems which contain an explicitly time-dependent Hamiltonian and occurs naturally in the time-evolution operator. As the inclusion of time ordering generally increases the complexity of the underlying equations of motion, it is an important question whether consequent effects have a significant impact or if they can be neglected. Furthermore, the general question arises if such effects may cause nonclassicality, or not. To answer this issue, the Magnus expansion [40, 41] can be used, as this method allows for an unitary description of the time-evolution operator with the advantage that arbitrary orders of time ordering can be included.

An ideal testbed for studying such time-dependent effects is the dynamics of a trapped ion which can be described by the nonlinear Jaynes-Cummings model [42]. The model describes an ion caught in a Paul trap in which the motion of the ion can be described in a quantized manner [43–45]. Because of the, in good approximation, harmonic trap potential, it is possible to introduce the usual bosonic ladder operators, which describe the vibrational/motional states of the ion. If the ion is driven, for example by a laser, the interaction yields a coupling of the electronic and motional states of the ion, which is collectively referred to as *vibronic coupling*. A short overview of the most important steps in the development of the nonlinear Jaynes-Cummings Hamiltonian will follow later in this thesis.

The outline of this thesis is as follows: It will start with a short recapitulation of the fundamentals—i.e., the description of a quantum mechanical state in phase space, the handling of the time-evolution, and nonclassicality [Chap. 2]. Afterwards, it will be shown how multi-time nonclassicality criteria can be derived which are based on the Fourier transform of the P functional [Chap. 3] and on the P functional itself [Chap. 4]. The latter includes a generalization of an established regularization procedure to the multi-time case. To demonstrate the applicability of both methods, they will be applied to degenerate

parametric down-conversion, and the influence of the time-ordering prescription in the common time-evolution operator will be discussed. In order to investigate more sophisticated systems with respect to time-dependent effects, the nonlinear Jaynes-Cummings model, in which a detuning is included, will be treated in Chap. 5. By using this model, non-standard quantum effects, namely anomalous correlations, and non-equal-time commutators of the corresponding Hamiltonian will be discussed. Throughout this thesis, my own contributions are cited as Roman numerals [I, II, . . .], whereas other literature is denoted by Arabic numerals [1, 2, . . .]. The published/submitted manuscripts are attached after the bibliography; see pages 54, 60, 72, 83, 95, and 104.

2. Fundamentals

In this chapter, the fundamentals that are required to understand the findings of this work will be briefly recapitulated. This includes a physical system's representation in phase space, as well as the general description of its temporal evolution. The equations are explicitly referenced whenever it is needed. Otherwise, the corresponding derivations can be found in most standard quantum optics text books. Note that throughout this work, only one frequency mode of the electromagnetic field under study is considered. This is due to the fact that temporal correlations are the topic of interest and, for this purpose, it is sufficient to restrict the considerations to the one-mode case¹.

2.1 Phase-space formalism

In the classical Hamiltonian mechanics, a dynamical system may be described by two canonically conjugated variables q and p . In classical mechanics, those variables may be the generalized position and momentum. In the context of electromagnetic fields, p and q are commonly referred to as field quadratures, since the complex-valued electric field can be represented as a classical superposition of p and q . They satisfy the Poisson bracket

$$\{q, p\} = 1. \quad (2.1)$$

Starting from classical Maxwell equations, the energy of one mode of a classical light field reads as, see for example Ref. [46],

$$H = \frac{1}{2}(p^2 + \omega^2 q^2), \quad (2.2)$$

in which ω is the mode frequency. The form of the latter equation yields the insight that a single mode of the electromagnetic field is a harmonic oscillator. This is a crucial point and should be kept in mind for later discussions. The statistical dynamics of the system can be described via its generally time-dependent probability density $P(q, p; t)$ with the normalization $\int dp dq P(q, p; t) = 1$. As the (q, p) space is referred to as phase space, P may be called a phase-space distribution or phase-space density. The expression $P(q, p; t) dq dp$ equals the probability to find a particle at time t in the intervals $[q, q + dq]$ and $[p, p + dp]$.

¹The presented methods can be extended to the multi-mode picture straightforwardly.

However, classical Hamilton mechanics is a purely macroscopic theory. It fails, for example, for the understanding of effects on the microscopic level. If the transition into the quantum regime (quantization) is performed, the variables q and p may formally be replaced with the operators $q \rightarrow \hat{q}$ and $p \rightarrow \hat{p}$. By using the correspondence rule, the Poisson bracket of q and p is replaced by the commutator of the corresponding operators,

$$\{q, p\} \rightarrow \frac{1}{i\hbar} [\hat{q}, \hat{p}] := \frac{1}{i\hbar} (\hat{q}\hat{p} - \hat{p}\hat{q}). \quad (2.3)$$

According to Heisenberg's uncertainty principle, the non-commutativity of \hat{p} and \hat{q} prevents from observing both values q and p at the same time with arbitrary precision. The question arises how a phase-space representation in the quantum regime can be formulated, since in this case a state can obviously not be represented as a localized point in phase space because of the uncertainty relation.

It is convenient to introduce the operators \hat{a} and \hat{a}^\dagger ,

$$\begin{aligned} \hat{a} &= \frac{1}{\sqrt{2\hbar}} \left(\sqrt{\omega} \hat{q} + \frac{i}{\sqrt{\omega}} \hat{p} \right), \\ \hat{a}^\dagger &= \frac{1}{\sqrt{2\hbar}} \left(\sqrt{\omega} \hat{q} - \frac{i}{\sqrt{\omega}} \hat{p} \right), \end{aligned} \quad (2.4)$$

in which $\hat{q}^\dagger = \hat{q}$ and $\hat{p}^\dagger = \hat{p}$. The operators \hat{a} and \hat{a}^\dagger enable the description of a single mode of the electric field (in one certain polarization direction) via

$$\hat{E}(\mathbf{r}) = E(\mathbf{r})\hat{a} + E^*(\mathbf{r})\hat{a}^\dagger, \quad (2.5)$$

in which $E(\mathbf{r})$ describes the mode structure of the field. These operators are referred to as bosonic creation (\hat{a}^\dagger) and annihilation (\hat{a}) operator and they fulfill the commutation relation

$$[\hat{a}, \hat{a}^\dagger] = \hat{1}. \quad (2.6)$$

The non-commutativity of \hat{p} and \hat{q} is directly translated to the non-commutativity of \hat{a} and \hat{a}^\dagger . If an arbitrary operator function $\hat{f}(\hat{a}, \hat{a}^\dagger)$ is considered, it is important to define a certain ordering of the operators. It makes a difference whether the operator function under study is in normal order (all creation operators are on the left of the annihilation operators), anti-normal order (all annihilation operators are on the left of the creation operators), or in yet another order. Of course, this issue is a pure quantum mechanical aspect and it will be seen that it has a crucial impact on possible phase-space representations.

The coherent state $|\alpha\rangle$ is introduced as the eigenstate of the operator \hat{a} with the complex eigenvalue α ,

$$\hat{a}|\alpha\rangle = \alpha|\alpha\rangle. \quad (2.7)$$

By using this eigenvalue equation, it is found that $\langle \alpha | \hat{a} | \alpha \rangle = \alpha$ and, hence, in this coherent state basis, it holds that

$$\begin{aligned} \text{Re}(\alpha) &\propto q, \\ \text{Im}(\alpha) &\propto p; \end{aligned} \quad (2.8)$$

cf. Eq. (2.4). Thus, the complex amplitude α determines one point in phase space. Remarkably, if the radiation field is prepared in a coherent state, the equations of motion of the operators \hat{a} and \hat{a}^\dagger attain the form of a harmonic oscillator. The findings from Eq. (2.2) indicate that the coherent state yields the most possible classical description of a quantum state. Furthermore, the coherent states may serve as a basis for the expansion of each operator function and, therefore, phase-space densities $P(\alpha, \alpha^*; t; s)$ at a time t may be defined. The new parameter s is used to define a specific operator ordering. An extensive treatment of this topic is a sophisticated issue itself, which was particularly investigated in the 1960s by many authors; see Refs. [16, 17, 47–52]. In this thesis, the parameter $s = 1$ (normal ordering) will be considered, whose corresponding phase-space representation is called Glauber-Sudarshan P function [16, 17]:

$$P(\alpha, \alpha^*; t; s = 1) \equiv P(\alpha; t). \quad (2.9)$$

Other phase-space representations that should be mentioned are the Husimi Q function [48, 49] for $s = -1$ (anti-normal ordering) and the Wigner function [47] for $s = 0$ (symmetric ordering). However, those phase-space functions are not always suitable for the revelation of nonclassicality via negative values. In fact, the Q function is always non-negative and the Wigner function is known to be non-negative for Gaussian states [53]. As in Eq. (2.9), throughout this work the dependence on α^* and \hat{a}^\dagger will not be explicitly indicated; i.e., $f(\alpha, \alpha^*) \equiv f(\alpha)$, $\hat{f}(\hat{a}, \hat{a}^\dagger) \equiv \hat{f}(\hat{a})$, and so on.

2.2 Time evolution and time ordering

Given a physical state, represented by the ket-vector $|\psi(t)\rangle$ at time t , its temporal evolution can be described with the time-dependent Schrödinger equation:

$$i\hbar \frac{\partial}{\partial t} |\psi(t)\rangle = \hat{H}(t) |\psi(t)\rangle. \quad (2.10)$$

Here, $\hat{H}(t)$ is the generally time-dependent Hamiltonian, which characterizes the system's properties. It may contain contributions of different subsystems, for example free radiation, atomic source fields, and their mutual interactions. The unitary time-evolution operator $\hat{U}(t, t_0)$, introduced via $|\psi(t)\rangle = \hat{U}(t, t_0) |\psi(t_0)\rangle$, has to obey a similar differential equation as in Eq. (2.10):

$$i\hbar \frac{\partial}{\partial t} \hat{U}(t, t_0) = \hat{H}(t) \hat{U}(t, t_0), \quad (2.11)$$

with the initial condition $\hat{U}(t_0, t_0) = \hat{1}$. The formal solution of Eq. (2.11) reads as

$$\hat{U}(t, t_0) = \sum_{n=0}^{\infty} \left(-\frac{i}{\hbar} \right)^n \int_{t_0}^t dt_1 \cdots \int_{t_0}^{t_{n-1}} dt_n \left\{ \hat{H}(t_1) \cdots \hat{H}(t_n) \right\}, \quad (2.12)$$

which is only unitary if all (infinite) orders are taken into account. Thus, the representation in Eq. (2.12) may not be suitable for numerical calculations. Note that for most dynamics $[\hat{H}(t), \hat{H}(t')] \neq 0$ for $t \neq t'$ holds. Introducing the time-ordering operator \mathcal{T} , one may rewrite this equation to

$$\hat{U}(t, t_0) = \mathcal{T} \exp \left[-\frac{i}{\hbar} \int_{t_0}^t dt' \hat{H}(t') \right], \quad (2.13)$$

in which \mathcal{T} orders the Hamiltonians according to

$$\mathcal{T} \left\{ \hat{H}(t_1) \cdots \hat{H}(t_n) \right\} = \hat{H}(t_{p_1}) \cdots \hat{H}(t_{p_n}), \quad (2.14)$$

for $t_{p_1} \geq \cdots \geq t_{p_n}$. By using the Magnus expansion [40, 41], the equivalent expression

$$\hat{U}(t, t_0) = \exp \left[\hat{G}_1(t, t_0) + \sum_{n=2}^{\infty} \hat{G}_n(t, t_0) \right] \quad (2.15)$$

is formulated, in which the first two Magnus orders are defined as follows:

$$\hat{G}_1(t, t_0) = -\frac{i}{\hbar} \int_{t_0}^t dt_1 \hat{H}(t_1), \quad (2.16)$$

$$\hat{G}_2(t, t_0) = -\frac{1}{2\hbar^2} \int_{t_0}^t dt_1 \int_0^{t_1} dt_2 [\hat{H}(t_1), \hat{H}(t_2)]. \quad (2.17)$$

The higher orders contain additional contributions of nested non-equal-time commutators of the Hamiltonians, which are in general difficult to calculate. However, a great advantage of the representation in Eq. (2.15) is the fact that it is always unitary, independent of the number of Magnus orders taken into account.

Via inspection of Eqs. (2.13)-(2.17), the following is concluded: If $\hat{G}_n(t, t_0) = 0$, for $n > 1$, \mathcal{T} in (2.13) can be neglected. Thus, the Magnus orders $\hat{G}_{n>1}(t, t_0)$ can be referred to as *time-ordering effects* or *time-ordering corrections* [I, 54–58]. It is clear that these effects are a direct consequence of non-vanishing non-equal-time commutators of the Hamiltonian, which can only be described in terms of quantum mechanics. From the physical point of view, the influence of those effects is of interest as the dynamics are easier to solve if time-ordering effects can be neglected in good approximation. Additionally, it might yield a deeper insight into the general structure of temporal evolution with respect to non-commuting Hamiltonians.

2.3 Nonclassicality in terms of the P function

In fact, by using the P function from Eq. (2.9), any quantum state, which is represented by its density operator $\hat{\rho}(t)$, can be expressed as a statistical pseudo-mixture of coherent states

$$\hat{\rho}(t) = \int d^2\alpha P(\alpha; t) |\alpha\rangle \langle\alpha|. \quad (2.18)$$

Nonclassicality—i.e., the impossibility to describe the state under study by using only classical electrodynamics (namely Maxwell's equations) and physical statistics—can be defined as follows [18, 59]: Whenever $P(\alpha; t)$ does not comply with the properties of a classical probability density (i.e., non-negativity), the state is referred to as nonclassical. According to Eq. (2.18), this means that any classical state can be expressed as a quasiclassical² pseudo-mixture of coherent states, ultimately defining the notion of a nonclassical state for a single time.

By using $P(\alpha; t)$, the expectation value of an arbitrary operator $\hat{O}(\hat{a}(t))$ can be calculated as follows:

$$\langle \hat{O}(\hat{a}(t)) \rangle = \int d^2\alpha P(\alpha; t) \langle \alpha | \hat{O}(\hat{a}(0)) | \alpha \rangle, \quad (2.19)$$

with $\hat{a}(0) = \hat{a}$. The P function itself is defined as the Fourier transformed expectation value of the normal-ordered displacement operator $\hat{D}(\beta; t)$. This expectation value is called the characteristic function of P and denoted with $\Phi(\beta; t)$:

$$P(\alpha; t) = \pi^{-2} \int d^2\beta e^{\alpha\beta^* - \alpha^*\beta} \Phi(\beta; t), \quad (2.20)$$

with

$$\Phi(\beta; t) := \langle : \hat{D}(\beta; t) : \rangle = \langle : e^{\beta\hat{a}^\dagger(t) - \beta^*\hat{a}(t)} : \rangle = \langle e^{\beta\hat{a}^\dagger(t)} e^{-\beta^*\hat{a}(t)} \rangle. \quad (2.21)$$

The notation $: \dots :$ represents the normal-ordering prescription. It is worth noting that the possibly occurring singularities of P are reasoned by the fact that Φ may be an unbounded function. By using Eq. (2.19) and the assumption that $\hat{O}(t) = : \hat{f}^\dagger(t) \hat{f}(t) :$, with $\hat{f}(t) \equiv \hat{f}(\hat{a}(t))$, it is found that

$$\langle : \hat{f}^\dagger(t) \hat{f}(t) : \rangle = \int d^2\alpha |f(\alpha)|^2 P(\alpha; t). \quad (2.22)$$

Since $|f(\alpha)|^2 \geq 0$, the expectation value is always positive semi-definite (for all possible operator functions \hat{f}), as long as $P(\alpha; t)$ is not negative in the sense of distributions. On the contrary, if the expectation value attains negativities, they are exclusively caused by negativities of the P function. Hence, one can link the negativity of the expectation in Eq. (2.22) directly to the negativity of P and formulate the nonclassicality criterion

$$\exists \hat{f}(t) : \langle : \hat{f}^\dagger(t) \hat{f}(t) : \rangle < 0 \Leftrightarrow \hat{\rho}(t) \text{ nonclassical}. \quad (2.23)$$

²The term quasiclassical is used since a classical state does not imply a well-behaved P function; cf. Ref. [60].

Based on the latter findings and the characteristic function $\Phi(\beta; t)$, a plethora of necessary and sufficient nonclassicality criteria were derived [22, 25, 27]. Those approaches circumvent the difficulty of dealing with a highly singular P functions. Remarkably, in 2010, a method was presented that allows for a proper regularization—i.e., it does not affect the negativities—of the P function [28]. This technique was rigorously investigated and successfully applied to experimental data as well [29–33].

2.4 Normal- and time-ordered quantum correlations

In the previous section, in Eq. (2.23) a general definition of single-time nonclassicality has been presented. However, for the description of certain physical effects, the inclusion of multiple points in time is indispensable. The most prominent example is probably the effect of photon antibunching [13]. To divide those effects into a classical and nonclassical regime, a generalization of the criterion in Eq. (2.23) was formulated in 2008 [39]. There, general multi-time quantum correlations were defined via the inequality

$$\exists \hat{f} : \left\langle \circ \hat{f}^\dagger \hat{f} \circ \right\rangle^{\text{ncl.}} < 0, \quad (2.24)$$

in which the abbreviation “ncl.” means “nonclassical” and \hat{f} is an arbitrary operator function that depends on an arbitrary but fixed number r of points in time; i.e., $\hat{f} \equiv \hat{f}[\hat{a}(t_1), \dots, \hat{a}(t_r), \hat{a}^\dagger(t_1), \dots, \hat{a}^\dagger(t_r)]$. The notation $\circ \dots \circ$ means that the inherent expression is firstly normal ordered and secondly time ordered in such a way that the time arguments of the creation operators increase, while the time arguments of the annihilation operators decrease (from left to right). In the special case $r = 1$, the time-ordering prescription in Eq. (2.24) becomes meaningless and the single-time criterion in Eq. (2.23) is recovered. On the basis of a power series expansion of \hat{f} in Eq. (2.24), a hierarchy of nonclassicality criteria was derived in Ref. [39]. The exact physical meaning of normal- and time-ordered correlation functions depends on the particular situation under study. A prominent example is the photodetection theory introduced first by Kelley and Kleiner [19]; see also Refs. [38, 61]. If the joint probability of the events of multiple detectors at different space-time-points is studied, it is found that the former equals a normal- and time-ordered expectation value.

However, as has been discussed in the previous section, the Glauber-Sudarshan P function solely depends on a single point in time and hence, it is only an appropriate tool to investigate nonclassical properties of a physical system with respect to one specific time point. Thus, the description of general multi-time-dependent correlation functions, as in Eq. (2.24) for example, requires a generalization of the P function to the multi-time picture. This generalization, the so-called P functional [39], is in the single-mode case defined as

$$P[\alpha_1, \dots, \alpha_r; t_1, \dots, t_r] = \left\langle \circ \prod_{i=1}^r \hat{\delta}(\hat{a}(t_i) - \alpha_i) \circ \right\rangle, \quad (2.25)$$

in which $\prod_{i=1}^r \hat{A}_i = \hat{A}_1 \dots \hat{A}_r$ simply means the successive execution of the operators \hat{A}_i . The operator-valued version of the Dirac delta distribution reads as

$$\hat{\delta}(\hat{a} - \alpha) = \frac{1}{\pi^2} \int d^2\beta e^{(\hat{a}^\dagger - \alpha^*)\beta - (\hat{a} - \alpha)\beta^*}, \quad (2.26)$$

and is a straightforward generalization of the complex-valued Dirac delta distribution; see for example Chap. 4 of Ref. [38]. In Eq. (2.25), each coherent amplitude α_i spans the phase space at time t_i via its real and imaginary part. In contrast to the P function, the P functional can be used to express general normal- and time-ordered correlation functions formally as classical stochastic processes. Therefore, the negativity (in the sense of distributions) of the P functional is directly related to the negativity of the expectation value in Eq. (2.24).

2.5 Summary of Chapter 2

In this chapter, the key points, which are required to understand the topics which will be treated in this thesis, have been summarized: (i) the description of a quantum state in phase space, (ii) how the time evolution of a state is handled and at which point time ordering emerges, (iii) the notion of nonclassicality that will be used in this thesis. By using these techniques, the next chapter covers the investigation of multi-time nonclassicality within the notion of the P functional.

3. Multi-time nonclassicality via characteristic functions

As the P function itself, the P functional in Eq. (2.25) may be highly singular, caused by an unbounded but well-behaved Fourier transform. Thus, a direct investigation of the P functional is mostly not possible. Instead, the attention will be restricted to the Fourier transform in this section. The Fourier transform of the P functional reads [I]

$$\Phi(\beta_1, \dots, \beta_r; t_1, \dots, t_r) = \left\langle \circ \prod_{i=1}^n \hat{D}(\beta_i; t_i) \circ \right\rangle \quad (3.1)$$

and will be referred to as *multi-time-dependent characteristic function* (MTCF) throughout this work. Here,

$$\hat{D}(\beta; t) = e^{\beta \hat{a}^\dagger(t) - \beta^* \hat{a}(t)} \quad (3.2)$$

is the time-evolved displacement operator. The MTCF is normalized according to $\Phi(0, \dots, 0; t_1, \dots, t_r) = 1$ and is a continuous function. As the single-time characteristic function is accessible by balanced homodyne detection experiments [62], it is expected that the MTCF can be reconstructed by extended time-correlated detection setups in a similar way; cf. Ref. [II].

3.1 Multi-time-dependent nonclassicality criteria

To formulate nonclassicality criteria in terms of the MTCF in Eq. (3.1), the definition of multi-time-dependent quantum correlations in Eq. (2.24) can be used, together with operator functions of the form

$$\hat{f} = \sum_{j=1}^{\mathcal{O}} f_j \prod_{i=1}^r \hat{D}(\beta_{i,j}; t_i), \quad (3.3)$$

in which the integer number \mathcal{O} will determine the order of the arising criterion and f_j is a complex number. By inserting the expansion in Eq. (3.3) in the condition in Eq. (2.24) and making use of the fact that the operators may be rearranged arbitrarily inside the normal- and time-ordering prescription, one

obtains

$$\left\langle \circ \hat{f}^\dagger \hat{f} \circ \right\rangle = \sum_{j,l=0}^{\mathcal{O}} f_l^* f_j \Phi(\beta_{1,j} - \beta_{1,l}, \dots, \beta_{r,j} - \beta_{r,l}; t_1, \dots, t_r), \quad (3.4)$$

with the definition of Φ given in Eq. (3.1). Obviously, via the expansion of \hat{f} in terms of a product of time-dependent displacement operators, the general definition of normal- and time-ordered correlation properties [Eq. (2.24)] is linked to the Fourier transform of the P functional.

Apparently, the expression in Eq. (3.4) can be rewritten in a vectorized form,

$$\left\langle \circ \hat{f}^\dagger \hat{f} \circ \right\rangle = \mathbf{f}^\dagger \Phi(t_1, \dots, t_r) \mathbf{f}, \quad (3.5)$$

with $\mathbf{f} = (f_1, \dots, f_{\mathcal{O}})$ and $\Phi(t_1, \dots, t_r) = [\Phi(\beta_{1,j} - \beta_{1,l}, \dots, \beta_{r,j} - \beta_{r,l}; t_1, \dots, t_r)]_{l,j=1}^{\mathcal{O}}$. A similar expression was found in the single-time case by applying the theorem of Bochner [20,63]. According to Eq. (3.5), the expectation value $\left\langle \circ \hat{f}^\dagger \hat{f} \circ \right\rangle$ is non-negative for all possible \hat{f} if and only if the matrix $\Phi(t_1, \dots, t_r)$ is positive-semidefinite. The latter means that Φ is a classical characteristic function—i.e., the characteristic function of a classical (non-negative) P functional. By using Sylvester's criterion¹ in Eq. (3.5), the following nonclassicality condition is obtained: The characteristic function $\Phi(\beta_1, \dots, \beta_r; t_1, \dots, t_r)$ corresponds to a nonclassical P functional $P[\alpha_1, \dots, \alpha_r; t_1, \dots, t_r]$ if and only if

$$\exists \mathcal{O} \in \mathbb{N}, [\{\beta_{i,j}\}_{i=1}^r]_{j=1}^{\mathcal{O}} : \det_{\mathcal{O}}[\Phi(t_1, \dots, t_r)]^{\text{ncl.}} < 0. \quad (3.6)$$

Here, $\det_{\mathcal{O}}$ is the determinant of the order \mathcal{O} . In words, the criterion has the following meaning: If at least one principal minor of the matrix $\Phi(t_1, \dots, t_r)$ is not positive-semidefinite for an arbitrary order \mathcal{O} and any arguments $[\{\beta_{i,j}\}_{i=1}^r]_{j=1}^{\mathcal{O}}$, then the corresponding dynamics is nonclassical with respect to the definition in Eq. (2.24). Note that the derived criterion in Eq. (3.6) is only necessary if all generally infinite orders are taken into account. This means, for a finite \mathcal{O} the criterion is mostly only sufficient. It is noteworthy that the criterion in (3.6) contains the single-time case. Thus, if $r = 1$ is chosen, the corresponding single-time criteria are recovered, which have already been known; cf. Refs. [22, 25, 26]. Finally, it should be emphasized that the derived hierarchy of inequalities is not the only criterion which can be used to uncover multi-time-dependent nonclassicality. Other expansions of \hat{f} in Eq. (3.3) allow for the derivation of various criteria. Especially, it is possible to derive criteria containing MTCFs, which depend on different points in time within one inequality.

As the general form of the criterion in Eq. (3.6) is rather complicated, one may start with the lowest order, $\mathcal{O} = 2$:

$$\begin{aligned} 0 &\stackrel{\text{ncl.}}{>} \det_2 [\Phi(t_1, \dots, t_r)] \\ &= \begin{vmatrix} \Phi(0, \dots, 0; t_1, \dots, t_r) & \Phi(\beta_{1,2} - \beta_{1,1}, \dots, \beta_{r,2} - \beta_{r,1}; t_1, \dots, t_r) \\ \Phi(\beta_{1,2} - \beta_{1,1}, \dots, \beta_{r,2} - \beta_{r,1}; t_1, \dots, t_r)^* & \Phi(0, \dots, 0; t_1, \dots, t_r) \end{vmatrix} \\ &= 1 - |\Phi(\beta_{1,2} - \beta_{1,1}, \dots, \beta_{r,2} - \beta_{r,1}; t_1, \dots, t_r)|^2 := 1 - |\Phi(\gamma_1, \dots, \gamma_r; t_1, \dots, t_r)|^2. \end{aligned} \quad (3.7)$$

¹A (Hermitian) matrix is positive semi-definite if and only if all leading principal minors are non-negative.

In the last step, $\beta_{i,2} - \beta_{i,1} := \gamma_i$ was defined for $i = 1, \dots, r$. The final result reads as

$$|\Phi(\gamma_1, \dots, \gamma_r; t_1, \dots, t_r)|^2 \stackrel{\text{ncl.}}{>} 1. \quad (3.8)$$

Thus, to verify nonclassicality, it has to be shown the squared absolute value of the MTCF [Eq. (3.1)] exceeds the value 1.

3.2 Application to degenerate parametric down-conversion

In the following, the applicability of the findings from the previous section will be demonstrated. A fundamental system of interest in quantum optics is parametric down-conversion (sometimes referred to as parametric oscillator), which allows for the generation of many quantum states, like single photons [64–68], entangled photon pairs [69–71], and Einstein-Podolsky-Rosen states [72, 73]. Here, this model is considered in the degenerated case: A pump photon with frequency ω_p is down-converted into two photons, each with the same frequency ω_a ; see Fig. 3.1. If the pump frequency is matched but slightly detuned, the constraint

$$\omega_p = 2\omega_a + \delta \quad (3.9)$$

is obtained, in which δ is the detuning. If

$\delta > 0$, the corresponding Hamiltonian is explicitly time-dependent in the interaction picture and reads as

$$\hat{H}_{\text{PDC}}(t) = \hbar\kappa [e^{-i\delta t}\hat{a}^{\dagger 2} + e^{i\delta t}\hat{a}^2], \quad (3.10)$$

in which the real-valued κ describes the coupling of the pump to the nonlinear crystal. An adequate overview of the model can be found in Ref. [54]. The corresponding time-evolution operator reads as

$$\hat{U}_{\text{PDC}}(t) = \mathcal{T} \exp \left\{ -\frac{i}{\hbar} \int_{t_0}^t d\tau \hat{H}_{\text{PDC}}(\tau) \right\}. \quad (3.11)$$

Due to the time-dependence of the Hamiltonian, the study time-ordering effects, which have been recapitulated in Sec. 2.2, is possible. For the Hamiltonian in Eq. (3.10), the Magnus expansion will be employed² [see Eq. (2.15)]. Although, there are some works that should be mentioned in which time-ordering effects were investigated [54–58], none of them considered time-ordering effects with respect to nonclassicality. Instead of directly applying the Magnus expansion to \hat{U} , the equations of motion may be derived and solved by using the Magnus expansion [I]. This yields an expression of the

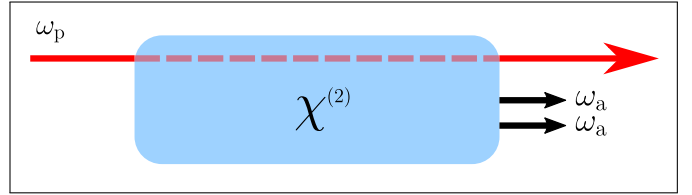


Figure 3.1: Sketch of degenerate parametric down-conversion described by the Hamiltonian in Eq. (3.10).

²Note that it is possible to solve the equations of motion analytically; see Sec. 4.2. However, at this point, the time-ordering corrections are of interest and for this purpose, the Magnus expansion is a suitable tool for investigation.

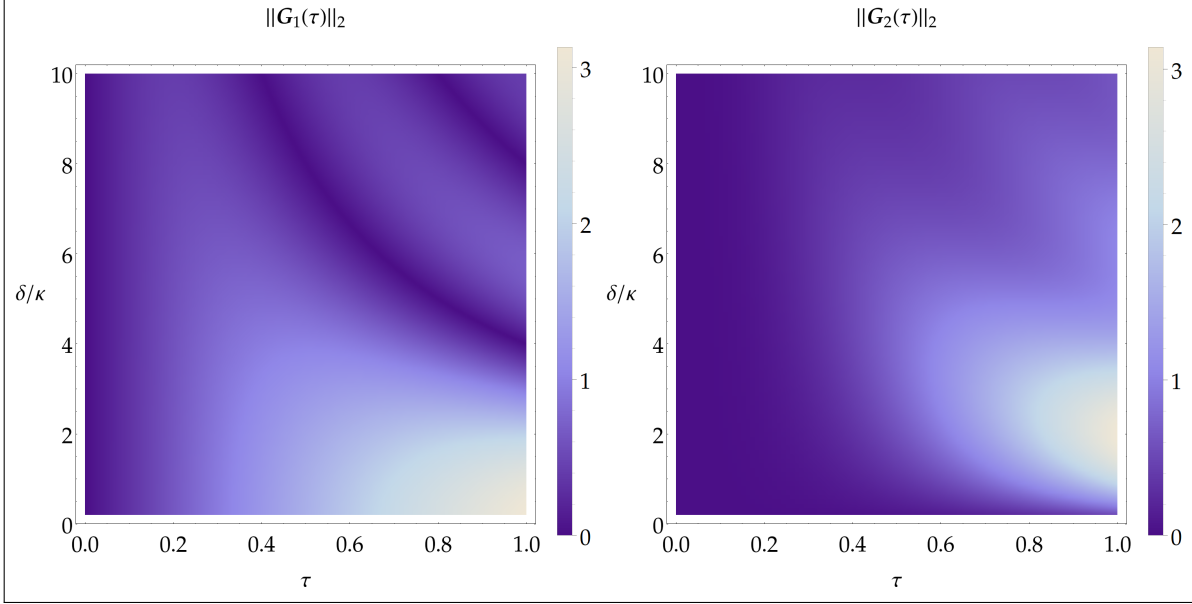


Figure 3.2: The Euclidean norm of the first two complex-valued Magnus orders in Eq. (3.12) in dependence of the dimensionless time τ (within the radius of convergence) and mismatch δ/κ . More orders are plotted in Ref. [I].

form

$$\begin{pmatrix} \hat{a}(t) \\ \hat{a}^\dagger(t) \end{pmatrix} = \exp \left\{ \sum_{n=1}^{\infty} \mathbf{G}_n(t) \right\} \begin{pmatrix} \hat{a}(t_0) \\ \hat{a}^\dagger(t_0) \end{pmatrix}, \quad (3.12)$$

with the 2×2 complex matrices \mathbf{G}_n . The non-commutativity of the Hamiltonian—i.e., the time-ordering effects in Eq. (2.13)—is now contained in the matrices $\mathbf{G}_{n>1}$. Especially, $\mathbf{G}_1(\tau)$ represents the impact of the integrated Hamiltonian [cf. Eq. (2.16)] and $\mathbf{G}_2(\tau)$ is the complex-valued version of the commutator of the Hamiltonian; cf. Eq. (2.17). The advantage of the representation in Eq. (3.12) is that the complex-valued matrices are easier to handle in numerical calculations than the corresponding Hilbert-space operators. However, one disadvantage of the Magnus expansion is the generally finite radius of convergence. Thus, it might not be possible to access arbitrary interaction times. For the dynamics discussed here, convergence in terms of the Magnus expansion is assured as long as $\tau < 1$ for the dimensionless time $\tau = 2\kappa t/\pi$; for further details see [I]. Above this radius of convergence, the correctness of the obtained dynamics cannot be ensured.

3.2.1 Time-ordering corrections

Before the derived multi-time dependent nonclassicality criterion in Eq. (3.8) will be investigated, the time-ordering corrections in \hat{U}_{PDC} will be examined in more detail. In Fig. 3.2, a plot of $\|\mathbf{G}_1(\tau)\|_2$ and $\|\mathbf{G}_2(\tau)\|_2$ in dependence of the time τ and the frequency mismatch δ is presented. The magnitude of the first-order time-ordering correction, $\|\mathbf{G}_1(\tau)\|_2$, is most prominent for large interaction times and

moderate δ/κ . This coincides with the fact that if low pump powers are considered, the first-order perturbation theory is sufficiently accurate to describe the dynamics of the system [74]. By inspection of the plot of $\|G_1(\tau)\|_2$, regions are found in which this quantity is nearly zero. This means that for those scenarios the dynamics may be primarily determined by time-ordering corrections—i.e., by the $G_{n>1}$. Since the influence of such corrections is the main interest, $\delta/\kappa \approx 3.18$ will be chosen in the following discussions, because in this case a significant impact of higher Magnus orders is expected. To investigate the effect of time ordering on nonclassicality, the modulus squared of the single-time characteristic function [Eq. (3.1) for $r = 1$] is derived, which, after a principal axis transformation, attains the form

$$|\Phi(\gamma; \tau)|^2 = e^{\mu_1(\tau)\text{Re}[\gamma]^2 + \mu_2(\tau)\text{Im}[\gamma]^2}. \quad (3.13)$$

If the maximal value $\lambda_{\max} \equiv \lambda_{\max}(\tau) = \max(\mu_1(\tau), \mu_2(\tau))$ in Eq. (3.13) is positive, then $|\Phi(\gamma; \tau)|^2$ exceeds one, which is an evidence of nonclassicality [22, 25, 26]. The time dependence of λ_{\max} is depicted in Fig. 3.3. The impact of time ordering is revealed via the differences in the contributions of $n_{\max} = 1$ (no time-ordering corrections) and $n_{\max} > 1$ (time-ordering corrections included). On small time scales, the first Magnus order is sufficiently accurate—i.e., time ordering is negligible. However, for larger interaction times, higher Magnus orders must be included to obtain the correct dynamics; i.e., the time-ordering corrections have a significant impact. Due to the algebraic structure of the $G_n(\tau)$, the even and odd orders converge alternately to the exact solution; see Ref. [1] for details. That is why the first correction term $G_2(\tau)$ yields worse results than the negligence of time ordering. The overall influence of time ordering is contained in the differences of the red and black curve.

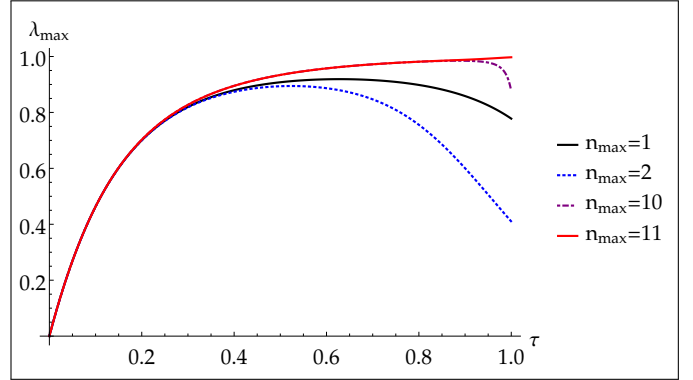


Figure 3.3: λ_{\max} for $G(\tau) = \sum_{n=1}^{n_{\max}} G_n(\tau)$ [see Eq. (3.12)] in dependence on the rescaled time $\tau = 2\kappa t/\pi$. Parameters: $\delta/\kappa \approx 3.18$.

3.2.2 Multi-time scenario

Coming back to the multi-time picture—i.e., to the criterion in Eq. (3.8)—two points in time will be discussed in the following ($r = 2$). Such a scenario corresponds to, e.g., a detector scheme involving two detectors, where each detector detects the light field at a different point in time. The joint probability of the detector events equals normal- and time-ordered correlation functions [19,38,61]. For the investigation of the criterion in Eq. (3.8), the modulus squared of the MTCF [Eq. (3.1)] is plotted in Fig. 3.4 for two times. The time evolution is described by the Magnus expansion up to the eleventh order which yields sufficiently accurate results. It is seen that the derived

criterion is clearly violated for all two points in time under study since the function is always greater than one. This certifies a negative P functional and, hence, multi-time nonclassicality with respect to Eq. (2.24). This means that in Eq. (2.24), at least one possible operator function \hat{f} exists which yields negative values of the expectation value. Advantageously, because of the developed criterion, that particular operator function does not need to be known.

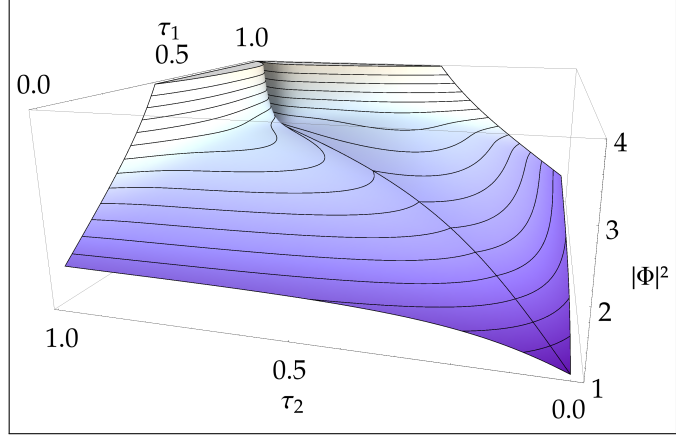


Figure 3.4: Plot of the modulus squared of the MTCF, $|\Phi(\gamma_1, \gamma_2; \tau_1, \tau_2)|^2$, which is defined in Eq. (3.1) for the dynamics of the Hamiltonian in Eq. (3.10). Parameters: $|\gamma_1|^2 + |\gamma_2|^2 = 1$, $\arg \gamma_1 = \arg \gamma_2 = \pi/2$, $\delta/\kappa \approx 3.18$, and $\tau_i = 2\kappa t_i/\pi$ for $i = 1, 2$.

3.3 Summary of Chapter 3

In this chapter, novel techniques for the identification of multi-time dependent nonclassical stochastic processes in radiation fields in terms of characteristic functions have been developed. Those techniques clearly extend the established single-time criteria. The introduced multi-time criteria are, in their general form, necessary and sufficient and they are able to uncover multi-time dependent quantum effects. Additionally, since they are based on normal- and time-ordered correlation functions, it is expected that they are measurable by appropriate correlation setups. The methods have been applied to the model of parametric down-conversion including a frequency mismatch. In the course of the application, time-ordering effects within the time-evolution operator have been investigated. They are present whenever an explicitly time-dependent Hamiltonian is studied. With those new tools, it is possible to analyze time-dependent processes and assess the impact of time ordering

4. Multi-time nonclassicality via generalized quasiprobabilities

The problem around the criterion in Eq. (3.6), which has already been mentioned, is the sufficiency of its applicable form. Lower orders of the criterion might fail to uncover nonclassicality, while the MTCF in Eq. (3.1) is unbounded. In such a case, the corresponding P functional is highly singular and, thus, a further analysis is hardly possible. The question arises whether it is possible to derive a criterion which is also necessary on an applicable basis—e.g., a criterion based on the negativities of an appropriately regularized version of the P functional. Naively, one would tend to use the same regularization procedure as was introduced in Ref. [28] for the single-time scenario: In the latter case the characteristic function is bounded as

$$|\Phi(\beta; t)|^2 \leq e^{|\beta|^2} \quad (4.1)$$

for all times. Thus, $\Phi(\beta; t)$ might be not square-integrable and the Fourier transform (the P function) does not exist in a well defined manner. However, an appropriate filter function $\Omega_w(\beta)$, with a width w , can be introduced that suppresses this maximal possible rising behavior of the characteristic function. The *filtered* characteristic function is accordingly defined as $\Phi_\Omega(\beta; t) := \Phi(\beta; t)\Omega_w(\beta)$. Some remarks concerning the phrase *appropriate* follow in the next section. The filtered characteristic function $\Phi_\Omega(\beta; t)$ is then a proper square-integrable function and the corresponding P function is regular. However, the same procedure is not simply expandable to the multi-time scenario.

4.1 Universal multi-time filters

In the multi-time case, an estimation comparable to the one in Eq. (4.1) is mostly not feasible. The difficulty is that especially non-equal-time commutators need to be taken into account, which may, depending on the dynamics under study, be a cumbersome task to evaluate. Those contributions may overcome the bound given in Eq. (4.1) and can cause stronger singularities than in the single-time case¹. It should be emphasized that this means that it is insufficient to simply employ a filter that is compounded out of single-time filters, which are chosen to suppress the slope in Eq. (4.1). To overcome this issue, a special kind of filters is suitable: *compact-support filter functions*.

¹A detailed investigation of the singularities of the P function can be found in Ref. [60].

Formally, the filtered P functional can be defined as follows [II]:

$$P_\Omega[\alpha_1, \dots, \alpha_r; t_1, \dots, t_r] = \pi^{-2k} \int d^2\beta_1 \dots \int d^2\beta_r e^{\alpha_1\beta_1^* - \alpha_1^*\beta_1} \times \dots \times e^{\alpha_r\beta_r^* - \alpha_r^*\beta_r} \underbrace{\Phi(\beta_1, \dots, \beta_r; t_1, \dots, t_r) \Omega_w(\beta_1, \dots, \beta_r)}_{:=\Phi_\Omega(\beta_1, \dots, \beta_r; t_1, \dots, t_r)}, \quad (4.2)$$

with the filtered MTCF $\Phi_\Omega(\beta_1, \dots, \beta_r; t_1, \dots, t_r)$. As already mentioned, the filter function Ω_w has to fulfill several requirements [28]:

1. The Fourier transform of $\Phi_\Omega(\beta_1, \dots, \beta_r; t_1, \dots, t_r)$ exists for all widths w . This means that Φ_Ω is always a rapidly decaying function with respect to the real- and imaginary parts of all β_i .
2. The Fourier transform of the filter function $\Omega_w(\beta_1, \dots, \beta_r)$ is non-negative. This requirement ensures that occurring negativities are caused exclusively by the P functional.
3. In the limit of an infinite broad filter, the standard P functional is recovered:
 $\lim_{w \rightarrow \infty} P_\Omega[\alpha_1, \dots, \alpha_r; t_1, \dots, t_r] = P[\alpha_1, \dots, \alpha_r; t_1, \dots, t_r]$. This means that P_Ω is still a complete representation of the quantum state.

A possible choice of a compact support filter reads as

$$\Omega_w(\beta_1, \dots, \beta_r) = \prod_{i=1}^k \left\{ \text{tri} \left(\frac{\text{Re}[\beta_i]}{w} \right) \text{tri} \left(\frac{\text{Im}[\beta_i]}{w} \right) \right\}, \quad (4.3)$$

with the triangular function

$$\text{tri}(z) = \begin{cases} (1+z) & \text{for } z \in [-1, 0], \\ (1-z) & \text{for } z \in [0, 1], \\ 0 & \text{else.} \end{cases} \quad (4.4)$$

The mathematical details which are concerned with the applicability of this filter are extensively discussed in Sec. III of Ref. [II]: The filtered continuous MTCF $\Phi_\Omega(\beta_1, \dots, \beta_r; t_1, \dots, t_r)$ has a compact support and hence, it decays faster than any polynomial. Therefore, according to Sobolev's lemma, all orders of the derivatives of the Fourier transform of Φ_Ω exist². In short, the regularized functional P_Ω exists and furthermore is a smooth function. The procedure which has been introduced applies to general dynamics under study and, due to its compact support, suppresses any rising behavior of Φ . This novel feature of multi-time regularization was not known before. It is worth noting that there is a plethora of suitable filter functions; an adequate overview is offered in Ref. [33]. As already pointed out in Chap. 3, a measurement of Φ (and consequently of P_Ω as well) is possible by a correlation measurement which includes multiple photodetectors. Details concerning this issue are discussed in Ref. [II].

²More details can be found in Refs. [31, 60] and references therein.

4.2 Application to degenerate parametric down-conversion

In order to apply the previously derived findings, the degenerate parametric down-conversion-Hamiltonian will be reconsidered; see Eq. (3.10). In this section, time-ordering effects are not of interest and hence the dynamics will be solved exactly via the equations of motion. The analytic solution of the dynamics of the Hamiltonian in Eq. (3.10) reads as³

$$\hat{a}(\tau) = u_1(\tau)\hat{a} + u_2(\tau)\hat{a}^\dagger, \quad (4.5)$$

with

$$u_1(\tau) = e^{-i\pi\tau\delta/(4\kappa)} \left[\cosh(\vartheta\tau) + \frac{i\pi\delta/\kappa}{4\vartheta} \sinh(\vartheta\tau) \right], \text{ and} \\ u_2(\tau) = \frac{-i\pi}{\vartheta} e^{-i\frac{\pi}{4}\tau\delta/\kappa} \sinh(\vartheta\tau), \quad (4.6)$$

in which $\vartheta = \pi\sqrt{16 - (\delta/\kappa)^2}/4$ and $\tau = 2\kappa t/\pi$. By using this solution and the filter specified in Eqs. (4.3) and (4.4), the regularized P functional for two times is calculated as

$$P_\Omega[\alpha_1, \alpha_2; \tau_1, \tau_1] = w^4 T(w\frac{f_{10}}{2i}, -w^2 f_{20}) T(w\frac{f_{01}}{2i}, -w^2 f_{02}) T(w\frac{d_{10}}{2i}, -w^2 d_{20}) T(w\frac{d_{01}}{2i}, -w^2 d_{02}), \quad (4.7)$$

in which [60]

$$T(y, g) = \text{Re} \left(\frac{2}{\pi} \int_0^1 dz e^{-gz^2 + 2iyz} (1 - z) \right). \quad (4.8)$$

The coefficients f_{mn} and d_{mn} are obtained numerically; see Ref. [II] for details. With the equation given in Eq. (4.7), the regularized version of the two-time dependent P functional can be derived for the dynamics of degenerate parametric down-conversion. A plot of P_Ω is depicted in Fig. 4.1 for $\delta/\kappa \approx 3.18$. The negative values of P_Ω clearly verify nonclassical normal- and time-ordered correlation properties of the dynamics under study. That is, at least one operator function \hat{f} exists so that the expectation value in Eq. (2.24) attains negative values. This result confirms the violation of the sufficient criterion visualized in Fig. 3.4. Yet, the negativities of P_Ω are necessary (besides being known to be sufficient, as well). Note that in the characteristic function of P_Ω in Eq. (4.7), no stronger rising behavior occurs, which would require a compact filter. This is reasoned by the solution of the dynamics given in

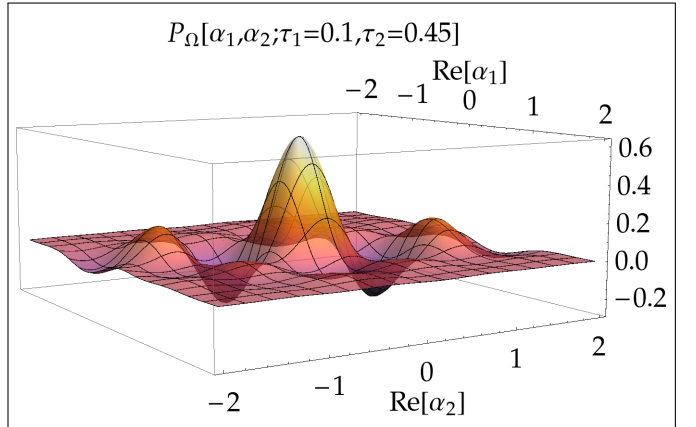


Figure 4.1: Plot of the regularized two-time-dependent P functional for the cross sections $\text{Im}(\alpha_1) = \text{Im}(\alpha_2) = 0$ and two distinct points in time, $\tau_1 = 0.1$ and $\tau_2 = 0.45$.

³The solution is explicitly derived in Ref. [II], however, it can be found in quantum optics textbooks as well.

Eq. (4.5), since $[\hat{a}(t), \hat{a}^\dagger(t')] = c(t, t')\hat{1}$ holds. A more complex dynamics in which such a commutation relation is generally not present, will be discussed in the following section.

4.3 Stronger divergences in the multi-time scenario

In this section, $\Phi(\beta_1, \beta_2; t_1, t_2)$ will be investigated with respect to its rising behavior. For this purpose, the Hamiltonian of a trapped ion whose electronic transition is not driven [75] will be considered⁴. To compare the rising behavior of the two-time case ($r = 2$) with the two-mode (but single-time) case, the quantity

$$\Delta\Phi_{\text{ion}}(\beta_1, \beta_2; 0, t) := |\Phi_{\text{ion}}(\beta_1, \beta_2; 0, t)|^2 - e^{|\beta_1|^2 + |\beta_2|^2} \quad (4.9)$$

will be examined; cf. Ref. [II]. If $\Delta\Phi_{\text{ion}}$ is positive, the slope of the modulus squared of the two-time-dependent characteristic function $|\Phi_{\text{ion}}(\beta_1, \beta_2; 0, t)|^2$ overcomes the maximal possible slope of the corresponding two-mode characteristic function $e^{|\beta_1|^2 + |\beta_2|^2}$. To put it more briefly, if $\Delta\Phi_{\text{ion}}(\beta_1, \beta_2; 0, t) > 0$ then, according to the findings of the previous section, a non-compact-support filter may fail to properly regularize the corresponding P functional. A plot of $\Delta\Phi_{\text{ion}}$ for the trapped ion dynamics is depicted in Fig. 4.2 for the case of an input Fock state $\hat{\rho}_{\text{ion}}(0) = |3\rangle\langle 3|$. Since $\Delta\Phi_{\text{ion}}$ exceeds the value of zero (pink areas), it is confirmed that the MTCF is differently bounded compared to the two-mode single-time case and the choice of a compact-support filter is justified, as the absolute value of the two-time characteristic function cannot be estimated as a product of single-time bounds; cf. Eq. (4.1).

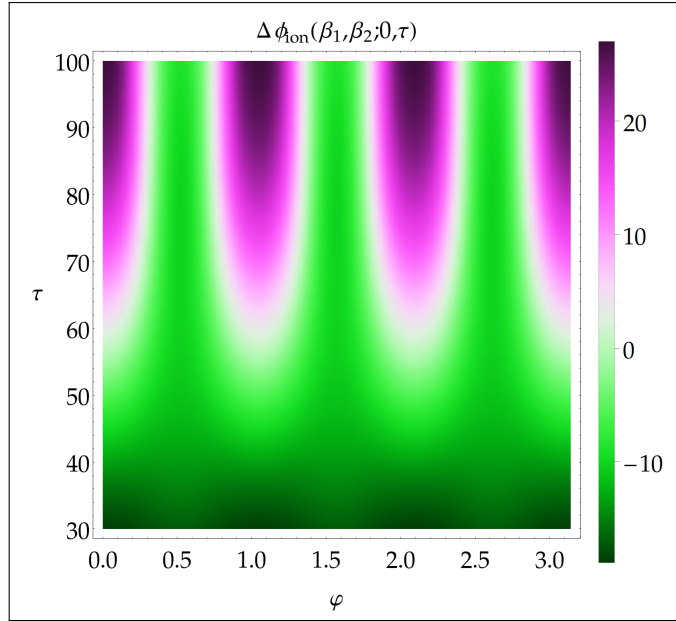


Figure 4.2: $\Delta\Phi_{\text{ion}}$ [Eq. (4.9)] for the dynamics of a trapped ion for an input Fock state $|3\rangle\langle 3|$ in dependence of the phase φ and the dimensionless time τ . Parameters: $|\beta_1| = |\beta_2| = 1.3$, $\varphi_1 = \varphi_2 \equiv \varphi$, and $\beta_j = |\beta_j|e^{i\varphi_j}$, ($j = 1, 2$).

4.4 Summary of Chapter 4

In this chapter, a method for visualizing general multi-time quantum correlations in terms of regular phase-space quasi-probabilities has been derived, which is a continuation of the idea presented in Chap. 3. For this purpose, the regularization procedure of the P function has been extended to the

⁴A detailed discussion of the dynamics of a trapped ion follows in Chap. 5.

multi-time picture. The negativities of the regularized P functional are always necessary and sufficient for uncovering multi-time dependent quantum correlations. Remarkably, the regularization procedure applies to arbitrary dynamics, which is far from trivial, since multi-time-dependent commutators need to be taken into account. Thus, the technique regularizes arbitrary strong singularities due to the usage of a compact-support filter. It should be mentioned that it was unclear until now, whether a general applicable regularization procedure of the P functional is possible. As in Chap. 3, the findings have been applied to the parametric oscillator. The occurring nonclassical two-time correlations have been directly visualized via negativities of P_Ω in phase space. In order to justify the approach, the dynamics of a trapped ion has been considered and it has been shown that the slope of the two-time dependent characteristic function can exceed the slope which is maximal possible for single-time (but multi-mode) characteristic functions.

5. Off-resonantly driven nonlinear Jaynes-Cummings model

Investigating time-dependent quantum phenomena, it is desirable to apply the developed techniques to a realistic model, which is not only sophisticated itself, but exactly solvable as well. This concerns the investigation of an explicitly time-dependent Hamiltonian, especially. Unfortunately, such models are rarely available. In this context, an interesting model to be studied is the Jaynes-Cummings model, which was introduced in 1963 [76, 77]. At this time, it was doubted whether the model is of practical relevance, as the underlying scenario of this model is rather idealized: A single radiation mode interacts with a two-level system. However, due to technical progress, it was possible to verify many of its predictions [78–81]. Note that, although the model is rather compact, it can be used to demonstrate many physical effects like Rabi oscillations [82–84], collapse and revivals [81, 85, 86], squeezing [87, 88], atom-field entanglement [89–91], antibunching [92–94], and nonclassical states such as Schrödinger cat [95, 96] and Fock states [97–99]. Furthermore, it was found that the model is not only suitable to describe the interaction of a two-level system with a radiation mode, but can also be applied in many other scenarios, as well [100–114].

This section covers the description of the dynamics of a trapped ion. The vibrational center-of-mass motion of an ion caught in a trap can be described in a quantized manner [43–45]; see also Chap. 13 of Ref. [38]. Beyond the standard Lamb-Dicke regime [115, 116], the dynamics can be described by a nonlinear generalization of the standard Jaynes-Cummings Hamiltonian [42]. The interaction of a trapped ion with optical radiation led to the generation of a variety of motional states [75, 115, 117–124], especially nonclassical states. It should be mentioned that related experiments were part of the Nobel prize in 2012 [125].

5.1 Solution of the dynamics

As mentioned earlier, the Hamiltonian which describes the quantized motion of a trapped ion in the resolved sideband regime was first introduced and solved for the resonant case (Ref. [42]), in which the Hamiltonian is not time-dependent. In case of a frequency mismatch $\Delta\omega > 0$ of the driving laser, the

corresponding Hamiltonian in the interaction picture reads as [III]

$$\hat{H}_{\text{NLJC}}(t) = \hbar\kappa' e^{-i\Delta\omega t} \hat{A}_{21} \hat{f}_k(\hat{a}^\dagger \hat{a}; \eta) \hat{a}^k + \text{H.c.}, \quad (5.1)$$

in which

$$\hat{f}_k(\hat{a}^\dagger \hat{a}; \eta) = \frac{1}{2} e^{i\Delta\phi - \eta^2/2} \sum_{n=0}^{\infty} |n\rangle\langle n| \frac{(i\eta)^k n!}{(n+k)!} L_n^{(k)}(\eta^2) + \text{H.c.} \quad (5.2)$$

describes the mode structure of the standing-wave-forming pump laser at the operator-valued relative position (defined by $\Delta\phi$) of the ion. The interaction is schematically depicted in Fig. 5.1. Furthermore, κ' is the coupling constant¹, η is the Lamb-Dicke parameter, and \hat{a} and \hat{a}^\dagger are the operators destroying and creating one vibrational quantum, respectively. $\hat{A}_{ij} = |i\rangle\langle j|$ is the atomic flip operator which accounts for the electronic transitions ($|j\rangle \rightarrow |i\rangle$) of the ion. The $L_n^{(k)}$ denote the generalized Laguerre polynomials. The frequency mismatch is specified by the relation

$$\omega_L = \omega_{21} - k\nu + \Delta\omega. \quad (5.3)$$

Here, ω_L is the frequency of the incident pump laser, ω_{21} is the separation of the electronic levels, ν is the trap frequency, and $k = 0, 1, \dots$ denotes the excited sideband. Note that the Hamiltonian in Eq. (5.1) is time-dependent in the Schrödinger picture, as well. As the Hamiltonian in Eq. (5.1) is explicitly time-dependent, the time-evolution operator cannot be solved straightforwardly, as in Ref. [42], since time-ordering effects need to be taken into account; cf. Eqs. (2.13)-(2.15). In Ref. [III], it was shown that the time-ordering corrections must not be neglected as they contribute significantly to the dynamics. To circumvent this issue, the pump field will be quantized². By using this approach, the full Hamiltonian in the Schrödinger picture reads as

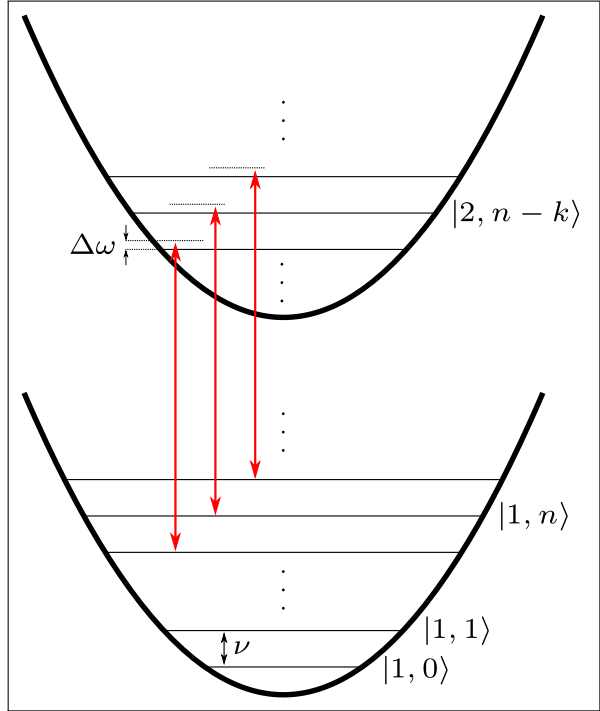


Figure 5.1: Visualization of the interaction described by the Hamiltonian in Eq. (5.1). The electronic ground state $|1\rangle$ and excited state $|2\rangle$ are separated by the electronic transition frequency $\omega_{21} = \omega_2 - \omega_1$. Due to the approximately harmonic trap potential, the energy surfaces are neither displaced, nor distorted and the vibrational levels are equidistantly separated by the trap frequency ν . The laser frequency ω_L (red arrows) is driven off-resonantly with respect to the $|1, n\rangle \leftrightarrow |2, n-k\rangle$ transition, including a detuning $\Delta\omega \ll \nu$.

$$\hat{\mathcal{H}}_{\text{NLJC}} = \hbar\nu \hat{a}^\dagger \hat{a} + \hbar\omega_L \hat{b}^\dagger \hat{b} + \hbar\omega_{21} \hat{A}_{22} + \left(\hbar\kappa'' \hat{A}_{21} \hat{b} \hat{f}_k(\hat{a}^\dagger \hat{a}; \eta) \hat{a}^k + \text{H.c.} \right). \quad (5.4)$$

¹The prime denotes the different coupling constants of the various models.

²Note that the Hamiltonian in Eq. (5.1) can be solved directly as well, by using the spinor formalism; see Ref. [IV] for details. The solution will be treated in Sec. 5.3.

The interaction described by this Hamiltonian proceeds as follows: As soon as a pump photon is absorbed (\hat{b}), the ion switches to its excited state (\hat{A}_{21}). The vibrational transitions ($\hat{f}_k(\hat{a}^\dagger \hat{a}; \eta) \hat{a}^k$) obey the chosen quasiresonance condition. The Hermitian conjugate (H.c.) term describes the reversal process—i.e., a pump photon (\hat{b}^\dagger) is created, accompanied by the electronic $|2\rangle \rightarrow |1\rangle$ and the vibrational transition $|n-k\rangle \rightarrow |n\rangle$. Since the Hamiltonian in Eq. (5.4) is not time-dependent, the time-evolution operator reads as

$$\hat{\mathcal{U}}_{\text{NLJC}}(t) = \exp \left\{ -\frac{i(t-t_0)}{\hbar} \hat{\mathcal{H}}_{\text{NLJC}} \right\}. \quad (5.5)$$

The time ordering which would be present in the time-evolution operator of the Hamiltonian in Eq. (5.1) is contained in the extension of the Hilbert space. Inserting the Hamiltonian from Eq. (5.4) in Eq. (5.5) yields

$$\begin{aligned} \hat{\mathcal{U}}_{\text{NLJC}}(t) = & \sum_{\sigma=\pm} \sum_{m,n=0}^{\infty} e^{-i\omega_{mn}^\sigma(t-t_0)} |\psi_{mn}^\sigma\rangle \langle \psi_{mn}^\sigma| + \sum_{n=0}^{\infty} e^{-i\nu n(t-t_0)} |1, 0, n\rangle \langle 1, 0, n| \\ & + \sum_{m=0}^{\infty} \sum_{q=0}^{k-1} e^{-i[\nu q + \omega_L(m+1)](t-t_0)} |1, m+1, q\rangle \langle 1, m+1, q|. \end{aligned} \quad (5.6)$$

The parameters are defined as follows:

$$\begin{aligned} |\psi_{mn}^\pm\rangle &= c_{mn}^\pm (|2, m, n\rangle + \alpha_{mn}^\pm |1, m+1, n+k\rangle), \quad \alpha_{mn}^\pm = \frac{\Delta\omega \pm \sqrt{\Delta\omega^2 + |\Omega_{mn}|^2}}{\Omega_{mn}}, \\ \omega_{mn}^\pm &= \frac{1}{2} \{ \Delta\omega(2m+1) + \nu(2n-2km) + \omega_{21}(2m+2) \pm \sqrt{\Delta\omega^2 + |\Omega_{mn}|^2} \}, \\ c_{mn}^\pm &= \frac{1}{\sqrt{1 + |\alpha_{mn}^\pm|^2}}, \quad \Omega_{mn} = 2\kappa'' \sqrt{m+1} f_k(n; \eta) \sqrt{\frac{(n+k)!}{n!}}, \text{ and} \\ f_k(n; \eta) &= \langle n | \hat{f}_k(\hat{a}^\dagger \hat{a}; \eta) | n \rangle. \end{aligned} \quad (5.7)$$

The $|i, m, n\rangle$ denotes the electronic ($i = 1, 2$), pump-photon ($m = 0, 1, 2, \dots$), and motional excitations ($n = 0, 1, 2, \dots$). To briefly recapitulate: The starting point was the explicitly time-dependent Hamiltonian in Eq. (5.1). The quantization of the pump field—i.e., an extension of the Hilbert space—led to a time-independent Hamiltonian [Eq. (5.4)]. The corresponding dynamics of this Hamiltonian has been solved straightforwardly.

To demonstrate the validity of the approach, the occupation probability of the excited electronic state of the ion will be considered, which is defined as

$$\sigma_{22}(t) = \sum_{m,n} \langle 2, n, m | \hat{\rho}(t) | 2, n, m \rangle, \quad (5.8)$$

in which $\hat{\rho}(t) = \hat{\mathcal{U}}_{\text{NLJC}}(t) \hat{\rho}(0) \hat{\mathcal{U}}_{\text{NLJC}}^\dagger(t)$ denotes the full density matrix of the system with $\hat{\rho}(0) = |2\rangle\langle 2| \otimes |\alpha_0\rangle\langle \alpha_0| \otimes |\beta_0\rangle\langle \beta_0|$. Thus, the ion is initially prepared in its excited electronic state, the pump is prepared in a coherent state $|\beta_0\rangle$, and likewise, the quantized motion is initially in a coherent state $|\alpha_0\rangle$. Combining

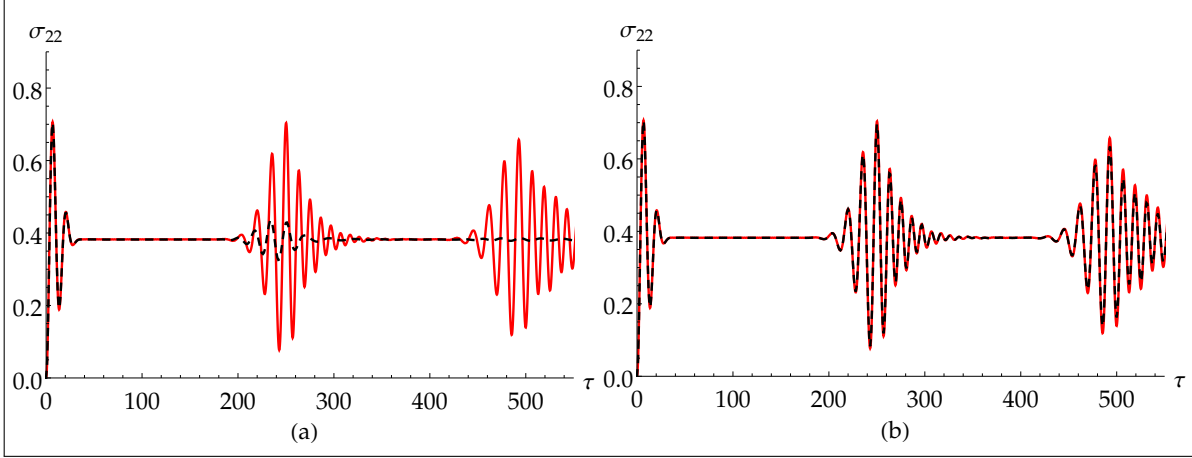


Figure 5.2: Comparison of the analytical solution for the quantized pump field [Hamiltonian in Eq. (5.4)] (dashed, black line) for $\beta_0 = 20$ (a) and $\beta_0 = 100$ (b) with the corresponding dynamics of the semiclassical solution (solid, red line) [Hamiltonian in Eq. (5.1)]. The latter is obtained numerically by using the PYTHON package QUTIP [126, 127]. The dimensionless time is defined as $\tau = |\kappa''|t$. The initial state of the quantized motion was assumed to be a coherent state $|\alpha_0\rangle$. Parameters: $\Delta\omega/|\kappa''| = 0.2$, $\alpha_0 = \sqrt{12}$, $k = 2$, $\Delta\phi = 0$, and $\eta = 0.2$.

the latter statements with Eqs. (5.5) and (5.8) it is found that

$$\sigma_{22}(t) = \sum_{m,n=0}^{\infty} \sum_{\sigma,\sigma'=\pm} e^{i[\omega_{mn}' - \omega_{mn}^{\sigma}]t} |c_{mn}^{\sigma} c_{mn}^{\sigma'}|^2 (\alpha_{mn}^{\sigma})^* \alpha_{mn}^{\sigma'} \frac{|\beta_0|^{(2m+2)} |\alpha_0|^{(2n+2k)}}{(m+1)!(n+k)!} e^{-|\beta_0|^2 - |\alpha_0|^2}. \quad (5.9)$$

Plots of $\sigma_{22}(t)$ are presented in Fig. 5.2. The solid (red) line corresponds to the solution of the dynamics of a classical pump, which is derived numerically using the PYTHON package QUTIP [126, 127]. The black (dashed) line visualizes the solution given in Eq. (5.9). It can be seen that the solution differs from the semiclassical one for a weak coherent input field $\beta_0 = 20$ of the pump. However, for a strong coherent amplitude $\beta_0 = 100$, the solution is very similar to the semiclassical case. In summary, not only a way to solve the dynamics of the detuned and nonlinear Jaynes-Cummings model has been found, but the model has been extended so that arbitrary pump fields may be considered. The issue of different—e.g. nonclassical—pump fields will be considered in Sec. 5.3.

5.2 Nonclassicality

In this section, the nonclassical properties of the derived solution [Eq. (5.6)] will be investigated in more detail. As a first qualitative analysis, the regularized Glauber-Sudarshan P representation will be calculated. In Fock basis, P_{Ω} , with respect to the motional subsystem, is calculated via

$$P_{\Omega}(\alpha; t) = \sum_{m,n=0}^{\infty} \rho_{\text{vib},mn}(t) P_{\Omega,nm}(\alpha). \quad (5.10)$$

This representation of the (motional) quantum state under study in phase space has the advantage that the values $P_{\Omega,nm}(\alpha)$ need to be computed only once and can be applied to arbitrary density matrices afterwards. By using the radial-symmetric compact-support filter [33]

$$\Omega_w(|\beta|) = \frac{2}{\pi} \left[\arccos\left(\frac{|\beta|}{2w}\right) - \frac{|\beta|}{2w} \sqrt{1 - \frac{|\beta|^2}{4w^2}} \right] \text{rect}\left(\frac{|\beta|}{4w}\right), \quad (5.11)$$

with $\text{rect}(x) = 1$ if $x \leq 1/2$ and $\text{rect}(x) = 0$ elsewhere,

$$P_{\Omega,nm}(\alpha) = \frac{16}{\pi^2} w^2 e^{i(n-m)\varphi_\alpha} \int_0^1 dz \Lambda_{nm}(2wz) z J_{n-m}(4w|\alpha|z) \left[\arccos(z) - z\sqrt{1-z^2} \right] \quad (5.12)$$

is obtained [III]. Here, $J_n(x)$ are the Bessel functions of the first kind, $\alpha = |\alpha|e^{i\varphi_\alpha}$, and

$$\begin{aligned} \Lambda_{nm}(x) &= \begin{cases} (-x)^{m-n} \sqrt{\frac{n!}{m!}} L_n^{(m-n)}(x^2) & m \geq n \\ x^{n-m} \sqrt{\frac{m!}{n!}} L_m^{(n-m)}(x^2) & m < n. \end{cases} \\ & \quad (5.13) \end{aligned}$$

The reduced density matrix is calculated via $\hat{\rho}_{\text{vib}}(t) = \sum_{i=1,2} \sum_{m=0}^{\infty} \langle i, m | \hat{\rho}(t) | i, m \rangle$. By using the input state $\hat{\rho}(0) = |2, \beta_0, \alpha_0\rangle\langle 2, \beta_0, \alpha_0|$, the quasiprobability in Fig. 5.3 is obtained. The motional coherent input state with amplitude $\alpha_0 = \sqrt{5}$ evolved into a distorted nonclassical state. The presented phase-space representation yields full insight into the (reduced) motional subsystem of the trapped ion. To get more insight into the nonclassical nature, the following distinct quantum effects will be considered. The motional states will be investigated with respect to squeezing, sub-Poisson statistics, and anomalous quantum correlations [128]. The related criteria read as

$$\mathcal{C}_{\text{Sq}} := \min_{\varphi \in [0, 2\pi)} \{ \langle : [\Delta \hat{x}(\varphi; \tau)]^2 : \rangle \} < 0, \quad (5.14)$$

$$\mathcal{C}_{\text{SP}} := Q(\tau) = \frac{\langle : [\Delta \hat{n}(\tau)]^2 : \rangle}{\langle \hat{n}(\tau) \rangle} < 0, \text{ and} \quad (5.15)$$

$$\mathcal{C}_{\text{AC}} := \min_{\varphi \in [0, 2\pi)} \{ \langle : [\Delta \hat{n}(\tau)]^2 : \rangle \langle : [\Delta \hat{x}(\varphi; \tau)]^2 : \rangle - | \langle : \Delta \hat{x}(\varphi; \tau) \Delta \hat{n}(\tau) : \rangle |^2 \} < 0, \quad (5.16)$$

in case of squeezing (Sq), sub-Poisson statistics (SP), and anomalous quantum correlations (AC). Here, $Q(\tau)$ is the commonly used definition of the Mandel Q parameter. As before, $\hat{\rho}(0) = |2, \beta_0, \alpha_0\rangle\langle 2, \beta_0, \alpha_0|$ is assumed. The input coherent pump amplitude β_0 is chosen to be sufficiently large, so that the dynamics is close to the semiclassical one. The results are depicted in Fig. 5.4 (after Ref. [V]). In the case of the excitation to the zeroth sideband [$k = 0$, figure (a)], only the anomalous quantum-correlations condition is able to certify nonclassicality. More interestingly, if the second sideband is excited [$k = 2$, figure (b)],

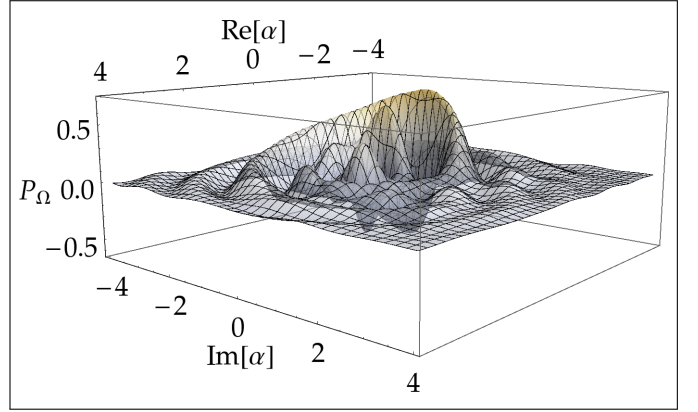


Figure 5.3: The regularized Glauber-Sudarshan P function [Eq. (5.12)] is shown for the initial coherent state $|\alpha_0\rangle$ at $|\kappa''|t = 50$. Parameters: $\alpha_0 = \sqrt{5}$, $k = 3$, $\Delta\phi = \pi/2$, $\eta = 0.2$, $\nu/|\kappa''| = 5000$, $\beta_0 = 40$, $\Delta\omega/|\kappa''| = 8$, and $w = 1.7$.

only small areas of squeezing are visible. This is surprising, as the Hamiltonian contains quadratic terms of the creation and annihilation operators, as it is the case in the ordinary squeezing operator. This counterintuitive behavior is caused by the nonlinearities—i.e., the Lamb-Dicke parameter being greater than zero. Thus, when it comes to the investigation of its exact physical relevance (e.g. with respect to application in future quantum technologies), a trapped ion in the resolved sideband regime seems to be a promising model to be studied.

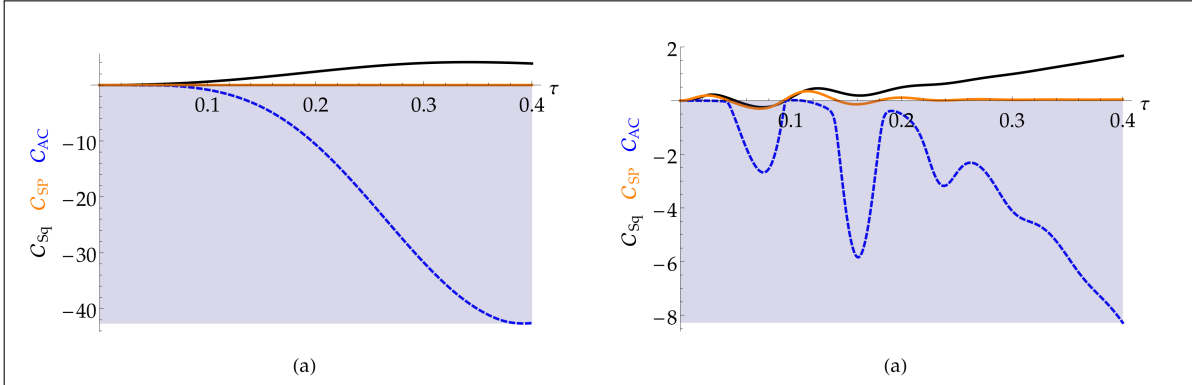


Figure 5.4: The nonclassicality criteria given in Eqs. (5.14) (C_{Sq} —squeezing; solid black line), (5.15) (C_{Sp} —sub-Poisson statistics; solid orange line), and (5.16) (C_{AC} —anomalous quantum correlations; dashed blue line) for the excitation to the zeroth sideband, $k = 0$ (a), and to the second sideband, $k = 2$ (b). Negative values (shaded area) certify nonclassicality. Note that the phase φ is optimized for each criterion separately. Parameters: $\alpha_0 = \sqrt{8}$, $\eta = 0.3$, $\Delta\omega/|\kappa''| = 20$, $\Delta\Phi = 0$, $\nu/|\kappa''| = 5000$, and $\beta_0 = 100$.

5.3 Quantum-pump dynamics

As mentioned before, the Hamiltonian in Eq. (5.1) can be solved directly, as well; see Ref. [IV]. The derived semiclassical solution in the latter reference is on the one hand easier to handle (as the additional “pump-Hilbert-space” is not needed), but on the other hand it does not allow for the consideration of more general pump/cavity input states. For example, by using the solutions in Eq. (5.6), one may consider

$$\hat{\rho}_{cav}(0) = |\Psi_{SV}\rangle\langle\Psi_{SV}| \quad (5.17)$$

with the squeezed vacuum state

$$|\Psi_{SV}\rangle = \frac{1}{\cosh \xi} \sum_{n=0}^{\infty} (-\tanh \xi)^n \frac{\sqrt{(2n)!}}{2^n n!} |2n\rangle, \quad (5.18)$$

in which ξ denotes the squeezing parameter. The regularized P function is derived in the same way as in Sec. 5.2. The result is depicted in Fig. 5.5, in which the electronic and motional input states are $|2\rangle\langle 2|$ and $|\alpha_0\rangle\langle\alpha_0|$, respectively. While figure (a) corresponds to the semiclassical solution of the Hamiltonian in Eq. (5.1), figure (b) shows the solution which has been discussed in Sec. 5.2 by using the input state

in Eq. (5.17). Due to the nonclassical cavity input field, a ring-formed structure appeared, which cannot be explained by using solely the semiclassical solution. Finally, note that Fig. 5.5 (a) could also be derived with the solution in Sec. 5.2 by using a coherent pump/cavity-input state $|\beta_0\rangle$ with $\beta_0 \gg 1$.

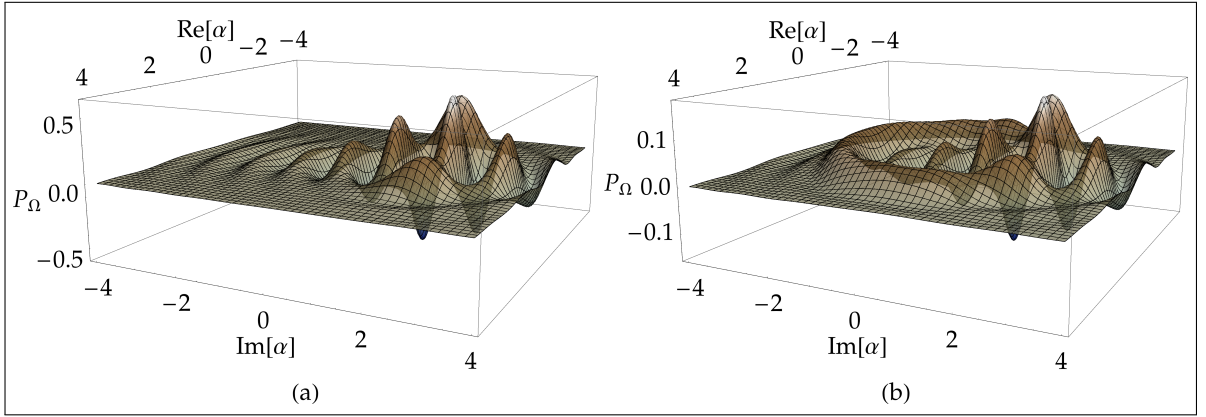


Figure 5.5: Comparison of the exact, semiclassical solution (Ref. [IV]) in figure (a) and the solution given in Eq. (5.6) for a cavity field prepared initially in a squeezed vacuum in figure (b) at $|\kappa'|t = 50$ for $k = 2$ in terms of the regularized P function [Eq. (5.10)]. Parameters: $\xi = 2$, $\eta = 0.2$, $\alpha_0 = \sqrt{5}$, and $\Delta\omega/|\kappa| = 0.1$.

5.4 Measurement of the trapped ion's total quantum state

A possible measurement scheme to reconstruct the total quantum state of a trapped ion in terms of a generalization of the Wigner function was introduced in Ref. [129]. The phrase *total quantum state* includes even entanglement between the electronic and motional degrees of freedom, which is not observable if only the reduced density matrix of one subsystem is considered. The measurement scheme

is depicted in Fig. 5.6 and discussed in depth in Ref. [129] and Sec. IV of Ref. [V]. With the strong $|1\rangle \leftrightarrow |3\rangle$ transition, the ground (or excited) electronic state probability of the ion is determined. The weak $|1\rangle \leftrightarrow |2\rangle$ transition leads to the interaction Hamiltonian

$$\hat{\mathcal{H}}_{\text{int}} = \hbar|\kappa'|f_0(\hat{n};\eta)\hat{A}_{12} + \text{H.c.} \quad (5.19)$$

Due to the measurement of the ion's electronic state via the strong transition, the density matrix of the complete system reduces to

$$\hat{\rho}^{(1)}(\tau_1) = |2\rangle\langle 2| \otimes \hat{\rho}_{\text{red}}^{(1)}(\tau_1), \quad (5.20)$$

in case the ion is in its electronically excited state. In Eq. (5.20),

$\hat{\rho}_{\text{red}}^{(1)}(\tau) = \langle 2|\hat{\mathcal{U}}_{\text{int}}(\tau_1)\hat{\rho}(\alpha)\hat{\mathcal{U}}_{\text{int}}^\dagger(\tau_1)|2\rangle$ was defined, in which $\hat{\rho}(\alpha) = \hat{D}^\dagger(\alpha)\hat{\rho}(0)\hat{D}(\alpha)$ is the displaced motional state and $\hat{\rho}(0)$ denotes the density operator of the vibronic degrees of freedom. After applying multiple probe cycles and choosing appropriate interaction times, the diagonal density matrix elements $\rho_{ij}^{nn}(\alpha) \equiv \langle i, n|\hat{\rho}(\alpha)|j, n\rangle$ for $i, j = 1, 2$ are recovered. By using these elements, multiple representations of the state under study can be derived. Ref. [129] relates the elements to a so-called Wigner-function matrix which is a generalization of the ordinary Wigner function, including a description of possibly entangled electronic and motional degrees of freedom. Meanwhile a hybrid-version of the Glauber-Sudarshan P function was introduced in Ref. [130], which uncovers quantum correlations between the subsystems beyond entanglement [131]. The hybrid-version of the P function is defined as

$$P_{ij}(\alpha) = \langle \hat{A}_{ji} \otimes : \hat{\delta}(\hat{a} - \alpha) : \rangle \quad (5.21)$$

and can be derived out of the elements $\rho_{ij}^{nn}(\alpha)$ in two ways. One way is to derive the Wigner-function matrix, Fourier transform it, rewrite the resulting expression in normal order, and Fourier transform it back (including an appropriate filtering) to obtain the regularized P -function matrix. Another way is to apply the method of nonclassicality witnesses, introduced in Ref. [132]. These two approaches yield the expressions

$$P_{ij,\Omega}(\alpha) = \frac{2}{\pi^3} \sum_{n=0}^{\infty} (-1)^n \int d^2\alpha' \Lambda_{\Omega}(\alpha, \alpha') \rho_{ij}^{nn}(\alpha') \quad (5.22)$$

and

$$P_{ij,\text{disc}}(\alpha) = \frac{w^2}{16} \sum_{m=0}^{\infty} \frac{(-w^2/4)^m}{[(m+1)!]^2} \binom{2m+2}{m} \sum_{n=m}^{\infty} \rho_{ij}^{nn}(\alpha) \frac{n!}{(n-m)!}. \quad (5.23)$$

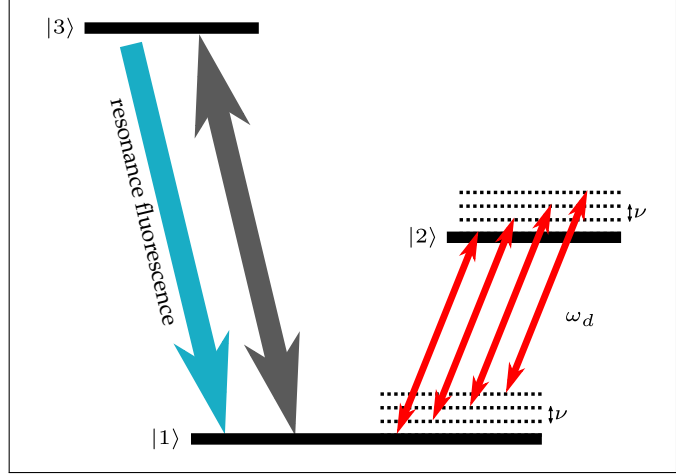


Figure 5.6: Measurement scheme after Ref. [129] to reconstruct the, possibly entangled, quantum state of a trapped ion, with respect to the vibronic states. The driving laser (red arrows) is detuned to the zeroth sideband: $\omega_d = \omega_{21}$; see text for further explanations.

The index “disc” in the second expression denotes that this result is obtained by using a disc-function filter. In Eq. (5.22), $\Lambda_\Omega(\alpha, \alpha') := \int d^2\beta \Omega_w(\beta) e^{|\beta|^2/2} e^{\beta^*(\alpha-\alpha')-\beta(\alpha^*-\alpha'^*)}$ was defined. Thus, the elements $\rho_{ij}^{nn}(\alpha)$ which are obtained from the measurement, directly yield the regularized version of the P -function matrix. The latter is obtained either over the complete phase space via integration [Eq. (5.22)] or at one particular point in phase space [Eq. (5.23)]. The anomalous quantum correlations can be derived accordingly in Fourier space via the derivatives of the characteristic-function matrix; cf. Ref. [V].

5.5 Non-commuting Hamiltonians

At the beginning of this thesis, in Sec. 2.2, the problems of non-commuting Hamiltonians have been recapitulated. The problems arise naturally in the solution of the time-evolution operator if the corresponding Hamiltonian is explicitly time-dependent. Can this quantity be somehow extracted out of measured data? Even though this problem is a keystone of quantum mechanics, it is rarely investigated. A related but simpler problem is the verification of the commutation relation $[\hat{a}, \hat{a}^\dagger] = \hat{1}$. Although this commutation rule is of fundamental importance, a direct experimental proof was not reported before 2007; see Refs. [133–135].

Given an interaction Hamiltonian in the interaction picture, $\hat{H}_{\text{int},I}$, the time evolution of the Hamiltonian itself can be described via

$$\hat{U}_I^\dagger(t) \hat{H}_{\text{int},I}(t) \hat{U}_I(t) = \underbrace{\hat{H}_{\text{int},I}(t)}_{\propto |\kappa'|} + \frac{i}{\hbar} \int_0^t d\tau_1 \underbrace{\left[\hat{H}_{\text{int},I}(\tau_1), \hat{H}_{\text{int},I}(t) \right]}_{\propto |\kappa'|^2} + \mathcal{O}(|\kappa'|^3), \quad (5.24)$$

in which $\hat{U}_I(t)$ is the ordinary time-evolution operator, containing solely the interaction Hamiltonian. Here, $|\kappa'|$ denotes some coupling constant to which the interaction Hamiltonian is assumed to be proportional. Thus, the measurement of the interaction Hamiltonian in dependence of $|\kappa'|$ yields the Hamiltonian in the interaction picture (term proportional to $|\kappa'|$) and its partially integrated time-dependent commutator (term proportional to $|\kappa'|^2$).

The first question arising is whether or not it is possible to measure the time evolution of the interaction Hamiltonian alone. Since the operator $\hat{A}_{22} = |2\rangle\langle 2|$ commutes with the free field Hamiltonian and the excited state occupation probability equals the expectation value of \hat{A}_{22} it is found that, for $\Delta\omega \neq 0$, [VI]

$$\sigma_{22}(t) - \sigma_{22}(0) = \frac{1}{\hbar\Delta\omega} \left(\left\langle \hat{U}_I^\dagger(t) \hat{H}_{\text{int},I}(t) \hat{U}_I(t) \right\rangle - \left\langle \hat{U}_I^\dagger(0) \hat{H}_{\text{int},I}(0) \hat{U}_I(0) \right\rangle \right). \quad (5.25)$$

The measurement of σ_{22} , which is achieved via probing for resonance fluorescence, allows for the determination of the time evolution of solely the interaction Hamiltonian. From the latter, the explicit time-dependent Hamiltonian itself and the corresponding commutator can be derived; see Eq. (5.24).

To demonstrate the applicability, the technique will be applied to simulated data, i.e., random events will be generated that resemble the evolution of σ_{22} . The generation scheme is:

1. creation of random events that resemble the evolution of σ_{22} with respect to the coupling.

2. polynomial approximation of those data for small couplings at each time point.
3. determination of the linear and quadratic coefficients of this polynomial, which equal the first and second term in Eq. (5.24), respectively.

Depending on the scenario, this procedure needs to be repeated multiple times. The results are depicted in Fig. 5.7. The interaction Hamiltonian [Eq. (5.1)] in Fock basis reads as

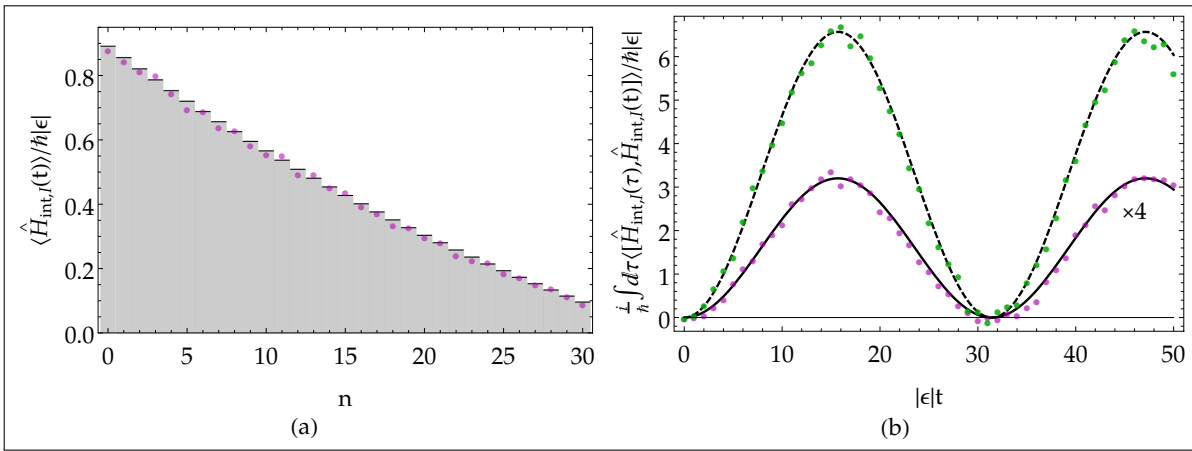


Figure 5.7: Plot of the simulated data, represented by the dots, in comparison to the analytical results. Figure (a) shows the determination of the interaction Hamiltonian in Fock basis, $\langle n | \hat{H}_{\text{int},I}(t) | n \rangle$ in Eq. (5.26) at $|\epsilon|t = 10$. The gray bars are the analytical results. $|\epsilon|$ denotes the rescaled and dimensionless coupling; for details see Ref. [VI]. Figure (b) shows the analytically derived curves of the commutator in Eq. (5.27) (black lines) for a coherent state $|\alpha_0\rangle$, with $\alpha_0 = \sqrt{12}$, together with simulated data for $k = 0$ (green dots) and $k = 2$ (magenta dots). Parameters: $\eta = 0.2$, $\Delta\omega/|\epsilon| = 0.2$, $\Delta\Phi = 0$, and $\nu = 5000$.

$$\langle n | \hat{H}_{\text{int},I}(t) | n \rangle = \hbar |\kappa'| f_0(n; \eta) (\gamma_1 \gamma_2^* e^{-i\Delta\omega t} + \gamma_2 \gamma_1^* e^{i\Delta\omega t}) \quad (5.26)$$

and is presented as the gray bars in Fig. 5.7 (a). The commutator for a motional coherent input state is

$$\frac{i}{\hbar} \int_0^t d\tau \langle 1, \alpha_0 | [\hat{H}_{\text{int},I}(\tau), \hat{H}_{\text{int},I}(t)] | 1, \alpha_0 \rangle = \frac{2|\kappa'|^2 \hbar}{\Delta\omega} (1 - \cos \Delta\omega t) \sum_{n=0}^{\infty} |f_k(n; \eta)|^2 \frac{|\alpha_0|^{2(n+k)}}{n!} e^{-|\alpha_0|^2} \quad (5.27)$$

and is shown as the black dashed and solid line in Fig. 5.7 (b), for $k = 0$ and $k = 2$, respectively. The simulation resembles the theoretical prediction sufficiently well. It is noteworthy that statistically significant non-zero contributions of real data in figure (b) would be a clear experimental evidence of non-equal-time commutators of the interaction Hamiltonian. Especially, solely the electronic-state occupation probability is needed to reveal the behavior of the non-equal-time commutators which account for time-ordering effects.

5.6 Summary of Chapter 5

In this chapter, the time-dependent Hamiltonian of the quasiresonantly driven nonlinear Jaynes-Cummings model has been investigated. Since time ordering must not be neglected, the dynamics has been solved via an extension of the Hilbert space; more precisely, the pump field has been quantized. Due to this procedure, the full Hamiltonian became time-independent. The dynamics of the Hamiltonian has been solved analytically and the solutions have been verified using numerical methods. Especially, for a strong coherent pump input state, it has been shown that the solutions resemble the semiclassical behavior. Furthermore, the temporal evolution of the regularized P function of the motional states of the ion has been visualized. The model has been used as a basis for various considerations and it could be shown that (i) for the excitation to the zeroth sideband, anomalous quantum correlations of non-commuting observables of the motional states can be revealed where neither quadrature squeezing nor sub-Poisson number statistics occur, (ii) the treatment of the pump in a quantized manner yields a more general description of the corresponding dynamics, (iii) the discussed quantities can be measured via an appropriate measurement scheme, and (iv) the model is suitable for the investigation of non-equal-time commutators of Hamiltonians, which are a keystone of quantum mechanics. In fact, the further investigation of the model is very promising since there may be more so far undiscovered effects. Nonetheless, it is still an open question whether the investigated effects—e.g., anomalous quantum correlations of the motional states—can be useful for applications in quantum technologies.

6. Conclusion

In this final section, the findings of this thesis and the corresponding publications will be summarized. For a better overview, this chapter is structured according to the different topics which have been treated during the research.

Time ordering.— If a system's Hamiltonian is explicitly time-dependent, time-ordering effects arise naturally in the dynamics. Albeit this issue is a keystone of the fundamentals of quantum dynamics, these effects are rarely considered in current research. This may be due to the fact that most approaches include the time-ordering effects in the final solution automatically. In experiments, certain scenarios are preferred, e.g., the restriction to certain pump pulses in parametric down-conversion, which are well approximated without time ordering, leading to untapped resources. It has been shown that for degenerate parametric down-conversion which includes a frequency mismatch (and algebraically comparable systems), the operator-valued time-ordering problem can be transferred into the complex-valued domain, in which the time ordering can be treated in terms of non-commutative matrices. By using these results and the Magnus expansion, it has been demonstrated that, within the radius of convergence, terms up to the eleventh Magnus order may significantly contribute to the complete dynamics. Especially, it has been shown that they affect the evolution of nonclassicality, which has been considered in terms of the slope of the Fourier transform of the Glauber-Sudarshan P function.

Quasiresonantly driven nonlinear Jaynes-Cummings Hamiltonian.— Apart from the model of degenerate parametric down-conversion, time ordering within the quasiresonantly driven nonlinear Jaynes-Cummings model has been discussed. In order to justify the need of analytical solutions, including time ordering, it has been argued that even for a small detuning, the impact of time ordering is crucial. Therefore, an exact solution via the extension of the Hilbert space has been derived, in the form of a quantized pump field. This way, via treating the incident laser in a quantized manner, the time-dependence of the Hamiltonian in the Schrödinger picture vanished. The solution of the time-evolution operator has been derived straightforwardly. If the input state of the pump is a strong coherent state, the solutions converge to the semiclassical case (where the pump is treated classically). However, it has been shown that, e.g., nonclassical pump input-fields reveal a different dynamics compared to the semiclassical case and, thus, the solution which include a quantized pump field yields a more general description of the system. By using the regularized version of the Glauber-Sudarshan P function, the temporal nonclassicality evolution of the motional state of the trapped ion in phase space has been visualized.

Furthermore, for this particular system, nonclassicality in terms of squeezing, sub-Poisson statistics, and anomalous quantum correlations has been investigated. Comparing these criteria, scenarios have been revealed, in which nonclassicality is only certified by anomalous quantum correlations. Thus, to investigate the usefulness of those correlations with respect to future quantum technologies, the nonlinear and detuned Jaynes-Cummings model is a promising candidate. Additionally, an established measurement scheme has been reconsidered, which was initially thought to uncover entanglement between the electronic and motional states in terms of a generalization of the Wigner function. It has been shown that, in principle, the anomalous quantum correlations and other normal-ordered moments can be recovered out of the measured quantities. Moreover, the hybrid version of the Glauber-Sudarshan P function can be reconstructed from the same data.

Another important topic which have been discussed in terms of the nonlinear Jaynes-Cummings model is the verification of non-equal-time commutators. By using the semiclassical solutions, simulated data has been used to demonstrate that the expectation value of a partially integrated non-equal-time commutator of the corresponding Hamiltonian can be reconstructed out of the excited electronic-state occupation probability. In principle, this can be achieved as long as the data are well resolved for weak couplings.

Multi-time-dependent nonclassicality.— Besides the nonclassicality with respect to a single point in time, a complete framework has been developed to uncover multi-time-dependent nonclassicality. The latter means nothing but the negativity of the P functional introduced in 2008, which is a generalization of the Glauber-Sudarshan P function. It can be used to express normal- and time-ordered correlations functions formally as a classical stochastic process. Unfortunately, the P functional is an ill-behaved function for most states and its singularities may become stronger in multi-time scenarios. Thus, the Fourier transform of the P functional has been investigated, which is referred to as a multi-time-dependent characteristic function and is always well-behaved. Based on this function, a hierarchy of necessary and sufficient criteria has been derived to verify nonclassical stochastic processes for radiation fields, including an arbitrary number of points in time. The approach has been applied to two points in time to degenerate parametric-down conversion and it has been shown that for all times under study the derived criterion is violated and hence, the corresponding two-time-dependent P functional is negative in the sense of distributions. However, the derived criteria are only necessary if all generally infinite orders are taken into account. Thus, in certain situations, if low orders fail to uncover nonclassicality, it may be reasonable to consider the P functional instead.

For this purpose, the procedure of P function regularization has been extended to the multi-time scenario. It has been demonstrated that the multi-time-dependent regularization procedure needs to fulfill additional constraints compared to the single-time case. This is caused by the fact that in the latter case, the bound of the characteristic function, which is the same for all times under study, is well-known. However, for multiple points in time, a general bound is not known as, e.g., non-equal-time commutators play an important role. By using the developed multi-time regularization procedure of the P functional, multi-time nonclassicality can be directly visualized via negativities in the “multi-time phase space”. It has been discussed that the method applies to arbitrary dynamics. As a physical example and in close relation to previous works, degenerate parametric down-conversion has been reconsidered

and its regularized two-time-dependent P functional has been derived. The clearly visible negativities were in accordance with the approach in terms of the multi-time-dependent characteristic function. For the dynamics of a trapped ion, it has been presented that a product of single-time bounds cannot be used to estimate the slope of the two-time-dependent characteristic function. This justifies the derived regularization procedure. Moreover, the discussed multi-time-dependent quantities are accessible in experiments as, according to the photodetection theory of Kelly and Kleiner, the joint statistics of multiple detectors at different space-time-points equals a normal- and time-ordered correlation function.

In summary, the thesis concerns novel approaches that address the paramount question of time-dependence in quantum systems. A number of new techniques have been developed to theoretically describe the quantum nature of time-dependent processes in optical systems and beyond, overcoming the limitations of previously existing methods. Moreover, measurable criteria to probe such quantum phenomena have been derived and interacting systems of practical relevance have been extensively studied. New insights have been gathered into fundamental and application-oriented aspects of temporal quantum correlations, which hopefully will be useful for upcoming research and in future implementations of quantum technologies.

Bibliography

- [1] H. P. YUEN, *Two-photon coherent states of the radiation field*, *Phys. Rev. A* **13**, 2226 (1976).
- [2] D. F. WALLS, *Squeezed states of light*, *Nature* **306**, 141 (1983).
- [3] C. M. CAVES and B. L. SCHUMAKER, *New formalism for two-photon quantum optics. I. Quadrature phases and squeezed states*, *Phys. Rev. A* **31**, 3068 (1985).
- [4] B. L. SCHUMAKER and C. M. CAVES, *New formalism for two-photon quantum optics. II. Mathematical foundation and compact notation*, *Phys. Rev. A* **31**, 3093 (1985).
- [5] R. LOUDON and P. KNIGHT, *Squeezed Light* *J. Mod. Opt.* **34**, 709 (1987).
- [6] V. V. DODONOV, ‘Nonclassical’ states in quantum optics: a ‘squeezed’ review of the first 75 years, *J. Opt. B: Quantum Semiclass. Opt.* **4**, R1 (2002).
- [7] L. MANDEL, *Sub-Poissonian photon statistics in resonance fluorescence*, *Opt. Lett.* **4**, 205 (1979).
- [8] R. SHORT and L. MANDEL, *Observation of Sub-Poissonian Photon Statistics*, *Phys. Rev. Lett.* **51**, 384 (1983).
- [9] M. C. TEICH and B. E. A. SALEH, *Observation of sub-Poisson Franck–Hertz light at 253.7 nm*, *J. Opt. Soc. Am. B*, **2**, 275 (1985).
- [10] X. T. ZOU and L. MANDEL, *Photon-antibunching and sub-Poissonian photon statistics*, *Phys. Rev. A* **41**, 475 (1990).
- [11] H. J. CARMICHAEL and D. F. WALLS, *Proposal for the measurement of the resonant Stark effect by photon correlation techniques*, *J. Phys. B: At. Mol. Opt. Phys.* **9**, L43 (1976).
- [12] H. J. KIMBLE and L. MANDEL, *Theory of resonance fluorescence*, *Phys. Rev. A* **13**, 2123 (1976).
- [13] H. J. KIMBLE, M. DAGENAIS, and L. MANDEL, *Photon Antibunching in Resonance Fluorescence*, *Phys. Rev. Lett.* **39**, 691 (1977).
- [14] A. MIRANOWICZ, J. BAJER, H. MATSUEDA, M. R. B. WAHIDDIN, and R. TANAS, *Comparative study of photon antibunching of non-stationary fields*, *Journal of Optics B: Quantum and Semiclassical Optics* **1**, 511 (1999).
- [15] A. MIRANOWICZ, M. BARTKOWIAK, X. WANG, Y. LIU, and F. NORI, *Testing nonclassicality in multimode fields: a unified derivation of classical inequalities*, *Phys. Rev. A* **82**, 031824 (2010).
- [16] R. J. GLAUBER, *Coherent and Incoherent States of the Radiation Field*, *Phys. Rev.* **131**, 2766 (1963).

- [17] E. C. G. SUDARSHAN, *Equivalence of Semiclassical and Quantum Mechanical Descriptions of Statistical Light Beams*, *Phys. Rev. Lett.* **10**, 277 (1963).
- [18] U. M. TITULAER and R. J. GLAUBER, *Correlation Functions for Coherent Fields*, *Phys. Rev.* **140**, B676 (1965).
- [19] P. L. KELLEY and W. H. KLEINER, *Theory of Electromagnetic Field Measurement and Photoelectron Counting*, *Phys. Rev.* **136**, A316 (1964).
- [20] W. VOGEL, *Nonclassical States: An Observable Criterion*, *Phys. Rev. Lett.* **84**, 1849 (2000).
- [21] A. I. LVOVSKY and J. H. SHAPIRO, *Nonclassical character of statistical mixtures of the single-photon and vacuum optical states*, *Phys. Rev. A* **65**, 033830 (2002).
- [22] Th. RICHTER and W. VOGEL, *Nonclassicality of Quantum States: A Hierarchy of Observable Conditions*, *Phys. Rev. Lett.* **89**, 283601 (2002).
- [23] A. ZAVATTA, V. PARIGI, and M. BELLINI, *Experimental nonclassicality of single-photon-added thermal light states*, *Phys. Rev. A* **75**, 052106 (2007).
- [24] A. MARI, K. KIELING, B. M. NIELSEN, E. S. POLZIK, and J. EISERT, *Directly Estimating Nonclassicality*, *Phys. Rev. Lett.* **106**, 010403 (2011).
- [25] E. SHCHUKIN, Th. RICHTER, and W. VOGEL, *Nonclassicality criteria in terms of moments*, *Phys. Rev. A* **71**, 011802(R) (2005).
- [26] E. V. SHCHUKIN and W. VOGEL, *Nonclassicality moments and their measurements*, *Phys. Rev. A* **72**, 043808 (2005).
- [27] S. RYL, J. SPERLING, E. AGUDELO, M. MRAZ, S. KÖHNKE, B. HAGE, and W. VOGEL, *Unified nonclassicality criteria*, *Phys. Rev. A* **92**, 011801(R) (2015).
- [28] T. KIESEL and W. VOGEL, *Nonclassicality filters and quasi-probabilities*, *Phys. Rev. A* **82**, 032107 (2010).
- [29] T. KIESEL, W. VOGEL, B. HAGE, and R. SCHNABEL, *Direct sampling of negative quasiprobabilities of a squeezed state*, *Phys. Rev. Lett.* **107**, 113604 (2011).
- [30] T. KIESEL, W. VOGEL, M. BELLINI, and A. ZAVATTA, *Nonclassicality quasiprobability of single-photon-added thermal states*, *Phys. Rev. A* **83**, 032116 (2011).
- [31] E. AGUDELO, J. SPERLING, and W. VOGEL, *Quasiprobabilities for multipartite quantum correlations of light*, *Phys. Rev. A* **87**, 033811 (2013).
- [32] S. RAHIMI-KESHARI, T. KIESEL, W. VOGEL, S. GRANDI, A. ZAVATTA, and M. BELLINI, *Quantum Process Nonclassicality*, *Phys. Rev. Lett.* **110**, 160401 (2013).
- [33] B. KÜHN and W. VOGEL, *Visualizing nonclassical effects in phase space*, *Phys. Rev. A* **90**, 033821 (2014).
- [34] J. SPERLING, *Characterizing maximally singular phase-space distributions*, *Phys. Rev. A* **94**, 013814

- (2016).
- [35] E. AGUDELO, J. SPERLING, L. S. COSTANZO, M. BELLINI, A. ZAVATTA, and W. VOGEL, *Conditional Hybrid Nonclassicality*, *Phys. Rev. Lett.* **119**, 120403 (2017).
- [36] B. KÜHN and W. VOGEL, *Quantum non-Gaussianity and quantification of nonclassicality*, *Phys. Rev. A* **97**, 053807 (2018).
- [37] B. KÜHN and W. VOGEL, *Preparation of quantum states with regular P functions*, *Phys. Rev. A* **98**, 053807 (2018).
- [38] W. VOGEL and D.-G. WELSCH, *Quantum optics*, 3rd ed. (Wiley-VCH, New York, 2006).
- [39] W. VOGEL, *Nonclassical correlation properties of radiation fields*, *Phys. Rev. Lett.* **100**, 013605 (2008).
- [40] W. MAGNUS, *On the exponential solution of differential equations for a linear operator*, *Comm. Pure and Appl. Math.* **7**, 649 (1954).
- [41] S. BLANES, F. CASAS, J. A. OTEO, and J. ROS, *The Magnus expansion and some of its applications*, *Phys. Rep.* **470**, 151 (2009).
- [42] W. VOGEL and R. L. DE MATOS FILHO, *Nonlinear Jaynes-Cummings dynamics of a trapped ion*, *Phys. Rev. A* **52**, 4214 (1995).
- [43] C. A. BLOCKLEY, D. F. WALLS, and H. RISKEN, *Quantum Collapses and Revivals in a Quantized Trap*, *Europhys. Lett.* **17**, 509 (1992).
- [44] C. A. BLOCKLEY and D. F. WALLS, *Cooling of a trapped ion in the strong-sideband regime*, *Phys. Rev. A* **47**, 2115 (1993).
- [45] J. I. CIRAC, R. BLATT, A. S. PARKINS, and P. ZOLLER, *Quantum collapse and revival in the motion of a single trapped ion*, *Phys. Rev. A* **49**, 1202 (1994).
- [46] C. GERRY and P. KNIGHT, *Introductory Quantum Optics*, (Cambridge University Press, Cambridge, 2004).
- [47] E. WIGNER, *On the Quantum Correction For Thermodynamic Equilibrium*, *Phys. Rev.* **40**, B749 (1932).
- [48] K. HUSIMI, *Some Formal Properties of the Density Matrix*, *Proc. Phys. Math. Soc. Japan* **22**, 264 (1940).
- [49] Y. KANO, *A New Phase-Space Distribution Function in the Statistical Theory of the Electromagnetic Field*, *J. Math. Phys.* **6**, 1913 (1965).
- [50] K. E. CAHILL and R. J. GLAUBER, *Ordered Expansions in Boson Amplitude Operators*, *Phys. Rev.* **177**, 1857 (1969).
- [51] G. S. AGARWAL and E. WOLF, *Calculus for Functions of Noncommuting Operators and General Phase-Space Methods in Quantum Mechanics. I. Mapping Theorems and Ordering of Functions of Noncommuting Operators*, *Phys. Rev. D* **2**, 2161 (1970).

- [52] H.-W. LEE, *Theory and application of the quantum phase-space distribution functions*, *Phys. Rep.* **259**, 149-211 (1995).
- [53] G. ADESSO, S. RAGY, and A. R. LEE, *Continuous Variable Quantum Information: Gaussian States and Beyond*, *Open Syst. Inf. Dyn.* **21**, 1440001 (2014).
- [54] A. CHRIST, B. BRECHT, W. MAUERER, and C. SILBERHORN, *Theory of quantum frequency conversion and type-II parametric down-conversion in the high-gain regime*, *New J. Phys.* **15**, 053038 (2013).
- [55] N. QUESADA and J. E. SIPE, *Effects of time ordering in quantum nonlinear optics*, *Phys. Rev. A* **90**, 063840 (2014).
- [56] N. QUESADA and J. E. SIPE, *Time-Ordering Effects in the Generation of Entangled Photons Using Nonlinear Optical Processes*, *Phys. Rev. Lett.* **114**, 093903 (2015).
- [57] N. QUESADA and J. E. SIPE, *High efficiency in mode-selective frequency conversion*, *Opt. Lett.* **41**, 364-367 (2016).
- [58] T. LIPFERT, D. B. HOROSHKO, G. PATERA, and M. I. KOLOBOV, *Bloch-Messiah decomposition and Magnus expansion for parametric down-conversion with monochromatic pump*, *Phys. Rev. A* **98**, 013815 (2018).
- [59] L. MANDEL, *Non-Classical States of the Electromagnetic Field*, *Phys. Scr.* **T12**, 34 (1986).
- [60] J. SPERLING, *Characterizing maximally singular phase-space distributions*, *Phys. Rev. A* **94**, 013814 (2016).
- [61] R. J. GLAUBER, *Quantum Optics and Electronics*, (Gordon and Breach, New York, 1965).
- [62] T. KIESEL, W. VOGEL, B. HAGE, J. DIGUGLIELMO, A. SAMBLOWSKI, and R. SCHNABEL, *Experimental test of nonclassicality criteria for phase-diffused squeezed states*, *Phys. Rev. A* **79**, 022122 .
- [63] S. BOCHNER, *Monotone Funktionen, Stieltjessche Integrale und harmonische Analyse*, *Math. Ann.* **108**, 378 (1933).
- [64] C. K. HONG, Z. Y. OU, and L. MANDEL, *Measurement of subpicosecond time intervals between two photons by interference*, *Phys. Rev. Lett.* **59**, 2044 (1987).
- [65] A. B. U'REN, C. SILBERHORN, K. BANASZEK, and I. A. WALMSLEY, *Efficient Conditional Preparation of High-Fidelity Single Photon States for Fiber-Optic Quantum Networks*, *Phys. Rev. Lett.* **93**, 093601 (2004).
- [66] P. J. MOSLEY, J. S. LUNDEEN, B. J. SMITH, P. WASYLCHYK, A. B. U'REN, C. SILBERHORN, and I. A. WALMSLEY, *Heralded Generation of Ultrafast Single Photons in Pure Quantum States*, *Phys. Rev. Lett.* **100**, 133601 (2008).
- [67] T. B. PITTMAN, B. C. JACOBS, and J. D. FRANSON, *Heralding single photons from pulsed parametric down-conversion*, *Opt. Commun.* **246**, 545-550 (2005).
- [68] A. L. MIGDALL, D. BRANNING, and S. CASTELLETTO, *Tailoring single-photon and multiphoton*

- probabilities of a single-photon on-demand source*, *Phys. Rev. A* **66**, 053805 (2002).
- [69] Paul G. KWIAT, Klaus MATTLE, Harald WEINFURTER, Anton ZEILINGER, Alexander V. SERGIENKO, and Yanhua SHIH, *New High-Intensity Source of Polarization-Entangled Photon Pairs*, *Phys. Rev. Lett.* **75**, 4337 (1995).
- [70] Paul G. KWIAT, Edo WAKS, Andrew G. WHITE, Ian APPELBAUM, and Philippe H. EBERHARD, *Ultra-bright source of polarization-entangled photons*, *Phys. Rev. A* **60**, R773(R) (1999).
- [71] C. KURTSIEFER, M. OBERPARLEITER, and H. WEINFURTER, *High-efficiency entangled photon pair collection in type-II parametric fluorescence*, *Phys. Rev. A* **64**, 023802 (2001).
- [72] S. M. BARNETT and P. M. RADMORE, *Methods in Theoretical Quantum Optics*, (Oxford University Press, Oxford, 2002).
- [73] A. CHRIST, K. LAIHO, A. ECKSTEIN, K. N. CASSEMIRO, and C. WEINFURTER, *Probing multimode squeezing with correlation functions*, *New J. Phys.* **13**, 033207 (2011).
- [74] W. P. GRICE and I. A. WALMSLEY, *Spectral information and distinguishability in type-II down-conversion with a broadband pump*, *Phys. Rev. A* **56**, 1627 (1997).
- [75] S. WALLENTOWITZ and W. VOGEL, *Quantum-mechanical counterpart of nonlinear optics*, *Phys. Rev. A* **55**, 4438 (1997).
- [76] E. T. JAYNES and F. W. CUMMINGS, *Comparison of Quantum and Semiclassical Radiation Theories with Application to the Beam Maser*, *Proc. IEEE* **51**, 89 (1963).
- [77] H. PAUL, *Induzierte Emission bei starker Einstrahlung*, *Ann, Phys. (Leipzig)* **11**, 411 (1963).
- [78] S. HAROCHE, *Les Houches Lecture Notes*, Session XXXVIII ed, in *New Trends in Atomic Physics*, edited by G. Grynberg and R. Stora (Elsevier, New York , 1984), p. 195.
- [79] S. HAROCHE and J. M. RAIMOND, *Radiative Properties of Rydberg States in Resonant Cavities*, *Adv. At. Mol. Phys.* **20**, 347 (1985).
- [80] D. MESCHÉDE, H. WALTHER, and G. MÜLLER, *One-Atom Maser*, *Phys. Rev. Lett.* **54**, 551 (1985).
- [81] G. REMPE, H. WALTHER and N. KLEIN, *Observation of Quantum Collapse and Revival in a One-Atom Maser*, *Phys. Rev. Lett.* **58**, 353 (1987).
- [82] I. I. RABI, *On the Process of Space Quantization*, *Phys. Rev.* **49**, 324 (1936).
- [83] I. I. RABI, *Space Quantization in a Gyating Magnetic Field*, *Phys. Rev.* **51**, 652 (1937).
- [84] D. ESTEVE, J.-M. RAIMOND, and J. DALIBARD, *Entanglement and Information Processing*, 1st ed., (Elsevier, Amsterdam, 2003).
- [85] J. H. EBERLY, N. B. NAROZHNY, and J. J. SANCHEZ-MONDRAGON, *Periodic Spontaneous Collapse and Revival in a Simple Quantum Model*, *Phys. Rev. Lett.* **44**, 1323 (1980).
- [86] N. B. NAROZHNY, J. J. SANCHEZ-MONDRAGON, and J. H. EBERLY, *Coherence versus incoherence:*

- Collapse and revival in a simple quantum model*, *Phys. Rev. A* **23**, 236 (1981).
- [87] J. R. KUKLIŃSKI and J. L. MADAJCZYK, *Strong squeezing in the Jaynes-Cummings model*, *Phys. Rev. A* **37**, 3175(R) (1988).
- [88] M. HILLERY, *Squeezing and photon number in the Jaynes-Cummings model*, *Phys. Rev. A* **39**, 1556 (1989).
- [89] S. J. D. PHOENIX and P. L. KNIGHT, *Establishment of an entangled atom-field state in the Jaynes-Cummings model*, *Phys. Rev. A* **44**, 6023 (1991).
- [90] S. FURUICHI and M. OHYA, *Entanglement Degree in the Time Development of the Jaynes-Cummings Model*, *Lett. Math. Phys.* **49**, 279 (1999).
- [91] S. BOSE, I. FUENTES-GURIDI, P. L. KNIGHT, and V. VEDRAL, *Subsystem Purity as an Enforcer of Entanglement*, *Phys. Rev. Lett.* **87**, 050401 (2001).
- [92] H. J. CARMICHAEL, *Photon Antibunching and Squeezing for a Single Atom in a Resonant Cavity*, *Phys. Rev. Lett.* **56**, 539 (1986).
- [93] M. HENNRICH, A. KUHN, and G. REMPE, *Transition from Antibunching to Bunching in Cavity QED*, *Phys. Rev. Lett.* **94**, 053604 (2005).
- [94] F. DUBIN, D. ROTTER, M. MUKHERJEE, C. RUSSO, J. ESCHNER, and R. BLATT, *Photon Correlation versus Interference of Single-Atom Fluorescence in a Half-Cavity*, *Phys. Rev. Lett.* **98**, 183003 (2007).
- [95] M. BRUNE, S. HAROCHE, J. M. RAIMOND, L. DAVIDOVICH, and N. ZAGURY, *Manipulation of photons in a cavity by dispersive atom-field coupling: Quantum-nondemolition measurements and generation of "Schrödinger cat" states*, *Phys. Rev. A* **45**, 5193 (1992).
- [96] G.-C. GUO and S.-B. ZHENG, *Generation of Schrödinger cat states via the Jaynes-Cummings model with large detuning*, *Phys. Lett. A* **223**, 332 (1996).
- [97] J. J. SLOSSER, P. MEYSTRE, and S. L. BRAUNSTEIN, *Harmonic Oscillator Driven by a Quantum Current*, *Phys. Rev. Lett.* **63**, 934 (1989).
- [98] M. WEIDINGER, B. T. H. VARCOE, R. HEERLEIN, and H. WALTHER, *Trapping States in the Micromaser*, *Phys. Rev. Lett.* **82**, 3795 (1999).
- [99] S. BRATTKE, B. T. H. VARCOE, and H. WALTHER, *Generation of Photon Number States on Demand via Cavity Quantum Electrodynamics*, *Phys. Rev. Lett.* **86**, 3534 (2001).
- [100] E. K. IRISH and K. SCHWAB, *Quantum measurement of a coupled nanomechanical resonator-Cooper-pair box system*, *Phys. Rev. B* **68**, 155311 (2003).
- [101] A. WALLRAFF, D. I. SCHUSTER, A. BLAIS, L. FRUNZIO, R.-S. HUANG, J. MAJER, S. KUMAR, S. M. GIRVIN, and R. J. SCHOELKOPF, *Strong coupling of a single photon to a superconducting qubit using circuit quantum electrodynamics*, *Nature* **431**, 162 (2004).
- [102] I. CHIORESCU, P. BERTET, K. SEMBA, Y. NAKAMURA, C. J. P. M. HARMANS, and J. E. MOOIJ,

- Coherent dynamics of a flux qubit coupled to a harmonic oscillator*, *Nature* **431**, 159 (2004).
- [103] N. HATAKENAKA and S. KURIHARA, *Josephson cascade micromaser*, *Phys. Rev. A* **54**, 1729 (1996).
- [104] C. C. GERRY, *Schrödinger cat states in a Josephson junction*, *Phys. Rev. B* **57**, 7474 (1998).
- [105] A. T. SORNBORGER, A. N. CLELAND, and M. R. GELLER, *Superconducting phase qubit coupled to a nanomechanical resonator: Beyond the rotating-wave approximation*, *Phys. Rev. A* **70**, 052315 (2004).
- [106] T. KEATING, C. H. BALDWIN, Y.-Y. JAU, J. LEE, G. W. BIEDERMANN, and I. H. DEUTSCH, *Arbitrary Dicke-State Control of Symmetric Rydberg Ensembles*, *Phys. Rev. Lett.* **117**, 213601 (2016).
- [107] J. LEE, M. J. MARTIN, Y. JAU, T. KEATING, I. H. DEUTSCH, and G. W. BIEDERMANN, *Demonstration of the Jaynes-Cummings ladder with Rydberg-dressed atoms*, *Phys. Rev. A* **95**, 041801(R) (2017).
- [108] F. MEIER and D. D. AWSCHALOM, *Spin-photon dynamics of quantum dots in two-mode cavities*, *Phys. Rev. B* **70**, 205329 (2004).
- [109] J. KASPRZAK, S. REITZENSTEIN, E. A. MULJAROV, C. KISTNER, C. SCHNEIDER, M. STRAUSS, S. HÖFLING, A. FORCHEL, and W. LANGBEIN, *Up on the Jaynes-Cummings ladder of a quantum-dot/microcavity system*, *Nature Materials* **9**, 304 (2010).
- [110] J. BASSET, D.-D. JARAUSCH, A. STOCKKLAUSER, T. FREY, C. REICHL, W. WEGSCHEIDER, T. M. IHN, K. ENSSLIN, and A. WALLRAFF, *Single-electron double quantum dot dipole-coupled to a single photonic mode*, *Phys. Rev. B* **88**, 125312 (2013).
- [111] A. de FREITAS, L. SANZ, and J. M. VILLAS-BOAS, *Coherent control of the dynamics of a single quantum-dot exciton qubit in a cavity*, *Phys. Rev. B* **95**, 115110 (2017).
- [112] J. M. FINK, M. GÖPPL, M. BAUR, R. BIANCHETTI, P. J. LEEK, A. BLAIS, and A. WALLRAFF, *Climbing the Jaynes-Cummings ladder and observing its nonlinearity in a cavity QED system*, *Nature* **454**, 315 (2008).
- [113] F. P. LAUSSY, E. DEL VALLE, M. SCHRAPP, A. LAUCHT, and J. J. FINLEY, *Climbing the Jaynes-Cummings ladder by photon counting*, *J. of Nanophotonics*, **6**, 061803 (2012).
- [114] T. NIEMCZYK, F. DEPPE, H. HUEBL, E. P. MENZEL, F. HOCKE, M. J. SCHWARZ, J. J. GARCIA-RIPOLL, D. ZUECO, T. HÜMMER, E. SOLANO, A. MARX, and R. GROSS, *Circuit quantum electrodynamics in the ultrastrong-coupling regime*, *Nature Physics* **6**, 772 (2010).
- [115] D. M. MEEKHOF, C. MONROE, B. E. KING, W. M. ITANO, and D. J. WINELAND, *Generation of Nonclassical Motional States of a Trapped Atom*, *Phys. Rev. Lett.* **76**, 1796 (1996).
- [116] D. LEIBFRIED, R. BLATT, C. MONROE, and D. WINELAND, *Quantum dynamics of single trapped ions*, *Rev. Mod. Phys.* **75**, 281 (2003).
- [117] J. I. CIRAC, A. S. PARKINS, R. BLATT, and P. ZOLLER, *"Dark" squeezed states of the motion of a trapped ion*, *Phys. Rev. Lett.* **70**, 556 (1993).
- [118] R. L. DE MATOS FILHO and W. VOGEL, *Even and Odd Coherent States of the Motion of a Trapped*

- Ion*, *Phys. Rev. Lett.* **76**, 608 (1996).
- [119] R. L. DE MATOS FILHO and W. VOGEL, *Nonlinear Coherent States*, *Phys. Rev. A* **54**, 4560 (1996).
 - [120] S.-C. GOU, J. STEINBACH, and P. L. KNIGHT, *Dark pair coherent states of the motion of a trapped ion*, *Phys. Rev. A* **54**, R1014(R) (1996).
 - [121] S.-C. GOU, J. STEINBACH, and P. L. KNIGHT, *Vibrational pair cat states*, *Phys. Rev. A* **54**, 4315 (1996).
 - [122] C. C. GERRY, S.-C. GOU, and J. STEINBACH, *Generation of motional $SU(1,1)$ intelligent states of a trapped ion*, *Phys. Rev. A* **55**, 630 (1997).
 - [123] C. MONROE, D. M. MEEKHOF, B. E. KING, and D. J. WINELAND, *A "Schrödinger Cat" Superposition State of an Atom*, *Science* **272**, 1131 (1996).
 - [124] C. C. GERRY, *Generation of Schrödinger cats and entangled coherent states in the motion of a trapped ion by a dispersive interaction*, *Phys. Rev. A* **55**, 2478 (1997).
 - [125] D. J. WINELAND, *Nobel Lecture: Superposition, entanglement, and raising Schrödinger's cat*, *Rev. Mod. Phys.* **85**, 1103 (2013).
 - [126] J. R. JOHANSSON, P. D. NATION, and F. NORI, *QuTiP: An open-source Python framework for the dynamics of open quantum systems*, *Comp. Phys. Comm.* **183**, 1760–1772 (2012).
 - [127] J. R. JOHANSSON, P. D. NATION, and F. NORI, *QuTiP 2: A Python framework for the dynamics of open quantum systems*, *Comp. Phys. Comm.* **184**, 1234 (2013).
 - [128] W. VOGEL, *Squeezing and anomalous moments in resonance fluorescence*, *Phys. Rev. Lett.* **67**, 2450 (1991).
 - [129] S. WALLENTOWITZ, R. L. DE MATOS FILHO, and W. VOGEL, *Determination of entangled quantum states of a trapped atom*, *Phys. Rev. A* **56**, 1205 (1997).
 - [130] E. AGUDELO, J. SPERLING, L. S. COSTANZO, M. BELLINI, A. ZAVATTA, and W. VOGEL, *Conditional Hybrid Nonclassicality*, *Phys. Rev. Lett.* **119**, 120403 (2017).
 - [131] J. SPERLING, E. AGUDELO, I. A. WALMSLEY, and W. VOGEL, *Quantum correlations in composite systems*, *J. Phys. B: At. Mol. Opt. Phys.* **50**, 134003 (2017).
 - [132] T. KIESEL and W. VOGEL, *Universal nonclassicality witnesses for harmonic oscillators*, *Phys. Rev. A* **85**, 062106 (2012).
 - [133] V. PARIGI, A. ZAVATTA, M. KIM, and M. BELLINI, *Probing Quantum Commutation Rules by Addition and Subtraction of Single Photons to/from a Light Field*, *Science* **317**, 1890 (2007).
 - [134] M. S. KIM, H. JEONG, A. ZAVATTA, V. PARIGI, and M. BELLINI, *Scheme for Proving the Bosonic Commutation Relation Using Single-Photon Interference*, *Phys. Rev. Lett.* **101**, 260401 (2008).
 - [135] A. ZAVATTA, V. PARIGI, M. S. KIM, H. JEONG, and M. BELLINI, *Experimental Demonstration of the Bosonic Commutation Relation via Superpositions of Quantum Operations on Thermal Light Fields*,

Phys. Rev. Lett. **103**, 140406 (2009).

Own Publications

The following publications have been prepared and published during my PhD studies. For each work my own contributions are declared. The page numbers refer to the attached manuscripts.

Published

- [I] F. KRUMM, J. SPERLING, and W. VOGEL, *Multitime correlation functions in nonclassical stochastic processes*, *Phys. Rev. A* **93**, 063843 (2016).
—F.K.: Derivation of the theoretical results, discussion, visualization of the results and preparation of the manuscript. page 54
- [II] F. KRUMM, W. VOGEL, and J. SPERLING, *Time-dependent quantum correlations in phase space*, *Phys. Rev. A* **95**, 063805 (2017).
—F.K.: Derivation of the theoretical results, discussion, visualization of the results and preparation of the manuscript. page 60
- [III] F. KRUMM and W. VOGEL, *Time-dependent nonlinear Jaynes-Cummings dynamics of a trapped ion*, *Phys. Rev. A* **97**, 043806 (2018).
—F.K.: Derivation of the theoretical results, discussion, visualization of the results and preparation of the manuscript. page 72

Submitted

- [IV] T. LIPFERT, F. KRUMM, M. I. KOLOBOV, and W. VOGEL, *Time ordering in the classically driven nonlinear Jaynes-Cummings model*, *Phys. Rev. A* **98**, 063817 (2018).
—F.K.: Complete creation of Sections II.A, IV, and VI. Contributions to the introduction, the conclusion and the preparation of the paper. page 83
- [V] F. KRUMM and W. VOGEL, *Anomalous quantum correlations in the motion of a trapped ion*, *Phys. Scr.* **94**, 085101 (2019).
—F.K.: Derivation of the theoretical results, discussion, visualization of the results and preparation of the manuscript. page 95

- [VI] F. KRUMM and W. VOGEL, *Accessing the non-equal-time commutators of a trapped ion*, *Phys. Rev. A* **99**, 063816 (2019).

—F.K.: Derivation of the theoretical results, discussion, visualization of the results and preparation of the manuscript. page 104

Multitime correlation functions in nonclassical stochastic processes

F. Krumm,^{*} J. Sperling, and W. Vogel*Arbeitsgruppe Theoretische Quantenoptik, Institut für Physik, Universität Rostock, D-18051 Rostock, Germany*

(Received 30 March 2016; published 27 June 2016)

A general method is introduced for verifying multitime quantum correlations through the characteristic function of the time-dependent P functional that generalizes the Glauber-Sudarshan P function. Quantum correlation criteria are derived which identify quantum effects for an arbitrary number of points in time. The Magnus expansion is used to visualize the impact of the required time ordering, which becomes crucial in situations when the interaction problem is explicitly time dependent. We show that the latter affects the multi-time-characteristic function and, therefore, the temporal evolution of the nonclassicality. As an example, we apply our technique to an optical parametric process with a frequency mismatch. The resulting two-time-characteristic function yields full insight into the two-time quantum correlation properties of such a system.

DOI: 10.1103/PhysRevA.93.063843

I. INTRODUCTION

The determination of nonclassical effects, such as squeezing [1] or entanglement [2,3], is a cumbersome, yet necessary task for employing these phenomena in future quantum technologies. However, most approaches are restricted to single-time quantum effects, albeit it is well known that there exist multitime correlations [4] and quantum effects. For instance, the fundamental photon antibunching experiment requires correlating two points in time [5].

To uncover the dynamics of nonclassicality, the treatment of multitime nonclassicality is therefore a desirable aspect to be studied. Based on the well-known Glauber-Sudarshan P function [6,7], an approach to infer space-time-dependent quantum correlations of radiation fields was introduced by defining a generalized P functional [8]. The resulting nonclassicality criteria yield a general insight into multitime quantum correlation functions beyond the photon antibunching effect.

Other characterization techniques have been introduced by Leggett and Garg [9]. They prove that temporal correlations can violate Bell-like equalities based on assumptions of macroscopic realism and noninvasive measurements. Such a test was recently applied to multilevel systems [10]. Another approach is the consideration of bits of classical communication that are required to simulate a temporal correlation function of a multilevel system [11]. Considering other types of correlation functions, one can study the temporal dynamics of a coupled optomechanical system [12].

To keep the close relation between the treatment of the P function and the P functional, we will consider its Fourier transform, i.e., its characteristic function. For a single point in time, it is known that the characteristic function yields necessary and sufficient nonclassicality certifiers [13], which can be directly applied to measurements [14,15]. Moreover, the characteristic function method can be related to moment-based techniques [16] to formulate unified nonclassicality criteria [17].

In the present contribution, we generalize the nonclassicality criteria in terms of characteristic functions to identify multitime nonclassical correlations. The derived conditions lead to

an infinite hierarchy of necessary and sufficient nonclassicality probes for temporal quantum correlations in radiation fields. In general, the investigation of temporal correlations requires appropriate techniques, in particular, when the interaction problem under study is explicitly time dependent. For this purpose, we will apply the Magnus expansion of the unitary time-evolution operator to analyze the impact of time ordering on the evolution of nonclassicality. As a fundamental example, we provide a detailed study of the quantum correlations of a parametric process with a frequency mismatch.

The paper is structured as follows. In Sec. II we recapitulate the concept of multitime nonclassicality. Necessary and sufficient conditions for time-dependent quantum correlations are derived in terms of multi-time-characteristic functions in Sec. III. Section IV deals with the application of the methods to a parametric process with frequency mismatch. The corresponding time-dependent quantum effects are uncovered in Sec. V. A summary and some conclusions are given in Sec. VI.

II. MULTITIME NONCLASSICALITY

A well-established definition of nonclassicality of a radiation field is related to the Glauber-Sudarshan P function [6,7,18–20],

$$P(\alpha) = \langle : \hat{\delta}(\hat{a} - \alpha) : \rangle. \quad (1)$$

Herein, $\hat{\delta}$ denotes the operator-valued δ distribution, and \hat{a} is the bosonic annihilation operator of the radiation mode under study. The prescription $: \dots :$ orders creation operators to the left of annihilation operators. On this basis, a quantum state is referred to as nonclassical if the P function fails to have the properties of a classical probability density [18,19]. That is, $P(\alpha)$ cannot be described by the classical theory of light. Note that a generalization to multimode fields is straightforward.

In correlation measurements, observables become relevant which depend on a set $\{t_i\}_{i=1}^k$ of points in time. For example, two-time intensity correlation functions are recorded in photon antibunching experiments [5]. Higher-order correlations of general field operators describe the full quantum statistics of the radiation field in chosen space-time points [8,21]. Thus, to completely cover the multitime nonclassicality, we consider

^{*}fabian.krumm@uni-rostock.de

the P functional [8],

$$P[\{\alpha(t_i); t_i\}_{i=1}^k] = \left\langle \circ \prod_{i=1}^k \hat{\delta}(\hat{a}(t_i) - \alpha(t_i)) \circ \right\rangle. \quad (2)$$

The symbol $\circ \cdots \circ$ represents the normal- and time-ordering prescriptions. Due to the latter, creation (annihilation) operators are sorted with increasing (decreasing) time arguments from left to right [20] as it occurs in the photocounting theory [22].

With the introduced functional, the normally and time-ordered expectation value of an arbitrary observable $\hat{O} = \hat{O}(\hat{a}(t_1), \dots, \hat{a}(t_k))$, which depends on the bosonic creation and annihilation operators at different times, can be written as

$$\begin{aligned} & \langle \circ \hat{O}(\hat{a}(t_1), \dots, \hat{a}(t_k)) \circ \rangle \\ &= \int d^2\alpha_1 \cdots \int d^2\alpha_k O(\alpha_1, \dots, \alpha_k) P[\{\alpha_i; t_i\}_{i=1}^k], \end{aligned} \quad (3)$$

where we identified $\alpha_i = \alpha(t_i)$. Using Eqs. (2) and (3), multitime nonclassicality can be defined as follows [8]: A radiation field shows nonclassical correlation properties if and only if

$$\exists \hat{f}: \langle \circ \hat{f}^\dagger \hat{f} \circ \rangle < 0. \quad (4)$$

Here, $\hat{f} = \hat{f}(\hat{a}(t_1), \dots, \hat{a}(t_k))$ connotes an operator function of the bosonic creation and annihilation operators at different times. Note that these nonclassicality conditions include the ones in Refs. [18,19] for a single time.

III. CHARACTERISTIC FUNCTIONS AND QUANTUM CORRELATIONS

A. Space-time nonclassicality criteria

The Fourier transform of the multitime P functional in Eq. (2) defines the corresponding characteristic function,

$$\Phi(\{\beta_i; t_i\}_{i=1}^k) = \langle \circ \hat{D}(\{\beta_i; t_i\}_{i=1}^k) \circ \rangle. \quad (5)$$

Here, the multi-time-displacement operator reads as

$$\hat{D}(\{\beta_i; t_i\}_{i=1}^k) = \prod_{i=1}^k \exp[\beta_i \hat{a}(t_i)^\dagger - \beta_i^* \hat{a}(t_i)]. \quad (6)$$

Characteristic functions are experimentally accessible, for example, via balanced homodyne correlation measurements [21] of the multi-time-characteristic function (5). In the classical probability theory of stochastic processes, the coherent amplitudes $\{\alpha_i(t_i)\}_{i=1}^k$ define a set of random variables, distributed according to the classical analog of the P functional (2). Their characteristic function (5) is a unique characterization in Fourier-transformed phase space, given by the variables $\{\beta_i; t_i\}_{i=1}^k$. As the P function at a single time can be highly singular, the same holds true for the general multitime functional. However, the characteristic function is always well behaved, which will also be discussed in the continuation of this paper and, therefore, much better suited for uncovering nonclassical features.

We may expand each operator function in Eq. (4) in terms of a Fourier series,

$$\hat{f} = \sum_{j=1}^O f_j \hat{D}(\{\beta_{i,j}; t_i\}_{i=1}^k) \quad (7)$$

for some complex amplitudes (index j) at different points in time (index i), $\beta_{i,j}$, and a given order O . This expansion (7) is the multitime generalization of the single-time case [16,23]. Inserting Eq. (7) into Eq. (4) and using the definitions in Eqs. (5) and (6), we obtain

$$\begin{aligned} 0 > \langle \circ \hat{f}^\dagger \hat{f} \circ \rangle &= \sum_{l,j=1}^O f_l^* f_j \Phi(\{\beta_{i,l} - \beta_{i,j}; t_i\}_{i=1}^k) \\ &= \mathbf{f}^\dagger \Phi(\{t_i\}_{i=1}^k) \mathbf{f}, \end{aligned} \quad (8)$$

where the latter vector-matrix notion consists of the matrix $\Phi(\{t_i\}_{i=1}^k) = [\Phi(\{\beta_{i,l} - \beta_{i,j}; t_i\}_{i=1}^k)]_{l,j=1}^O$ and the coefficient vector $\mathbf{f} = (f_1, \dots, f_O)^T$.

Applying Bochner's theorem for classical probabilities [24], condition (8) certifies that the characteristic function (5) cannot be interpreted as the Fourier transform of the classical analog of the P functional (2). Moreover, Bochner's conditions are necessary and sufficient if all orders O and all $\beta_{i,j}$ are considered. Applying Sylvester's criterion and in analogy to Ref. [13], we get a multitime generalization of hierarchies of nonclassicality conditions. Namely, $\Phi(\{\beta_i; t_i\}_{i=1}^k)$ is the characteristic function of a nonclassical P functional if and only if

$$\exists O \in \mathbb{N}, \quad [\{\beta_{i,j}\}_{i=1}^k]_{j=1}^O : \det_O[\Phi(\{t_i\}_{i=1}^k)] < 0. \quad (9)$$

Herein, \det_O denotes the determinant of the order O . As $\det_1[\Phi(\{t_i\}_{i=1}^k)] = \Phi(\{0; t_i\}_{i=1}^k) = 1$ (the normalization of P), the lowest-order nontrivial nonclassicality criterion is obtained for $O = 2$. It reads

$$0 > \det_2[\Phi(\{t_i\}_{i=1}^k)] = 1 - |\Phi(\{\beta_{i,2} - \beta_{i,1}; t_i\}_{i=1}^k)|^2. \quad (10)$$

This lowest-order criterion only provides a sufficient condition for nonclassicality, whereas the general nonclassicality condition (9) is necessary and sufficient if all orders O are considered. Again, for one point in time, we recover the single-time nonclassicality condition established in Ref. [25].

Let us relate the definition of nonclassicality of multiple points in time, i.e., the functional in Eq. (2) does not describe a classical stochastic process [8] with the derived criteria in inequality (9). The here introduced method is based on the characteristic function. In contrast to the P functional, this function is always well behaved and does not exhibit singularities which are often present in the Glauber-Sudarshan representation. As the characteristic function includes all information about the quantum systems for the considered times, our approach can identify all nonclassical features which are present in the P functional. In this sense, our method is equivalent to the approach in Ref. [8], which, however, formulates the conditions for nonclassical correlations in terms of time-dependent correlation functions. Alternatively, the here presented technique relies on a regular phase-space distribution in terms of the characteristic function and the corresponding criteria in (9).

B. Time evolution and time ordering

In order to rigorously study the propagation of quantum correlations in time, let us formulate the dynamic behavior of quantum systems. The most general way to implement the propagation in time is formulated in terms of the unitary time-evolution operator $\hat{\mathcal{U}}(t)$. For an explicitly time-dependent Hamiltonian $\hat{H}(t)$, the latter is given by

$$\hat{\mathcal{U}}(t) = \mathcal{T} \exp \left[-\frac{i}{\hbar} \int_0^t dt' \hat{H}(t') \right], \quad (11)$$

where \mathcal{T} denotes exclusively the time-ordering prescription, which is required if $[\hat{H}(t_1), \hat{H}(t_2)] \neq 0$ for $t_1 \neq t_2$. As such a formal solution is not very helpful, one can apply the Dyson expansion $\hat{\mathcal{U}}(t) = \hat{1} - i\hbar^{-1} \int_0^t dt_1 \hat{H}(t_1) - \hbar^{-2} \int_0^t dt_1 \int_0^{t_1} dt_2 \hat{H}(t_1) \hat{H}(t_2) + \dots$, which resembles a time-ordered Taylor expansion of the exponential function in (11). Alternatively, this problem can be handled by the Magnus expansion [26,27], which yields the time-evolution operator in the form

$$\hat{\mathcal{U}}(t) = \exp \left[\sum_{n=1}^{n_{\max}} \hat{\Omega}_n(t) \right], \quad (12)$$

with $\hat{\Omega}_n(t)$ being the n th Magnus order and for $n_{\max} = \infty$, the true evolution is recovered. In contrast to the Dyson series, the Magnus expansion is unitary in each order. The first two orders read as

$$\begin{aligned} \hat{\Omega}_1(t) &= -\frac{i}{\hbar} \int_0^t dt_1 \hat{H}(t_1), \\ \hat{\Omega}_2(t) &= -\frac{1}{2\hbar^2} \int_0^t dt_1 \int_0^{t_1} dt_2 [\hat{H}(t_1), \hat{H}(t_2)]. \end{aligned} \quad (13)$$

Hence, nonequal time commutators of the Hamiltonian $\hat{H}(t)$ have to be evaluated. The first-order approximation (12) $n_{\max} = 1$ is equivalent to disregarding the time-ordering \mathcal{T} in Eq. (11). Higher Magnus orders, $\hat{\Omega}_n(t)$ with $n > 1$, can be referred to as *time-ordering corrections*.

Thus, an effect of the time ordering can be observed if the higher-order corrections are nonzero. In particular for the second order, this means that the Hamiltonians of the system for different times do not commute, see Eq. (13). The Magnus expansion and the hierarchy of introduced nonclassicality criteria (9)—including the special case (10)—enable us to directly investigate the impact of time-ordering effects on the nonclassicality.

IV. APPLICATION TO PARAMETRIC PROCESSES

As a fundamental example, we study the particular process of degenerate parametric down-conversion for a strong classical pump field in the following. In the interaction picture, the time-dependent interaction Hamiltonian reads as

$$\hat{H}_{\text{int}}(t) = \hbar\kappa [e^{-i\delta t} \hat{a}^{\dagger 2} + e^{i\delta t} \hat{a}^2], \quad (14)$$

where κ denotes the coupling constant and $\delta = \omega_p - 2\omega_a$ is a nonlinear frequency mismatch between the pump frequency ω_p and the signal frequency ω_a . For a perfectly matched pump, $\delta = 0$, Eq. (11) without the time ordering already gives the exact solution.

A related system has been studied recently [28,29]. There, a two-mode Hamiltonian was considered with the frequency spectrum using the Magnus expansion. In Ref. [30], the authors have also studied parametric down-conversion with respect to time-ordering corrections. In contrast to those works, we aim at demonstrating the impact of time ordering on the continuous evolution of quantum phenomena.

Equivalent to the time-evolution operator in Eq. (11), one can establish the coupled equation of motion in the interaction picture for the signal field operators \hat{a} and \hat{a}^\dagger . This reads as

$$\begin{aligned} \frac{d}{dt} \begin{pmatrix} \hat{a}(t) \\ \hat{a}(t)^\dagger \end{pmatrix} &= \begin{pmatrix} 0 & -2i\kappa e^{-i\delta t} \\ 2i\kappa e^{i\delta t} & 0 \end{pmatrix} \begin{pmatrix} \hat{a}(t) \\ \hat{a}(t)^\dagger \end{pmatrix} \\ &= \mathbf{M}(t) \begin{pmatrix} \hat{a}(t) \\ \hat{a}(t)^\dagger \end{pmatrix}. \end{aligned} \quad (15)$$

Now, the formal solution in Eq. (11) is given by $-i\hbar^{-1} \hat{H}(t) \mapsto \mathbf{M}(t)$ which also replaces the operator $\hat{\mathcal{U}}(t)$ by the unitary matrix $\mathbf{U}(t)$. This approach allows us to express the time evolution in terms of matrices which, then, can be directly applied to \hat{a} and \hat{a}^\dagger . In the same way $[\hat{H}(t_1), \hat{H}(t_2)] \neq 0$ translates to noncommuting matrices $\mathbf{M}(t_1)$ and $\mathbf{M}(t_2)$.

For a rigorous formulation of our treatment, one has to mention the convergence radius of the Magnus series. The series converges if the inequality,

$$\int_0^t ds \|\mathbf{M}(s)\|_2 < \pi \quad (16)$$

is fulfilled [27]. The convergence radius is the supreme value for which this inequality is satisfied. Using Eq. (15), one obtains the spectral norm as $\|\mathbf{M}(s)\|_2 = 2\kappa$. For convenience we introduce the dimensionless time $\tau = 2\kappa t/\pi$. Thus, convergence is assured for $\tau < 1$. To access times $\tau \geq 1$, one can subdivide the evolution in adjacent time intervals, known as the Euler method.

For our studied model, the Magnus expansion is completely determined by τ and δ/κ . This means that the time evolution is given by the ratio of the mismatch and the coupling constant as well as the characteristic system time $\pi/(2\kappa)$. Using the matrix $\mathbf{M}(t)$ in Eq. (15), we explicitly show that each Magnus order has the form

$$\mathbf{\Omega}_n(\tau) = \begin{cases} i|C_n| \begin{pmatrix} -1 & 0 \\ 0 & 1 \end{pmatrix} & \text{for } n \text{ even,} \\ |S_n| \begin{pmatrix} 0 & e^{i\varphi_n} \\ e^{-i\varphi_n} & 0 \end{pmatrix} & \text{for } n \text{ odd,} \end{cases} \quad (17)$$

where we use τ instead of the time t for parametrization. The quantities $|C_n|$, $|S_n|$, and φ_n are obtained numerically, for details see Ref. [27].

With Eq. (17), the time-evolution matrix reads as

$$\begin{aligned} \mathbf{U}(\tau) &= \exp \left[\sum_n \mathbf{\Omega}_n(\tau) \right] = \exp[\mathbf{\Omega}(\tau)] \\ &= \cosh(p) \begin{pmatrix} 1 & 0 \\ 0 & 1 \end{pmatrix} + \frac{\sinh(p)}{p} \begin{pmatrix} -iC & S \\ S^* & iC \end{pmatrix}, \end{aligned} \quad (18)$$

with $C = \sum_{n \text{ even}} |C_n|$, $S = \sum_{n \text{ odd}} |S_n| e^{i\varphi_n}$, and $p = [-\det \mathbf{\Omega}(\tau)]^{1/2} = [|S|^2 - C^2]^{1/2}$. The nondiagonal entries of $\mathbf{U}(\tau)$ correspond to a map $\hat{a} \mapsto \hat{a}^\dagger$ (and $\hat{a}^\dagger \mapsto \hat{a}$). Such a transformation yields squeezing. The diagonal elements can

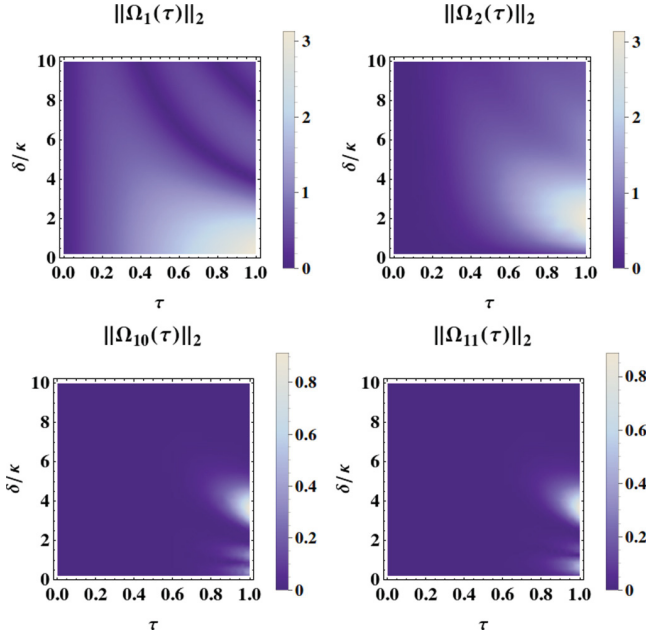


FIG. 1. Density plots of the spectral norm of different Magnus orders $\|\Omega_n(\tau)\|_2$ for $n = 1, 2, 10, 11$. The time-ordering corrections are most significant at values of τ and δ/κ , where $\|\Omega_n(\tau)\|_2$ for $n > 1$ attains its largest values.

be related to rotations in phase space, which is a classical effect.

An additional advantage of the dynamical representation in terms of Eq. (15) and its Magnus expansion is the possibility of analyzing non-equal-time-commutation relations of the fundamental bosonic annihilation (or creation) operators,

$$[\hat{a}(\tau), \hat{a}(\tau + \Delta\tau)] = \mathcal{U}_{11}(\tau)\mathcal{U}_{12}(\tau + \Delta\tau) - \mathcal{U}_{12}(\tau)\mathcal{U}_{11}(\tau + \Delta\tau), \quad (19)$$

where the components of the evolution operator are used $\mathcal{U}(\tau) = (\mathcal{U}_{ij}(\tau))_{i,j=1}^2$. The commutator (19) is, in general, nonzero for time-dependent Hamiltonians and unequal times $\Delta\tau \neq 0$. Such commutation relations for different points in time play a fundamental role in multitime correlation functions, see Ref. [20] for an overview.

The impact of the different Magnus orders (17) is visualized in Fig. 1 by showing the spectral norm of different contributions $\|\Omega_n(\tau)\|_2$. A large value of this matrix norm relates to a more significant contribution to the evolution operator (18). The plot $n = 1$ describes the case without any time ordering. The norms for $n > 1$ are maximal in the range of $1 \leq \delta/\kappa \leq 5$. Thus, the strongest time-ordering corrections are expected to occur in this region. In particular, we will use the value $\delta/\kappa \approx 3.18$ for the following discussions.

V. TIME-DEPENDENT QUANTUM EFFECTS

After discussing the modeling of the evolution with time-dependent Hamiltonians, let us come back to the verification of nonclassicality. According to our criterion (10), we are able to verify nonclassical multitime correlations if $|\Phi(\{\beta_{i,2} - \beta_{i,1}; t_i\}_{i=1}^k)|^2 > 1$. Let us apply this test to our considered

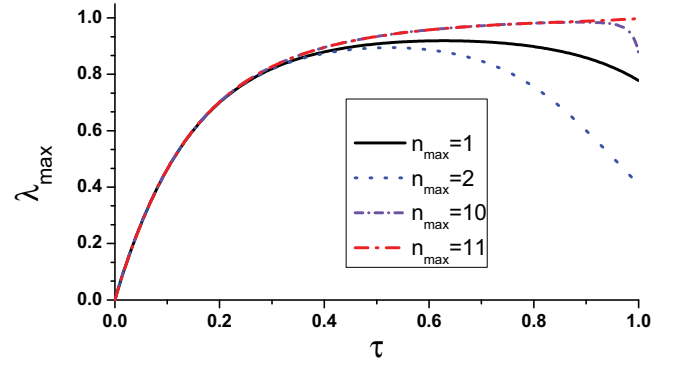


FIG. 2. λ_{\max} , cf. Eq. (20), for $\Omega(\tau) = \sum_{n=1}^{n_{\max}} \Omega_n(\tau)$ and $\delta/\kappa \approx 3.18$ in dependence on the rescaled time τ . A positive λ_{\max} verifies nonclassicality. The influence of time ordering is clearly visible in the contributions of the higher-order Magnus terms $n_{\max} > 1$.

system. Again, we will replace the times t_i with the scaled ones $\tau_i = 2\kappa t_i/\pi$.

First, we study the evolution of the nonclassicality by considering a single time $k = 1$ for discussing the time-ordering corrections. Initially, the system is assumed to be in the vacuum state. Thus, after a principal axis transformation of $\beta = \beta_{1,2} - \beta_{1,1}$ to a rotated complex amplitude γ , we can write the modulus of the characteristic function (5) in the form

$$|\Phi(\gamma; \tau)|^2 = e^{\lambda(\text{Re } \gamma)^2 + \mu(\text{Im } \gamma)^2}. \quad (20)$$

If the maximal value $\lambda_{\max} = \lambda_{\max}(\tau) = \max(\lambda, \mu)$ is positive, then the characteristic function exceeds one.

The results for different Magnus orders are given in Fig. 2, where λ_{\max} is plotted as a function of τ . One can see the time-ordering effects in the evolution for $n_{\max} > 1$, which significantly affect the rising behavior of the characteristic function and, therefore, the nonclassical character of the corresponding state. Note that times close to the convergence radius $\tau = 1$ show oscillations when comparing even and odd n_{\max} values because of the alternating form of the contributions $\Omega_n(\tau)$ in Eq. (17).

Second, we study two-time nonclassical correlations. We follow the same approach, such as in the single-time case, i.e., a principal axis transformation: $(\beta_{1,2} - \beta_{1,1}, \beta_{2,2} - \beta_{2,1}) \mapsto (\gamma_1, \gamma_2)$. Consequently, the two-time characteristic function for the nonclassicality condition (10) reduces to a form similar to (20),

$$|\Phi(\{\gamma_i; \tau_i\}_{i=1}^2)|^2 = \exp\left(\sum_{i=1}^2 [\lambda_i(\text{Re } \gamma_i)^2 + \mu_i(\text{Im } \gamma_i)^2]\right). \quad (21)$$

The modulus square of the two-time characteristic function is shown in Fig. 3. Note that due to the time-ordering prescription in Eq. (5), one has to consider actually two scenarios $\tau_1 \geq \tau_2$ and $\tau_2 \geq \tau_1$. The quantity (21) depends on two complex parameters (γ_1, γ_2) . We restricted ourselves to a unit circle ($|\gamma_1|^2 + |\gamma_2|^2 = 1$) and selected phase values ($\arg \gamma_1 = \arg \gamma_2 = \pi/2$), which maximize the function (21). As the two-time-characteristic function is larger than one, we directly uncover two-time quantum correlations for all times, except for $\tau_{1,2} = 0$. It is important to mention that

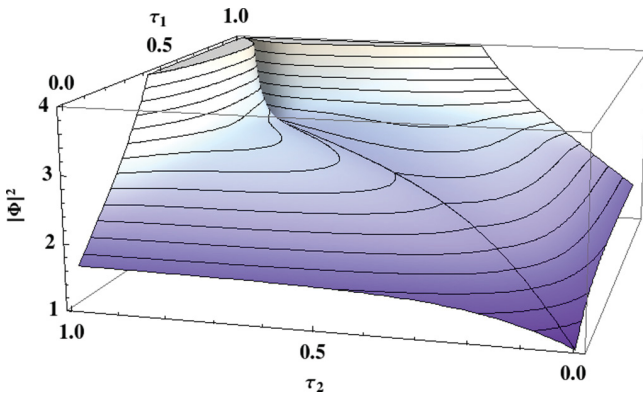


FIG. 3. We show $|\Phi|^2 \equiv |\Phi(\{\gamma_i; \tau_i\}_{i=1}^2)|^2$. As the value of one is exceeded for all times $\tau_{1,2} \neq 0$, the state is clearly two-time quantum correlated. We included all Magnus orders up to $n_{\max} = 11$ in the evolution for $\delta/\kappa \approx 3.18$.

the corresponding P functional will be highly singular as an inverse Fourier transform of Φ is only possible in terms of singular distributions as Eq. (21) is an unbounded function for $\max\{\lambda_1, \lambda_2, \mu_1, \mu_2\} > 0$. Our results clearly visualize the two-time quantum correlations of our system.

Finally, another advantage of our approaches is the fact that measurement schemes, e.g., as proposed in Ref. [21], can be implemented which enables us to sample multi-time-characteristic functions of arbitrary orders. This allows one to directly implement our nonclassicality criteria (9). Thus, quantum correlations between an arbitrary number of points in time are experimentally accessible and reconstructible.

VI. CONCLUSIONS

To summarize, we presented techniques for identifying nonclassical stochastic processes in radiation fields in terms of

characteristic functions. The latter are the Fourier transforms of the multi-time-dependent P functional, generalizing the Glauber-Sudarshan representation. We constructed a hierarchy of necessary and sufficient criteria for the characteristic functions that can be applied to infer nonclassical correlations between an arbitrary number of points in time. The influence of the time ordering on the evolution of nonclassicality has been studied via the Magnus expansion.

To demonstrate the applicability, we studied a degenerated parametric-down-conversion process with a frequency mismatch. We identified time intervals where the time-ordering corrections have the most significant impact for our time-dependent Hamiltonian. Whenever the temporal evolution of nonclassicality is studied in the presence of a Hamiltonian not commuting with itself at different points in time, this influences the nonclassicality of the system. Based on the characteristic function, we studied this temporal behavior of the nonclassicality and demonstrated nonclassical correlations between two points in time.

Our method can be generalized in a straightforward way to simultaneously study multimode and multitime correlations. Moreover, the decomposition of the light field into a free-field and a source-field contribution allows one to study nonclassical processes in light-matter interactions. Especially the investigation of non-equal-time commutation relations—including the description of a dynamic source—is an interesting problem for future studies. Eventually, this will lead to a deeper understanding of the nonclassical evolution of quantum systems and their resulting nonclassical correlations.

ACKNOWLEDGMENTS

This work has received funding from the Deutsche Forschungsgemeinschaft through SFB 652 and the European Union's Horizon 2020 research and innovation program under Grant Agreement No. 665148.

-
- [1] D. F. Walls, Squeezed states of light, *Nature (London)* **306**, 141 (1983).
 - [2] A. Einstein, B. Podolsky, and N. Rosen, Can quantum-mechanical description of physical reality be considered complete? *Phys. Rev.* **47**, 777 (1935).
 - [3] E. Schrödinger, Die gegenwärtige Situation in der Quantenmechanik, *Naturwiss.* **23**, 807 (1935).
 - [4] Y. Aharonov, S. Popescu, J. Tollaksen, and L. Vaidman, Multiple-time states and multiple-time measurements in quantum mechanics, *Phys. Rev. A* **79**, 052110 (2009).
 - [5] H. J. Kimble, M. Dagenais, and L. Mandel, Photon Antibunching in Resonance Fluorescence, *Phys. Rev. Lett.* **39**, 691 (1977).
 - [6] R. J. Glauber, Coherent and incoherent states of the radiation field, *Phys. Rev.* **131**, 2766 (1963).
 - [7] E. C. G. Sudarshan, Equivalence of Semiclassical and Quantum Mechanical Descriptions of Statistical Light Beams, *Phys. Rev. Lett.* **10**, 277 (1963).
 - [8] W. Vogel, Nonclassical Correlation Properties of Radiation Fields, *Phys. Rev. Lett.* **100**, 013605 (2008).
 - [9] A. J. Leggett and A. Garg, Quantum Mechanics Versus Macroscopic Realism: Is the Flux there when Nobody Looks? *Phys. Rev. Lett.* **54**, 857 (1985).
 - [10] C. Budroni and C. Emary, Temporal Quantum Correlations and Leggett-Garg Inequalities in Multilevel Systems, *Phys. Rev. Lett.* **113**, 050401 (2014).
 - [11] S. Brierley, A. Kosowski, M. Markiewicz, T. Paterek, and A. Przysieszna, Nonclassicality of Temporal Correlations, *Phys. Rev. Lett.* **115**, 120404 (2015).
 - [12] S. K. Singh and S. V. Muniandy, Temporal dynamics and nonclassical photon statistics of quadratically coupled optomechanical systems, *Int. J. Theor. Phys.* **55**, 287 (2016).
 - [13] T. Richter and W. Vogel, Nonclassicality of Quantum States: A Hierarchy of Observable Conditions, *Phys. Rev. Lett.* **89**, 283601 (2002).
 - [14] A. I. Lvovsky and J. H. Shapiro, Nonclassical character of statistical mixtures of the single-photon and vacuum optical states, *Phys. Rev. A* **65**, 033830 (2002).

- [15] A. Mari, K. Kieling, B. M. Nielsen, E. S. Polzik, and J. Eisert, Directly Estimating Nonclassicality, *Phys. Rev. Lett.* **106**, 010403 (2011).
- [16] E. Shchukin, T. Richter, and W. Vogel, Nonclassicality criteria in terms of moments, *Phys. Rev. A* **71**, 011802(R) (2005).
- [17] S. Ryl, J. Sperling, E. Agudelo, M. Mraz, S. Köhnke, B. Hage, and W. Vogel, Unified nonclassicality criteria, *Phys. Rev. A* **92**, 011801(R) (2015).
- [18] U. M. Titulaer and R. J. Glauber, Correlation functions for coherent fields, *Phys. Rev.* **140**, B676 (1965).
- [19] L. Mandel, Non-classical states of the electromagnetic field, *Phys. Scr.*, **T12**, 34 (1986).
- [20] W. Vogel and D.-G. Welsch, *Quantum Optics*, 3rd ed. (Wiley-VCH, New York, 2006)
- [21] E. Shchukin and W. Vogel, Universal Measurement of Quantum Correlations of Radiation, *Phys. Rev. Lett.* **96**, 200403 (2006).
- [22] P. L. Kelley and W. H. Kleiner, Theory of electromagnetic field measurement and photoelectron counting, *Phys. Rev.* **136**, A316 (1964).
- [23] E. V. Shchukin and W. Vogel, Nonclassicality moments and their measurements, *Phys. Rev. A* **72**, 043808 (2005).
- [24] S. Bochner, Monotone funktionen, stieltjessche integrale und harmonische analyse, *Math. Ann.* **108**, 378 (1933).
- [25] W. Vogel, Nonclassical States: An Observable Criterion, *Phys. Rev. Lett.* **84**, 1849 (2000).
- [26] W. Magnus, On the exponential solution of differential equations for a linear operator, *Comm. Pure and Appl. Math.* **7**, 649 (1954).
- [27] S. Blanes, F. Casas, J. A. Oteo, and J. Ros, The Magnus expansion and some of its applications, *Phys. Rep.* **470**, 151 (2009).
- [28] N. Quesada and J. E. Sipe, Effects of time ordering in quantum nonlinear optics, *Phys. Rev. A* **90**, 063840 (2014).
- [29] N. Quesada and J. E. Sipe, Time-Ordering Effects in the Generation of Entangled Photons Using Nonlinear Optical Processes, *Phys. Rev. Lett.* **114**, 093903 (2015).
- [30] A. Christ, B. Brecht, W. Maurer, and C. Silberhorn, Theory of quantum frequency conversion and type-II parametric down-conversion in the high-gain regime, *New J. Phys.* **15**, 053038 (2013).

Time-dependent quantum correlations in phase space

F. Krumm* and W. Vogel

Arbeitsgruppe Theoretische Quantenoptik, Institut für Physik, Universität Rostock, D-18059 Rostock, Germany

J. Sperling

Clarendon Laboratory, University of Oxford, Parks Road, Oxford OX1 3PU, United Kingdom

(Received 8 February 2017; published 6 June 2017)

General quasiprobabilities are introduced to visualize time-dependent quantum correlations of light in phase space. They are based on the generalization of the Glauber-Sudarshan P function to a time-dependent P functional [W. Vogel, *Phys. Rev. Lett.* **100**, 013605 (2008)], which fully describes temporal correlations of radiation fields on the basis of continuous phase-space distributions. This approach is nontrivial, as the P functional itself is highly singular for many quantum states and nonlinear processes. In general, it yields neither a well-behaved nor an experimentally accessible description of quantum stochastic processes. Our regularized version of this multitime-dependent quasiprobability is a smooth function and applies to stronger divergences compared to the single-time and multimode scenario. The technique is used to characterize an optical parametric process with frequency mismatch and a strongly nonlinear evolution of the quantized center-of-mass motion of a trapped ion. A measurement scheme, together with a sampling approach, is provided which yields direct experimental access to the regularized P functional from measured data.

DOI: 10.1103/PhysRevA.95.063805

I. INTRODUCTION

Nonclassical effects, such as photon antibunching [1], squeezing [2–6], and entanglement [7,8], have been known for many decades. Their verification, classification, quantification, and application remain challenging tasks of modern quantum optics. For the distinction of genuine quantum interferences from classical optical effects, two major techniques have been established. The first one is the application of various types of nonclassicality criteria based on observable quantities. The second one is the investigation of different kinds of phase-space distributions. The implementation of each of these techniques brings along its own characteristic advantages and challenges.

A variety of nonclassicality criteria are suitable for different applications, depending on the quantum system or effect under consideration. Some of them consist of an infinite hierarchy of necessary and sufficient nonclassicality probes. Examples are criteria based on characteristic functions, moments, and their combination [9–11]. Yet, the full characterization of quantum effects requires the study of all orders of these hierarchies. Even though this is impossible in general, these methods provide a plethora of sufficient nonclassicality conditions to successfully identify various types of quantum effects; cf. Ref. [12] for an overview. However, low-order criteria may fail to uncover the nonclassical character of particular quantum states.

In such cases, the investigation of phase-space distributions may be advantageous. Prominent examples are the Husimi Q function [13], the Wigner function [14], the Glauber-Sudarshan P function [15,16], their unification in terms of s -parameterized quasiprobability distributions [17], and the general distributions introduced by Agarwal and Wolf [18]. Nonclassicality is commonly defined via comparison of such

quasiprobabilities with their classical counterparts. The widely accepted definition of nonclassicality by Titulaer and Glauber relies on the P function [19,20]: Whenever P cannot be interpreted as a classical probability density, i.e., when it contains negativities, the state is referred to as nonclassical. Hence, this very quasiprobability will be our benchmark to identify quantum effects. However, the study of the P function can become a cumbersome task, as it is highly singular for many quantum states [21]. In general, an experimental reconstruction of the P function is only possible if a proper regularization procedure is introduced [22]. Based on such a technique, one can also implement a direct sampling approach for the regularized P functions [23], which yields direct access to the full information on general quantum states.

The P function itself represents the full information on the quantum state $\hat{\rho}$ of a radiation mode at an arbitrary but fixed time in a diagonal representation,

$$\hat{\rho} = \int d^2\alpha P(\alpha) |\alpha\rangle\langle\alpha|, \quad (1)$$

with coherent states $|\alpha\rangle$ with complex amplitudes α . Yet, correlations between multiple points in time (i.e., temporal correlations) play a fundamental role in quantum optics and quantum information theory. For instance, the early demonstration of the quantum nature of light via photon antibunching was based on the detection of two-time intensity correlation properties [1]. Also, the photocounting theory depends on multitime correlation functions of the light field to be measured [24]. It is noteworthy that the corresponding field correlations are normal and time ordered. In particular, this is relevant when the interaction dynamics is described by an explicitly time-dependent Hamiltonian or when the radiation field is emitted by atomic sources. Recently, the Keldysh-ordered full counting statistics has been studied in the context of negativities of quasiprobabilities [25,26].

Early studies of parametric processes in terms of time-dependent correlation functions were reported by Mollow [27].

*fabian.krumm@uni-rostock.de

Temporal correlations have also been studied in the quantum dynamical theory of the fluctuations in a degenerate optical parametric oscillator [28]. More recently, the multimode parametric dynamics has been further investigated by including time-ordering effects [29]. For an explicitly time-dependent parametric interaction, temporal quantum correlations have also been considered in terms of characteristic functions [30].

Another field where time ordering is important is the passive filtering of light emitted from atomic sources. A general theory for the effects of passive optical systems on quantum light was developed in Ref. [31]. In this context, a careful treatment of non-equal-time commutators is crucial. Although such commutation rules are not explicitly known in general, their effects can be handled in a closed form; for details see Chap. 2.7 in Ref. [32]. Yet another example stems from the spectral filtering of quantum light from atomic sources for which spectral squeezing [33] and spectral intensity correlations [34,35] of the atomic resonance fluorescence have been studied to some extent.

Temporal correlations are also considered in the framework of the Leggett-Garg inequalities [36,37]—sometimes referred to as *temporal Bell inequalities*. Recently, the latter were extended to continuous-variable systems placed in a squeezed state [38]. It turns out that the application areas of temporal correlation properties of radiation fields are a wide-ranging field of research [24,27–41]. Hence, a complete characterization of such correlations is a subject of broad interest.

Also, for applications of time-dependent quantum correlations of light in quantum technology, a full characterization of such complex quantum effects is indispensable. For this purpose, a space-time-dependent phase-space representation has been introduced by generalizing the Glauber-Sudarshan P function to a space-time-dependent P functional [42]. This functional renders it possible to formulate an infinite set of nonclassicality conditions in terms of normal- and time-ordered field correlation functions, which are accessible by homodyne correlation measurements [43]. However, such a verification of quantum correlations is hardly used, as it requires the detection of a manifold of correlation functions.

In conclusion, a direct study of the P functional would be favorable and would lead to a deep and general understanding of temporal quantum correlations. However, even for a single time, the P functional can be highly singular. Even more severely, the singularities of the multitime P functional are even not clearly understood yet. Although it is well known that the singularities of the Glauber-Sudarshan P function are caused by the normal-ordering prescription, it is—to our best knowledge—presently unknown whether or not the time-ordering prescription, occurring in the P functional, can give rise to singularities stronger than those of a multimode (but single-time) P function. In our recent contribution [30], we formulated nonclassicality tests to uncover time-dependent quantum effects. This method was based on the characteristic function, i.e., the Fourier transform of the P functional, which is indeed a regular function. Still, until now, a proper regularization procedure for the P functional itself has not been established for the multitime case. Such a method, however, would be important for a comprehensive understanding and potential applications of general quantum correlations of radiation fields. Here, it is also noteworthy that

the general quantum correlations under study even include entanglement as a subset [44].

In the present paper, we develop a rigorous formalism that describes nonclassical multitime correlations in terms of smooth nonclassicality quasiprobabilities. The regularity of our phase-space function applies to any evolution of the optical system. This enables us to verify quantum effects through the negativity of our quasiprobability representation for quantum states of general radiation fields. For example, we apply our method to an explicitly time-dependent parametric process and to a nonlinear dynamics of the quantized motion of a trapped ion. It is shown that the multitime scenario implies singularities of the P functional stronger than those of the single-time multimode P function. Even those singularities are suppressed by our regularization technique. Eventually, we formulate the measurement theory for the direct sampling of the regularized P functional, which allows for an experimental visualization of multitime quantum correlations of light in phase space.

The paper is structured as follows. Section II recapitulates the concept of single- and multitime nonclassicality. In Sec. III, we formulate the regularization procedure of the multitime-dependent P functional. Afterwards, in Sec. IV we apply the introduced techniques to an optical parametric process with frequency mismatch. The nonlinear evolution of a laser-driven trapped ion is analyzed in Sec. V, which includes more complex time-dependent commutation rules and strongly enhanced singularities of the P functional. In Sec. VI, we propose an experimental scheme for efficiently measuring the quantities under study. Finally, a summary and some conclusions follow in Sec. VII.

II. NONCLASSICALITY

A. Single-time nonclassicality filters

In the single-time scenario, the P function can be used to express any quantum state as a formal mixture of coherent states [15,16,19,20,32]; cf. Eq. (1). However, it is due to the singular behavior of P , which occurs for many quantum states, such as Fock or squeezed states, that a direct experimental access to this distribution is impossible. The singularity is equivalent to an unbounded characteristic function Φ , being the Fourier transform of P .

To resolve the issue of singularities and to identify the nonclassicality of quantum states in experiments through negativities of properly defined quasiprobabilities, a regularization procedure was introduced [22]. The resulting regularized P function is consequently defined via the Fourier transform \mathcal{F} or convolution $*$,

$$P_{\Omega}(\alpha) = \mathcal{F}_{\beta}[\Omega_w(\beta)\Phi(\beta)](\alpha) = (P * \tilde{\Omega}_w)(\alpha), \quad (2)$$

with the filter function Ω_w or its inverse Fourier transform $\tilde{\Omega}_w$ and both depending on a width parameter $w > 0$. This, in general, non-Gaussian filter function needs to satisfy several conditions [22]:

(1) $\Omega_w(\beta)\Phi(\beta)$ is rapidly decaying for all (finite) values w . This is necessary to assure that the regularized P function exists and is even smooth for all states and for all filter widths (cf. also Ref. [45], Appendix A).

(2) The Fourier transform $\tilde{\Omega}_w$ is a probability density. Especially, its nonnegativity is important, as we want to

visualize the negativities of the original P function, which define the nonclassicality. Thus, the filter must not contribute negativities.

(3) The limit $\lim_{w \rightarrow \infty} \Omega_w(\beta) = 1$ assures that the original P function is recovered for $w \rightarrow \infty$.

The regularized N -mode and single-time P function is obtained from the generalization [45]

$$P_\Omega(\alpha) = \mathcal{F}_\beta[\Omega_w(\beta)\Phi(\beta)](\alpha), \quad (3)$$

where $\alpha, \beta \in \mathbb{C}^N$. One possibility for constructing a multimode filter is a product of single-mode filters, $\tilde{\Omega}_w(\alpha) = \prod_{j=1}^N \tilde{\Omega}_w(\alpha_j)$. Note that the multimode characteristic function Φ is, in general, unbounded, $\sup_{\beta \in \mathbb{C}^N} |\Phi(\beta)| = \infty$, but can be bounded through a diverging function,

$$|\Phi(\beta)| \leq \exp[|\beta|^2/2], \quad (4)$$

which can be easily derived: Using the definition of the multimode characteristic function and the displacement operators $\hat{D}(\beta_j) = \exp[\beta_j \hat{a}_j^\dagger - \beta_j^* \hat{a}_j]$ with $\beta = (\beta_1, \dots, \beta_N)^T$, one obtains

$$|\Phi(\beta)| = \left| \left\langle : \prod_{j=1}^N \hat{D}(\beta_j) : \right\rangle \right| = \left| \left\langle e^{\sum_{j=1}^N \beta_j \hat{a}_j^\dagger} e^{-\sum_{j=1}^N \beta_j^* \hat{a}_j} \right\rangle \right|, \quad (5)$$

where \hat{a}_l labels the annihilation operator of the l th radiation mode and $: \dots :$ connotes the normal ordering prescription. That is, all creation operators are placed to the left of the annihilation operators without making use of the bosonic commutation relations. As $[\hat{a}_i, \hat{a}_j] = 0$ and $[\hat{a}_i, \hat{a}_j^\dagger] = \delta_{ij}$ hold (δ is the Kronecker symbol), one can use the standard (i.e., first-order) Baker-Campbell-Hausdorff (BCH) formula to obtain

$$|\Phi(\beta)| = \left| \left\langle \prod_{j=1}^N \hat{D}(\beta_j) \right\rangle \right| e^{|\beta|^2/2}. \quad (6)$$

As for the unitary displacement operators $\hat{D}(\beta_j)$ it holds that $\|\prod_{j=1}^N \hat{D}(\beta_j)\| \leq 1$, and one readily verifies Eq. (4). This estimation also holds true for any time evolution of a quantum state $\hat{\rho}(t)$ for a single time t . Hence, one finds that the slope of the characteristic function of the N -mode P function is bounded by an inverse Gaussian factor, which also bounds the singularities of the multimode P function [21]. However, the regularization procedure so far recapitulated is restricted to single-time properties of a quantum system.

B. Multitime P functional

In the more general multitime scenario, the situation is very different. It is nontrivial to give a similar expansion as in Eq. (1), because it is a cumbersome task to define the corresponding multitime density matrix [46]. Thus, one needs a generalized, multitime-dependent version of the P function [42]. We discuss this concept in the continuation of this section. The resulting P functional is formulated by using normal- and time-ordered expressions which are accessible in quantum correlation measurements [32,43]. They also occur in the photocounting theory [24] whenever source fields play a significant role in the description of a quantum state of light.

Let us consider an observable $\hat{O}[\{\hat{a}(t_i)\}_{i=1}^k]$, which depends on the bosonic annihilation operators $\hat{a}(t_i)$ and creation operators $\hat{a}(t_i)^\dagger$ (not explicitly written as an argument in \hat{O}) at arbitrarily chosen points in time, $t_1 \leq \dots \leq t_k$. Throughout this work, k denotes the number of different points in time. For simplicity, we treat the case of a single spatial-frequency optical mode but k nonmonochromatic (temporal) modes. The extension to N spatial-frequency modes is straightforward, via $\hat{a}^{(\dagger)} \rightarrow (\hat{a}_1^{(\dagger)}, \dots, \hat{a}_N^{(\dagger)})^T$, as exemplified in the previous subsection for a single time. The definition of the singular P functional was introduced in terms of space-time-dependent field operators in Ref. [42], which already includes the most general scenario. It is a function of the k coherent amplitudes at the considered k points in time, $P[\alpha_1, \dots, \alpha_k; t_1, \dots, t_k]$.

Using this P functional, a multitime-dependent expectation value of the given observable \hat{O} may be written as

$$\begin{aligned} \langle \hat{O}[\{\hat{a}(t_i)\}_{i=1}^k] \rangle &= \int d^2\alpha_1 \dots \int d^2\alpha_k O(\alpha_1, \dots, \alpha_k) \\ &\times P[\alpha_1, \dots, \alpha_k; t_1, \dots, t_k], \end{aligned} \quad (7)$$

where we omitted the dependence on the complex conjugated variables and operators. The symbol $\langle \dots \rangle = \mathcal{T} : \dots :$ represents the normal ($: \dots :$)- and time (\mathcal{T})-ordering prescription. Namely, the operators in Eq. (7) have to be normal ordered—creation operators to the left of annihilation operators—and then time ordering is performed, i.e., the time-dependent creation (annihilation) operators are sorted with increasing (decreasing) time arguments from left to right [32]. Note that from the theory of photoelectric detection of light it is well known that observable correlation functions are subjected to normal and time ordering. An example of such a function is the second-order intensity correlation function, $g^{(2)}$, which corresponds to the expectation value of the operator $\hat{O} \sim \hat{a}^\dagger(t) \hat{a}^\dagger(t + \Delta t) \hat{a}(t + \Delta t) \hat{a}(t)$. This quantity is essential for the verification of photon antibunching [1,47].

From the general structure of Eq. (7), we can observe that the P functional has formally the meaning of a joint probability distribution of the coherent amplitudes $\alpha_i \equiv \alpha(t_i)$ at k points in time. We use the term “formally” here, as P , in general, does not fulfill all the properties of a probability density in the sense of classical stochastics. This means that the P functional is a joint quasiprobability, defined as the quantum expectation value [42]

$$P[\{\alpha_i; t_i\}_{i=1}^k] = \left\langle \prod_{i=1}^k \hat{\delta}(\hat{a}(t_i) - \alpha_i) \right\rangle, \quad (8)$$

where $\hat{\delta}$ denotes the operator-valued δ distribution. To clarify the terms, let us stress the following: The notion P function is used for characterizing the quantum state at a single (arbitrary but fixed) time. The notion P functional, on the other hand, applies when field amplitudes including their time dependencies are relevant. This also means that in the case $k = 1$, the time-ordering prescription becomes meaningless, $\langle \dots \rangle \rightarrow : \dots : \dots$. In this scenario, the Glauber-Sudarshan P function in Eq. (1) is recovered.

The classicality (nonnegativity) of the multitime functional, (8), leads to a hierarchy of classical inequalities in term of moments. Their violation certifies general quantum

correlations of light [42]. Special cases were also studied in Ref. [48] for characterizing two-photon quantum interferences.

III. THE FILTERED P FUNCTIONAL

Starting from the definition (8), one can always express the P functional through its characteristic function Φ ,

$$P[\{\alpha_i; t_i\}_{i=1}^k] = \mathcal{F}_{\{\beta_i\}_{i=1}^k}[\Phi(\{\beta_i; t_i\}_{i=1}^k)](\{\alpha_i\}_{i=1}^k), \quad (9)$$

where $\mathcal{F}_{\{\beta_i\}_{i=1}^k} = \mathcal{F}_{\beta_1} \dots \mathcal{F}_{\beta_k}$ is a product of Fourier transforms for the k different degrees of freedom. Let us recall that the (time-dependent) operator-valued δ distribution is defined as the Fourier transform of the (time-dependent) displacement operator, $\hat{\delta}(\hat{a}(t) - \alpha) = \mathcal{F}_{\beta}[\hat{D}(\beta; t)](\alpha)$, with $\hat{D}(\beta; t) = \exp[\beta \hat{a}(t)^\dagger - \beta^* \hat{a}(t)]$. Hence, one readily gets that

$$\begin{aligned} \Phi(\{\beta_i; t_i\}_{i=1}^k) &= \left\langle \circ \prod_{i=1}^k \hat{D}(\beta_i; t_i) \circ \right\rangle \\ &= \left\langle \prod_{i=1}^k e^{\beta_i \hat{a}^\dagger(t_i)} \prod_{i=1}^k e^{-\beta_{k+1-i}^* \hat{a}(t_{k+1-i})} \right\rangle, \end{aligned} \quad (10)$$

which is the multitime-dependent characteristic function (MTCF) of the P functional for $t_1 \leq \dots \leq t_k$ [30]. The operator product for arbitrary $\hat{A}(t)$ is defined as $\prod_{i=1}^k \hat{A}(t_i) = \hat{A}(t_1) \dots \hat{A}(t_k)$. Since the operators are in general not commuting, the operator products contain the time ordering from the first line in Eq. (10).

At first sight, the above expression, (10), resembles that for the multimode characteristic function [Eq. (5)]. However, there are two significant differences when considering the multitime scenario:

(i) One needs to consider non-equal-time commutators of the field operators, which are, in general, nonvanishing or not even proportional to unity [31,32,49,50]. This means that $[\hat{a}(t), \hat{a}(t')^\dagger] \not\propto \hat{1}$ for $t \neq t'$, which is a crucial point, as such commutators do not necessarily commute with other operators. Hence, the standard BCH formula is insufficient and higher-order terms need to be taken into account. Their calculation and the related convergence considerations are complex problems [51], which complicates the issue of finding a bound of the absolute square of the MTCF. This result is a major difference compared to the multimode (single-time) case [Eq. (4)].

(ii) Resulting from the structure of the functional, (8), the time-ordering prescription (beside the normal-ordering prescription) has to be considered. As we saw in the derivation of Eq. (4), the factor $e^{|\beta|^2/2}$ for a single radiation mode is caused by the normal ordering. The question arises whether or not the time ordering itself does cause a stronger rising behavior of the MTCF.

Altogether, the MTCF may be a more strongly growing function of β_1, \dots, β_k compared with the single-time but multimode scenario. However, this asymptotic behavior is important as it could lead to stronger singularities of the corresponding P functional compared with the multimode P function. This problem, to our best knowledge, has not been studied yet. Our rigorous regularization procedure in the multitime scenario has to include this eventuality. This

also means that our approach, to be formulated, needs to be applicable to any dynamics of a quantum optical system.

A. Universal multitime regularization

As emphasized above, the singularities of P in Eq. (9) are caused by the fact that the characteristic function $\Phi(\{\beta_i; t_i\}_{i=1}^k)$ [Eq. (10)] is, in general, unbounded. Hence, the integrals of the Fourier transforms in Eq. (9) do not converge. When generalizing the approach in Eq. (2), our multitime filter Ω_w needs to assure the fast decay of the filtered characteristic function,

$$\Phi_\Omega(\{\beta_i; t_i\}_{i=1}^k) = \Phi(\{\beta_i; t_i\}_{i=1}^k) \Omega_w(\{\beta_i; t_i\}_{i=1}^k). \quad (11)$$

Consequently, the regularized P functional in terms of the Fourier transform is defined as

$$P_\Omega[\{\alpha_i; t_i\}_{i=1}^k] = \mathcal{F}_{\{\beta_i\}_{i=1}^k}[\Phi_\Omega(\{\beta_i; t_i\}_{i=1}^k)](\{\alpha_i\}_{i=1}^k), \quad (12)$$

where w denotes a tuple of width parameters that is specified later.

In the following, let us formulate some simple observations. We consider a continuous function $\varphi(z)$ depending on a real-valued parameter z that might diverge for $|z| \rightarrow \infty$. In addition, we employ the triangular function,

$$\text{tri}(z) = \begin{cases} (1+z) & \text{for } z \in [-1, 0], \\ (1-z) & \text{for } z \in [0, 1], \\ 0 & \text{otherwise.} \end{cases} \quad (13)$$

It holds that the product $\varphi(z)\text{tri}(z)$ is bounded and continuous since the product of two continuous functions is continuous, and since the triangular function has the compact support $[-1, 1]$, it is identical to 0 for $|z| > 1$. Further on, it is easy to check that the one-dimensional Fourier transform of $\text{tri}(z)$ is a probability density. Rescaling the argument with $w > 0$, $\text{tri}(z/w)$, yields a rescaled probability density, with the support of $\text{tri}(z/w)$ changing to the interval $[-w, w]$. In particular, for $w \rightarrow \infty$, this rescaled triangular function converges pointwise to the constant function 1, for which the Fourier transform is a δ distribution.

Returning to our initial filtering problem and keeping those observations in mind, we define the filter function

$$\Omega_w(\{\beta_i\}_{i=1}^k) = \prod_{i=1}^k (\text{tri}(\text{Re}[\beta_i]/w_i) \text{tri}(\text{Im}[\beta_i]/w_i)) \quad (14)$$

using different filter parameters for each time, $w = (w_1, \dots, w_k)$, with $\text{Re}[\beta]$ and $\text{Im}[\beta]$ denoting the real and imaginary part of β , respectively. From our observation above it directly follows that requirements 1–3 (cf. Sec. II) for a filter are satisfied. In particular and due to its compact support, the filter, (14), suppresses any rising behavior of the MTCF. This also means that the filtered P functional, (12), exists always as a smooth function [52].

For illustration, a plot of the filter, multiplied by a factor $\exp[\text{Re}[\beta]^m]$ for $m = 2, 4, 6$, is given in Fig. 1. In the case $m = 2$, the factor resembles the growth factor of a single-time-characteristic function [53]. The parameters $m = 4, 6$ correspond to faster increments that might result from non-equal-time commutation relations of nonlinear interactions.

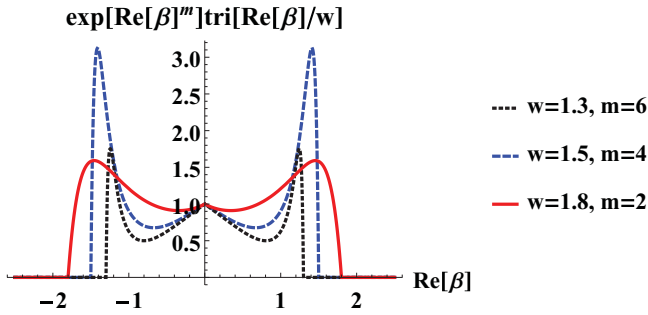


FIG. 1. Plot of the triangular function $\text{tri}(\text{Re}[\beta]/w)$ multiplied by an exponential rising function $\exp[|\beta|^m]$. We see that the resulting function is bounded, and thus, its Fourier transform is a continuous function.

Note that a filter of this type is needed for multitime-dependent phenomena, as the behavior of the MTCF cannot be estimated in general. The multitime commutation rules of the bosonic operators are unknown for general interaction problems; for details see Chap. 2.7 of [32]. With our filters in Eq. (14), however, we ensure that the multitime nonclassicality quasiprobabilities are smooth functions and they can be directly sampled in experiments, which is shown in Sec. VI.

B. Discussion

Let us formulate some preliminary conclusions. The problem of regularizing the P functional has been treated. Although the singularities of this multitime quasiprobability are unknown, we formulated a regularization approach via a compact filter function, (14), which applies to any nonlinear interaction dynamics of radiation fields. On this basis, the well-behaved quasiprobability, (12), exists and it is negative for a width w if and only if the light field under study is nonclassical—including multitime quantum correlations. Our applied filter suppresses any rising behavior of the MTCF for $|\beta| \rightarrow \infty$. This also includes scenarios where the slope of the MTCF increases more rapidly than an inverse Gaussian, which might result from the dynamics of complex interactions.

Remarkably, a triangular filter has already been used for the single-mode and -time scenario [22]. There, the compact support was considered a deficiency because parts of the characteristic function are multiplied by 0 and, thus, do not contribute to the filtered P function. Here, however, this compactness serves as a beneficial resource which renders it possible to filter a multitime P functional. Moreover, similarly to the multimode scenario [45], we have a filter in a product form, (14). It is worth mentioning that we could also and equivalently employ any filter with a compact support, including radial symmetric filters and higher-order autocorrelation-function filters [54,55].

The basic definition of the multitime nonclassicality is the inability to interpret the singular P functional, (8), as a joint probability distribution of a classical stochastic process [42]. Also in Ref. [42], a hierarchy of quantum correlation conditions has been formulated on the basis of measurable space-time-dependent field correlation functions. An approach to formulating multitime nonclassicality tests on

the basis of the MTCF was subsequently formulated as well [30]. Here, in contrast, we introduce regular nonclassicality quasiprobabilities that enable us to study quantum correlations between multiple points in time directly via the corresponding negativities of smooth phase-space distributions of quantum stochastic, optical processes.

IV. PARAMETRIC PROCESSES

Let us now apply our approach to the characterization of temporal quantum effects on a specific physical system. In our recent work [30], we studied the parametric process based on the MTCF. This and related parametric interactions are a fundamental tool for generating nonclassical light in modern experimental quantum optics, e.g., squeezed light [3–6]. Note that various single-photon sources are based on parametric down-conversion [56–61]. Due to the resulting wide range of applications of this process, let us reconsider this system from the perspective of the technique derived here.

The effective Hamiltonian of the quantum system in the interaction picture is

$$\hat{H}_{\text{int}}(t) = \hbar\kappa(\hat{a}^{\dagger 2}e^{-i\delta t} + \hat{a}^2e^{i\delta t}), \quad (15)$$

with a positive frequency mismatch $\delta = \omega_p - 2\omega_a$ and with ω_p and ω_a being the pump and signal frequency, respectively. In this process, a strong (classically described) pump field creates pairs of (equal-frequency) signal photons. Due to the violation of multitime-dependent classical inequalities, we have already demonstrated the presence of two-time quantum correlations [30] for this process. We also stress that the dynamical behavior exhibits a nontrivial dependence on time, as we have, in general, a nonvanishing commutator $[\hat{H}_{\text{int}}(t), \hat{H}_{\text{int}}(t')] \neq 0$ for different times t and t' . In this section, let us focus on the visualization of quantum correlations directly in terms of negativities of the regularized P functional, which has not been considered before.

The coupled equations of motion of the signal field operators \hat{a} and \hat{a}^\dagger read as

$$\frac{d}{dt} \begin{pmatrix} \hat{a}(t) \\ \hat{a}^\dagger(t) \end{pmatrix} = \begin{pmatrix} 0 & -2i\kappa e^{-i\delta t} \\ 2i\kappa e^{i\delta t} & 0 \end{pmatrix} \begin{pmatrix} \hat{a}(t) \\ \hat{a}^\dagger(t) \end{pmatrix}. \quad (16)$$

After decoupling, one obtains second-order equations of motion,

$$\frac{d^2}{dt^2} \hat{a}(t) + i\delta \frac{d}{dt} \hat{a}(t) - 4\kappa^2 \hat{a}(t) = 0. \quad (17)$$

The solution can be found via standard algebra,

$$\hat{a}(\tau) = u_1(\tau)\hat{a} + u_2(\tau)\hat{a}^\dagger, \quad (18)$$

where we have defined the following dimensionless quantities: $\vartheta_r = \pi\sqrt{16-r^2}/4$ (representing the eigenfrequency), $r = \delta/\kappa$ (the coupling ratio), $\tau = 2\kappa t/\pi$ (a time in “natural” units of the system), and the two functions

$$u_1(\tau) = e^{-i\pi r\tau/4} \left[\cosh(\vartheta_r \tau) + \frac{i\pi r}{4\vartheta_r} \sinh(\vartheta_r \tau) \right],$$

$$u_2(\tau) = \frac{-i\pi}{\vartheta_r} e^{-i\frac{\pi}{4}r\tau} \sinh(\vartheta_r \tau). \quad (19)$$

The initial condition is $\hat{a}(\tau = 0) \equiv \hat{a}$.

A. Single-time scenario

To clarify the filtering procedure and to demonstrate the applicability of the filter to the single-time dynamics of the system, we first consider the single-time scenario. In this case, $k = 1$, the P functional in Eq. (9) is obtained from the inverse Fourier transform, (10):

$$P[\alpha'; \tau] = \frac{1}{\pi^2} \int d^2\beta e^{\beta'^* \alpha' - \beta' \alpha'^*} \langle \hat{D}(\beta'; \tau) \rangle. \quad (20)$$

$$\langle \hat{D}(\beta; \tau) \rangle \equiv \Phi(\beta; \tau) = \exp \left[\begin{pmatrix} \beta_r \\ \beta_i \end{pmatrix}^T \begin{pmatrix} \frac{1}{2}(1 - |u_2^* - u_1|^2) & \text{Im}[u_1 u_2] \\ \text{Im}[u_1 u_2] & \frac{1}{2}(1 - |u_2^* + u_1|^2) \end{pmatrix} \begin{pmatrix} \beta_r \\ \beta_i \end{pmatrix} \right]. \quad (21)$$

Here, we have supposed that the initial state is the vacuum state and omitted to write the explicit time dependence, $u_l = u_l(\tau)$.

To simplify the integration, we diagonalize the coefficient matrix in Eq. (21). The transformation matrix S , containing the normalized eigenvectors χ_l ($l = +, -$), reads

$$S = (\chi_+, \chi_-) = \begin{pmatrix} \frac{-b_+}{\sqrt{1+|b_+|^2}} & \frac{-b_-}{\sqrt{1+|b_-|^2}} \\ \frac{1}{\sqrt{1+|b_+|^2}} & \frac{1}{\sqrt{1+|b_-|^2}} \end{pmatrix}, \quad (22)$$

with $b_{\pm} = (-\text{Re}[u_1 u_2] \pm |u_1 u_2|)/\text{Im}[u_1 u_2] \in \mathbb{R}$. The obtained normal coordinates are described via the classical rotation $(\beta_r, \beta_i)^T = S(\gamma_r, \gamma_i)^T$ and we find

$$\Phi(\gamma; \tau) = \exp \left[\begin{pmatrix} \gamma_r \\ \gamma_i \end{pmatrix}^T \begin{pmatrix} -c_+ & 0 \\ 0 & -c_- \end{pmatrix} \begin{pmatrix} \gamma_r \\ \gamma_i \end{pmatrix} \right],$$

with $c_{\pm} = -\frac{1}{2}(1 - |u_2^* - u_1|^2) \pm 2 \frac{|u_1 u_2|}{1 + b_{\pm}^2}$. (23)

Including the free-field propagation, we further obtain

$$P[\alpha; \tau] = \frac{1}{\pi^2} \int_{-\infty}^{\infty} d\gamma_r \int_{-\infty}^{\infty} d\gamma_i \times \exp[2iA_r \gamma_r - 2iA_i \gamma_i - c_+ \gamma_r^2 - c_- \gamma_i^2], \quad (24)$$

with

$$A_r = -(1 + b_+^2)^{-1/2}(\text{Re}[\alpha] + b_+ \text{Im}[\alpha]),$$

$$A_i = (1 + b_-^2)^{-1/2}(\text{Re}[\alpha] + b_- \text{Im}[\alpha]). \quad (25)$$

The application of our regularization procedure, (12), to a single point in time yields

$$P_{\Omega}[\alpha; \tau] = \int_{-\infty}^{\infty} \frac{d\gamma_r}{\pi} e^{2iA_r \gamma_r - c_+ \gamma_r^2} \text{tri}(\gamma_r/w) \times \int_{-\infty}^{\infty} \frac{d\gamma_i}{\pi} e^{2i(-A_i) \gamma_i - c_- \gamma_i^2} \text{tri}(\gamma_i/w). \quad (26)$$

The integral can be simplified (cf. Appendix C in [21]) via defining the function

$$T(y, g) = \text{Re} \left[\frac{2}{\pi} \int_0^1 dz e^{-gz^2 + 2iyz} (1 - z) \right], \quad (27)$$

Since we treat the time evolution in the interaction picture, the impact of the free-field Hamiltonian $\hat{H}_0 = \hbar \omega_a \hat{a}^\dagger \hat{a}$ is not directly included in the parameters u_l . However, it only acts as a classical rotation in phase space, $\hat{D}(\beta'; \tau) \mapsto \hat{D}(\beta' e^{i\omega_a \tau}; \tau)$, which can be ignored, as we can perform a transformation $\beta' e^{i\omega_a \tau} = \beta$ (likewise, $e^{i\omega_a \tau} \alpha' = \alpha$ in the original phase space). Using Eq. (10) for $k = 1$, inserting the solution of the time evolution, (18), using the decomposition $\beta = \beta_r + i\beta_i$ ($\beta_r, \beta_i \in \mathbb{R}$), and reordering the terms using the BCH formula, we get

which relates to complex error functions, and we finally arrive at

$$P_{\Omega}[\alpha; \tau] = w^2 T(wA_r, w^2 c_+) T(-wA_i, w^2 c_-). \quad (28)$$

The temporal evolution in terms of $P_{\Omega}[\alpha; \tau]$ is shown in Fig. 2 for different times $\tau = 2\kappa t/\pi$. The negativities clearly display the nonclassicality of the system in terms of a regular and time-dependent quasiprobability.

B. Singularities due to explicit time dependence

Let us now extend our studies to the more general multitime case. As discussed earlier, the main features of multitime correlations are due to (i) non-equal-time commutation relations and (ii) the time-ordering prescription; see the beginning of Sec. III. The commutators for (i) can be straightforwardly computed for the system under study by using the exact solution, (18),

$$[\hat{a}(\tau), \hat{a}(\tau + \Delta\tau)] = \det \begin{pmatrix} u_1(\tau) & u_2(\tau) \\ u_1(\tau + \Delta\tau) & u_2(\tau + \Delta\tau) \end{pmatrix} \hat{1}, \quad (29)$$

with $u_l(\tau)$ given in Eq. (19). The effect of the time-ordering prescription in Eqs. (8) and (10) can be analyzed in terms of

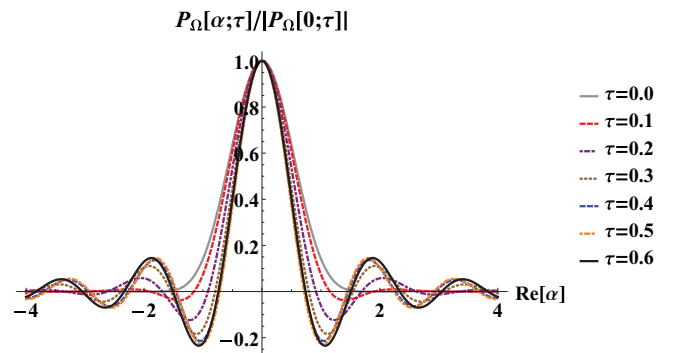


FIG. 2. Plot of the regularized and scaled phase-space distribution $P_{\Omega}[\alpha; \tau]$ for several system times τ . We chose $\text{Im}[\alpha] = 0$, $w = 2.3$ for the triangular filter and $r = \delta/\kappa = 10/\pi \approx 3.18$. The negativities for $\tau > 0$ clearly show the evolution of the nonclassicality.

the ratio

$$\tilde{\Phi} = \frac{|\langle \circ \hat{D}(\beta_1, \beta_2; \tau, \tau + \Delta\tau) \circ \rangle|}{|\langle \hat{D}(\beta_1, \beta_2; \tau, \tau + \Delta\tau) \rangle|}, \quad (30)$$

which relates the time- and normal-ordered quantities to solely normal-ordered ones. Since all appearing commutators are multiples of the identity, we get

$$\begin{aligned} \tilde{\Phi} &= |\exp\{-\beta_1^* \beta_2^* [\hat{a}(\tau), \hat{a}(\tau + \Delta\tau)]\}| \\ &= \exp\{-|\beta_1 \beta_2| \text{Re}[e^{-i(\varphi_{\beta_1} + \varphi_{\beta_2})} [\hat{a}(\tau), \hat{a}(\tau + \Delta\tau)]]\}, \end{aligned} \quad (31)$$

where $\varphi_{\beta_j} = \arg \beta_j$ for $j = 1, 2$. Using the solutions, (19), one finds for $|r| \leq 4$ and $\vartheta_r = \pi \sqrt{16 - r^2}/4$ that

$$\begin{aligned} &\text{Re}[e^{-i(\varphi_{\beta_1} + \varphi_{\beta_2})} [\hat{a}(\tau), \hat{a}(\tau + \Delta\tau)]] \\ &= -\frac{\pi}{\vartheta_r} \sin \left[\frac{\pi r}{4} (2\tau + \Delta\tau) + \varphi_{\beta_1} + \varphi_{\beta_2} \right] \sinh[\vartheta_r \Delta\tau] \hat{1}. \end{aligned} \quad (32)$$

In other words, the influence of the time-ordering prescription is an additional term proportional to $\exp\{\pm|\beta_1 \beta_2|\}$, where the sign depends on the sine (sin) term in Eq. (32). As the hyperbolic sine (sinh) is monotonically increasing, the strength of this factor increases with $\Delta\tau$. For the P functional (i.e., performing a Fourier transformation), this factor increases (for $\exp\{+|\beta_1 \beta_2|\}$) or decreases (for $\exp\{-|\beta_1 \beta_2|\}$) the strength of the singularities.

Let us apply our filter procedure introduced in Sec. III A. We use identical filter widths, $w_1 = w_2 = w$ [cf. Eqs. (12) and (14)]. The general procedure to compute $P_\Omega[\alpha_1, \alpha_2; \tau_1, \tau_1]$ is a straightforward extension of the one presented in Sec. IV A. After some algebra, we get the two-time regularized P functional,

$$\begin{aligned} P_\Omega[\alpha_1, \alpha_2; \tau_1, \tau_1] &= w^4 T \left(w \frac{f_{10}}{2i}, -w^2 f_{20} \right) T \left(w \frac{f_{01}}{2i}, -w^2 f_{02} \right) \\ &\times T \left(w \frac{d_{10}}{2i}, -w^2 d_{20} \right) T \left(w \frac{d_{01}}{2i}, -w^2 d_{02} \right), \end{aligned} \quad (33)$$

with the definition of T in Eq. (27). The coefficients f_{mn} and d_{mn} together with a proper rotation of phase space can be obtained numerically as described in detail in Sec. IV A and generalized to four dimensions.

The two-time regularized P functional, (33), is depicted in Fig. 3. The negativities directly reveal the quantum correlations of the system under study. Note that for any time pairings (τ_1, τ_2) and cross sections other than those used in Fig. 3, negativities are revealed as well; cf. also Ref. [30]. Let us stress that the existence of negativities for a certain filter width is necessary and sufficient for the existence of quantum correlations within the singular P functional.

V. TRAPPED-ION DYNAMICS

In the previous section, we discuss multitime effects for a time-dependent parametric oscillator. In this case, however, the rather simple commutator $[\hat{a}(t), \hat{a}(t')] \propto \hat{1}$ for $t \neq t'$ holds [Eq. (29)], and hence, the standard BCH formula is applicable. Furthermore, one is able to solve the equations of motion

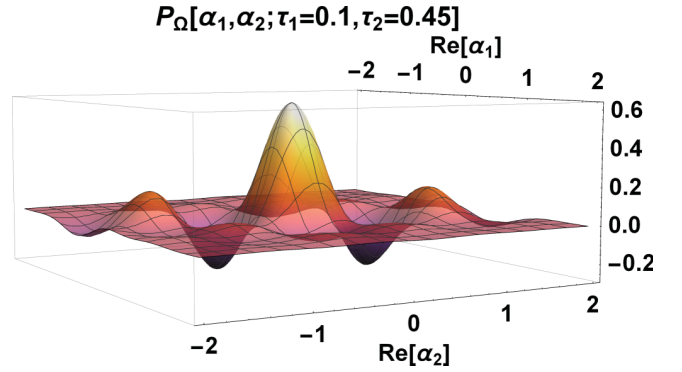


FIG. 3. Plot of the two-time regularized functional $P_\Omega(\alpha_1, \alpha_2; \tau_1, \tau_2)$ for $w = 2.9$. Here, we used $\tau_1 = 0.1$, $\tau_2 = 0.45$, and the cross section $\text{Im}[\alpha_2] = \text{Im}[\alpha_1] = 0$. The negativities of the quasiprobability reveal nonclassical normally and time-ordered correlation properties of the considered system.

analytically. The question arises how such systems shall be examined if the exact dynamics is not explicitly given. In this section, we therefore study more general structures of the MTCF and the corresponding dynamics for which the commutators are not central—i.e., they do not commute with the field operators itself, $[[\hat{a}(t), \hat{a}(t')], \hat{a}(t'')] \neq 0$.

Let us first rewrite the MTCF [Eq. (10)] for the two-time case $k = 2$ and an input state $\hat{\rho}_{\text{in}}$,

$$\Phi(\beta_1, \beta_2; t_1, t_2) = \text{Tr}[\hat{\rho}_{\text{in}}(t_1, t_0) e^{\beta_1 \hat{a}^\dagger} \hat{D}(\beta_2; t_2, t_1) e^{-\beta_1^* \hat{a}}] e^{|\beta_2|^2/2}. \quad (34)$$

Here we have used $\hat{\rho}_{\text{in}}(t_1, t_0) = \hat{U}(t_1, t_0) \hat{\rho}_{\text{in}} \hat{U}^\dagger(t_1, t_0)$ and the time-evolved displacement operator $\hat{D}(\beta_2; t_2, t_1) = \hat{U}(t_2, t_1)^\dagger \hat{D}(\beta_2) \hat{U}(t_2, t_1)$. This form of Φ reveals a major difficulty: $e^{\beta_1 \hat{a}^\dagger}$ and $e^{-\beta_1^* \hat{a}}$ are unbounded operators [62], and they cannot be rewritten in a simple manner when the commutators are not central.

Let us therefore consider the limit $t_1 \rightarrow t_0$ and $t_0 \rightarrow 0$, i.e., $t_1 = t_0 = 0$. As in general $[\hat{a}(0), \hat{a}(t_2)] \neq 0$ (even $\propto \hat{1}$) holds true, this situation differs from the single-time case. Let us emphasize that the time-ordering prescription still applies. Setting $t_2 \equiv t$, we arrive at

$$\Phi(\beta_1, \beta_2; 0, t) = \text{Tr}[\hat{\rho}_{\text{in}} e^{\beta_1 \hat{a}^\dagger} \hat{D}(\beta_2; t) e^{-\beta_1^* \hat{a}}] e^{|\beta_2|^2/2}. \quad (35)$$

Evaluations of this expression depend on the input state $\hat{\rho}_{\text{in}}$ and on the dynamics under study. Here we focus on Fock states as input states, i.e., $\hat{\rho}_{\text{in}} = |p\rangle\langle p|$. This yields

$$\begin{aligned} \Phi(\beta_1, \beta_2; 0, t) &= \sum_{m,n=0}^p \frac{\beta_1^n (-\beta_1^*)^m}{m!n!} \frac{p!(p-n)! \langle \hat{D}(\beta_2; t) | p-m \rangle}{\sqrt{(p-n)!(p-m)!}} e^{|\beta_2|^2/2}, \end{aligned} \quad (36)$$

which is obtained via expanding the exponential functions in power series and using the standard actions of \hat{a} (\hat{a}^\dagger) on the Fock states $|p\rangle$ ($\langle p|$).

First, we study Eq. (36) for $p = 0$, i.e., $\hat{\rho}_{\text{in}} = |\text{vac}\rangle\langle \text{vac}|$. We obtain

$$\Phi_{\text{vac}}(\beta_1, \beta_2; 0, t) = \langle 0 | \hat{D}(\beta_2; t) | 0 \rangle e^{|\beta_2|^2/2}, \quad (37)$$

which is always bound by an inverse Gaussian factor. Furthermore, $\Phi_{\text{vac}}(\beta_1, \beta_2; 0, t)$ equals a single-time characteristic function, and the corresponding P functional [Eq. (9)] will attain for any dynamics the form

$$P_{\text{vac}}[\alpha_1, \alpha_2; 0, t] = P_{\text{vac}}[\alpha_2; t] \delta(\alpha_1). \quad (38)$$

As the delta distribution is a nonnegative distribution, the two-time P functional describes a nonclassical system if and only if the single-time P function fails to be a classical probability distribution. In this scenario, there are no genuine temporal correlations. However, the situation is different for other input states, which can be observed for our second example, $p = 1$. Because $e^{-\beta_1^\dagger \hat{a}} |1\rangle = |1\rangle - \beta_1^* |0\rangle$, we get

$$\Phi_1(\beta_1, \beta_2; 0, t) = [(\langle 1| + \langle 0|\beta_1| \hat{D}(\beta_2; t) [|1\rangle - \beta_1^* |0\rangle] e^{|\beta_2|^2/2} \quad (39)$$

and, therefore, additional terms due to the inclusion of a second point in time. This holds even if we set the first time to be 0. Note, a similar behavior can be observed for any $p \geq 1$.

For clarification, let us consider a realistic interaction Hamiltonian [63],

$$\hat{H}_3 = \hbar \varepsilon \hat{f}_3(\hat{a}^\dagger \hat{a}; \eta) (i\eta \hat{a})^3 + \text{H.c.}, \quad (40)$$

which results in a time evolution obeying a noncentral commutator algebra and whose time evolution is solved numerically. It describes a nonlinear vibrational dynamics of a laser-driven trapped ion. Therein, ε is the effective two-photon coupling strength, and η is the Lamb-Dicke parameter. The nonlinear operator function $\hat{f}_3(\hat{a}^\dagger \hat{a}; \eta)$ of the vibrational number operator $\hat{a}^\dagger \hat{a}$ accounts for the recoil effects due to absorption and emission of laser photons by the trapped atom. It reads [63]

$$\hat{f}_3(\hat{a}^\dagger \hat{a}; \eta) = e^{-\eta^2/2} \sum_{l=0}^{\infty} (-1)^l \frac{\eta^{2l}}{l!(l+3)!} \hat{a}^{\dagger l} \hat{a}^l. \quad (41)$$

The action on Fock states of the ion's center-of-mass motion yields

$$\hat{f}_3(\hat{a}^\dagger \hat{a}; \eta) |n\rangle = e^{-\eta^2/2} \frac{n!}{(n+3)!} L_n^{(3)}(\eta^2) |n\rangle \equiv f_3(n; \eta) |n\rangle, \quad (42)$$

with $L_n^{(k)}(x)$ being the generalized Laguerre polynomials. Using the completeness relation of the Fock states, $\sum_{n=0}^{\infty} |n\rangle \langle n| = \hat{1}$, the Hamiltonian, (40), can be written in the Fock basis as

$$\hat{H}_3 = i\hbar \varepsilon \eta^3 \sum_{n=0}^{\infty} g_3(n; \eta) |n+3\rangle \langle n| - g_3(n; \eta) |n\rangle \langle n+3|, \quad (43)$$

with $g_3(n; \eta) = f_3(n; \eta) \sqrt{(n+1)(n+2)(n+3)}$.

The time evolution can be numerically solved via evaluating the time evolution operator

$$\hat{U}(t, t_0) = \exp \left[-\frac{i}{\hbar} (t - t_0) \hat{H}_3 \right], \quad (44)$$

in matrix representation, where a sufficiently high cutoff of the Fock space has to be chosen. Using the MTCF in Eq. (35), we

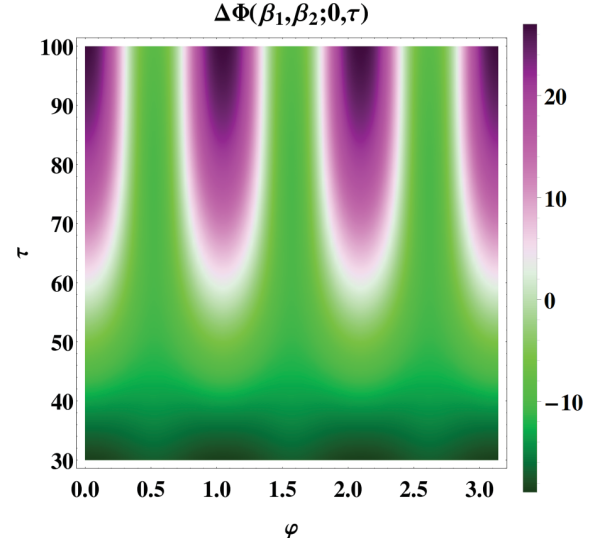


FIG. 4. Plot of $\Delta\Phi$ as defined in Eq. (45) for fixed $|\beta_1| = |\beta_2| = 1.3$ and $\varphi_1 = \varphi_2 \equiv \varphi$, where $\beta_j = |\beta_j| e^{i\varphi_j}$, $j = 1, 2$. We vary the common phase φ and the dimensionless time $\tau = \varepsilon t$. As $\Delta\Phi$ clearly exceeds the value of 0 (pink areas), we confirm that the MTCF is differently bounded compared to the two-mode single-time case.

can investigate the difference between the squared modulus of the MTCF and the inverse Gaussian bound,

$$\Delta\Phi(\beta_1, \beta_2; 0, \tau) := |\Phi(\beta_1, \beta_2; 0, \tau)|^2 - e^{|\beta_1|^2 + |\beta_2|^2}, \quad (45)$$

with the dimensionless system time $\tau \equiv \varepsilon t$. If this function $\Delta\Phi$ exceeds 0, the MTCF is—due to temporal correlations—differently bounded compared to the two-mode single-time characteristic function. This means that the temporal correlations increase the divergences of the P functional to an extent which cannot occur for any two-mode correlations at equal time; cf. Eq. (4).

A visualization of (45) is given in Fig. 4 for a particular choice of the parameters. We used $p = 3$ ($\hat{\rho}_{\text{in}} = |3\rangle\langle 3|$) and numerically evaluated $\Delta\Phi$ in a 200-dimensional Fock space to ensure approximation errors of the order of those of the numerical arithmetic. As for several parameters $\Delta\Phi > 0$ holds, the temporal correlations obviously exceed the slope one can maximally expect for an equal-time two-mode characteristic function. As discussed earlier, the strength of the excess depends on the chosen input state. This deviation from the inverse Gaussian bound of the MTCF could be even stronger for other dynamical systems. However, our filter approach, introduced in Sec. III A, is suitable for regularization of the P functional for any dynamics. Based on the strongly nonlinear trapped-ion interaction Hamiltonian and the discussion of the impact of the input state, we have demonstrated our approach's requirement for regularization of multitime P functionals.

VI. SAMPLING OF THE P FUNCTIONAL

The first experimental reconstruction of a phase-insensitive and single-time filtered P_Ω function with negativities was performed for single-photon-added thermal states [64]—based on the measurement of quadratures in balanced homodyne detection. A direct sampling of a single-time P_Ω function for a squeezed state was then performed [65]—including

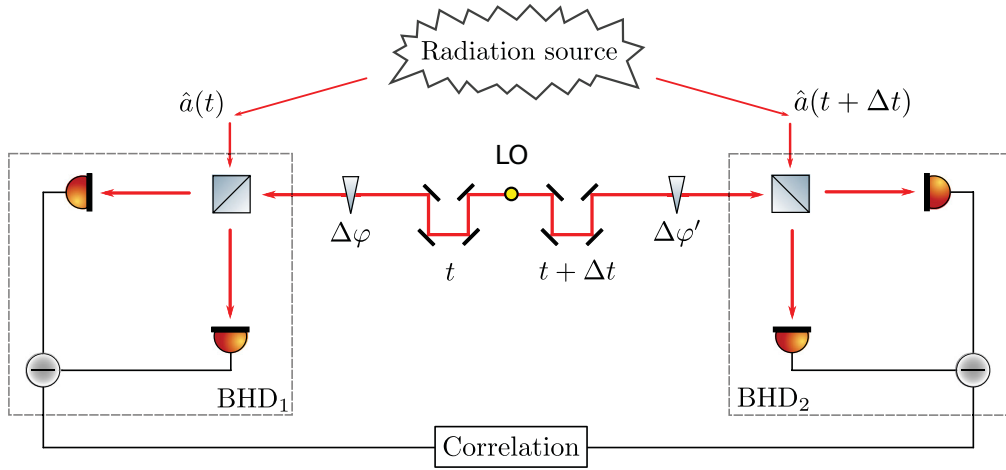


FIG. 5. Experimental scheme to directly measure two-time quantum correlations in terms of two-time quasiprobabilities. The scheme consists of two balanced homodyne detection (BHD) setups whose difference signals are additionally correlated. The creation operators $\hat{a}(t)$ and $\hat{a}(t + \Delta t)$ label the different travel times of the field. The resulting correlated difference statistics of the detector events can be directly related to $P_\Omega[\alpha_1, \alpha_2; \tau_1, \tau_2]$, where the phases for the local oscillator (LO) of each BHD setup are controlled continuously through the phase shifters $\Delta\varphi$ and $\Delta\varphi'$. The temporal matching of the LO to the signal fields is ensured through a proper path-length control.

the formulation of suitable pattern functions for discrete phase measurements. More recently, a method was presented to sample the filtered P function via continuous-in-phase measurement [23]. In the following we study an optical measurement scheme for reconstructing the filtered P functional that allows one to apply our technique in experiments. Additionally note that a corresponding measurement technique can also be provided for the motional quantum state of a trapped ion, which can be directly based on the motional-state reconstruction as proposed in Ref. [66].

The setup of our scheme is shown in Fig. 5; it correlates the radiation field at two times. According to the quantum theoretical model for photodetection [24,32,67], the joint probability of four detectors is

$$P_{n_1, n_2, n_3, n_4} = \left\langle \prod_{i=1}^4 \frac{[\eta_i \hat{n}_i(t_i)]^{n_i}}{n_i!} e^{-\eta_i \hat{n}_i(t_i)} \right\rangle, \quad (46)$$

where n_i denotes the number of photons at the i th detector, η_i is the detector efficiency, and $\hat{n}_i(t_i)$ is the photon number operator at time t_i in the corresponding detector path. As we correlate two points in time in our setup, we set $t_1 = t_2 \equiv t$ and $t_3 = t_4 \equiv t + \Delta t$. The phases of the local oscillator modes can be controlled separately by the phase shifters $\Delta\varphi$ and $\Delta\varphi'$. Note that the layout is scalable and could be further extended to more points in time.

In close analogy to the procedure in Ref. [68], the correlated difference statistics is found to be

$$p_{t, t+\Delta t}(v, v'; \varphi, \varphi') = \frac{1}{2\pi R^2 \sqrt{\eta\eta'}} \left\langle \exp \left\{ -\frac{[v - \eta R \hat{x}(\varphi - \pi/2; t)]^2}{2\eta R^2} \right\} \times \exp \left\{ -\frac{[v' - \eta' R \hat{x}(\varphi' - \pi/2; t + \Delta t)]^2}{2\eta' R^2} \right\} \right\rangle, \quad (47)$$

with the difference events $n_1 - n_2 = v$ and $n_3 - n_4 = v'$, the phases φ and φ' , the common amplitude R of the two local

oscillators, and the quadrature operator

$$\hat{x}(\varphi - \pi/2; t) = \hat{a}(t)e^{-i\varphi} + \hat{a}(t)^\dagger e^{i\varphi}. \quad (48)$$

To arrive at Eq. (47), we replaced n_i with continuous variables, which can be done in the strong local oscillator limit and for a sufficiently large number of events. The distribution, (47), is obviously the quantum expectation value of the time- and normal-ordered product of two Gaussian distributions of the quadratures at t and $t + \Delta t$. Via the two-dimensional Fourier transform of the measured difference statistics,

$$F_{t, t+\Delta t}(y, y', \varphi, \varphi') = \int dv \int dv' e^{ivy} e^{iv'y'} p_{t, t+\Delta t}(v, v'; \varphi, \varphi'), \quad (49)$$

one gets

$$F_{t, t+\Delta t}(y, y', \varphi, \varphi') = e^{y^2 R^2 \eta/2 + y'^2 R^2 \eta'/2} \Phi(y\eta R e^{i\varphi}, y'\eta' R e^{i\varphi'}; t, t + \Delta t). \quad (50)$$

Here Φ is the desired two-time characteristic function of the P functional. Hence, by adjusting the parameters and properly scaling the complex numbers y and y' , Φ can be directly sampled with our setup. If we use the representations $\beta_1 = b_1 e^{i\varphi}$ and $\beta_2 = b_2 e^{i\varphi'}$ and identify $y\eta R \equiv b_1$ and $y'\eta' R \equiv b_2$, we can rewrite the previous results as

$$\Phi(b_1 e^{i\varphi}, b_2 e^{i\varphi'}; t, t + \Delta t) = \exp \left[\frac{b_1^2}{2\eta} + \frac{b_2^2}{2\eta'} \right] \int dv \int dv' p_{t, t+\Delta t}(v, v'; \varphi, \varphi') \times \exp \left[\frac{ib_1}{\eta R} v + \frac{ib_2}{\eta' R} v' \right]. \quad (51)$$

The regularized P functional can be reconstructed in the following way. First, we recall that [cf. Eq. (12)

for $k = 2$]

$$P_{\Omega}[\alpha_1, \alpha_2; t, t + \Delta t] = \int \frac{d^2\beta_1}{\pi^2} e^{\beta_1^* \alpha_1 - \beta_1 \alpha_1^*} \int \frac{d^2\beta_2}{\pi^2} e^{\beta_2^* \alpha_2 - \beta_2 \alpha_2^*} \times \Phi(\beta_1, \beta_2; t, t + \Delta t) \Omega_w(\beta_1) \Omega_w(\beta_2). \quad (52)$$

Since we have used a product filter [cf. Eq. (14)], we can simply insert Eq. (51) and, following the procedure in Ref. [65], rewrite the previous formula as

$$P_{\Omega}[\alpha_1, \alpha_2; t, t + \Delta t] = \int dv \int dv' \int_0^{\pi} d\varphi \int_0^{\pi} d\varphi' \frac{P_{t, t+\Delta t}(v, v'; \varphi, \varphi')}{\pi^2} \times f_{\Omega}(v, \varphi; \alpha_1, w) f_{\Omega}(v', \varphi'; \alpha_2, w). \quad (53)$$

Here, the so-called pattern function f_{Ω} is

$$f_{\Omega}(z, \varphi; \alpha_i, w) = \int db_i \frac{b_i}{\pi} \Omega_w(b_i) \exp \left[\frac{izb_i}{\eta_z r} + \frac{b_i^2}{2\eta_z} \right] \times \exp[2ib_i |\alpha_i| \sin[\varphi_{\alpha_i} - \varphi - \pi/2]], \quad (54)$$

with $z \in \{v, v'\}$, $\eta_v \equiv \eta$, and $\eta_{v'} \equiv \eta'$. Finally, the regularized P functional can be sampled from M measured quadrature data points $(v_j, \varphi_j, v'_j, \varphi'_j)_{j=1}^M$ in the two channels via its empirical estimate

$$P_{\Omega}[\alpha_1, \alpha_2; t, t + \Delta t] \approx \frac{1}{M} \sum_{j=1}^M f_{\Omega}(v_j, \varphi_j; \alpha_1, w) f_{\Omega}(v'_j, \varphi'_j; \alpha_2, w), \quad (55)$$

where the time dependences are included in the set of data, $v \equiv v(t)$ and $v' \equiv v(t + \Delta t)$. For convenience, we used a radial symmetric filter, such that the filter functions Ω_w depend only on the b_i and not on the phases φ and φ' [cf. Eqs. (53) and (54)].

Hence, we have formulated the theory of our proposed measurement scheme in Fig. 5 that renders it possible to directly obtain the two-time regularized P functional via the sampling of measured (correlated) quadrature data using pattern functions. We may stress again that this approach is scalable to an arbitrary number of points in time by employing multiple BHDs. In addition, some remarks concerning the sampling error estimation can be found in Ref. [23].

VII. SUMMARY AND CONCLUSIONS

In summary, we have derived a method for visualizing general multitime quantum correlations in terms of regular phase-space quasiprobabilities. For this purpose, we significantly generalized the approach of filtering the Glauber-Sudarshan P function for a single time to a regularization of the P functional that correlates an arbitrary number of points in time. This generalizes the commonly accepted definition of nonclassicality by Titulaer and Glauber to capture multitime quantum phenomena in terms of regular and accessible phase-space distributions. Hence, our formulation of multitime and regular nonclassicality quasiprobabilities is not restricted to particular correlation functions or observables. Additionally, we have proved that our method is applicable to arbitrarily complex evolutions of light fields. In our general approach, nonclassical correlations, if present, are directly visualized by negativities of this regular quasiprobability density for properly chosen filter widths. Beyond previously studied methods, our treatment enables us to visualize general quantum correlations of radiation fields, including quantum entanglement as a subset.

We applied this technique to characterization of the temporal quantum features of a parametric oscillator with a frequency mismatch. We studied the impact of the time-dependent Hamiltonian on the dynamical properties of this system, including the multitime correlations. In particular, we uncovered quantum correlations via a negative and regular two-time quasiprobability description of this process. We also studied a strongly nonlinear dynamics of the motional quantum state of a laser-driven trapped ion. In this case, nontrivial time-dependent commutator rules become important, leading to singularities of the P functional much stronger than those occurring for equal-time two-mode correlations. Our technique regularizes these unexpectedly strong singularities. Eventually, we presented an experimental setup—consisting of two correlated balanced homodyne detection layouts. Based on the derived pattern functions, this allows one to directly sample the regularized quasiprobabilities in experiments. Altogether, this yields a powerful tool for the characterization of general, time-dependent quantum correlations in phase space.

ACKNOWLEDGMENTS

We thank Regina Kruse for helpful comments. This work was supported by the Deutsche Forschungsgemeinschaft through SFB 652, project B12. J.S. and W.V. acknowledge funding from the European Union's Horizon 2020 research and innovation program under Grant Agreement No. 665148.

-
- [1] H. J. Kimble, M. Dagenais, and L. Mandel, Photon Antibunching in Resonance Fluorescence, *Phys. Rev. Lett.* **39**, 691 (1977).
 - [2] D. F. Walls, Squeezed states of light, *Nature (London)* **306**, 141 (1983).
 - [3] R. E. Slusher, L. W. Hollberg, B. Yurke, J. C. Mertz, and J. F. Valley, Observation of Squeezed States Generated by Four-Wave Mixing in an Optical Cavity, *Phys. Rev. Lett.* **55**, 2409 (1985).

- [4] L.-A. Wu, H. J. Kimble, J. L. Hall, and H. Wu, Generation of Squeezed States by Parametric Down Conversion, *Phys. Rev. Lett.* **57**, 2520 (1986).
- [5] H. Vahlbruch, M. Mehmet, S. Chelkowski, B. Hage, A. Franzen, N. Lastzka, S. Goßler, K. Danzmann, and R. Schnabel, Observation of Squeezed Light with 10-dB Quantum-Noise Reduction, *Phys. Rev. Lett.* **100**, 033602 (2008).

- [6] H. Vahlbruch, M. Mehmet, K. Danzmann, and R. Schnabel, Detection of 15 dB Squeezed States of Light and Their Application for the Absolute Calibration of Photoelectric Quantum Efficiency, *Phys. Rev. Lett.* **117**, 110801 (2016).
- [7] A. Einstein, N. Rosen, and B. Podolsky, Can quantum-mechanical description of physical reality be considered complete? *Phys. Rev.* **47**, 777 (1935).
- [8] E. Schrödinger, Die gegenwärtige Situation in der Quantenmechanik, *Naturwissenschaften* **23**, 807 (1935).
- [9] T. Richter and W. Vogel, Nonclassicality of Quantum States: A Hierarchy of Observable Conditions, *Phys. Rev. Lett.* **89**, 283601 (2002).
- [10] E. V. Shchukin and W. Vogel, Nonclassical moments and their measurements, *Phys. Rev. A* **72**, 043808 (2005).
- [11] S. Ryl, J. Sperling, E. Agudelo, M. Mraz, S. Köhnke, B. Hage, and W. Vogel, Unified nonclassicality criteria, *Phys. Rev. A* **92**, 011801(R) (2015).
- [12] A. Miranowicz, M. Bartkowiak, X. Wang, Y.-X. Liu, and F. Nori, Testing nonclassicality in multimode fields: A unified derivation of classical inequalities, *Phys. Rev. A* **82**, 013824 (2010).
- [13] K. Husimi, Some formal properties of the density matrix, *Proc. Phys. Math. Soc. Jpn.* **22**, 264 (1940).
- [14] E. Wigner, On the quantum correction for thermodynamic equilibrium, *Phys. Rev.* **40**, 749 (1932).
- [15] E. C. G. Sudarshan, Equivalence of Semiclassical and Quantum Mechanical Descriptions of Statistical Light Beams, *Phys. Rev. Lett.* **10**, 277 (1963).
- [16] R. J. Glauber, Coherent and incoherent states of the radiation field, *Phys. Rev.* **131**, 2766 (1963).
- [17] K. E. Cahill and R. J. Glauber, Ordered expansions in boson amplitude operators, *Phys. Rev.* **177**, 1857 (1969).
- [18] G. S. Agarwal and E. Wolf, Calculus for functions of noncommuting operators and general phase-space methods in quantum mechanics. I. Mapping theorems and ordering of functions of noncommuting operators, *Phys. Rev. D* **2**, 2161 (1970).
- [19] U. M. Titulaer and R. J. Glauber, Correlation functions for coherent fields, *Phys. Rev.* **140**, B676 (1965).
- [20] L. Mandel, Non-classical states of the electromagnetic field, *Phys. Scripta T* **12**, 34 (1986).
- [21] J. Sperling, Characterizing maximally singular phase-space distributions, *Phys. Rev. A* **94**, 013814 (2016).
- [22] T. Kiesel and W. Vogel, Nonclassicality filters and quasiprobabilities, *Phys. Rev. A* **82**, 032107 (2010).
- [23] E. Agudelo, J. Sperling, W. Vogel, S. Köhnke, M. Mraz, and B. Hage, Continuous sampling of the squeezed-state nonclassicality, *Phys. Rev. A* **92**, 033837 (2015).
- [24] P. L. Kelley and W. H. Kleiner, Theory of electromagnetic field measurement and photoelectron counting, *Phys. Rev.* **136**, A316 (1964).
- [25] P. P. Hofer and A. A. Clerk, Negative Full Counting Statistics Arise from Interference Effects, *Phys. Rev. Lett.* **116**, 013603 (2016).
- [26] P. P. Hofer, Quasi-probability distributions for observables in dynamic systems, [arXiv:1702.00998](https://arxiv.org/abs/1702.00998) [quant-ph].
- [27] B. R. Mollow, Photon correlations in the parametric frequency splitting of light, *Phys. Rev. A* **8**, 2684 (1973).
- [28] L. I. Plimak and D. F. Walls, Dynamical restrictions to squeezing in a degenerate optical parametric oscillator, *Phys. Rev. A* **50**, 2627 (1994).
- [29] A. Christ, B. Brecht, W. Maurer, and C. Silberhorn, Theory of quantum frequency conversion and type-II parametric down-conversion in the high-gain regime, *New J. Phys.* **15**, 053038 (2013).
- [30] F. Krumm, J. Sperling, and W. Vogel, Multitime correlation functions in nonclassical stochastic processes, *Phys. Rev. A* **93**, 063843 (2016).
- [31] L. Knöll, W. Vogel, and D.-G. Welsch, Action of passive, lossless optical systems in quantum optics, *Phys. Rev. A* **36**, 3803 (1987).
- [32] W. Vogel and D.-G. Welsch, *Quantum Optics*, 3rd ed. (Wiley-VCH, New York, 2006).
- [33] L. Knöll, W. Vogel, and D.-G. Welsch, Quantum noise in spectral filtering of light, *J. Opt. Soc. Am. B* **3**, 1315 (1986).
- [34] L. Knöll and G. Weber, Theory of n -fold time-resolved correlation spectroscopy and its application to resonance fluorescence radiation, *J. Phys. B* **19**, 2817 (1986).
- [35] J. D. Cresser, Intensity correlations of frequency-filtered light fields, *J. Phys. B* **20**, 4915 (1987).
- [36] A. J. Leggett and A. Garg, Quantum Mechanics Versus Macroscopic Realism: Is the Flux there When Nobody Looks? *Phys. Rev. Lett.* **54**, 857 (1985).
- [37] C. Emary, N. Lambert, and F. Nori, Leggett-Garg inequalities, *Rep. Prog. Phys.* **77**, 039501 (2014).
- [38] J. Martin and V. Vennin, Leggett-Garg inequalities for squeezed states, *Phys. Rev. A* **94**, 052135 (2016).
- [39] S. Brierley, A. Kosowski, M. Markiewicz, T. Paterek, and A. Przysieszna, Nonclassicality of Temporal Correlations, *Phys. Rev. Lett.* **115**, 120404 (2015).
- [40] T. Xin, J. S. Pedernales, L. Lamata, E. Solano, and G.-L. Long, Measurement of linear response functions in NMR, [arXiv:1606.00686](https://arxiv.org/abs/1606.00686) [quant-ph].
- [41] R. Di Candia, J. S. Pedernales, A. del Campo, E. Solano, and J. Casanova, Quantum simulation of dissipative processes without reservoir engineering, *Sci. Rep.* **5**, 9981 (2015).
- [42] W. Vogel, Nonclassical Correlation Properties of Radiation Fields, *Phys. Rev. Lett.* **100**, 013605 (2008).
- [43] E. Shchukin and W. Vogel, Universal Measurement of Quantum Correlations of Radiation, *Phys. Rev. Lett.* **96**, 200403 (2006).
- [44] J. Sperling and W. Vogel, Representation of entanglement by negative quasiprobabilities, *Phys. Rev. A* **79**, 042337 (2009).
- [45] E. Agudelo, J. Sperling, and W. Vogel, Quasiprobabilities for multipartite quantum correlations of light, *Phys. Rev. A* **87**, 033811 (2013).
- [46] Y. Aharonov, S. Popescu, J. Tollaksen, and L. Vaidman, Multiple-time states and multiple-time measurements in quantum mechanics, *Phys. Rev. A* **79**, 052110 (2009).
- [47] H. Paul, Photon antibunching, *Rev. Mod. Phys.* **54**, 1061 (1982).
- [48] Z. Y. Ou, *Multi-photon Quantum Interference* (Springer, New York, 2007).
- [49] J. D. Cresser, Theory of the spectrum of the quantised light field, *Phys. Rep.* **94**, 47 (1983).
- [50] J. D. Cresser, Electric field commutation relation in the presence of a dipole atom, *Phys. Rev. A* **29**, 1984 (1984).
- [51] S. Blanes and F. Casas, On the convergence and optimization of the Baker-Campbell-Hausdorff formula, *Linear Algebra Appl.* **378**, 135 (2004).
- [52] A function with a compact support decays more rapidly than any polynomial. Thus, due to Sobolev's lemma, all orders of

- derivatives of its Fourier transform exist; see, e.g., Refs. [21] and [45] and references therein.
- [53] A. M. Perelomov, *Generalized Coherent States and Their Applications* (Springer-Verlag, Berlin, 1986).
 - [54] T. Kiesel and W. Vogel, Universal nonclassicality witnesses for harmonic oscillators, *Phys. Rev. A* **85**, 062106 (2012).
 - [55] B. Kühn and W. Vogel, Visualizing nonclassical effects in phase space, *Phys. Rev. A* **90**, 033821 (2014).
 - [56] C. K. Hong, Z. Y. Ou, and L. Mandel, Measurement of Subpicosecond Time Intervals Between two Photons by Interference, *Phys. Rev. Lett.* **59**, 2044 (1987).
 - [57] A. Christ and C. Silberhorn, Limits on the deterministic creation of pure single-photon states using parametric down-conversion, *Phys. Rev. A* **85**, 023829 (2012).
 - [58] S. Castelletto, I. P. Degiovanni, V. Schettini, and A. Migdall, Optimizing single-photon-source heralding efficiency and detection efficiency metrology at 1550 nm using periodically poled lithium niobate, *Metrologia* **43**, S56 (2006).
 - [59] T. B. Pittman, B. C. Jacobs, and J. D. Franson, Heralding single photons from pulsed parametric down-conversion, *Opt. Commun.* **246**, 545 (2005).
 - [60] A. B. U'Ren, C. Silberhorn, K. Banaszek, and I. A. Walmsley, Efficient Conditional Preparation of High-Fidelity Single Photon States for Fiber-Optic Quantum Networks, *Phys. Rev. Lett.* **93**, 093601 (2004).
 - [61] A. I. Lvovsky, H. Hansen, T. Aichele, O. Benson, J. Mlynek, and S. Schiller, Quantum State Reconstruction of the Single-Photon Fock State, *Phys. Rev. Lett.* **87**, 050402 (2001).
 - [62] V. Potocek and S. M. Barnett, On the exponential form of the displacement operator for different systems, *Phys. Scripta* **90**, 065208 (2015).
 - [63] S. Wallentowitz and W. Vogel, Quantum-mechanical counterpart of nonlinear optics, *Phys. Rev. A* **55**, 4438 (1997).
 - [64] T. Kiesel, W. Vogel, M. Bellini, and A. Zavatta, Nonclassicality quasi-probability of single-photon-added thermal states, *Phys. Rev. A* **83**, 032116 (2011).
 - [65] T. Kiesel, W. Vogel, B. Hage, and R. Schnabel, Direct Sampling of Negative Quasiprobabilities of a Squeezed State, *Phys. Rev. Lett.* **107**, 113604 (2011).
 - [66] S. Wallentowitz and W. Vogel, Reconstruction of the Quantum-Mechanical State of a Trapped Ion, *Phys. Rev. Lett.* **75**, 2932 (1995).
 - [67] R. J. Glauber, *Quantum Optics and Electronics* (Gordon and Breach, New York, 1965).
 - [68] W. Vogel and J. Grabow, Statistics of difference events in homodyne detection, *Phys. Rev. A* **47**, 4227 (1993).

Time-dependent nonlinear Jaynes-Cummings dynamics of a trapped ion

F. Krumm* and W. Vogel

Arbeitsgruppe Theoretische Quantenoptik, Institut für Physik, Universität Rostock, D-18059 Rostock, Germany

(Received 22 February 2018; published 6 April 2018)

In quantum interaction problems with explicitly time-dependent interaction Hamiltonians, the time ordering plays a crucial role for describing the quantum evolution of the system under consideration. In such complex scenarios, exact solutions of the dynamics are rarely available. Here we study the nonlinear vibronic dynamics of a trapped ion, driven in the resolved sideband regime with some small frequency mismatch. By describing the pump field in a quantized manner, we are able to derive exact solutions for the dynamics of the system. This eventually allows us to provide analytical solutions for various types of time-dependent quantities. In particular, we study in some detail the electronic and the motional quantum dynamics of the ion, as well as the time evolution of the nonclassicality of the motional quantum state.

DOI: [10.1103/PhysRevA.97.043806](https://doi.org/10.1103/PhysRevA.97.043806)**I. INTRODUCTION**

The verification and quantification of nonclassical effects, that is, phenomena which cannot be explained by Maxwell's equations, is a main concern of theoretical and experimental quantum optics. Many of those effects, like squeezing [1–5], entanglement [6,7], and photon antibunching [8], were intensively investigated over many decades. However, there are effects beyond this set, like, for example, anomalous quantum correlations [9–11], which arise from the violation of field-intensity inequalities. In such and related scenarios a subject of interest is the investigation of the interplay of free fields and fields which are attributed to sources, which play an important role in the theory of spectral filtering of light [12,13]. The relationships between field correlation functions of free-field and source-field operators were, for example, considered in [14,15]. Hence, the treatment of a physical system containing contributions from both kinds of fields is an interesting aspect to be studied, especially when the corresponding dynamics is exactly solvable. A suitable model for this purpose is the Jaynes-Cummings model, which contains not only free-field parts but a source-attributed part as well. In the following we will briefly reconsider its history and possible areas of application.

When the Jaynes-Cummings model was proposed in 1963 [16,17], its practical relevance was doubted, as it describes an idealized scenario of the resonant interaction of a two-level system with only a single radiation mode. However, in the 1980s the model's importance was vastly enhanced, since, due to technical progress, it was possible to experimentally prove many of its predictions [18–21]. Remarkably, despite its simplicity, the Jaynes-Cummings model exhibits plenty of physical effects, e.g., Rabi oscillations [22–24], collapse and revivals [21,25,26], squeezing [27,28], atom-field entanglement [29–31], antibunching [32–34], and nonclassical states such as Schrödinger cat [35,36] and Fock states [37–39].

Initially intended for describing the interaction of a single atom with a single radiation mode, the Jaynes-Cummings model could be applied to a variety of physical scenarios. Examples are Cooper-pair boxes [40,41], “flux” qubits [42], and Josephson junctions [43–45]. It can also be applied in solid-state systems to describe the (strong) coupling of qubits to a cavity mode, for example in quantum dots [46–49] or superconducting circuits [50–52]. Another recent application of the Jaynes-Cummings model is the description of Rydberg-blockaded atomic ensembles [53,54].

The Jaynes-Cummings model also became relevant for the vibronic dynamics of trapped ions, where the quantized mode of the electromagnetic field is replaced by the quantized center-of-mass-motion of the ion [55–57]. Later on, a nonlinear Jaynes-Cummings model (NJCM) was introduced [58], which describes the dynamics of a trapped ion beyond the standard Lamb-Dicke regime [59,60]. The motional degrees of freedom are coupled to the electronic states of the ion by a classical pump field in the resolved sideband regime. On this basis it became possible to generate many motional states for trapped ions, such as Fock states, squeezed states [59,61], even and odd coherent states [62], nonlinear coherent states [63], pair coherent states [64], superpositions of the latter [65], SU(1,1) intelligent states [66], Schrödinger cat states [67,68], entangled coherent states [68], and generalized Kerr-type states [69]. As for the standard Jaynes-Cummings Hamiltonian (see, for example, [70]), the trapped-ion dynamics based on the nonlinear Jaynes-Cummings model was also considered beyond the rotating-wave approximation [71–74].

In the present paper we study the vibronic nonlinear Jaynes-Cummings model, when the classical driving laser field is slightly detuned from the k th sideband. Such a mismatch yields an explicitly time-dependent Hamiltonian in the Schrödinger picture, the corresponding dynamics of which is not easily solved due to the relevance of time-ordering effects. We will demonstrate that these difficulties can be resolved by extending the Hilbert space of the problem to include the driving field in the quantum description. On this basis, the full dynamics will become exactly solvable. This renders it possible to study

*fabian.krumm@uni-rostock.de

sophisticated problems of explicitly time-dependent dynamics on the basis of the exactly solvable extended problem. This yields deeper insight into the yet rarely studied quantum dynamics in cases when explicitly time-dependent Hamiltonians and the resulting time-ordering prescriptions are relevant. Also the quantum effects and the nonclassical correlation properties of the system can be studied by this method in great depth.

The paper is structured as follows. Section II introduces the Hamiltonian used in this paper and briefly discusses its physical meaning as well as time-ordering effects. In Sec. III, we solve the dynamics using the eigenstates of the generalized Hamiltonian. Afterwards, in Sec. IV, we use the regularized Glauber-Sudarshan P function to study the nonclassical evolution of the motional quantum properties of the ion. Finally, a summary and some conclusions follow in Sec. V.

II. EXPLICITLY TIME-DEPENDENT NONLINEAR JAYNES-CUMMINGS MODEL

The NJCM for the vibronic coupling between the electronic and motional degrees of freedom of a trapped ion was introduced for the situation of the exactly resonant interaction of a laser field with the k th vibronic sideband of the ion [58,75]. This interaction Hamiltonian can be exactly diagonalized. It was experimentally demonstrated that it properly describes the dynamics of a trapped ion for the case of $k = 1$ [59]. In the present paper we are interested in more sophisticated time-dependent quantum phenomena of such a system. For this reason, in a first step we generalize the NJCM to allow for the explicitly time-dependent dynamics. In this case, however, an exact solution of the problem seems to be not feasible and numerical solutions are required.

A. Explicitly time-dependent Hamiltonian

Let us start with the following Hamiltonian, describing an ion, trapped in a harmonic trap potential, interacting with a classical laser field (see [58] and Chap. 13 of [75]):

$$\hat{H}(t) = \underbrace{(\hbar\nu\hat{a}^\dagger\hat{a} + \hbar\omega_{21}\hat{A}_{22})}_{=\hat{H}_0} \quad (1)$$

$$+ \underbrace{\{\hbar\kappa|\beta_{cl}|e^{-i\omega_L t}\hat{A}_{21}\hat{g}[\eta(\hat{a} + \hat{a}^\dagger)] + \text{H.c.}\}}_{=\hat{H}_{\text{int}}(t)}. \quad (2)$$

\hat{H}_0 describes the free motion of the vibrational center-of-mass and electronic degrees of freedom of the two-level ion, with the vibrational frequency ν and the electronic transition frequency $\omega_{21} = \omega_2 - \omega_1$. The laser is assumed to be monochromatic and quasis resonant with the electronic $|1\rangle \leftrightarrow |2\rangle$ transition, $\omega_L \approx \omega_{21}$, and to have only one nonvanishing wave-vector component, such that only one motional degree of freedom appears in the interaction term. The complex amplitude β_{cl} describes the pump laser. The operators \hat{a}^\dagger (\hat{a}) are the creation (annihilation) operators of the vibrational frequency ν . The electronic flip operators $\hat{A}_{ij} = |i\rangle\langle j|$ ($i, j = 1, 2$) describe the atomic $|j\rangle \rightarrow |i\rangle$ transitions, κ is a projection of the electric-dipole matrix element on the direction of the electrical field, and $g[\eta(\hat{a} + \hat{a}^\dagger)]$ describes the mode structure of the pump laser at the operator-valued position of the ion. For a standing

wave it reads as

$$g[\eta(\hat{a} + \hat{a}^\dagger)] = \cos[\eta(\hat{a} + \hat{a}^\dagger) + \Delta\phi], \quad (3)$$

where $\Delta\phi$ defines the relative position of the trap potential to the laser wave. The Lamb-Dicke parameter η describes the effects of momentum transfer on the atomic wave packet due to recoil effects.

Applying the Baker-Campbell-Hausdorff formula in \hat{g} together with a power series expansion, we get

$$\hat{g}[\eta(\hat{a} + \hat{a}^\dagger)] = \frac{1}{2}e^{i\Delta\phi - \eta^2/2} \sum_{l,m=0}^{\infty} \frac{(i\eta)^{l+m}}{l!m!} \hat{a}^{\dagger l} \hat{a}^m + \text{H.c.} \quad (4)$$

The interaction Hamiltonian in the interaction picture (indicated by the tilde) reads as

$$\begin{aligned} \hat{\tilde{H}}_{\text{int}}(t) &= \frac{1}{2}\hbar\kappa|\beta_{cl}|\hat{A}_{21}e^{-\eta^2/2} \\ &\times \sum_{l,m=0}^{\infty} \frac{\hat{a}^{\dagger l} \hat{a}^m}{l!m!} e^{-i[\omega_L - \omega_{21} + (m-l)\nu]t} \\ &\times \{e^{i\Delta\phi}(i\eta)^{l+m} + e^{-i\Delta\phi}(-i\eta)^{l+m}\} + \text{H.c.} \end{aligned} \quad (5)$$

If the laser is exactly resonant to the k th vibrational sideband, this yields the exactly solvable nonlinear Jaynes-Cummings interaction [58,75].

For the purpose of the present paper, we are interested in the situation when the laser is slightly detuned from the k th sideband:

$$\omega_L = \omega_{21} - k\nu + \Delta\omega, \quad (6)$$

with $\Delta\omega \ll \nu$. We still assume that the ion is in the resolved sideband limit, i.e., we can resolve the single sidebands very well. This means that the linewidths of the vibronic transitions and the coupling strength $|\kappa|$ are small compared to the vibrational frequency ν . In this case one only excites vibronic transitions which are quasis resonant according to the condition in Eq. (6), which are the $|1, n\rangle \leftrightarrow |2, n-k\rangle$ transitions for $k \geq 0$. Hence, we perform a vibrational rotating-wave approximation,

$$e^{\mp i n \nu t} = 0 \quad \forall n \neq 0, \quad (7)$$

in Eq. (5). This yields the interaction Hamiltonian

$$\hat{\tilde{H}}_{\text{int}}(t) = \hbar\kappa|\beta_{cl}|e^{-i\Delta\omega t}\hat{A}_{21}\hat{f}_k(\hat{a}^\dagger\hat{a}; \eta)\hat{a}^k + \text{H.c.}, \quad (8)$$

where

$$\begin{aligned} \hat{f}_k(\hat{a}^\dagger\hat{a}; \eta) &= \frac{1}{2}e^{i\Delta\phi - \eta^2/2} \sum_{l=0}^{\infty} \frac{(i\eta)^{2l+k}}{l!(l+k)!} \hat{a}^{\dagger l} \hat{a}^l + \text{H.c.} \\ &= \frac{1}{2}e^{i\Delta\phi - \eta^2/2} \sum_{n=0}^{\infty} |n\rangle\langle n| \\ &\times \frac{(i\eta)^k n!}{(n+k)!} L_n^{(k)}(\eta^2) + \text{H.c.}, \end{aligned} \quad (9)$$

with $L_n^{(k)}$ denoting the generalized Laguerre polynomials. The Hamiltonian (8) describes the nonlinear k th sideband coupling of the vibrational mode and the electronic transition, $|1, n\rangle \leftrightarrow |2, n-k\rangle$ (see Fig. 1). It is important that this nonlinear interaction is explicitly time dependent, as long as $\Delta\omega \neq 0$.

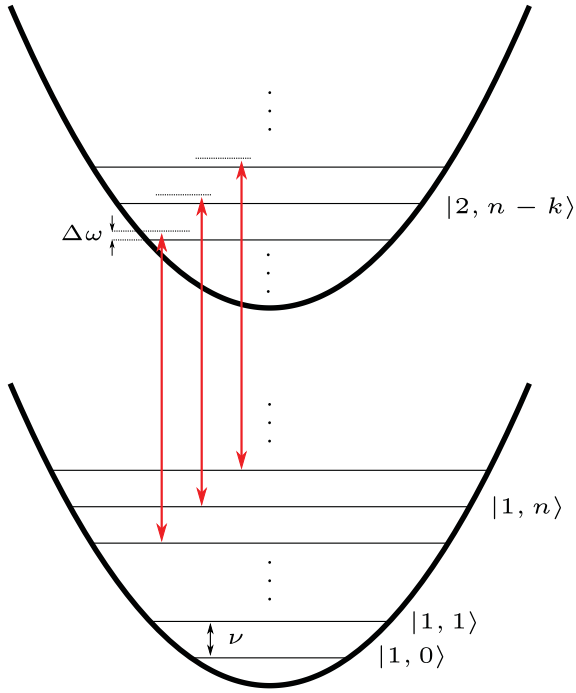


FIG. 1. Scheme of the dynamics described by the interaction Hamiltonian (8). The two electronic states, ground state $|1\rangle$ (lower potential-energy surface) and excited state $|2\rangle$ (upper potential-energy surface), are separated by the electric transition frequency $\omega_{21} = \omega_2 - \omega_1$. Since the (harmonic) trap potential is not influenced by the ion dynamics, the energy surfaces are neither displaced nor distorted and the vibronic levels are separated equidistantly by ν . The laser frequency $\omega_L = \omega_{21} - kv + \Delta\omega$ (red arrows) is not in exact resonance with the $|1, n\rangle \leftrightarrow |2, n-k\rangle$ transition but slightly detuned by $\Delta\omega$.

B. Solution of the time-dependent interaction and time-ordering effects

The most general solution of the time evolution of a quantum system, described by its Hamiltonian $\hat{H}(t)$, is given by its time-evolution operator:

$$\hat{U}(t) = \mathcal{T} \exp \left\{ \frac{-i}{\hbar} \int_{t_0}^t \hat{H}(t') dt' \right\}, \quad (10)$$

where \mathcal{T} denotes the time-ordering prescription. The latter accounts for the temporal order of the Hamiltonians with different time arguments contained in the exponential function. If the Hamiltonian, however, is not explicitly time dependent or commuting with itself at different times, the ordering symbol \mathcal{T} becomes superfluous and the standard exponential power series of \hat{H} is recovered.

Alternatively, the representation (10) can also be given in the form of the Magnus expansion [76,77]:

$$\hat{U}(t) = \exp \left\{ \frac{-i}{\hbar} \int_{t_0}^t \hat{H}(t') dt' + \sum_{n=1}^{\infty} \hat{\Omega}_n(t) \right\}, \quad (11)$$

which is unitary in each order n , with $n = 1, \dots, \infty$. Herein, the contributions of $\hat{\Omega}_n(t)$ are referred to as *time-ordering effects* or *time-ordering corrections* [78–82]. However, the $\hat{\Omega}_n(t)$ contain multiple integrals of nested commutators of the

Hamiltonians at different times which are, especially for higher orders, difficult to handle. A possibility to circumvent this problem was presented in [83], where only one commutator needs to be evaluated. However, in this representation a needed diagonalization of the operator-valued problem is not trivial, as the different orders of the expansion do not necessarily possess a common eigenbasis. For certain physical models and regimes, the time-ordering symbol \mathcal{T} in (10) can be neglected, for example for parametric down-conversion with not too high pump powers [78]. Hence, let us begin to study the influence of time-ordering effects on the dynamics described by the Hamiltonian in Eq. (8).

For this purpose we use the open-source software package QUTIP [84,85] in PYTHON to obtain numerically the time-ordered solutions based on Eq. (10) together with the Hamiltonian (8). To visualize the effects of time ordering, we compare the solutions with those when the time ordering is discarded, $\hat{U} \rightarrow \hat{U}'$:

$$\hat{U}'(t) = \exp \left\{ \frac{-i}{\hbar} \int_{t_0}^t \hat{H}_{\text{int}}(t') dt' \right\}. \quad (12)$$

In this case the integral can be directly evaluated:

$$\begin{aligned} \int_{t_0}^t \hat{H}_{\text{int}}(t') dt' &= \hbar \kappa |\beta_{\text{cl}}| \frac{i}{\Delta\omega} (e^{-i\Delta\omega t} - e^{-i\Delta\omega t_0}) \\ &\times \hat{A}_{21} \hat{f}_k(\hat{a}^\dagger \hat{a}; \eta) \hat{a}^k + \text{H.c.} \end{aligned} \quad (13)$$

For convenience we introduce the dimensionless quantities

$$r := \frac{\Delta\omega}{|\kappa\beta_{\text{cl}}|}, \quad (14)$$

$$\tau_{(0)} := |\kappa\beta_{\text{cl}}| t_{(0)}, \quad (15)$$

such that

$$\Delta\omega t_{(0)} = r \tau_{(0)}. \quad (16)$$

Furthermore, we define $h(\tau) := i(e^{-ir\tau} - e^{-ir\tau_0})$. Hence, we have

$$\hat{U}'(t) = \exp \left\{ -i \left[\frac{h(\tau)}{r} e^{i \arg(\kappa)} \hat{A}_{21} \hat{f}_k(\hat{a}^\dagger \hat{a}; \eta) \hat{a}^k + \text{H.c.} \right] \right\} \quad (17)$$

and we assume $\arg(\kappa) = 0$ from now on.

The eigenstates of the integrated Hamiltonian (13) read as

$$|\psi_n^\pm\rangle = c_n^\pm (|2, n\rangle + \alpha_n^\pm |1, n+k\rangle), \quad (18)$$

with $|i, n\rangle$ denoting the electronic ($i = 1, 2$) and motional ($n = 0, 1, 2, \dots$) excitations (see, e.g., Chap. 12 of [75]). Due to normalization we find immediately $c_n^\pm = \frac{1}{\sqrt{1+|\alpha_n^\pm|^2}}$. These states $|\psi_n^\pm\rangle$ are often referred to as “dressed states.” Solving

$$\left[\frac{h(\tau)}{r} \hat{A}_{21} \hat{f}_k(\hat{a}^\dagger \hat{a}; \eta) \hat{a}^k + \text{H.c.} \right] |\psi_n^\pm\rangle \stackrel{!}{=} \omega_n^\pm |\psi_n^\pm\rangle \quad (19)$$

yields the parameters

$$\begin{aligned} \alpha_n^\pm &= \pm e^{-i \arg[f_k(n; \eta) h(\tau)]}, \quad c_n^\pm = \frac{1}{\sqrt{2}}, \\ \omega_n^\pm &= \pm \frac{|f_k(n; \eta) h(\tau)|}{r} \sqrt{\frac{(n+k)!}{n!}} \equiv \omega_n^\pm(\tau), \end{aligned} \quad (20)$$

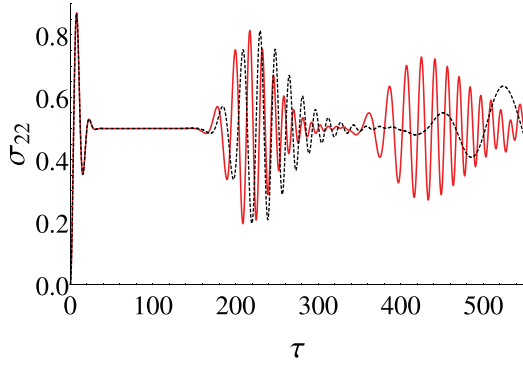


FIG. 2. Influence of the time ordering on the population dynamics of the excited electronic state of the ion. The curves represent the numerical solution $\sigma_{22}(\tau)$ (solid, red line) for a small mismatch $r = 0.005$ and, for the same r , the analytical solution without time ordering, $\sigma'_{22}(\tau)$ (dashed, black line). The motional degree of freedom is initially prepared in the coherent state $|\alpha_0\rangle$. Parameters: $\alpha_0 = \sqrt{12}$, $k = 2$, $\Delta\phi = 0$, and $\eta = 0.2$.

where $f_k(n; \eta) = \langle n | \hat{f}_k(\hat{a}^\dagger \hat{a}; \eta) | n \rangle$ [see Eq. (9)]. The completeness relation of these states reads

$$\hat{1} = \sum_{\sigma=\pm} \sum_{n=0}^{\infty} |\psi_n^\sigma\rangle \langle \psi_n^\sigma| + \sum_{q=0}^{k-1} |1, q\rangle \langle 1, q|. \quad (21)$$

This yields the time evolution operator (17) in the form

$$\hat{U}'(\tau) = \sum_{\sigma=\pm} \sum_{n=0}^{\infty} e^{-i\omega_n^\sigma(\tau)} |\psi_n^\sigma\rangle \langle \psi_n^\sigma|, \quad (22)$$

since the $\sum_{q=0}^{k-1} |1, q\rangle \langle 1, q|$ part cancels, as $\hat{a}^k |q\rangle = 0$ for $q < k$.

For further investigations let us consider the population probability of the excited electronic state, which was studied only for $\Delta\omega = 0$ in [58]:

$$\sigma'_{22}(\tau) = \sum_{n=0}^{\infty} \langle 2, n | \hat{U}'(\tau) \hat{U}_0(\tau) \hat{\rho}(0) \hat{U}_0(\tau)^\dagger \hat{U}'(\tau)^\dagger | 2, n \rangle, \quad (23)$$

which is given now in dependence on the scaled time τ . For the visualization we chose the input state $|1, \alpha_0\rangle$ at $\tau_0 = 0$. The atom is initially prepared in the electronic ground state and the motional state of the ion is a coherent state. Details concerning the coherent-state preparation of the motional state of the ion can be found in [59,86]. This eventually yields

$$\begin{aligned} \sigma'_{22}(\tau) &= \frac{1}{4} \sum_{n=0}^{\infty} \sum_{\sigma, \sigma'=\pm} e^{i[\omega_n^\sigma(\tau) - \omega_n^{\sigma'}(\tau)]} \\ &\times (\alpha_n^{\sigma'})^* \alpha_n^\sigma \frac{|\alpha_0|^{2n+2k}}{(n+k)!} e^{-|\alpha_0|^2}. \end{aligned} \quad (24)$$

Note that the $\hat{U}_0(\tau)$ contributions cancel each other. The temporal evolution of $\sigma'_{22}(\tau)$ is depicted in Fig. 2.

The correct numerical solution significantly differs from the analytical one without time ordering. That is, neglecting the time-ordering effects, even for a very small frequency mismatch r , strongly falsifies the electronic population dynamics.

Hence, the \mathcal{T} ordering plays an important role and it must not be omitted.

III. NONLINEAR JAYNES-CUMMINGS MODEL WITH QUANTIZED PUMP

In this section we will overcome the shortcoming of the nonlinear Jaynes-Cummings model with frequency mismatch by quantization of the pump field. In practice, this can be realized by placing the trapped ion in a high- Q cavity. Now a mode of the quantized cavity field pumps the vibronic transition. We will see that this extension of the Hilbert space allows us to exactly solve the full interaction problem. This opens new possibilities to study problems underlying time ordering analytically, which are not solvable in a semiclassical approach.

A. Quantization of the pump field

As shown above, the explicit time dependence of the Hamiltonian (8) prevents an analytical solution of the dynamics as we cannot discard—even approximately—the time-ordering effects. Hence, our aim is to eliminate the time dependence in the Hamiltonian $\hat{H}(t)$. For this purpose we return to the Hamiltonian (2) and quantize the pump field by replacing

$$|\beta_{cl}| e^{-i\omega_L t} \rightarrow \hat{b}, \quad (25)$$

where \hat{b} is the annihilation operator of the pump quanta in the Schrödinger picture. The semiclassical time dependence is thus transformed into the free evolution of the operator \hat{b} . In practice this can be realized via QED with a trapped ion (for theory and corresponding experiments, see [87,88] and [89,90], respectively).

The total Hamiltonian $\hat{\mathcal{H}}$, in the Schrödinger picture, including the quantized pump field, reads as

$$\hat{\mathcal{H}} = \underbrace{(\hbar\nu\hat{a}^\dagger\hat{a} + \hbar\omega_L\hat{b}^\dagger\hat{b} + \hbar\omega_{21}\hat{A}_{22})}_{=\hat{\mathcal{H}}_0} \quad (26)$$

$$+ \underbrace{\{\hbar\kappa\hat{A}_{21}\hat{b}\hat{g}[\eta(\hat{a} + \hat{a}^\dagger)] + \text{H.c.}\}}_{=\hat{\mathcal{H}}_{\text{int}}}, \quad (27)$$

which is now time independent. As in the semiclassical case [see Eq. (2)], this Hamiltonian is again based on the optical rotating-wave approximation. The modified free Hamiltonian, $\hat{\mathcal{H}}_0$, now includes the free evolution of the quantized pump field with the frequency ω_L . Here, we again assume that we operate in the resolved sideband regime and quasiresonantly drive the $|1, n\rangle \leftrightarrow |2, n-k\rangle$ transitions in the vibronic rotating-wave approximation. As before, only those terms of \hat{g} are relevant which belong to this transition [see Eq. (4)]:

$$\hat{g}[\eta(\hat{a} + \hat{a}^\dagger)] \rightarrow \hat{f}_k(\hat{a}^\dagger \hat{a}; \eta) \hat{a}^k, \quad (28)$$

with \hat{f}_k being defined in Eq. (9). Thus, we arrive at

$$\hat{\mathcal{H}}_{\text{int}} = \hbar\kappa\hat{A}_{21}\hat{b}\hat{f}_k(\hat{a}^\dagger \hat{a}; \eta)\hat{a}^k + \text{H.c.} \quad (29)$$

The interpretation of the Hamiltonian (29) is the following: A pump photon is absorbed (\hat{b}) and the ion is excited (\hat{A}_{21}). The vibrational transitions ($\hat{f}_k(\hat{a}^\dagger \hat{a}; \eta)\hat{a}^k$) occur according to our chosen quasiresonance condition, $|n\rangle \rightarrow |n-k\rangle$. The H.c. term in addition describes the emission of a pump photon

(\hat{b}^\dagger), accompanied by the electronic transition $|2\rangle \rightarrow |1\rangle$ and the vibrational transition $|n-k\rangle \rightarrow |n\rangle$. As before, the pump field is not exactly on resonance, as $\Delta\omega \neq 0$. In the case of interest, $\Delta\omega \ll \nu$, only the wanted transitions significantly contribute to the dynamics. Since the resulting Hamiltonian is not explicitly time dependent anymore, we obtain the time-evolution operator in the form

$$\hat{U}(t) = \exp \left\{ -\frac{i(t-t_0)}{\hbar} [\hat{H}_0 + \hat{H}_{\text{int}}] \right\}, \quad (30)$$

with the definitions of the Hamiltonian according to Eqs. (26) and (29).

B. Solution for the quantized pump field

In this section we solve the time-evolution problem based on the operator (30), i.e., we derive an analytical expression for $\hat{U}(t)$. Our full Hamiltonian [see Eqs. (26) and (29)] reads as

$$\begin{aligned} \hat{H} = & (\hbar\nu\hat{a}^\dagger\hat{a} + \hbar\omega_L\hat{b}^\dagger\hat{b} + \hbar\omega_{21}\hat{A}_{22}) \\ & + [\hbar\kappa\hat{A}_{21}\hat{b}^\dagger\hat{f}_k(\hat{a}^\dagger\hat{a};\eta)\hat{a}^k + \text{H.c.}], \end{aligned} \quad (31)$$

The eigenstates of this Hamiltonian are

$$|\psi_{mn}^\pm\rangle = c_{mn}^\pm(|2,m,n\rangle + \alpha_{mn}^\pm|1,m+1,n+k\rangle), \quad (32)$$

where $|i,m,n\rangle$ denotes the electronic, pump-photon ($m = 0, 1, 2, \dots$), and motional excitations. The normalization yields $c_{mn}^\pm = \frac{1}{\sqrt{1+|\alpha_{mn}^\pm|^2}}$. The general procedure resembles that in Sec. II B. However, now we have an additional mode and we will solve the problem in the Schrödinger picture.

The parameters are found to be

$$\begin{aligned} \alpha_{mn}^\pm &= \frac{\Delta\omega \pm \sqrt{\Delta\omega^2 + |\Omega_{mn}|^2}}{\Omega_{mn}}, \\ \omega_{mn}^\pm &= \frac{1}{2} \{ \Delta\omega(2m+1) + \nu(2n-2km) + \omega_{21}(2m+2) \\ &\quad \pm \sqrt{\Delta\omega^2 + |\Omega_{mn}|^2} \}, \end{aligned} \quad (33)$$

where we used Eq. (6) and defined

$$\Omega_{mn} = 2\kappa\sqrt{m+1}f_k(n;\eta)\sqrt{\frac{(n+k)!}{n!}}. \quad (34)$$

Here, ω_{mn}^\pm are the eigenvalues of \hat{H} , associated with the eigenstates $|\psi_{mn}^\pm\rangle$, and Ω_{mn} is the nonlinear k -quantum Rabi frequency, which was already discussed in [58]. For the present problem there occurs in Eq. (34) the additional factor $\sqrt{m+1}$, which is caused by the quantum treatment of the pump field.

The completeness relation reads

$$\begin{aligned} \hat{1} = & \sum_{\sigma=\pm} \sum_{m,n=0}^{\infty} |\psi_{mn}^\sigma\rangle\langle\psi_{mn}^\sigma| + \sum_{n=0}^{\infty} |1,0,n\rangle\langle 1,0,n| \\ & + \sum_{m=0}^{\infty} \sum_{q=0}^{k-1} |1,m+1,q\rangle\langle 1,m+1,q|. \end{aligned} \quad (35)$$

Using the latter, we can rewrite the full time-evolution operator, Eq. (30), in the form

$$\begin{aligned} \hat{U}(t) = & \sum_{\sigma=\pm} \sum_{m,n=0}^{\infty} e^{-i\omega_{mn}^\sigma\Delta t} |\psi_{mn}^\sigma\rangle\langle\psi_{mn}^\sigma| \\ & + \sum_{n=0}^{\infty} e^{-i\nu n\Delta t} |1,0,n\rangle\langle 1,0,n| \\ & + \sum_{m=0}^{\infty} \sum_{q=0}^{k-1} e^{-i[\nu q + \omega_L(m+1)]\Delta t} \\ & \times |1,m+1,q\rangle\langle 1,m+1,q|, \end{aligned} \quad (36)$$

with $\Delta t = t - t_0$. For convenience we use the scaled (dimensionless) parameters:

$$\begin{aligned} \Delta\tilde{t} &:= |\kappa|\Delta t, \quad \tilde{\nu} := \nu/|\kappa|, \quad \tilde{\omega}_{21,L} := \omega_{21,L}/|\kappa|, \\ \tilde{\Omega}_{mn} &:= \Omega_{mn}/|\kappa|, \quad \tilde{\Delta\omega} := \Delta\omega/|\kappa|, \end{aligned} \quad (37)$$

with $\Delta\tilde{t} = \tilde{t} - \tilde{t}_0$. In terms of these dimensionless quantities the unitary time-evolution operator reads as

$$\begin{aligned} \hat{U}(\tilde{t}) = & \sum_{\sigma=\pm} \sum_{m,n=0}^{\infty} e^{-i\tilde{\omega}_{mn}^\sigma\Delta\tilde{t}} |\psi_{mn}^\sigma\rangle\langle\psi_{mn}^\sigma| \\ & + \sum_{n=0}^{\infty} e^{-i\tilde{\nu}n\Delta\tilde{t}} |1,0,n\rangle\langle 1,0,n| \\ & + \sum_{m=0}^{\infty} \sum_{q=0}^{k-1} e^{-i[\tilde{\nu}q + \tilde{\omega}_L(m+1)]\Delta\tilde{t}} \\ & \times |1,m+1,q\rangle\langle 1,m+1,q|, \end{aligned} \quad (38)$$

where

$$\begin{aligned} \tilde{\omega}_{mn}^\pm &= \frac{1}{2} \{ \Delta\tilde{\omega}(2m+1) + \tilde{\nu}(2n-2km) + \tilde{\omega}_{21}(2m+2) \\ &\quad \pm \sqrt{[\Delta\tilde{\omega}]^2 + |\tilde{\Omega}_{mn}|^2} \}. \end{aligned} \quad (39)$$

C. Semiclassical versus quantized pump

Let us now compare the analytical results obtained from the solution of the quantized-pump dynamics with the numerical solutions (see Sec. II B) for a classical pump field, when the Hamiltonian is explicitly time dependent [see Eq. (8)]. As an example, we calculate the occupation probability of the excited electronic state:

$$\sigma_{22}(\tilde{t}) = \sum_{m,n} \langle 2,n,m | \hat{\rho}(\tilde{t}) | 2,n,m \rangle \quad (40)$$

where $\hat{\rho}(\tilde{t}) = \hat{U}(\tilde{t})\hat{\rho}(0)\hat{U}(\tilde{t})^\dagger$ is the full density matrix of the state. Using the input state $\hat{\rho}(0) = |1,\beta_0,\alpha_0\rangle\langle 1,\beta_0,\alpha_0|$ at $\tilde{t}_0 = 0$, the analytical treatment yields

$$\begin{aligned} \sigma_{22}(\tilde{t}) = & \sum_{m,n=0}^{\infty} \sum_{\sigma,\sigma'=\pm} e^{i[\tilde{\omega}_{mn}^{\sigma'} - \tilde{\omega}_{mn}^\sigma]\tilde{t}} |c_{mn}^\sigma c_{mn}^{\sigma'}|^2 \\ & \times (\alpha_{mn}^\sigma)^* \alpha_{mn}^{\sigma'} \frac{|\beta_0|^{(2m+2)} |\alpha_0|^{(2n+2k)}}{(m+1)!(n+k)!} e^{-|\beta_0|^2 - |\alpha_0|^2}. \end{aligned} \quad (41)$$

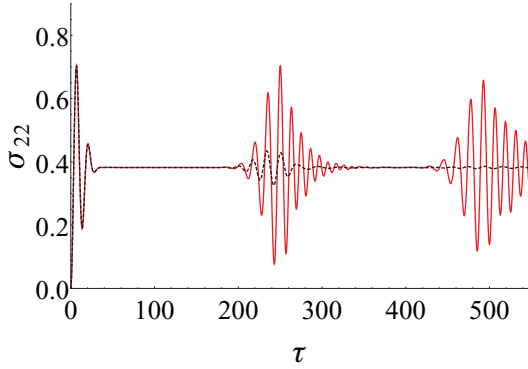


FIG. 3. Comparison of the numerical solution for the classical pump, using the Hamiltonian (8) in Eq. (10) (solid, red line) for $r = 0.2$ [see Eq. (14)], with the analytical solution for the quantized pump field for $\beta_0 = 20$ (dashed, black line). To obtain an equal time scaling of the semiclassical and quantum results, the latter solution was adjusted according to $\Delta\tilde{\omega} = |\beta_0|r = 4$ [see Eq. (14)] and $\tilde{t} = \tau/|\beta_0|$ [see Eq. (15)]. The initial state of the quantized motion was assumed to be a coherent state $|\alpha_0\rangle$. Parameters: $\alpha_0 = \sqrt{12}$, $k = 2$, $\Delta\phi = 0$, and $\eta = 0.2$.

Note that, due to the dependence on $\tilde{\omega}_{mn}^{\sigma'} - \tilde{\omega}_{mn}^{\sigma}$, there is no dependence of $\sigma_{22}(\tilde{t})$ on \tilde{v} and $\tilde{\omega}_{21}$.

Let us consider the evolution for a relatively weak pump amplitude (see Fig. 3). We see that, excluding the short-time dynamics, the solutions with classical and quantized pump differ significantly from each other. Hence, the used pump amplitude is by far not sufficiently large to be referred to as “quasiclassical.”

In the case of a stronger pump field (see Fig. 4), we indeed obtain a dynamics which is almost identical to the numerical solution for a classical pump field. This not only enables us to conclude which pump amplitudes are needed such that the pump can be treated as a classical one on the corresponding time scale but also reveals that the solution found via quantization of the pump yields a more general description of the quantum system under study, where the time ordering is contained via the extension of the Hilbert space

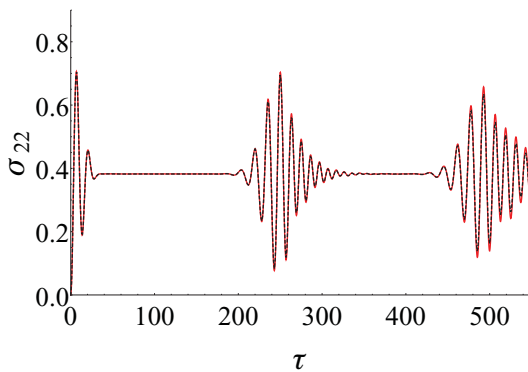


FIG. 4. The same as in Fig. 3, but for a strong quantized pump with $\beta_0 = 100$ and $\Delta\tilde{\omega} = |\beta_0|r = 20$.

IV. EVOLUTION OF NONCLASSICALITY

In this section we use the solution Eq. (38), to discuss the nonclassical properties of the system. Let us first introduce the notion of nonclassicality to be used in the following.

A. The regularized P function

Using the Glauber-Sudarshan P function [91,92], $P(\alpha; t)$, any quantum state, given by its density operator $\hat{\rho}(t)$ at time t , can be expressed as a mixture of coherent states $|\alpha\rangle$:

$$\hat{\rho}(t) = \int d^2\alpha P(\alpha; t) |\alpha\rangle \langle \alpha|. \quad (42)$$

We call a state *nonclassical* if it cannot be expressed as a classical mixture of coherent states. In such cases $P(\alpha; t)$ cannot be interpreted in terms of a classical probability density [93,94], i.e., it can attain negative values in the sense of distributions. However, for many states $P(\alpha; t)$ is highly singular and, hence, it is not accessible in experiments. To uncover the negativities of $P(\alpha; t)$ it is therefore necessary to use a regularization procedure which yields a regularized version of this function [95]. This procedure was successfully applied to experimental data [96–98] and generalized to different scenarios [99–101]. Here we will only recapitulate the basic idea.

The P function is defined by the Fourier transform of the characteristic function $\Phi(\beta; t) = \langle \hat{D}(\beta; t) \rangle e^{|\beta|^2/2}$ with $\hat{D}(\beta; t) = e^{\beta \hat{a}(t)^\dagger - \beta^* \hat{a}(t)}$:

$$P(\alpha; t) = \pi^{-2} \int d^2\beta e^{\beta^* \alpha - \beta \alpha^*} \Phi(\beta; t). \quad (43)$$

The possibly occurring singular behavior of P results from the fact that $\Phi(\beta; t)$ may be unbounded and, hence, not square-integrable. According to Eq. (43), the P function can therefore be highly singular. To get experimental access to the latter, one may introduce a filter function $\Omega_w(\beta)$ with some filter width w , to define the regularized P function [95] as

$$P_\Omega(\alpha; t) = \pi^{-2} \int d^2\beta e^{\beta^* \alpha - \beta \alpha^*} \Omega_w(\beta) \Phi(\beta; t). \quad (44)$$

The resulting function $P_\Omega(\alpha; t)$ is a regular and smooth [99] function as long as the following requirements to the filter function are fulfilled:

- (1) $\Omega_w(\beta) \Phi(\beta; t)$ can be Fourier transformed for all filter widths w , with $w < \infty$.
- (2) The Fourier transform of Ω_w is a probability density, so that it is non-negative.
- (3) For a filter which is infinitely broad, $w \rightarrow \infty$, we obtain the original P function, $P_\Omega \rightarrow P$.

For an overview and the discussion of different filter functions we refer to [102].

B. Calculation of P_Ω in Fock basis

In practical calculations, to obtain the full information on the quantum state, the density matrix of the state is calculated. In the following, we implement a suitable procedure to calculate

$P_\Omega(\alpha; t)$ directly out of $\hat{\rho}(t)$. Let us first rewrite the definition of P_Ω [see Eq. (44)] in Fock state basis:

$$\begin{aligned} P_\Omega(\alpha; t) &= \pi^{-2} \int d^2\beta e^{\beta^*\alpha - \beta\alpha^*} \Omega_w(\beta) e^{|\beta|^2/2} \text{Tr}\{\hat{\rho}(t) \hat{D}(\beta; 0)\} \\ &= \sum_{m,n=0}^{\infty} \rho_{mn}(t) \underbrace{\int \frac{d^2\beta}{\pi^2} e^{\beta^*\alpha - \beta\alpha^* + |\beta|^2/2} \Omega_w(\beta) D_{nm}(\beta; 0)}_{:= P_{\Omega,nm}(\alpha)}, \end{aligned} \quad (45)$$

with $\rho_{mn}(t) = \langle m | \hat{\rho}(t) | n \rangle$ and $D_{nm}(\beta) = \langle n | \hat{D}(\beta; 0) | m \rangle$. The functions $P_{\Omega,nm}(\alpha)$ are the regularized elements of the P function in the Fock basis. In Eq. (45), the complete time evolution is contained in the density matrix elements $\rho_{mn}(t)$. The functions $P_{\Omega,nm}(\alpha)$, however, only depend on the fixed parameter w and the phase-space coordinate α . Hence, it is possible to calculate these elements only once and after that we apply them to $\hat{\rho}(t)$, for arbitrary t . Let us therefore find a suitable expression of $P_{\Omega,nm}(\alpha)$.

We make use of [75]

$$\langle n | \hat{D}(\beta; 0) | m \rangle = e^{-|\beta|^2/2} e^{i\varphi_\beta(n-m)} \Lambda_{nm}(|\beta|), \quad (46)$$

with

$$\Lambda_{nm}(|\beta|) = \begin{cases} (-|\beta|)^{m-n} \sqrt{\frac{n!}{m!}} L_n^{(m-n)}(|\beta|^2) & m \geq n \\ |\beta|^{n-m} \sqrt{\frac{m!}{n!}} L_m^{(n-m)}(|\beta|^2) & m < n \end{cases}, \quad (47)$$

where $L_n^{(k)}(x)$ are the generalized Laguerre polynomials. Using a radial symmetric filter function [102], $\Omega_w(\beta) \equiv \Omega_w(|\beta|)$ with $x = |x|e^{i\varphi_x}$ for α and β , then $P_{\Omega,nm}(\alpha)$ may be rewritten as

$$\begin{aligned} P_{\Omega,nm}(\alpha) &= \pi^{-2} \int_0^\infty d|\beta| \Lambda_{nm}(|\beta|) \Omega_w(|\beta|) |\beta| \\ &\quad \times \int_0^{2\pi} d\varphi_\beta e^{2i|\alpha\beta| \sin(\varphi_\alpha - \varphi_\beta)} e^{i\varphi_\beta(n-m)}. \end{aligned} \quad (48)$$

The phase integral can be evaluated via substitution of the limits of integration:

$$\begin{aligned} &\int_0^{2\pi} d\varphi_\beta e^{2i|\alpha\beta| \sin(\varphi_\alpha - \varphi_\beta)} e^{i\varphi_\beta(n-m)} \\ &= (-1)^{n-m} \int_{-\pi}^{\pi} d\varphi e^{-2i|\alpha\beta| \sin(\varphi_\alpha - \varphi)} e^{i\varphi(n-m)} \\ &= 2\pi e^{i(n-m)\varphi_\alpha} J_{n-m}(2|\alpha\beta|), \end{aligned} \quad (49)$$

where $J_n(x)$ are the Bessel functions of the first kind.

Finally, we arrive at the expression

$$\begin{aligned} P_{\Omega,nm}(\alpha) &= \frac{2}{\pi} e^{i(n-m)\varphi_\alpha} \int_0^\infty d|\beta| \Lambda_{nm}(|\beta|) \Omega_w(|\beta|) |\beta| \\ &\quad \times J_{n-m}(2|\alpha\beta|). \end{aligned} \quad (50)$$

This relation holds true for all radial symmetric filters $\Omega_w(|\beta|)$. We will use the filter [102]

$$\Omega_w(|\beta|) = \frac{2}{\pi} \left[\arccos\left(\frac{|\beta|}{2w}\right) - \frac{|\beta|}{2w} \sqrt{1 - \frac{|\beta|^2}{4w^2}} \right] \text{rect}\left(\frac{|\beta|}{4w}\right), \quad (51)$$

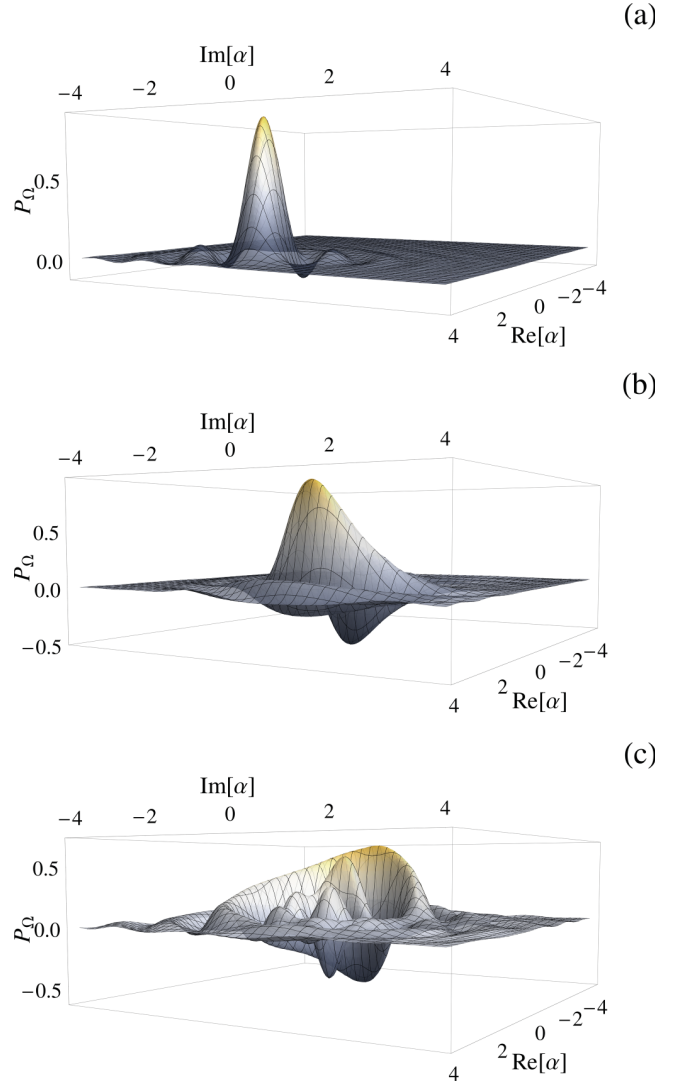


FIG. 5. The regularized Glauber-Sudarshan P function, derived via Eq. (45) together with Eq. (52), is shown for the initial coherent state $|\alpha_0\rangle$, at $\tilde{t} = 4$ (a), 13 (b), and 50 (c). Parameters: $\alpha_0 = \sqrt{5}$, $k = 3$, $\Delta\phi = \pi/2$, $\eta = 0.2$, $\tilde{\nu} = 5000$, $\beta_0 = 40$, $\Delta\tilde{\omega} = 8$, and $w = 1.7$.

with $\text{rect}(x) = 1$ if $x \leq 1/2$ and $\text{rect}(x) = 0$ elsewhere. Inserting Eq. (51) in Eq. (50) and using the substitution $z := |\beta|/(2w)$ yields

$$\begin{aligned} P_{\Omega,nm}(\alpha) &= \frac{16}{\pi^2} w^2 e^{i(n-m)\varphi_\alpha} \int_0^1 dz \Lambda_{nm}(2wz) z \\ &\quad \times J_{n-m}(4w|\alpha|z) [\arccos(z) - z\sqrt{1-z^2}]. \end{aligned} \quad (52)$$

The z integral needs to be evaluated numerically in general. Note that here $P_{\Omega,nm}(\alpha) = P_{\Omega,mn}(\alpha)^*$ holds. We stress that this procedure applies to any time evolution.

C. Nonclassicality in the nonlinear Jaynes-Cummings model

We are interested in the nonclassical properties of the vibrational states. Hence we calculate the reduced density

matrix:

$$\hat{\rho}_{\text{vib}}(\tilde{t}) = \sum_{i=1,2} \sum_{m=0}^{\infty} \langle i, m | \hat{\rho}(\tilde{t}) | i, m \rangle, \quad (53)$$

where the trace over the electronic states and the pump states is evaluated. Here we use $\hat{\rho}(\tilde{t}) = \hat{\mathcal{U}}(\tilde{t})\hat{\rho}(0)\hat{\mathcal{U}}(\tilde{t})^\dagger$ with the time-evolution operator given in Eq. (38) and $\hat{\rho}(0) = |2, \beta_0, \alpha_0\rangle\langle 2, \beta_0, \alpha_0|$ at $\tilde{t}_0 = 0$. This yields

$$\begin{aligned} \hat{\rho}_{\text{vib}}(\tilde{t}) = & \sum_{\sigma, \sigma' = \pm} \sum_{n, n' = 0}^{\infty} e^{i[\tilde{\omega}_{mn'}^{\sigma'} - \tilde{\omega}_{mn}^{\sigma}]\tilde{t}} |c_{mn}^{\sigma} c_{mn'}^{\sigma'}|^2 \\ & \times \frac{|\beta_0|^{2m} e^{-|\beta_0|^2}}{m!} \frac{\alpha_0^n \alpha_0^{*n'} e^{-|\alpha_0|^2}}{\sqrt{n!n'!}} \\ & \times \{ |n\rangle\langle n'| + \alpha_{mn}^{\sigma} (\alpha_{mn'}^{\sigma'})^* |n+k\rangle\langle n'+k| \}, \end{aligned} \quad (54)$$

which does not depend on $\tilde{\omega}_{21}$.

The surface plot of the regularized P function is given in Fig. 5. Due to the vibronic coupling the initial motional coherent state at $\tilde{t} = 0$ evolves into a nonclassical state. For a rather small time [see Fig. 5(a)], the state is still close to a coherent one. For larger times, one obtains more distorted states [see Figs. 5(b) and 5(c)]. The quantum character is displayed by the clearly visible negativities of the regularized P functions at the corresponding times. The choice of $\tilde{\nu}$ does not affect the nonclassical properties of the state but leads to a rotation in phase space. We note that the nonclassical effects shown in Fig. 5 become smaller for increasing frequency mismatch $\Delta\tilde{\omega}$, as the nonlinear vibronic interaction becomes weaker in this case.

Finally we would like to note that the nonclassicality quasiprobabilities shown in Fig. 5 can be determined straightforwardly in experiments. This can be done by the method introduced in [103] and realized in [104,105], which allows the direct measurement of the characteristic function $\Phi(\beta, t)$ of the P function [see Eq. (43)]. This technique can be readily combined with the direct sampling approaches as developed for the nonclassicality quasiprobabilities of radiation fields [97,98].

V. SUMMARY AND CONCLUSIONS

In this paper we considered the time-dependent Hamiltonian of a nonlinear Jaynes-Cummings system that is driven in quasiresonance. We showed, that time-ordering effects have a crucial impact on the system and can therefore not be omitted. As the general solution of a time-dependent Hamiltonian can become a cumbersome task, we introduce a method to circumvent this issue via quantizing the pump field. By extending the Hilbert space of the system, the dynamics becomes exactly solvable. Using the resulting time-independent Hamiltonian we derived an analytical expression of the time-evolution operator.

For a pump field prepared in a coherent state the solutions were shown to converge to the classical-pump scenario where the discrepancies shrink with increasing coherent amplitude. Furthermore, we visualized the temporal evolution of the nonclassicality quasiprobability of the motional states of the ion. This regularized version of the often strongly singular Glauber-Sudarshan P function has the advantage that it can be determined in experiments. Their negativities certify the quantum nature of the system under study. The introduced method to calculate this quasiprobability out of the density matrix applies to any time evolution.

In general, the derived algebra of the quasiresonantly driven trapped ion renders it possible to investigate complex scenarios where the interaction of the vibrational and the atomic (source) degrees of freedom is of interest. This may include the study of time-dependent motional quantum correlation effects. Furthermore, our analytical approach may yield a deeper insight into the properties of non-equal-time commutation rules, in cases with explicitly time-dependent interactions.

ACKNOWLEDGMENTS

We thank Ruynet Lima de Matos Filho for helpful comments. W.V. acknowledges funding from the European Union's Horizon 2020 research and innovation programme under Grant No. 665148.

-
- [1] D. F. Walls, Squeezed states of light, *Nature (London)* **306**, 141 (1983).
 - [2] R. E. Slusher, L. W. Hollberg, B. Yurke, J. C. Mertz, and J. F. Valley, Observation of Squeezed States Generated by Four-Wave Mixing in an Optical Cavity, *Phys. Rev. Lett.* **55**, 2409 (1985).
 - [3] L.-A. Wu, H. J. Kimble, J. L. Hall, and H. Wu, Generation of Squeezed States by Parametric Down Conversion, *Phys. Rev. Lett.* **57**, 2520 (1986).
 - [4] H. Vahlbruch, M. Mehmet, S. Chelkowski, B. Hage, A. Franzen, N. Lastzka, S. Goßler, K. Danzmann, and R. Schnabel, Observation of Squeezed Light with 10-dB Quantum-Noise Reduction, *Phys. Rev. Lett.* **100**, 033602 (2008).
 - [5] H. Vahlbruch, M. Mehmet, K. Danzmann, and R. Schnabel, Detection of 15 dB Squeezed States of Light and their Application for the Absolute Calibration of Photoelectric Quantum Efficiency, *Phys. Rev. Lett.* **117**, 110801 (2016).
 - [6] A. Einstein, N. Rosen, and B. Podolsky, Can quantum-mechanical description of physical reality be considered complete? *Phys. Rev.* **47**, 777 (1935).
 - [7] E. Schrödinger, Die gegenwärtige situation in der quantenmechanik, *Naturwiss.* **23**, 807 (1935).
 - [8] H. J. Kimble, M. Dagenais, and L. Mandel, Photon Antibunching in Resonance Fluorescence, *Phys. Rev. Lett.* **39**, 691 (1977).
 - [9] W. Vogel, Squeezing and Anomalous Moments in Resonance Fluorescence, *Phys. Rev. Lett.* **67**, 2450 (1991).
 - [10] B. Kühn, W. Vogel, M. Mraz, S. Köhnke, and B. Hage, Anomalous Quantum Correlations of Squeezed Light, *Phys. Rev. Lett.* **118**, 153601 (2017).
 - [11] S. Gerber, D. Rotter, L. Slodicka, J. Eschner, H. J. Carmichael, and R. Blatt, Intensity-Field Correlation of Single-Atom Resonance Fluorescence, *Phys. Rev. Lett.* **102**, 183601 (2009).
 - [12] L. Knöll, W. Vogel, and D.-G. Welsch, Quantum noise in spectral filtering of light, *J. Opt. Soc. Am. B* **3**, 1315 (1986).

- [13] J. D. Cresser, Intensity correlations of frequency-filtered light fields, *J. Phys. B* **20**, 4915 (1987).
- [14] L. Knöll, W. Vogel, and D.-G. Welsch, Action of passive, lossless optical systems in quantum optics, *Phys. Rev. A* **36**, 3803 (1987).
- [15] A. Stokes, Vacuum source-field correlations and advanced waves in quantum optics, *Quantum* **2**, 46 (2018).
- [16] E. T. Jaynes and F. W. Cummings, Comparison of quantum and semiclassical radiation theories with application to the beam maser, *Proc. IEEE* **51**, 89 (1963).
- [17] H. Paul, Induzierte emission bei starker einstrahlung, *Ann. Phys. (Leipzig)* **11**, 411 (1963).
- [18] S. Haroche, Les Houches Lecture Notes, Session XXXVIII ed., in *New Trends in Atomic Physics*, edited by G. Grynberg and R. Stora (Elsevier, New York, 1984), p. 195.
- [19] S. Haroche and J. M. Raimond, Radiative properties of rydberg states in resonant cavities, *Adv. At. Mol. Phys.* **20**, 347 (1985).
- [20] D. Meschede, H. Walther, and G. Müller, One-Atom Maser, *Phys. Rev. Lett.* **54**, 551 (1985).
- [21] G. Rempe, H. Walther and N. Klein, Observation of Quantum Collapse and Revival in a One-Atom Maser, *Phys. Rev. Lett.* **58**, 353 (1987).
- [22] I. I. Rabi, On the process of space quantization, *Phys. Rev.* **49**, 324 (1936).
- [23] I. I. Rabi, Space quantization in a gyrating magnetic field, *Phys. Rev.* **51**, 652 (1937).
- [24] D. Esteve, J.-M. Raimond, and J. Dalibard, *Entanglement and Information Processing*, 1st ed. (Elsevier, Amsterdam, 2003).
- [25] J. H. Eberly, N. B. Narozhny, and J. J. Sanchez-Mondragon, Periodic Spontaneous Collapse and Revival in a Simple Quantum Model, *Phys. Rev. Lett.* **44**, 1323 (1980).
- [26] N. B. Narozhny, J. J. Sanchez-Mondragon, and J. H. Eberly, Coherence versus incoherence: Collapse and revival in a simple quantum model, *Phys. Rev. A* **23**, 236 (1981).
- [27] J. R. Kukliński and J. L. Madajczyk, Strong squeezing in the Jaynes-Cummings model, *Phys. Rev. A* **37**, 3175(R) (1988).
- [28] M. Hillery, Squeezing and photon number in the Jaynes-Cummings model, *Phys. Rev. A* **39**, 1556 (1989).
- [29] S. J. D. Phoenix and P. L. Knight, Establishment of an entangled atom-field state in the Jaynes-Cummings model, *Phys. Rev. A* **44**, 6023 (1991).
- [30] S. Furuichi and M. Ohya, Entanglement degree in the time development of the jaynes-cummings model, *Lett. Math. Phys.* **49**, 279 (1999).
- [31] S. Bose, I. Fuentes-Guridi, P. L. Knight, and V. Vedral, Subsystem Purity as an Enforcer of Entanglement, *Phys. Rev. Lett.* **87**, 050401 (2001).
- [32] H. J. Carmichael, Photon Antibunching and Squeezing for a Single Atom in a Resonant Cavity, *Phys. Rev. Lett.* **56**, 539 (1986).
- [33] M. Hennrich, A. Kuhn, and G. Rempe, Transition from Antibunching to Bunching in Cavity QED, *Phys. Rev. Lett.* **94**, 053604 (2005).
- [34] F. Dubin, D. Rotter, M. Mukherjee, C. Russo, J. Eschner, and R. Blatt, Photon Correlation Versus Interference of Single-Atom Fluorescence in a Half-Cavity, *Phys. Rev. Lett.* **98**, 183003 (2007).
- [35] M. Brune, S. Haroche, J. M. Raimond, L. Davidovich, and N. Zagury, Manipulation of photons in a cavity by dispersive atom-field coupling: Quantum-nondemolition measurements and generation of “Schrödinger cat” states, *Phys. Rev. A* **45**, 5193 (1992).
- [36] G.-C. Guo and S.-B. Zheng, Generation of Schrödinger cat states via the Jaynes-Cummings model with large detuning, *Phys. Lett. A* **223**, 332 (1996).
- [37] J. J. Slosser, P. Meystre, and S. L. Braunstein, Harmonic Oscillator Driven by a Quantum Current, *Phys. Rev. Lett.* **63**, 934 (1989).
- [38] M. Weidinger, B. T. H. Varcoe, R. Heerlein, and H. Walther, Trapping States in the Micromaser, *Phys. Rev. Lett.* **82**, 3795 (1999).
- [39] S. Brattke, B. T. H. Varcoe, and H. Walther, Generation of Photon Number States on Demand via Cavity Quantum Electrodynamics, *Phys. Rev. Lett.* **86**, 3534 (2001).
- [40] E. K. Irish and K. Schwab, Quantum measurement of a coupled nanomechanical resonator-Cooper-pair box system, *Phys. Rev. B* **68**, 155311 (2003).
- [41] A. Wallraff, D. I. Schuster, A. Blais, L. Frunzio, R.-S. Huang, J. Majer, S. Kumar, S. M. Girvin, and R. J. Schoelkopf, Strong coupling of a single photon to a superconducting qubit using circuit quantum electrodynamics, *Nature (London)* **431**, 162 (2004).
- [42] I. Chiorescu, P. Bertet, K. Semba, Y. Nakamura, C. J. P. M. Harmans, and J. E. Mooij, Coherent dynamics of a flux qubit coupled to a harmonic oscillator, *Nature (London)* **431**, 159 (2004).
- [43] N. Hatakenaka and S. Kurihara, Josephson cascade micromaser, *Phys. Rev. A* **54**, 1729 (1996).
- [44] C. C. Gerry, Schrödinger cat states in a Josephson junction, *Phys. Rev. B* **57**, 7474 (1998).
- [45] A. T. Sornborger, A. N. Cleland, and M. R. Geller, Superconducting phase qubit coupled to a nanomechanical resonator: Beyond the rotating-wave approximation, *Phys. Rev. A* **70**, 052315 (2004).
- [46] F. Meier and D. D. Awschalom, Spin-photon dynamics of quantum dots in two-mode cavities, *Phys. Rev. B* **70**, 205329 (2004).
- [47] J. Kasprzak, S. Reitzenstein, E. A. Muljarov, C. Kistner, C. Schneider, M. Strauss, S. Höfling, A. Forchel, and W. Langbein, Up on the Jaynes-Cummings ladder of a quantum-dot/microcavity system, *Nat. Mater.* **9**, 304 (2010).
- [48] J. Basset, D.-D. Jarausch, A. Stockklauser, T. Frey, C. Reichl, W. Wegscheider, T. M. Ihn, K. Ensslin, and A. Wallraff, Single-electron double quantum dot dipole-coupled to a single photonic mode, *Phys. Rev. B* **88**, 125312 (2013).
- [49] A. de Freitas, L. Sanz, and J. M. Villas-Boas, Coherent control of the dynamics of a single quantum-dot exciton qubit in a cavity, *Phys. Rev. B* **95**, 115110 (2017).
- [50] J. M. Fink, M. Göppl, M. Baur, R. Bianchetti, P. J. Leek, A. Blais, and A. Wallraff, Climbing the Jaynes-Cummings ladder and observing its nonlinearity in a cavity QED system, *Nature (London)* **454**, 315 (2008).
- [51] F. P. Laussy, E. del Valle, M. Schrapp, A. Laucht, and J. J. Finley, Climbing the Jaynes-Cummings ladder by photon counting, *J. Nanophotonics* **6**, 061803 (2012).
- [52] T. Niemczyk, F. Deppe, H. Huebl, E. P. Menzel, F. Hocke, M. J. Schwarz, J. J. Garcia-Ripoll, D. Zueco, T. Hümmer, E. Solano, A. Marx, and R. Gross, Circuit quantum electrodynamics in the ultrastrong-coupling regime, *Nat. Phys.* **6**, 772 (2010).

- [53] T. Keating, C. H. Baldwin, Y.-Y. Jau, Jongmin Lee, G. W. Biedermann, and I. H. Deutsch, Arbitrary Dicke-State Control of Symmetric Rydberg Ensembles, *Phys. Rev. Lett.* **117**, 213601 (2016).
- [54] J. Lee, M. J. Martin, Y. Jau, T. Keating, I. H. Deutsch, and G. W. Biedermann, Demonstration of the Jaynes-Cummings ladder with Rydberg-dressed atoms, *Phys. Rev. A* **95**, 041801(R) (2017).
- [55] C. A. Blockley, D. F. Walls, and H. Risken, Quantum collapses and revivals in a quantized trap, *Europhys. Lett.* **17**, 509 (1992).
- [56] C. A. Blockley and D. F. Walls, Cooling of a trapped ion in the strong-sideband regime, *Phys. Rev. A* **47**, 2115 (1993).
- [57] J. I. Cirac, R. Blatt, A. S. Parkins, and P. Zoller, Quantum collapse and revival in the motion of a single trapped ion, *Phys. Rev. A* **49**, 1202 (1994).
- [58] W. Vogel and R. L. de Matos Filho, Nonlinear Jaynes-Cummings dynamics of a trapped ion, *Phys. Rev. A* **52**, 4214 (1995).
- [59] D. M. Meekhof, C. Monroe, B. E. King, W. M. Itano, and D. J. Wineland, Generation of Nonclassical Motional States of a Trapped Atom, *Phys. Rev. Lett.* **76**, 1796 (1996).
- [60] D. Leibfried, R. Blatt, C. Monroe, and D. Wineland, Quantum dynamics of single trapped ions, *Rev. Mod. Phys.* **75**, 281 (2003).
- [61] J. I. Cirac, A. S. Parkins, R. Blatt, and P. Zoller, “Dark” Squeezed States of the Motion of a Trapped Ion, *Phys. Rev. Lett.* **70**, 556 (1993).
- [62] R. L. de Matos Filho and W. Vogel, Even and Odd Coherent States of the Motion of a Trapped Ion, *Phys. Rev. Lett.* **76**, 608 (1996).
- [63] R. L. de Matos Filho and W. Vogel, Nonlinear Coherent States, *Phys. Rev. A* **54**, 4560 (1996).
- [64] S.-C. Gou, J. Steinbach, and P. L. Knight, Dark pair coherent states of the motion of a trapped ion, *Phys. Rev. A* **54**, R1014(R) (1996).
- [65] S.-C. Gou, J. Steinbach, and P. L. Knight, Vibrational pair cat states, *Phys. Rev. A* **54**, 4315 (1996).
- [66] C. C. Gerry, S.-C. Gou, and J. Steinbach, Generation of motional SU(1, 1) intelligent states of a trapped ion, *Phys. Rev. A* **55**, 630 (1997).
- [67] C. Monroe, D. M. Meekhof, B. E. King, and D. J. Wineland, A “schrodinger cat” superposition state of an atom, *Science* **272**, 1131 (1996).
- [68] C. C. Gerry, Generation of Schrödinger cats and entangled coherent states in the motion of a trapped ion by a dispersive interaction, *Phys. Rev. A* **55**, 2478 (1997).
- [69] S. Wallentowitz and W. Vogel, Quantum-mechanical counterpart of nonlinear optics, *Phys. Rev. A* **55**, 4438 (1997).
- [70] J. Larson, Dynamics of the Jaynes-Cummings and rabi models: old wine in new bottles, *Phys. Scr.* **76**, 146 (2007).
- [71] H. Moya-Cessa, F. Soto-Eguibar, J. M. Vargas-Martinez, R. Juarez-Amaro, and A. Zuniga-Segundo, Ion-laser interactions: The most complete solution, *Phys. Rep.* **513**, 229 (2012).
- [72] J. S. Pedernales, I. Lizuain, S. Felicetti, G. Romero, L. Lamata, and E. Solano, Quantum rabi model with trapped ions, *Sci. Rep.* **5**, 15472 (2015).
- [73] H. M. Moya-Cessa, Fast quantum rabi model with trapped ions, *Sci. Rep.* **6**, 38961 (2016).
- [74] X.-H. Cheng, I. Arrazola, J. S. Pedernales, L. Lamata, X. Chen, and E. Solano, Nonlinear quantum rabi model in trapped ions, *Phys. Rev. A* **97**, 023624 (2018).
- [75] W. Vogel and D.-G. Welsch, *Quantum Optics*, 3rd ed. (Wiley-VCH, New York, 2006).
- [76] W. Magnus, On the exponential solution of differential equations for a linear operator, *Commun. Pure Appl. Math.* **7**, 649 (1954).
- [77] S. Blanes, F. Casas, J. A. Oteo, and J. Ros, The Magnus expansion and some of its applications, *Phys. Rep.* **470**, 151 (2009).
- [78] A. Christ, B. Brecht, W. Maurer, and C. Silberhorn, Theory of quantum frequency conversion and type-II parametric down-conversion in the high-gain regime, *New J. Phys.* **15**, 053038 (2013).
- [79] N. Quesada and J. E. Sipe, Effects of time ordering in quantum nonlinear optics, *Phys. Rev. A* **90**, 063840 (2014).
- [80] N. Quesada and J. E. Sipe, Time-Ordering Effects in the Generation of Entangled Photons Using Nonlinear Optical Processes, *Phys. Rev. Lett.* **114**, 093903 (2015).
- [81] N. Quesada and J. E. Sipe, High efficiency in mode-selective frequency conversion, *Opt. Lett.* **41**, 364 (2016).
- [82] F. Krumm, J. Sperling, and W. Vogel, Multitime correlation functions in nonclassical stochastic processes, *Phys. Rev. A* **93**, 063843 (2016).
- [83] A. Alvermann and H. Fehske, High-order commutator-free exponential time-propagation of driven quantum systems, *J. Comput. Phys.* **230**, 5930 (2011).
- [84] J. R. Johansson, P. D. Nation, and F. Nori, QuTiP: An open-source Python framework for the dynamics of open quantum systems, *Comput. Phys. Commun.* **183**, 1760 (2012).
- [85] J. R. Johansson, P. D. Nation, and F. Nori, QuTiP 2: A Python framework for the dynamics of open quantum systems, *Comput. Phys. Commun.* **184**, 1234 (2013).
- [86] D. J. Heinzen and D. J. Wineland, Quantum-limited cooling and detection of radio-frequency oscillations by laser-cooled ions, *Phys. Rev. A* **42**, 2977 (1990).
- [87] C. Di Fidio, W. Vogel, R. L. de Matos Filho, and L. Davidovich, Single-trapped-ion vibronic Raman laser, *Phys. Rev. A* **65**, 013811 (2001).
- [88] C. Di Fidio, S. Maniscalco, W. Vogel, and A. Messina, Cavity QED with a trapped ion in a leaky cavity, *Phys. Rev. A* **65**, 033825 (2002).
- [89] A. B. Mundt, A. Kreuter, C. Becher, D. Leibfried, J. Eschner, F. Schmidt-Kaler, and R. Blatt, Coupling a Single Atomic Quantum Bit to a High Finesse Optical Cavity, *Phys. Rev. Lett.* **89**, 103001 (2002).
- [90] M. Keller, B. Lange, K. Hayasaka, W. Lange, and H. Walther, Continuous generation of single photons with controlled waveform in an ion-trap cavity system, *Nature (London)* **431**, 1075 (2004).
- [91] E. C. G. Sudarshan, Equivalence of Semiclassical and Quantum Mechanical Descriptions of Statistical Light Beams, *Phys. Rev. Lett.* **10**, 277 (1963).
- [92] R. J. Glauber, Coherent and incoherent states of the radiation field, *Phys. Rev.* **131**, 2766 (1963).
- [93] U. M. Titulaer and R. J. Glauber, Correlation functions for coherent fields, *Phys. Rev.* **140**, B676 (1965).

- [94] L. Mandel, Non-classical states of the electromagnetic field, *Phys. Scr.* **T12**, 34 (1986).
- [95] T. Kiesel and W. Vogel, Nonclassicality filters and quasi-probabilities, *Phys. Rev. A* **82**, 032107 (2010).
- [96] T. Kiesel, W. Vogel, M. Bellini, and A. Zavatta, Nonclassicality quasiprobability of single-photon-added thermal states, *Phys. Rev. A* **83**, 032116 (2011).
- [97] T. Kiesel, W. Vogel, B. Hage, and R. Schnabel, Direct Sampling of Negative Quasiprobabilities of a Squeezed State, *Phys. Rev. Lett.* **107**, 113604 (2011).
- [98] E. Agudelo, J. Sperling, W. Vogel, S. Köhnke, M. Mraz, and B. Hage, Continuous sampling of the squeezed-state nonclassicality, *Phys. Rev. A* **92**, 033837 (2015).
- [99] E. Agudelo, J. Sperling, and W. Vogel, Quasiprobabilities for multipartite quantum correlations of light, *Phys. Rev. A* **87**, 033811 (2013).
- [100] E. Agudelo, J. Sperling, L. S. Costanzo, M. Bellini, A. Zavatta, and W. Vogel, Conditional Hybrid Nonclassicality, *Phys. Rev. Lett.* **119**, 120403 (2017).
- [101] F. Krumm, W. Vogel, and J. Sperling, Time-dependent quantum correlations in phase space, *Phys. Rev. A* **95**, 063805 (2017).
- [102] B. Kühn and W. Vogel, Visualizing nonclassical effects in phase space, *Phys. Rev. A* **90**, 033821 (2014).
- [103] S. Wallentowitz and W. Vogel, Reconstruction of the Quantum-Mechanical State of a Trapped Ion, *Phys. Rev. Lett.* **75**, 2932 (1995).
- [104] P. C. Haljan, K. A. Brickman, L. Deslauriers, P. J. Lee, and C. Monroe, Spin-Dependent Forces on Trapped Ions for Phase-Stable Quantum Gates and Entangled States of Spin and Motion, *Phys. Rev. Lett.* **94**, 153602 (2005).
- [105] P. C. Haljan, P. J. Lee, K.-A. Brickman, M. Acton, L. Deslauriers, and C. Monroe, Entanglement of trapped-ion clock states, *Phys. Rev. A* **72**, 062316 (2005).

Time ordering in the classically driven nonlinear Jaynes-Cummings model

Tobias Lipfert,^{1,*} Fabian Krumm,^{2,†} Mikhail I. Kolobov,¹ and Werner Vogel²

¹*Laboratoire de Physique des Lasers Atomes et Molécules, Université Lille, CNRS, UMR No. 8523, 59000 Lille, France*

²*Arbeitsgruppe Theoretische Quantenoptik, Institut für Physik, Universität Rostock, 18059 Rostock, Germany*



(Received 13 September 2018; published 12 December 2018)

Recently [F. Krumm and W. Vogel, *Phys. Rev. A* **97**, 043806 (2018)], the detuned and nonlinear Jaynes-Cummings model describing the quantized motion of a trapped ion was introduced and its corresponding dynamics was solved via considering the driving laser in a quantized manner. For the dynamics with a classical driving laser an approximation in terms of neglected time ordering was considered to obtain analytical expressions and compared to numerically obtained exact dynamics, which revealed the insufficiency of this approximation. In the present work we reconsider this model and show that it can likewise be solved analytically, i.e., including time ordering, with a classical driving laser field. Using the analytical solution, we investigate the quantum time-ordering effects of the system with respect to nonclassicality and nonsimulatability of the motional states of the ion. Furthermore, we use the Magnus expansion to analyze the impact of certain orders of the time ordering. We derive an exact radius of convergence for these time-ordering corrections beyond the established and only sufficient criterion. Finally, the differences between the solution derived here and the previously found one using a quantized pump are discussed.

DOI: [10.1103/PhysRevA.98.063817](https://doi.org/10.1103/PhysRevA.98.063817)

I. INTRODUCTION

When the electromagnetic field is quantized, classical field variables are replaced by field operators (see, for example, [1–4]). The quantum nature of light is reflected in the noncommutative algebra of these operators, which in turn give rise to nonzero non-equal-time commutators of certain observables. Thus, temporal correlations may arise that are not covered by the classical theory of Maxwell. One phenomenon of this category is the quantum effect of photon antibunching [5,6], whose experimental verification [7] may be considered as the final proof to Einstein’s light quantum hypothesis [8]. A more general discussion of the underlying field inequalities is among others given in Refs. [9,10].

The evolution of dynamical systems with time-dependent perturbations are the subject of time-dependent perturbation theory (cf. [11–13]). Such systems are usually treated in terms of the Dyson series [14] and approximations based on the latter. In quantum optics non-equal-time commutators give rise to quantum time-ordering effects [15]. In Ref. [16] the latter were studied for the processes of sum frequency generation and parametric down-conversion. Recently, in the study of quantum time-ordering effects in dynamical systems, the Magnus expansion [17,18] has been considered as a useful representation of the corresponding evolution operators (cf. [19–24]). Let us note that, since noncommutativity of quantum-mechanical operators is a pure quantum effect, it can be used for quantitative measure of nonclassicality of a quantum state, as very recently proposed in Ref. [25].

Remarkably, the Magnus expansion allows for the formulation of approximations in terms of different orders of

nested non-equal-time commutators. As such approximations remain within the Lie algebra of whatever space is spanned by the non-equal-time commutators, important symmetries of the studied systems usually remain preserved [18–22]. Furthermore, the first-order approximation corresponds exactly to the case of neglecting ordering effects. This allows for a clear identification of ordering effects.

When approximations of the time-evolution operator are formulated in terms of the Magnus expansion, an increasing number of Magnus orders leads to a stepwise inclusion of time-ordering effects. That is, with higher orders one moves closer to the correct dynamics of the system, i.e., the incorporation of all time-ordering effects. However, this is limited by two factors: (i) the expressions for higher-order corrections can take quite complex forms (cf. [26]), which may make their evaluation quite tedious, and (ii) the Magnus expansion generally only works within a finite radius of convergence, that is, it may diverge at some point and the correct dynamics of the system cannot be recovered in terms of increasing orders of corrections.

In the case of divergence, a comparison of the cases of neglected time ordering with the case of time ordering in terms of the Magnus expansion will lead to misinterpretations. Admittedly, for small timescales the Magnus expansion does always converge, but significant deviations caused by the negligence of ordering effects may only arise after sufficiently long times. Thus, precise knowledge of the limits of convergence is in our case indispensable. Indeed, there exist sufficient upper bounds for evolution periods where convergence occurs [18], but exact upper bounds can generally only be found for generic cases.

Interestingly, for the detuned nonlinear Jaynes-Cummings dynamics of a trapped ion as studied in Ref. [24], an analytical solution of the dynamics could be found in the case

*tobias.lipfert@univ-lille.fr

†fabian.krumm@uni-rostock.de

of a quantized pump. With this ansatz, the system became time independent in the Schrödinger picture, i.e., no ordering effects occurred. For classical pump fields, the first-order Magnus expansion as an approximation to the exact dynamics was investigated. Comparison of this analytical approximation with numerically obtained dynamics of the exact model revealed that time-ordering effects cannot be neglected. Here we present how exact analytical solutions for the dynamics with a classical pump field can be obtained. Based on this exact analytical solution, we can give analytical expressions for density matrices as functions of time.

The spinor formalism we apply in this work to obtain such an analytical solution furthermore facilitates analysis of higher-order Magnus approximations, which we will present below. Presenting such time-ordering corrections only makes sense where the Magnus series converges. We show how an exact upper bound for the convergence time of the Magnus approximation can be obtained from the presented analytical solution. This allows us to guarantee convergence for times beyond those that are indicated by established sufficient criteria.

The paper is structured as follows. First we briefly reconsider the detuned nonlinear Jaynes-Cummings model and present the theoretical background in Sec. II. After that, an analytic solution for its dynamics is derived in Sec. III which we use to discuss the influence of time ordering on nonclassicality and nonsimulatability in Sec. IV. Then, in Sec. V, we further investigate the impact of certain orders of time-ordering corrections. In Sec. VI we give an exact upper bound for the convergence of these corrections. Afterward, in Sec. VII, we compare the solutions found in this work with the one derived in [24]. Finally, a summary and some conclusions are given in Sec. VIII.

II. MODEL

Let us briefly recapitulate the physical model to be studied and present the theoretical background. If an ion is caught in a Paul trap, its motion can be described in a quantized manner (see Refs. [27–29] or Chap. 13 of [1]). The resulting states of the ion are referred to as motional or vibrational states. Via the interaction of the ion with optical radiation, e.g., a laser, the generation of a plethora of motional states became feasible [30–39].

A. Detuned nonlinear Jaynes-Cummings Hamiltonian

The full dynamics describing the interaction of an ion with a laser is rather complicated and in general can only be solved numerically. However, under certain but realistic approximations, the interaction Hamiltonian of the system can be simplified to a nonlinear generalization of the Jaynes-Cummings Hamiltonian [40], describing the electronic coupling to the k th sideband. In the interaction picture, including a detuning $\Delta\omega$, it reads

$$\hat{H}_{\text{int}}(t) = \hbar|\kappa|e^{-i\Delta\omega t + i\theta} \hat{A}_{21} \hat{f}_k(\hat{a}^\dagger \hat{a}; \eta) \hat{a}^k + \text{H.c.} \quad (1)$$

A more detailed derivation of the Hamiltonian is given in Ref. [24]. The corresponding scheme is depicted in Fig. 1.

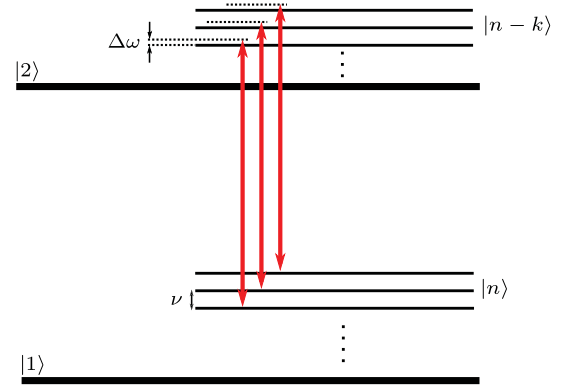


FIG. 1. Scheme of the physical system described by the interaction Hamiltonian in Eq. (1). The electronic ground state, denoted by $|1\rangle$, and the corresponding excited state $|2\rangle$ are separated by the electronic transition frequency $\omega_{21} = \omega_2 - \omega_1$. In a harmonic trap potential the vibrational levels are equidistantly separated by the trap frequency ν . The frequency of the driving laser (red arrows) is detuned from the k th sideband by $\Delta\omega$, that is, $\omega_L = \omega_{21} - k\nu + \Delta\omega$.

In Eq. (1) the following quantities and definitions are used: $\kappa = |\kappa|e^{i\theta}$ describes the strength of the coupling of the electronic to the vibrational levels of the ion (vibronic coupling), where $|\kappa|$ grows linearly with the pump amplitude; $\hat{A}_{ij} = |i\rangle\langle j|$ ($i, j = 1, 2$) are the atomic flip operators corresponding to the $|j\rangle \rightarrow |i\rangle$ transitions; and the operator function $\hat{f}_k(\hat{a}^\dagger \hat{a}; \eta)$ describes the mode structure of the laser field in the case of a standing wave at the (operator-valued) position of the ion and reads

$$\begin{aligned} \hat{f}_k(\hat{a}^\dagger \hat{a}; \eta) &= \frac{1}{2} e^{i\Delta\phi - \eta^2/2} \sum_{l=0}^{\infty} \frac{(i\eta)^{2l+k}}{l!(l+k)!} \hat{a}^{\dagger l} \hat{a}^l + \text{H.c.} \\ &= \frac{1}{2} e^{i\Delta\phi - \eta^2/2} \sum_{n=0}^{\infty} |n\rangle\langle n| \frac{(i\eta)^k n!}{(n+k)!} L_n^{(k)}(\eta^2) + \text{H.c.}, \end{aligned} \quad (2)$$

with $L_n^{(k)}$ denoting the generalized Laguerre polynomials, that is, via $\hat{f}_k(\hat{a}^\dagger \hat{a}; \eta)$ a nonlinear dependence of the dynamics on the excitation of the vibrational mode is obtained. The quantity $\Delta\phi$ is the relative position of the trap potential to the laser wave and η is the Lamb-Dicke parameter.

The operators \hat{a}^\dagger (\hat{a}) are the creation (annihilation) operators of the motional excitation with frequency ν . It is noteworthy that the operators, in contrast to the ordinary Jaynes-Cummings model, do not describe a photonic degree of freedom but the quantized center-of-mass motion of the trapped ion. The Hamiltonian of the free motion reads

$$\hat{H}_0 = \hbar\nu \hat{a}^\dagger \hat{a} + \hbar\omega_{21} \hat{A}_{22}, \quad (3)$$

where $\omega_{21} = \omega_2 - \omega_1$ is the separation of the electronic levels $|1\rangle$ and $|2\rangle$.

We are interested in the situation where the classically described laser, with the frequency ω_L , is slightly detuned from the k th sideband by $\Delta\omega$,

$$\omega_L = \omega_{21} - k\nu + \Delta\omega, \quad (4)$$

with $\Delta\omega \ll \nu$. Altogether, the Hamiltonian in Eq. (1) describes the nonlinear k th sideband coupling $|1, n\rangle \leftrightarrow |2, n - k\rangle$ including a frequency mismatch.

B. Time evolution

The time-dependent dynamics of the system is governed by the evolution operator $\hat{U}(t, t_0)$, which fulfills the standard Schrödinger equation

$$\frac{\partial}{\partial t} \hat{U}(t, t_0) = -\frac{i}{\hbar} \hat{H}(t) \hat{U}(t, t_0). \quad (5)$$

Note that in Eq. (5) the factor $1/\hbar$ always compensates the factor \hbar in the Hamiltonian \hat{H} . To avoid superfluous coefficients we introduce the notation

$$\hat{H}_{\text{int}}(t) = |\kappa| \hbar \hat{\mathcal{H}}(t), \quad (6)$$

in terms of the dimensionless Hamiltonian $\hat{\mathcal{H}}$ [cf. Eq. (1)], which also enables us to track the dependences on the coupling strength $|\kappa|$ throughout the following.

The formal solution to the reformulated evolution equation

$$\partial_t \hat{U}(t, t_0) = -i |\kappa| \hat{\mathcal{H}}(t) \hat{U}(t, t_0) \quad (7)$$

can be written in terms of the time-ordered exponential

$$\hat{U}(t, t_0) = \mathcal{T} \exp \left\{ -i |\kappa| \int_{t_0}^t d\tilde{t} \hat{\mathcal{H}}(\tilde{t}) \right\}, \quad (8)$$

where the time-ordering prescription \mathcal{T} orders operators with higher t to the right (see, for example, Refs. [1,2]). The time-ordered exponential can be represented in terms of the Magnus expansion [17,18]

$$\hat{U}(t, t_0) = \exp\{-i \hat{\mathcal{M}}(t, t_0)\}, \quad (9)$$

where the exponent is the so-called Magnus series

$$-i \hat{\mathcal{M}}(t, t_0) = \sum_{\ell=1}^{\infty} (-i |\kappa|)^{\ell} \hat{\mathcal{M}}^{[\ell]}(t, t_0). \quad (10)$$

As in the case of Dyson series [14], approximations of solutions may be obtained from this representation by truncating the series at any order of the coupling coefficients $|\kappa|$. The first-order Magnus expansion approximation, given by the first term of the series

$$\hat{\mathcal{M}}^{[1]}(t, t_0) = \int_{t_0}^t dt_1 \hat{\mathcal{H}}(t_1), \quad (11)$$

reads

$$\hat{U}^{[1]}(t, t_0) = \exp \left(-i |\kappa| \int_{t_0}^t d\tilde{t} \hat{\mathcal{H}}(\tilde{t}) \right), \quad (12)$$

which corresponds to Eq. (8) with neglected time ordering (cf. [24]). All other terms, $l > 1$, of the Magnus series are corrections in terms of time ordering and are therefore referred to as time-ordering effects [16,19–24]. These time-ordering terms consist of ordered integrals of linear combinations of nested commutators, e.g.,

$$\hat{\mathcal{M}}^{[2]}(t, t_0) = \frac{1}{2} \int_{t_0}^t dt_1 \int_{t_0}^{t_1} dt_2 [\hat{\mathcal{H}}(t_2), \hat{\mathcal{H}}(t_1)], \quad (13)$$

$$\begin{aligned} \hat{\mathcal{M}}^{[3]}(t, t_0) = & \frac{1}{6} \int_{t_0}^t dt_1 \int_{t_0}^{t_1} dt_2 \int_{t_0}^{t_2} dt_3 \\ & \times \{ [\hat{\mathcal{H}}(t_1), [\hat{\mathcal{H}}(t_2), \hat{\mathcal{H}}(t_3)]] \\ & + [\hat{\mathcal{H}}(t_3), [\hat{\mathcal{H}}(t_2), \hat{\mathcal{H}}(t_1)]] \}, \end{aligned} \quad (14)$$

and they can attain quite complex forms for higher orders (cf. [26]).

For larger time intervals, approximations of increasing orders in terms of the truncated series (10) do not necessarily converge towards the exact solution of the dynamics [18]. Thus, it is imperative to take into account such limitations on the convergence when analyzing time-ordering corrections. A precise knowledge of convergence bounds usually requires an *a priori* knowledge of the exact solution. Fortunately, as will be shown below, the Hamiltonian (1) belongs to the scarce class of time-dependent physical systems where exact solutions can be derived analytically.

III. EXPLICIT SOLUTION OF THE DYNAMICS

Below we derive a solution to Eq. (7) for the Hamiltonian (1) that includes all time-ordering effects. Based on this, we reproduce some results for dynamics of the population probability of the excited electronic state that could only be obtained numerically in Ref. [1]. Using the derived solution, we calculate analytical expressions for the time-dependent density matrices, in the Fock-basis representation, of the motional states for different initial configurations.

A. Decoupling and solving the evolution equation by a spinor formalism

From the dimensionless Fock basis representation of the Hamiltonian (1),

$$\hat{\mathcal{H}}(t) = \sum_{n=0}^{\infty} \omega_n [e^{-i\Delta\omega t} e^{i\theta} |2, n\rangle \langle 1, n+k| + \text{H.c.}],$$

with

$$w_n = \cos \left(\Delta\phi + \frac{\pi}{2} k \right) \eta^k e^{-\eta^2/2} \sqrt{\frac{n!}{(n+k)!}} L_n^{(k)}(\eta^2), \quad (15)$$

we can see that the interaction is entirely described in terms of projectors constructed from the states $|2, n\rangle$ and $|1, n+k\rangle$ with $n = 0, 1, \dots$. A compact notation for such projectors can be formulated in terms of the spinors

$$\Psi_n = \begin{pmatrix} \langle 2, n | e^{-i\theta/2} \\ \langle 1, n+k | e^{i\theta/2} \end{pmatrix} \Leftrightarrow \Psi_n^\dagger = \begin{pmatrix} e^{i\theta/2} \langle 2, n | \\ e^{-i\theta/2} \langle 1, n+k | \end{pmatrix}^T. \quad (16)$$

These spinors fulfill an orthogonality relation

$$\Psi_n \Psi_{n'}^\dagger = \delta_{n,n'} \mathbf{I}, \quad (17)$$

with

$$\mathbf{I} = \begin{pmatrix} 1 & 0 \\ 0 & 1 \end{pmatrix},$$

and allow us to formulate a completeness relation as (cf. [24])

$$\hat{1} = \sum_{n=0}^{\infty} \Psi_n^\dagger \mathbf{I} \Psi_n + \sum_{q=0}^{k-1} |1, q\rangle \langle 1, q|. \quad (18)$$

By applying this completeness relation, the Hamiltonian (15) can be written in the compact form

$$\hat{H}(t) = \sum_{n=0}^{\infty} \Psi_n^\dagger \mathbf{H}_n(t) \Psi_n, \quad (19)$$

with

$$\mathbf{H}_n(t) = \begin{pmatrix} 0 & w_n e^{-i\Delta\omega t} \\ w_n e^{i\Delta\omega t} & 0 \end{pmatrix}. \quad (20)$$

From the quasideagonal form of the Hamiltonian in the spinor basis it may be hypothesized that any evolution of the system will also be representable in this basis. Thus, a similarity ansatz for the evolution operator

$$\hat{\mathcal{U}}(t, t_0) = \sum_{n=0}^{\infty} \Psi_n^\dagger \mathbf{U}_n(t, t_0) \Psi_n + \sum_{q=0}^{k-1} |1, q\rangle \langle 1, q|, \quad (21)$$

with $\mathbf{U}_n(t, t_0) \in \mathbb{C}^{2 \times 2}$ and initial condition $\mathbf{U}_n(t, t_0)|_{t=t_0} = \mathbf{I}$, is suitable. Substituting (19) and (21) into (7) decouples the evolution equation in terms of the 2×2 matrix differential equations

$$\partial_t \mathbf{U}_n(t, t_0) = -i|\kappa| \mathbf{H}_n(t) \mathbf{U}_n(t, t_0) \quad (22)$$

for $n = 0, 1, \dots$

The time-dependent coefficient matrix (20) is representable as a linear combination of Pauli matrices that (multiplied by the imaginary unit i) generate the Lie group $SU(2)$. Thus, solutions to (22) are always representable as

$$\mathbf{U}_n(t, t_0) = \begin{pmatrix} a_n(t, t_0) & b_n(t, t_0) \\ -b_n^*(t, t_0) & a_n^*(t, t_0) \end{pmatrix}, \quad (23)$$

where

$$|a_n(t, t_0)|^2 + |b_n(t, t_0)|^2 = 1. \quad (24)$$

Note that in the treatment of parametric down-conversion with monochromatic pumps, the solutions to matrix differential equations with parameter-dependent coefficients of similar form are known [19,41].

Essentially, solutions to (22) can be obtained by transforming the equations into systems with constant coefficients. Such a system can then be directly solved in terms of matrix exponentials (see Appendix A for a stepwise derivation). The explicit solutions then read

$$\begin{aligned} a_n(t, t_0) &= e^{-i\Delta\omega[t-t_0]/2} \left[\cos(\Gamma_n[t-t_0]) \right. \\ &\quad \left. + \frac{i\Delta\omega}{2\Gamma_n} \sin(\Gamma_n[t-t_0]) \right], \\ b_n(t, t_0) &= e^{-i\Delta\omega[t+t_0]/2} \frac{|\kappa|w_n}{i\Gamma_n} \sin(\Gamma_n[t-t_0]) \end{aligned} \quad (25)$$

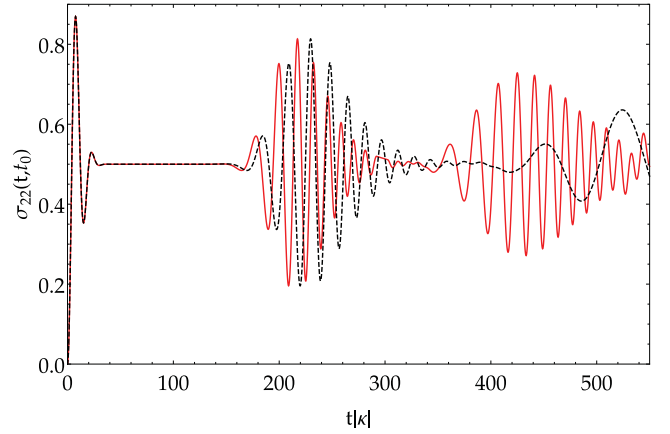


FIG. 2. Population probability of the excited electronic state $\sigma_{22}(t, t_0)$ as given in Eq. (26) obtained from the exact analytical solution for $\hat{\mathcal{U}}$ (red solid line) and for neglected time ordering (black dashed line) with the initial state $\hat{\rho}^{(1)}(t_0 = 0) = |1, \alpha_0\rangle \langle 1, \alpha_0|$. Here parameters have been chosen as $\Delta\omega/|\kappa| = 0.005$, $\Delta\phi = 0$, $k = 2$, and $\eta = 0.2$. The displayed result is a reproduction (and verification) of Fig. 2 in Ref. [24] by means of the analytical expression (26). In Ref. [24] the corresponding result was obtained numerically.

for $n = 0, 1, \dots$ with $\Gamma_n = \sqrt{(\frac{\Delta\omega}{2})^2 + w_n^2|\kappa|^2}$. In Ref. [24] an approximated solution was found in terms of neglected time ordering, i.e., in terms of (12). Here we have found an analytic expression that incorporates all time-ordering effects, i.e., an explicit representation of the time-ordered exponential (8) for the Hamiltonian (1).

This analytic expression allows us, e.g., to obtain the dynamics of the population probability of the excited electronic state

$$\begin{aligned} \sigma_{22}(t, t_0) &= \sum_{n=0}^{\infty} \langle 2, n | \hat{\mathcal{U}}(t, t_0) e^{-(i/\hbar)\hat{H}_0(t-t_0)} \hat{\rho}(t_0) \\ &\quad \times e^{(i/\hbar)\hat{H}_0(t-t_0)} \hat{\mathcal{U}}^\dagger(t, t_0) | 2, n \rangle \end{aligned} \quad (26)$$

and to compare it to the dynamics with neglected time ordering. This is illustrated in Fig. 2. Note that this is a reproduction of results that have been obtained numerically in Ref. [24]. Here, however, all results are based on analytical expressions. The discrepancy between the dynamics with neglected time ordering and exact dynamics was already pointed out in Ref. [24].

B. Density matrices

Let us apply the derived solution to investigate the evolution of the motional states of the ion. For this purpose we calculate the density matrix of the motional state

$$\rho_{m,n}(t) = \sum_{j=1,2} \langle j, m | \hat{\mathcal{U}}(t, t_0) e^{-(i/\hbar)\hat{H}_0(t-t_0)} \hat{\rho}(t_0) e^{(i/\hbar)\hat{H}_0(t-t_0)} \hat{\mathcal{U}}^\dagger(t, t_0) | j, n \rangle \quad (27)$$

with the electronic states traced out. For the initial coherent state in the electronic ground state $\hat{\rho}^{(1)}(t_0) = |1, \alpha_0\rangle\langle 1, \alpha_0|$ and in the excited electronic state $\hat{\rho}^{(2)}(t_0) = |2, \alpha_0\rangle\langle 2, \alpha_0|$, the motional density matrices read

$$\begin{aligned} \rho_{n,m}^{(1)}(t, t_0) &= \frac{\alpha_0^{n+k} \alpha_0^{*(m+k)} e^{-|\alpha_0|^2}}{\sqrt{(n+k)!(m+k)!}} e^{-i(\Phi_{1,n+k} - \Phi_{1,m+k})[t-t_0]} b_n(t, t_0) b_m^*(t, t_0) \\ &+ \frac{\alpha_0^n \alpha_0^{*m} e^{-|\alpha_0|^2}}{\sqrt{n!m!}} e^{-i(\Phi_{1,n} - \Phi_{1,m})[t-t_0]} a_{n-k}^*(t, t_0) a_{m-k}(t, t_0) \end{aligned} \quad (28)$$

and

$$\begin{aligned} \rho_{n,m}^{(2)}(t, t_0) &= \frac{\alpha_0^n \alpha_0^{*m} e^{-|\alpha_0|^2}}{\sqrt{n!m!}} e^{-i(\Phi_{1,n} - \Phi_{1,m})[t-t_0]} a_n(t, t_0) a_m^*(t, t_0) \\ &+ \frac{\alpha_0^{n-k} \alpha_0^{*(m-k)} e^{-|\alpha_0|^2}}{\sqrt{(n-k)!(m-k)!}} e^{-i(\Phi_{1,n-k} - \Phi_{1,m-k})[t-t_0]} b_{n-k}^*(t, t_0) b_{m-k}(t, t_0), \end{aligned} \quad (29)$$

respectively. Details regarding the preparation of coherent motional states can be found in Refs. [31,42]. Here $\Phi_{j,n} = n\nu + [j-1]\omega_{21}$ is the eigenvalue $\hat{H}_0|j, n\rangle = \hbar\Phi_{j,n}|j, n\rangle$ and we have defined $a_m(t, t_0) = 1$ and $b_m(t, t_0) = 0$ for negative indices $m < 0$.

In the case of neglected time ordering (12) we replace a_n and b_n in (29) and (28) by the corresponding terms $a_n^{[1]}$ and $b_n^{[1]}$ that one obtains in the first-order Magnus expansion approximation (12), i.e.,

$$\begin{aligned} a_n^{[1]}(t, t_0) &= \cos\left(w_n |\kappa| (t-t_0) \text{sinc}\left[\frac{(t-t_0)\Delta\omega}{2}\right]\right), \\ b_n^{[1]}(t, t_0) &= -e^{-i\Delta\omega[t+t_0]/2} \sin\left(w_n |\kappa| (t-t_0) \text{sinc}\left[\frac{(t-t_0)\Delta\omega}{2}\right]\right). \end{aligned} \quad (30)$$

Note that this corresponds exactly to the result derived in Ref. [24].

IV. QUANTUM TIME-ORDERING EFFECTS

Finally, using the derived results, we are able to rigorously investigate the effects of the time-ordering contributions, $\hat{\mathcal{M}}^{[n>1]}(t, t_0)$ in Eq. (9), on the nonclassicality of the system. The phrase *nonclassicality* is defined as follows: Noting that the density operator of a system (or of a subsystem) can be expressed as a mixture of coherent states using the Glauber-Sudarshan P representation [43,44],

$$\hat{\rho}(t) = \int d^2\alpha P(\alpha; t) |\alpha\rangle\langle\alpha|, \quad (31)$$

the system is classical if the density operator can be expressed as a classical mixture of coherent states.

The latter means that $P(\alpha; t) \geq 0$. That is, the coherent states serve as reference states to divide classicality from nonclassicality. If the P functions attain negative values (in the sense of distributions) the state is referred to as nonclassical as it cannot be expressed as a classical mixture of coherent states and hence it consists of superpositions of them, which is a clear signature of nonclassical behavior [45,46].

However, the P function is highly singular for many states and hence it cannot be observed in experiments. To circumvent this issue a regularization procedure was established [47] which converts the P function into a well-behaved quasiprobability P_Ω . Due to an appropriate choice of filter functions, the latter attains negative values only if the P function does. That is, if the regularized version reveals negativities, then the state

is referred to as a nonclassical state. The applicability was verified in several experiments (see, for example, Refs. [48,49]).

As presented in Ref. [24], the regularized P function can be calculated out of the, possibly reduced, density-matrix elements in the Fock basis via

$$P_\Omega(\alpha; t) = \sum_{m,n=0}^{\infty} \rho_{m,n}(t) P_{\Omega,n,m}(\alpha), \quad (32)$$

where $P_{\Omega,n,m}(\alpha)$ needs to be calculated only once and can be subsequently combined with the density-matrix elements $\rho_{m,n}(t) = \langle m | \hat{\rho}(t) | n \rangle$ for arbitrary times. The elements of the regularized P function are calculated via

$$\begin{aligned} P_{\Omega,n,m}(\alpha) &= \frac{16}{\pi^2} w^2 e^{i(n-m)\varphi_\alpha} \int_0^1 dz \Lambda_{n,m}(2wz) z \\ &\times J_{n-m}(4w|\alpha|z) [\arccos(z) - z\sqrt{1-z^2}], \end{aligned} \quad (33)$$

with $J_n(x)$ being the Bessel functions of the first kind, $\alpha = |\alpha|e^{i\varphi_\alpha}$, and

$$\Lambda_{n,m}(x) = \begin{cases} (-x)^{m-n} \sqrt{\frac{n!}{m!}} L_n^{(m-n)}(x^2), & m \geq n \\ x^{n-m} \sqrt{\frac{m!}{n!}} L_m^{(n-m)}(x^2), & m < n. \end{cases} \quad (34)$$

In Eq. (33) a radial symmetric filter was assumed. Details on appropriate filter functions can be found in Ref. [50].

The plots of the quasiprobability in Eq. (33) and the corresponding Wigner function [51] are depicted in Fig. 3 for $t|\kappa| = 500$, leading to differences in Figs. 3(a)–3(d), due to differences between exact solutions and first-order approximate solutions. We see that they have a crucial impact on the

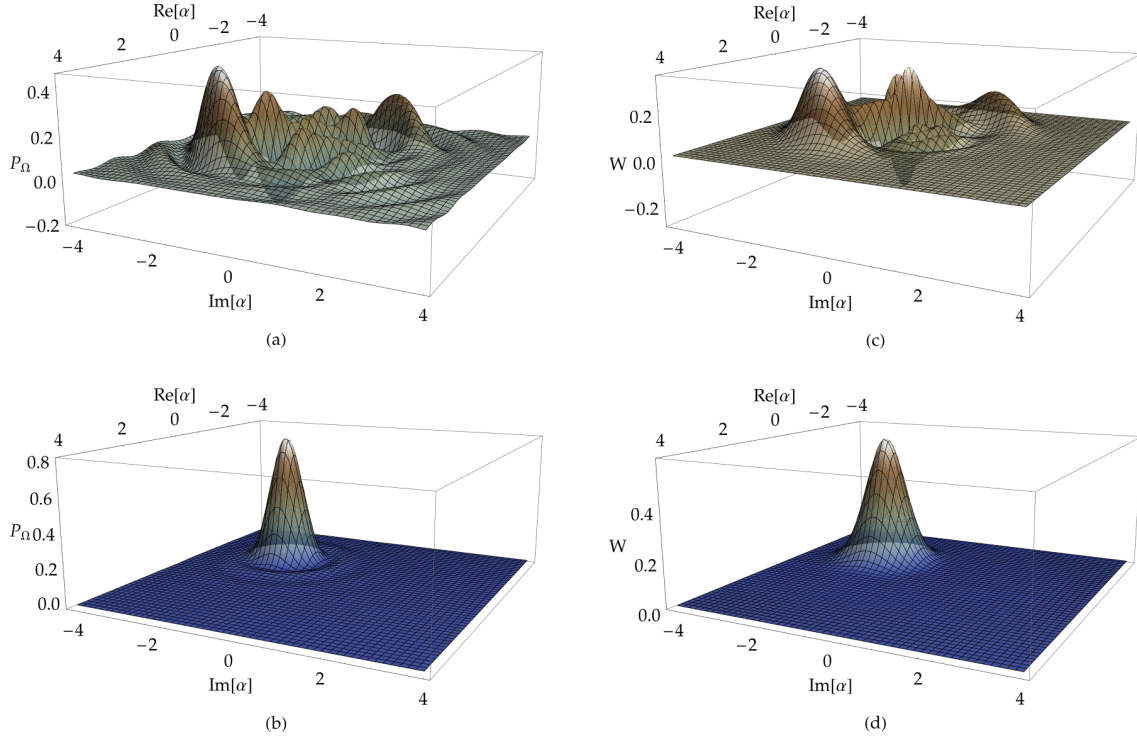


FIG. 3. (a) and (b) Regularized Glauber-Sudarshan P function and (c) and (d) the corresponding Wigner function for $t|\kappa| = 500$ and the excitation to the second sideband $k = 2$ and $\Delta\Phi = 0$ in Eq. (2). Here an electronic excited input state was chosen. (a) and (c) Analytic exact solution in Eq. (29), with full time ordering. (b) and (d) Solutions without time-ordering effects [Eq. (30)]. The parameters are $\eta = 0.2$, $\alpha_0 = \sqrt{5}$, and $\Delta\omega/|\kappa| = 0.1$.

dynamics of the system. In particular, the negligence of time ordering [Figs. 3(b) and 3(d)] yields non-negative phase-space representations.

Keeping in mind that the regularized P and Wigner function visualize the state under study in the phase space, one can see that at $t|\kappa| = 500$ the state resembles a quantum superposition of two coherent states of distinct amplitude where the strong negativities indicate quantum interferences [see Figs. 3(a) and 3(c)]. The negativities of P_Ω imply that the corresponding state cannot be expressed as a classical mixture of coherent states, whereas the negativities of the Wigner function indicate classical nonsimulatability [52]. Remarkably, the negativities of P_Ω can be used to investigate quantum non-Gaussianity and the degree of nonclassicality simultaneously, which is not possible using the Wigner function alone (for details see Ref. [53] and references therein).

In summary, for sufficiently large interaction times the nonclassical character in terms of P_Ω and W is contained in the time-ordering contributions of the corresponding time-evolution operator. Similar results are obtained using other η and $\Delta\omega$. On short timescales, however, the time-ordering effects do not have a decisive impact on nonclassicality.

V. TIME-ORDERING CORRECTIONS

One may now be interested in how different orders of time ordering affect the temporal evolution of the system under study. Based on the explicit solution, a generating function for arbitrary-order terms of the Magnus series can be defined. Using the orthogonality (17) of our spinor formalism (16), it

is easy to show that the non-equal-time commutators of (19) fulfill

$$[\hat{H}(t), \hat{H}(t')] = \sum_{n=0}^{\infty} \Psi_n^\dagger[\mathbf{H}_n(t), \mathbf{H}_n(t')] \Psi_n. \quad (35)$$

Consequently, there is a one-to-one correspondence to the non-equal-time commutators of the matrices \mathbf{H}_n . Thus it follows that the ℓ th-order Magnus expansion approximation to the solution of (7) corresponds exactly to the result one obtains by evaluating the ℓ th-order Magnus expansion approximation to the solution of Eq. (22).

The analytic solutions in Eq. (25) allow for the explicit formulation of the full Magnus series. This means that we can put (23) in exponential form as

$$\mathbf{U}_n(|\kappa|) = \exp\{-i\mathbf{M}_n(|\kappa|)\}. \quad (36)$$

Here and in the remainder of this section we drop the time dependence of the matrices from our notation and consider the appearing parameters as functions of the coupling parameter $|\kappa|$.

Evaluating the matrix exponential under application of the unitary condition (24) shows that the matrix-exponent can be chosen in the form

$$\mathbf{M}_n(|\kappa|) = \frac{\arccos\{\text{Re}[a_n(|\kappa|)]\}}{\sqrt{1 - \text{Re}^2[a_n(|\kappa|)]}} \times \begin{pmatrix} -\text{Im}[a_n(|\kappa|)] & ib_n(|\kappa|) \\ -ib_n^*(|\kappa|) & \text{Im}[a_n(|\kappa|)] \end{pmatrix}. \quad (37)$$

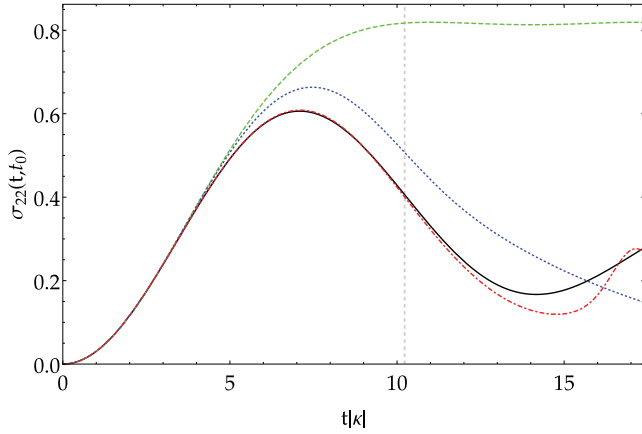


FIG. 4. Population probability of the excited electronic state $\sigma_{22}(t, t_0)$ as given in Eq. (26) obtained from the exact solution for \hat{U} (black solid line), from the first-order approximation, i.e., neglected time ordering (green dashed line), from the second-order approximation (blue dotted line), and from the fifth-order approximation (red dot-dashed line) with the initial state $\hat{\rho}^{(2)}(t_0 = 0) = |2, \alpha_0\rangle\langle 2, \alpha_0|$ in the range $0 \leq t|\kappa| < 17.4$. Here the parameters have been chosen as $\Delta\omega/|\kappa| = 0.224$, $\Delta\phi = \pi/4$, $k = 3$, and $\eta = 0.4$. This implies that $w_{\max} = 0.307$. A vertical grid line (gray dashed line) at $t|\kappa| = \pi/w_{\max}$ marks the region in which the sufficient condition [Eq. (40)] guarantees the convergence of the time-ordering corrections. In Sec. VI we develop criteria that allow us to state that the time-ordering corrections converge in the full displayed range.

This matrix can now serve as a generating function for the different orders of time-ordering corrections, i.e., a Taylor-series expansion of $\mathbf{M}_n(|\kappa|)$ in terms of $|\kappa|$ around $|\kappa| = 0$ yields the Magnus series as

$$\mathbf{M}_n(|\kappa|) = i \sum_{\ell=1}^{\infty} (-i|\kappa|)^{\ell} \mathbf{M}_n^{[\ell]}, \quad (38)$$

where

$$\mathbf{M}_n^{[\ell]} = \frac{i^{\ell-1}}{\ell!} \left. \frac{d^{\ell} \mathbf{M}_n(|\kappa|)}{d|\kappa|^{\ell}} \right|_{|\kappa|=0}. \quad (39)$$

We have verified the equivalence of these expressions with those obtained from nested commutators [cf. (14)] up to fifth order (see Appendix B) using expressions in Refs. [18,26]. This allows us to obtain time-ordering corrections to arbitrary order.

We want to point out that the Magnus series (38) may not always converge [18]. However, one can show that the Magnus series (38) converges for [18]

$$|\kappa| \int_{t_0}^t d\tilde{t} \|\mathbf{H}_n(\tilde{t})\|_2 = |\kappa w_n| [t - t_0] < \pi, \quad (40)$$

where $\|\cdots\|_2$ denotes the spectral norm [54]. In terms of the full operator (21) this means that we can guarantee convergence, as long as $w_{\max} |\kappa| [t - t_0] < \pi$ with $w_{\max} = \max_{n=0,1,\dots} |w_n|$ [also cf. Eq. (15)].

The upper bound (40) is nonetheless only a sufficient criterion for convergence. In Fig. 4 we give an illustrative example of convergence well above this upper bound. Here we compare the population probability of the excited electronic

state (26) in different orders of time-ordering corrections to the exact solution. The quality of approximation seemingly also improves above the bound (40).

VI. EXACT UPPER BOUND FOR CONVERGENCE OF TIME-ORDERING CORRECTIONS

The generating function derived in Sec. V allows us to perform an extensive study of the convergence of time-ordering corrections. We have seen that the sufficient convergence criterion (40) may underestimate the actual limits of convergence of Magnus expansion approximations. As we treat here a frequency-mismatch system one may wonder why the frequency mismatch $\Delta\omega$ does not appear in the criterion (40). Sharper bounds seem desirable in the treatment of time-ordering corrections and knowing the analytic expression for the exponents (37) indeed allows us to perform a more sophisticated analysis.

For these purposes we may substitute $w_n \mapsto \tau_n / (|\kappa| [t - t_0])$ and $\Delta\omega \mapsto 2\Lambda / [t - t_0]$ with the dimensionless parameters τ_n and Λ into (25). In this manner we find expressions of the form

$$\begin{aligned} a_n(|\gamma|) &\mapsto \tilde{a}_{\Lambda}(\tau_n), & b_n(|\gamma|) &\mapsto \tilde{b}_{\Lambda}(\tau_n) \\ \mathbf{M}_n(|\gamma|) &\mapsto \tilde{\mathbf{M}}_{\Lambda}(\tau_n). \end{aligned} \quad (41)$$

Applying the chain rule, it is now easy to show that

$$\mathbf{M}_n^{[\ell]} = \frac{\tau_n^{\ell}}{|\kappa|^{\ell}} \tilde{\mathbf{M}}_{\Lambda}^{[\ell]}, \quad (42)$$

with the partial derivatives at $\tau_n = 0$,

$$\tilde{\mathbf{M}}_{\Lambda}^{[\ell]} = \frac{i^{\ell-1}}{\ell!} \left. \frac{\partial^{\ell} \tilde{\mathbf{M}}_{\Lambda}(\tau_n)}{\partial \tau_n^{\ell}} \right|_{\tau_n=0}. \quad (43)$$

Thus it follows that the Magnus series (38) only converges if the Maclaurin series

$$\tilde{\mathbf{M}}_{\Lambda}(\tau_n) = i \sum_{\ell=1}^{\infty} (-i\tau_n)^{\ell} \tilde{\mathbf{M}}_{\Lambda}^{[\ell]} \quad (44)$$

converges. To analyze the convergence of the series (44), we consider the matrix elements of $\tilde{\mathbf{M}}_{\Lambda}(\tau_n)$ as complex functions by replacing $\tau_n \mapsto z$. It is then possible to determine the radii r_{Λ} of convergence [55] of these series, $|z| < r_{\Lambda}$, in terms of the singularities of the analytical expressions $\tilde{\mathbf{M}}_{\Lambda}(z)$ in the complex plane [18].

In this manner we can obtain exact limits of convergence for the Magnus series. Details on this rather elaborate procedure are given in Appendix C. The result reads [see Eq. (C10)]

$$|\tau_n| = |\kappa w_n| [t - t_0] < r_{\Lambda} = r_{\Delta\omega} [t - t_0] / 2. \quad (45)$$

Note that again w_n appears only as a factor here, thus for the full Magnus expansion of the full operator (21) we may define $w_{\max} = \max_{n=0,1,\dots} |w_n|$. Then the Magnus expansion for (21) converges for

$$0 \leq [t - t_0] < t_{\max}(\Delta\omega) = \min_{\tilde{t} \in \mathbb{R}_+ : |\kappa w_{\max} \tilde{t}| = r_{\Delta\omega} \tilde{t} / 2} \tilde{t}, \quad (46)$$

where $t_{\max}(\Delta\omega)$ is a function of the frequency mismatch. This exact upper bound of convergence is displayed in Fig. 5.

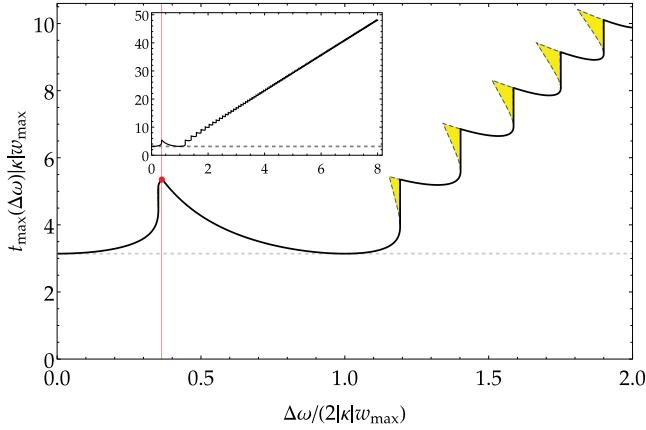


FIG. 5. Upper bound (black solid line) $t_{\max}(\Delta\omega)$ of the convergence time of the Magnus expansion as a function of the frequency mismatch $\Delta\omega$ as defined in (46); the inset illustrates its global behavior. The constant upper bound estimate (gray dashed line) as defined in (40). In the displayed regions (yellow with a blue dashed boundary) the Magnus expansion also converges but divergences have appeared at earlier times, i.e., at the upper bound. A vertical grid line (red) and a point (red) mark the position of the first local maximum of $t_{\max}(\Delta\omega)$.

Note that it may happen that the series becomes again convergent for $t > t_{\max}(\Delta\omega)$ in regions of t where Eq. (45) is fulfilled. However, $t_{\max}(\Delta\omega)$ is the exact upper limit of continuous convergence. Judging from the display of these regions in Fig. 5, they do not increase the range of convergence significantly. For a large frequency mismatch the convergence time increases in a linear fashion. Note that too large detunings may undermine the validity of the model in Eq. (1).

Based on this analysis, the frequency mismatch $\Delta\omega$ in Fig. 4 has been chosen such that the maximal displayed value t corresponds to the first local maximum of $t_{\max}(\Delta\omega)$ in Fig. 5. Thus, we can guarantee convergence of the time-ordering correction to the exact solution for all ranges of t displayed in Fig. 4.

VII. NONCLASSICAL PUMP FIELDS

Let us briefly recapitulate the findings so far. We reconsidered a model which was introduced and solved through a quantization of the pump field in Ref. [24]. In contrast, in the present work the model was solved for a classical pump, i.e., a driving laser. In this section we reconsider each solution and add some remarks regarding the strengths of each strategy. Note that even if in this contribution and in Ref. [24] the same physical model is considered, the investigated scenarios clearly differ.

In Ref. [24] the Hamiltonian, which is given in Eq. (1), was solved via quantization of the pump field. Thus, the Hilbert space was extended and the Hamiltonian became time-independent in the Schrödinger picture. This procedure corresponds formally to the replacement

$$\kappa e^{-i\omega_L t} \rightarrow \hat{b}|\kappa'\rangle. \quad (47)$$

The time-ordering effects, discussed in this work, were naturally contained in the straightforward solution of the time-independent Hamiltonian. The extension of the Hilbert space yields more cumbersome algebraic expressions for all observables under investigation. Additionally, the convergence to the semiclassical solution was only presented via numerical solutions obtained by the PYTHON package QUTIP [56,57]. However, the approach has the advantage of more general input pump fields. As the pump is treated in a quantized manner in its own Hilbert space, one can consider the scenario for arbitrary input states of the pump. In the case of a strong coherent input field, the semiclassical solution is obtained on a finite timescale. Nevertheless, the consideration of squeezed or catlike input states is possible without significant additional effort.

As an example, the input state for the pump field may be assumed,

$$\hat{\rho}_{\text{pump}} = |\Psi_{\text{SV}}\rangle\langle\Psi_{\text{SV}}|, \quad (48)$$

with the squeezed vacuum state

$$|\Psi_{\text{SV}}\rangle = \frac{1}{\cosh \xi} \sum_{n=0}^{\infty} (-\tanh \xi)^n \frac{\sqrt{(2n)!}}{2^n n!} |2n\rangle. \quad (49)$$

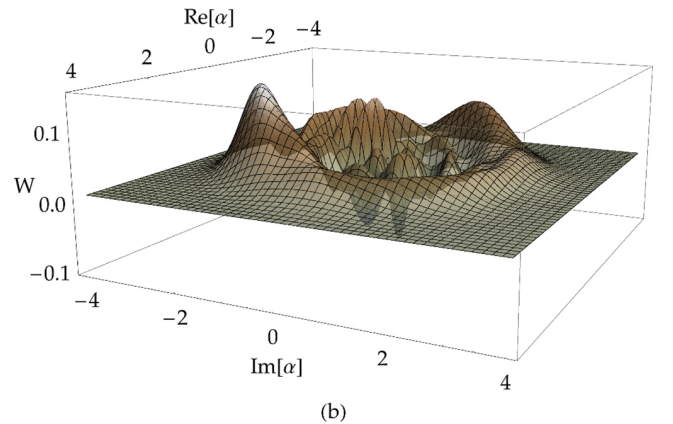
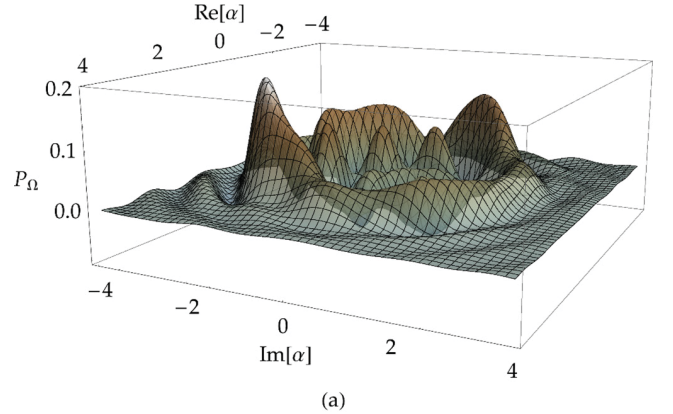


FIG. 6. (a) Regularized Glauber-Sudarshan P function and (b) the corresponding Wigner function for $t|\kappa'| = 500$ and the same parameters as in Fig. 3 but for a nonclassical input pump field as given in Eqs. (48) and (49), for $\xi = 2$.

The required algebra is explicitly given in Ref. [24]. On this basis one may calculate the reduced density matrix of the motional state and the resulting regularized P function [cf. Eq. (33)]. The results are depicted in Fig. 6, where we plotted the regularized P function and the Wigner function for $t|\kappa'| = 500$, considering a squeezing parameter of $\xi = 2$. This choice of ξ corresponds to a squeezing strength of approximately 17.4 dB, so far 15-dB squeezing is experimentally available [58]. We use $\xi = 2$ to visualize more significant effects of a nonclassical pump field. The presented quasiprobabilities in Fig. 6 are similar to those for the classical input [cf. Figs. 3(a) and 3(c)]. The phase-space representations in Fig. 6, however, exhibit an additional circular distribution surrounding the structures as they typically occur for the semiclassical pump. Hence, the usage of a nonclassical pump might lead to so far unstudied effects which need a more detailed treatment, which is beyond the scope of this work. In summary, the findings of this section clarify that the choice of the solution [Eq. (23) or Ref. [24]] of the system depends on the particular case under study.

VIII. CONCLUSION

In summary, we derived an exact solution for the dynamics corresponding to the classically driven detuned nonlinear Jaynes-Cummings model describing the quantized motion of a trapped ion. The solution was formulated by applying a spinor formalism which decoupled the dynamics in terms of 2×2 matrix differential equations. These matrix differential equations have been solved analytically, which resulted in analytical expressions for the evolution operator of the system. Applying the latter, we have reproduced results on the dynamics of the population probability of the excited electronic state that have been obtained numerically in Ref. [24].

The analytical expression for the time-evolution operator allows for the investigation of time-ordering effects. Using a regularized version of the Glauber-Sudarshan P function and the Wigner function, we have discussed the influence of time-ordering effects on the nonclassicality and nonsimulatability of the motional states of the ion. Especially on large timescales, the whole nonclassical and non-Gaussian character is contained in contributions which are connected to noncommuting Hamiltonians.

Furthermore, based on the analytical solution, a generating function for the time-ordering corrections could be derived. This function generates all terms up to arbitrary order of the Magnus expansion for the evolution operator of the nonlinear Jaynes-Cummings model. As an example for the impact of different orders of time-ordering corrections on observables, the population probability of the excited electronic state has been considered without time ordering, with full time ordering, and with different orders of time-ordering corrections. With increasing orders of corrections, the quality of approximation improved. By extending the generating function to the complex plane, we could determine the convergence of time-ordering corrections by locating the singularities of the former in the complex plane. It was shown that these exact upper bounds depend on the frequency mismatch and exceed known sufficient upper bounds over a wide range of detunings. Additionally we have observed

isolated regions of convergence above these upper bounds. The obtained exact upper bound has allowed us to analyze the impact of time-ordering corrections above the sufficient upper bound.

In the last part of the work we discussed the influence of a nonclassical pump field on the motional state. We used a squeezed vacuum state to reveal discrepancies to the semiclassical solutions in phase space. The findings suggest that a nonclassical pump causes a dynamics beyond the one derived in the semiclassical pump scenario.

ACKNOWLEDGMENTS

We thank Benjamin Kühn for helpful comments regarding the discussion of non-Gaussianity. T.L., M.I.K., and W.V. acknowledge funding from the European Union's Horizon 2020 Research and Innovation program under Grant Agreement No. 665148 (QCUMBER).

APPENDIX A: SOLUTION TO THE MATRIX DIFFERENTIAL EQUATION

To solve the matrix differential equations

$$\partial_t \mathbf{U}_n(t, t_0) = -i \begin{pmatrix} 0 & |\kappa| w_n e^{-i\Delta\omega t} \\ |\kappa| w_n e^{i\Delta\omega t} & 0 \end{pmatrix} \mathbf{U}_n(t, t_0) \quad (\text{A1})$$

with initial condition $\mathbf{U}_n(t, t_0)|_{t=t_0} = \mathbf{I}$ we write

$$\begin{pmatrix} 0 & |\kappa| w_n e^{-i\Delta\omega t} \\ |\kappa| w_n e^{i\Delta\omega t} & 0 \end{pmatrix} = \mathbf{S}^\dagger(t) \begin{pmatrix} 0 & |\kappa| w_n \\ |\kappa| w_n & 0 \end{pmatrix} \mathbf{S}(t),$$

with

$$\mathbf{S}(t) = \begin{pmatrix} e^{i\Delta\omega t/2} & 0 \\ 0 & e^{-i\Delta\omega t/2} \end{pmatrix}, \quad (\text{A2})$$

such that

$$\mathbf{S}(t) \partial_t \mathbf{U}_n(t, t_0) = -i \begin{pmatrix} 0 & |\kappa| w_n \\ |\kappa| w_n & 0 \end{pmatrix} \mathbf{S}(t) \mathbf{U}_n(t, t_0). \quad (\text{A3})$$

Adding the term $[\partial_t \mathbf{S}(t)] \mathbf{U}_n(t, t_0)$ on both sides of the equation, applying the product rule on the left-hand side, and executing the derivative

$$\partial_t \mathbf{S}(t) = -i \begin{pmatrix} -\Delta\omega/2 & 0 \\ 0 & \Delta\omega/2 \end{pmatrix} \mathbf{S}(t) \quad (\text{A4})$$

on the right-hand side yields the constant parameter differential equation

$$\partial_t [\mathbf{S}(t) \mathbf{U}_n(t, t_0)] = -i \begin{pmatrix} -\Delta\omega/2 & |\kappa| w_n \\ |\kappa| w_n & \Delta\omega/2 \end{pmatrix} [\mathbf{S}(t) \mathbf{U}_n(t, t_0)], \quad (\text{A5})$$

with initial condition $[\mathbf{S}(t) \mathbf{U}_n(t, t_0)]|_{t=t_0} = \mathbf{S}(t_0)$. The solution is easily found as

$$[\mathbf{S}(t) \mathbf{U}_n(t, t_0)] = \exp \left\{ -i(t - t_0) \begin{pmatrix} -\Delta\omega/2 & |\kappa| w_n \\ |\kappa| w_n & \Delta\omega/2 \end{pmatrix} \right\} \mathbf{S}(t_0), \quad (\text{A6})$$

which leads to

$$\begin{aligned} \mathbf{U}_n(t, t_0) &= \mathbf{S}^\dagger(t) \exp \left\{ -i(t - t_0) \begin{pmatrix} -\Delta\omega/2 & |\kappa|w_n \\ |\kappa|w_n & \Delta\omega/2 \end{pmatrix} \right\} \mathbf{S}(t_0) \\ &= \begin{pmatrix} a_n(t, t_0) & b_n(t, t_0) \\ -b_n^*(t, t_0) & a_n^*(t, t_0) \end{pmatrix}, \end{aligned} \quad (\text{A7})$$

with

$$\begin{aligned} a_n(t, t_0) &= e^{-i\Delta\omega[t-t_0]/2} \left[\cos(\Gamma_n[t - t_0]) \right. \\ &\quad \left. + \frac{i\Delta\omega}{2\Gamma_n} \sin(\Gamma_n[t - t_0]) \right], \\ b_n(t, t_0) &= e^{-i\Delta\omega[t-t_0]/2} \frac{|\kappa|w_n}{i\Gamma_n} \sin(\Gamma_n[t - t_0]), \end{aligned} \quad (\text{A8})$$

$$\text{and } \Gamma_n = \sqrt{(\frac{\Delta\omega}{2})^2 + w_n^2 |\kappa|^2}.$$

APPENDIX B: MAGNUS TERMS

The Magnus terms up to fifth order have been computed from the generating function (37) and the ordered nested non-equal-time commutators [cf. (14)]. The equivalence of the results verified that (37) is indeed the generating function of the Magnus terms. They read

$$\begin{aligned} \mathbf{M}_n^{[\ell]}(t, t_0) &= w_n^\ell [t - t_0]^\ell f_\ell \left(\frac{\Delta\omega[t - t_0]}{2} \right) \\ &\quad \times \begin{pmatrix} 0 & e^{-i\Delta\omega[t+t_0]/2} \\ e^{i\Delta\omega[t-r_0]/2} & 0 \end{pmatrix} \end{aligned} \quad (\text{B1})$$

for ℓ odd and

$$\mathbf{M}_n^{[\ell]}(t, t_0) = i w_n^\ell [t - t_0]^\ell f_\ell \left(\frac{\Delta\omega[t - t_0]}{2} \right) \begin{pmatrix} 1 & 0 \\ 0 & -1 \end{pmatrix} \quad (\text{B2})$$

for ℓ even, with the functions

$$f_1(z) = j_0(z), \quad (\text{B3})$$

$$f_2(z) = \frac{1}{2} [j_1(z) \cos(z) - j_0(z) \sin(z)], \quad (\text{B4})$$

$$f_3(z) = \frac{1}{6} [-j_0^3(z) + j_0(z) + j_2(z)], \quad (\text{B5})$$

$$\begin{aligned} f_4(z) &= \frac{1}{12} \left[\frac{1}{2} j_0^2(z) \sin(2z) - \frac{1}{2} j_0(z) \sin(z) - \frac{1}{2} j_1^2(z) \sin(2z) \right. \\ &\quad \left. - \frac{1}{2} j_2(z) \sin(z) - j_1(z) j_0(z) \cos(2z) \right. \\ &\quad \left. + \frac{3}{10} j_1(z) \cos(z) + \frac{3}{10} j_3(z) \cos(z) \right], \end{aligned} \quad (\text{B6})$$

$$\begin{aligned} f_5(z) &= \frac{1}{60} \left[\frac{j_0(z)}{2} + \frac{5j_2(z)}{7} + \frac{3j_4(z)}{14} + 2j_1^2(z) j_0(z) \sin^2(z) \right. \\ &\quad \left. - \frac{13}{6} j_1(z) j_0(z) \sin(z) \right. \\ &\quad \left. - \frac{1}{2} j_3(z) j_0(z) \sin(z) - \frac{5}{3} j_1(z) j_2(z) \sin(z) \right. \\ &\quad \left. + 2j_0^3(z) \cos^2(z) - \frac{5}{2} j_0^2(z) \cos(z) \right] \end{aligned}$$

$$- \frac{5}{2} j_2(z) j_0(z) \cos(z) + 4j_1(z) j_0^2(z) \sin(z) \cos(z) \Big] \quad (\text{B7})$$

that are defined in terms of the pole free spherical Bessel functions $j_0(z) = \text{sinc}(z)$. Evaluating the corresponding matrix exponentials, e.g., in second order

$$\mathbf{U}_n^{[2]}(t, t_0) = e^{-i|\kappa| \mathbf{M}_n^{[1]}(t, t_0) - |\kappa|^2 \mathbf{M}_n^{[2]}(t, t_0)} \quad (\text{B8})$$

yields the corresponding approximations for $a_n(t, t_0)$ and $b_n(t, t_0)$, i.e., $a_n^{[\ell]}(t, t_0)$ and $b_n^{[\ell]}(t, t_0)$.

APPENDIX C: CONVERGENCE TREATMENT

The replacement $\tau_n \mapsto z$ in the matrix elements of $\tilde{\mathbf{M}}_\Lambda(\tau_n)$ [cf. (41)] is performed after the conjugations in (37), i.e., z itself is not conjugated. In this manner we get the representations as

$$\begin{aligned} \tilde{\mathbf{M}}_\Lambda(z) &= \frac{\arccos[A_{R,\Lambda}(z)]}{\sqrt{1 - A_{R,\Lambda}^2(z)}} \\ &\quad \times \begin{pmatrix} -A_{I,\Lambda}(z) & e^{-i\Delta\omega[t+t_0]/2} B_\Lambda(z) \\ e^{i\Delta\omega[t+t_0]/2} B_\Lambda(z) & A_{I,\Lambda}(z) \end{pmatrix}, \end{aligned} \quad (\text{C1})$$

with

$$\begin{aligned} A_{R,\Lambda}(z) &= \cos(\Lambda) \cos[\gamma_\Lambda(z)] + \Lambda \sin(\Lambda) \text{sinc}[\gamma_\Lambda(z)], \\ A_{I,\Lambda}(z) &= -\sin(\Lambda) \cos[\gamma_\Lambda(z)] + \Lambda \cos(\Lambda) \text{sinc}[\gamma_\Lambda(z)], \\ B_\Lambda(z) &= z \text{sinc}[\gamma_\Lambda(z)], \end{aligned} \quad (\text{C2})$$

where $\gamma_\Lambda(z) = \sqrt{\Lambda^2 + z^2}$. Replacing $z \mapsto |\kappa|$ in (C1) yields (37). Thus, (C1) is a continuation of (37).

First, let us note that there is no branching in the functions (C2) as the square root $\gamma_\Lambda(z)$ only appears in the even cos and sinc functions. Furthermore, let us note that with the generating function [59]

$$\frac{1}{Z} \cos(\sqrt{Z^2 - 2ZT}) = \sum_{p=0}^{\infty} \frac{T^p}{p!} j_{p-1}(Z) \quad (\text{C3})$$

of the spherical Bessel functions

$$j_{-1}(Z) = \frac{\cos(Z)}{Z}, \quad j_p(Z) = (-Z)^p \left(\frac{1}{Z} \frac{d}{dZ} \right)^p \frac{\sin(Z)}{Z} \quad \text{for } p = 0, 1, \dots \quad (\text{C4})$$

and its derivative in terms of T , we can find the Maclaurin series representations

$$\begin{aligned} \cos[\gamma_\Lambda(z)] &= \Lambda \sum_{p=0}^{\infty} \frac{1}{p!} \left(\frac{-z^2}{2\Lambda} \right)^p j_{p-1}(\Lambda), \quad \text{sinc}[\gamma_\Lambda(z)] \\ &= \sum_{p=0}^{\infty} \frac{1}{p!} \left(\frac{-z^2}{2\Lambda} \right)^p j_p(\Lambda). \end{aligned} \quad (\text{C5})$$

Note that the series are entirely independent of the conjugated complex variable z^* .

With the help of $|j_p(Z)| \leq 1$ for $p = 0, 1, \dots$ and $Z \in [0, \infty)$, we can show absolute convergence of these series with

upper bounds

$$|\cos[\gamma_\Lambda(z)]| \leq |\cos(\Lambda)| + \Lambda \left(\exp \left[\frac{|z|^2}{2|\Lambda|} \right] - 1 \right),$$

$$|\text{sinc}[\gamma(z)]| \leq \exp \left[\frac{|z|^2}{2|\Lambda|} \right]. \quad (\text{C6})$$

Thus, the functions $A_{I,\Lambda}(z)$, $A_{R,\Lambda}(z)$, and $B_\Lambda(z)$ defined in (C2) are analytical functions in the full complex plane $z \in \mathbb{C}$. Thus, singularities of $\tilde{\mathbf{M}}_\Lambda(z)$ can only stem from the factor

$$f(A_{R,\Lambda}(z)) = \frac{\arccos[A_{R,\Lambda}(z)]}{\sqrt{1 - A_{R,\Lambda}^2(z)}}. \quad (\text{C7})$$

Note that

$$f(z) = \frac{dF(z)}{dz} \quad (\text{C8})$$

with $F(z) = -\frac{1}{2}\arccos^2(z)$. One can show that the function $F(z)$ has a branch point at $z = -1$ [but unlike $\arccos(z)$ not at $z = 1$] (a beautiful introduction to the concepts of branch points and branch cuts can be found in Ref. [55]).

Consequently, $f(z)$ has the same branch point as $F(z)$. Thus, the function $f(A_{R,\Lambda}(z))$ has branch points wherever $A_{R,\Lambda}(z) = -1$, i.e., the branch points of $f(A_{R,\Lambda}(z))$ correspond to the zeros of the analytic function

$$g_\Lambda(z) = A_{R,\Lambda}(z) + 1. \quad (\text{C9})$$

As we have shown that all other functions appearing in (C1) are analytic, $\tilde{\mathbf{M}}_\Lambda(z)$ also has branch points, where $g_\Lambda(z) = 0$. The branch cut lines, originating from the branch points, can always be chosen such that they point away from the origin and do not cross. Thus, a series expansion of $\tilde{\mathbf{M}}_\Lambda(z)$ around $z = 0$ will converge for $|z| < r_\Lambda$, where

$$r_\Lambda = \min_{z_0 \in \mathbb{C}: g_\Lambda(z_0)=0} |z_0|. \quad (\text{C10})$$

We have evaluated r_Λ in a range of Λ going from $\Lambda = 0.005\pi$ to $\Lambda = 200\pi$ in steps of 0.005π . This was achieved by extracting the line data from the ContourPlot function (contours $\text{Re}[g_\Lambda(z)] = 0$ and $\text{Im}[g_\Lambda(z)] = 0$) in *Mathematica* to get estimates for the location of the minimal absolute value zeros of $g(z)$, which were then refined by the FindRoot function in *Mathematica*.

-
- [1] W. Vogel and D.-G. Welsch, *Quantum Optics*, 3rd ed. (Wiley-VCH, Berlin, 2006).
 - [2] W. P. Schleich, *Quantum Optics in Phase Space* (Wiley-VCH, Berlin, 2001).
 - [3] G. S. Agarwal, *Quantum Optics* (Cambridge University Press, Cambridge, 2013).
 - [4] G. Grynberg, A. Aspect, and C. Fabre, *Introduction to Quantum Optics* (Cambridge University Press, Cambridge, 2010).
 - [5] H. J. Carmichael and D. F. Walls, A quantum-mechanical master equation treatment of the dynamical Stark effect, *J. Phys. B* **9**, 1199 (1976).
 - [6] H. J. Kimble and L. Mandel, Theory of resonance fluorescence, *Phys. Rev. A* **13**, 2123 (1976).
 - [7] H. J. Kimble, M. Dagenais, and L. Mandel, Photon Antibunching in Resonance Fluorescence, *Phys. Rev. Lett.* **39**, 691 (1977).
 - [8] A. Einstein, Über einen die Erzeugung und Verwandlung des Lichtes betreffenden heuristischen Gesichtspunkt, *Ann. Phys. (Leipzig)* **322**, 132 (1905).
 - [9] A. Miranowicz, J. Bajer, H. Matsueda, M. R. B. Wahiddin, and R. Tanas, Comparative study of photon antibunching of non-stationary fields, *J. Opt. B* **1**, 511 (1999).
 - [10] W. Vogel, Nonclassical Correlation Properties of Radiation Fields, *Phys. Rev. Lett.* **100**, 013605 (2008).
 - [11] L. D. Landau and E. M. Lifshitz, *Quantum Mechanics*, 3rd ed. (Elsevier, Oxford, 1977).
 - [12] D. J. Griffiths, *Introduction to Quantum Mechanics* (Prentice-Hall, London, 1995).
 - [13] T. Fließbach, *Quantenmechanik*, 5th ed. (Spektrum Akademischer, Heidelberg, 2008).
 - [14] F. J. Dyson, The radiation theories of Tomonaga, Schwinger, and Feynman, *Phys. Rev.* **75**, 486 (1949).
 - [15] L. Knöll, W. Vogel, and D.-G. Welsch, Action of passive, lossless optical systems in quantum optics, *Phys. Rev. A* **36**, 3803 (1987).
 - [16] A. Christ, B. Brecht, W. Mauere, and C. Silberhorn, Theory of quantum frequency conversion and type-II parametric down-conversion in the high-gain regime, *New J. Phys.* **15**, 053038 (2013).
 - [17] W. Magnus, On the exponential solution of differential equations for a linear operator, *Commun. Pure Appl. Math.* **7**, 649 (1954).
 - [18] S. Blanes, F. Casas, J. A. Oteo, and J. Ros, The Magnus expansion and some of its applications, *Phys. Rep.* **470**, 151 (2009).
 - [19] T. Lipfert, D. B. Horoshko, G. Patera, and M. I. Kolobov, Bloch-Messiah decomposition and Magnus expansion for parametric down-conversion with monochromatic pump, *Phys. Rev. A* **93**, 013815 (2018).
 - [20] N. Quesada and J. E. Sipe, Effects of time ordering in quantum nonlinear optics, *Phys. Rev. A* **90**, 063840 (2014).
 - [21] N. Quesada and J. E. Sipe, Time-Ordering Effects in the Generation of Entangled Photons Using Nonlinear Optical Processes, *Phys. Rev. Lett.* **114**, 093903 (2015).
 - [22] N. Quesada and J. E. Sipe, High efficiency in mode-selective frequency conversion, *Opt. Lett.* **41**, 364 (2016).
 - [23] F. Krumm, J. Sperling, and W. Vogel, Multi-time correlation functions in nonclassical stochastic processes, *Phys. Rev. A* **93**, 063843 (2016).
 - [24] F. Krumm and W. Vogel, Time-dependent nonlinear Jaynes-Cummings dynamics of a trapped ion, *Phys. Rev. A* **97**, 043806 (2018).
 - [25] S. De Bièvre, D. B. Horoshko, G. Patera, and M. I. Kolobov, Measuring nonclassicality of bosonic field quantum states via operator ordering sensitivity, [arXiv:1809.02047](https://arxiv.org/abs/1809.02047).
 - [26] D. Prato and P. W. Lamberti, A note on Magnus formula, *J. Chem. Phys.* **106**, 4640 (1997).
 - [27] C. A. Blockley, D. F. Walls, and H. Risken, Quantum collapses and revivals in a quantized trap, *Europhys. Lett.* **17**, 509 (1992).

- [28] C. A. Blockley and D. F. Walls, Cooling of a trapped ion in the strong-sideband regime, *Phys. Rev. A* **47**, 2115 (1993).
- [29] J. I. Cirac, R. Blatt, A. S. Parkins, and P. Zoller, Quantum collapse and revival in the motion of a single trapped ion, *Phys. Rev. A* **49**, 1202 (1994).
- [30] J. I. Cirac, A. S. Parkins, R. Blatt, and P. Zoller, “Dark” Squeezed States of the Motion of a Trapped Ion, *Phys. Rev. Lett.* **70**, 556 (1993).
- [31] D. M. Meekhof, C. Monroe, B. E. King, W. M. Itano, and D. J. Wineland, Generation of Nonclassical Motional States of a Trapped Atom, *Phys. Rev. Lett.* **76**, 1796 (1996).
- [32] R. L. de Matos Filho and W. Vogel, Even and Odd Coherent States of the Motion of a Trapped Ion, *Phys. Rev. Lett.* **76**, 608 (1996).
- [33] R. L. de Matos Filho and W. Vogel, Nonlinear coherent states, *Phys. Rev. A* **54**, 4560 (1996).
- [34] S.-C. Gou, J. Steinbach, and P. L. Knight, Dark pair coherent states of the motion of a trapped ion, *Phys. Rev. A* **54**, R1014(R) (1996).
- [35] S.-C. Gou, J. Steinbach, and P. L. Knight, Vibrational pair cat states, *Phys. Rev. A* **54**, 4315 (1996).
- [36] C. C. Gerry, S.-C. Gou, and J. Steinbach, Generation of motional SU(1, 1) intelligent states of a trapped ion, *Phys. Rev. A* **55**, 630 (1997).
- [37] C. Monroe, D. M. Meekhof, B. E. King, and D. J. Wineland, A “Schrödinger cat” superposition state of an atom, *Science* **272**, 1131 (1996).
- [38] C. C. Gerry, Generation of Schrödinger cats and entangled coherent states in the motion of a trapped ion by a dispersive interaction, *Phys. Rev. A* **55**, 2478 (1997).
- [39] S. Wallentowitz and W. Vogel, Quantum-mechanical counterpart of nonlinear optics, *Phys. Rev. A* **55**, 4438 (1997).
- [40] W. Vogel and R. L. de Matos Filho, Nonlinear Jaynes-Cummings dynamics of a trapped ion, *Phys. Rev. A* **52**, 4214 (1995).
- [41] M. I. Kolobov, The spatial behavior of nonclassical light, *Rev. Mod. Phys.* **71**, 1539 (1999).
- [42] D. J. Heinzen and D. J. Wineland, Quantum-limited cooling and detection of radio-frequency oscillations by laser-cooled ions, *Phys. Rev. A* **42**, 2977 (1990).
- [43] R. J. Glauber, Coherent and incoherent states of the radiation field, *Phys. Rev.* **131**, 2766 (1963).
- [44] E. C. G. Sudarshan, Equivalence of Semiclassical and Quantum Mechanical Descriptions of Statistical Light Beams, *Phys. Rev. Lett.* **10**, 277 (1963).
- [45] U. M. Titulaer and R. J. Glauber, Correlation functions for coherent fields, *Phys. Rev.* **140**, B676 (1965).
- [46] L. Mandel, Non-classical states of the electromagnetic field, *Phys. Scr.* **T12**, 34 (1986).
- [47] T. Kiesel and W. Vogel, Nonclassicality filters and quasiprobabilities, *Phys. Rev. A* **82**, 032107 (2010).
- [48] T. Kiesel, W. Vogel, B. Hage, and R. Schnabel, Direct Sampling of Negative Quasiprobabilities of a Squeezed State, *Phys. Rev. Lett.* **107**, 113604 (2011).
- [49] E. Agudelo, J. Sperling, W. Vogel, S. Köhnke, M. Mraz, and B. Hage, Continuous sampling of the squeezed-state nonclassicality, *Phys. Rev. A* **92**, 033837 (2015).
- [50] B. Kühn and W. Vogel, Visualizing nonclassical effects in phase space, *Phys. Rev. A* **90**, 033821 (2014).
- [51] E. Wigner, On the quantum correction for thermodynamic equilibrium, *Phys. Rev.* **40**, 749 (1932).
- [52] S. Rahimi-Keshari, T. C. Ralph, and C. M. Caves, Sufficient Conditions for Efficient Classical Simulation of Quantum Optics, *Phys. Rev. X* **6**, 021039 (2016).
- [53] B. Kühn and W. Vogel, Quantum non-Gaussianity and quantification of nonclassicality, *Phys. Rev. A* **97**, 053823 (2018).
- [54] R. A. Horn and C. R. Johnson, *Matrix Analysis*, 2nd ed. (Cambridge University Press, New York, 1985), p. 346.
- [55] T. Needham, *Visual Complex Analysis* (Oxford University Press, Oxford, 1997).
- [56] J. R. Johansson, P. D. Nation, and F. Nori, QuTiP: An open-source Python framework for the dynamics of open quantum systems, *Comput. Phys. Commun.* **183**, 1760 (2012).
- [57] J. R. Johansson, P. D. Nation, and F. Nori, QuTiP 2: A Python framework for the dynamics of open quantum systems, *Comput. Phys. Commun.* **184**, 1234 (2013).
- [58] H. Vahlbruch, M. Mehmet, K. Danzmann, and R. Schnabel, Detection of 15 dB Squeezed States of Light and their Application for the Absolute Calibration of Photoelectric Quantum Efficiency, *Phys. Rev. Lett.* **117**, 110801 (2016).
- [59] M. Abramowitz and I. A. Stegun, *Handbook of Mathematical Functions* (Dover, New York, 1974), Sec. 10.1.40.

PAPER

Anomalous quantum correlations in the motion of a trapped ion

To cite this article: F Krumm and W Vogel 2019 *Phys. Scr.* **94** 085101

View the [article online](#) for updates and enhancements.

Anomalous quantum correlations in the motion of a trapped ion

F Krumm  and W Vogel

Arbeitsgruppe Theoretische Quantenoptik, Institut für Physik, Universität Rostock, D-18059 Rostock, Germany

E-mail: fabian.krumm@uni-rostock.de

Received 16 November 2018, revised 16 January 2019

Accepted for publication 6 February 2019

Published 29 April 2019



Abstract

In a previous paper (Krumm and Vogel 2018 *Phys. Rev. A* **97** 043806) we presented a method to solve the nonlinear Jaynes–Cummings dynamics, describing the quantized motion of a trapped ion exactly, including detuning. Here we investigate this model with respect to nonclassical effects, such as squeezing and sub-Poisson statistics. We show that for the versatile model under study there exist quantum phenomena beyond squeezing and sub-Poisson statistics, such as anomalous quantum correlations of two non-commuting observables. In particular, it is shown that for the excitation of the zeroth sideband neither squeezing nor sub-Poisson statistics occur, but anomalous correlations can be verified. Furthermore, it is shown how these anomalous correlation functions can be derived from measured data.

Keywords: quantum physics, quantum optics, trapped ions

(Some figures may appear in colour only in the online journal)

1. Introduction

In the wide-ranging field of quantum optics, vital areas of interest are the identification, characterization and quantification of nonclassical effects—i.e. effects that can not be explained within Maxwell’s theory of classical electrodynamics. During the last decades significant efforts were made to develop techniques that allow not only for the theoretical description but also for the experimental verification of nonclassical states. Prominent examples are photon antibunching [1–3], squeezing [4–8], sub-Poisson statistics [9–11], and entanglement [12–17].

On a general basis, nonclassicality can be subdivided into two sets, namely single-time and multi-time nonclassicality. This means, there exist effects that can be characterized by using a single point in time and effects which need, for its description, two or more points in time. One example of the latter is photon antibunching as two points in time are required for its general analysis.

A general treatment of quantum correlations of radiation fields was introduced in [18]. Based on normal- and time-ordered correlation functions, it was shown that a plethora of multi-time nonclassicality criteria can be derived. They verify

nonclassical effects beyond photon antibunching and, in the special single-time scenario, nonclassicality beyond squeezing and sub-Poisson light. Those phenomena include so called anomalous correlations of non-commuting observables [19]. Such effects have recently been demonstrated to occur for squeezed coherent light, even for phase values when squeezing does not occur [20].

The question arises whether or not a similar behavior can be found in other, more sophisticated physical systems. An encouraging approach can be based on the Jaynes–Cummings model [21, 22], which was widely applied in cavity QED, see e.g. [23]. Using a vibrational rotating-wave approximation, this model also applies to describe the quantized center-of-mass motion of a trapped ion in a Paul trap [24, 25], for related experiments, see [26]. During the years it became feasible to study many nonclassical motional states of the ion [27–36]. Under more general conditions, the Hamiltonian describing the dynamics of a trapped ion attains the form of a nonlinear Jaynes–Cummings model [37]. Recently, the latter was extended to include some frequency mismatch, leading to an explicitly time-dependent dynamics [38]. It is noteworthy that related approaches can include the counter-rotating terms of the Hamiltonian, which are neglected withing the vibrational

rotating-wave approximation. The corresponding framework is referred to as Quantum Rabi Model, which is for example treated in [39–44].

In the present paper, we study the nonlinear Jaynes–Cummings dynamics to analyze quantum effects in the atomic center-of-mass motion of a trapped ion, with particular emphasis on anomalous quantum correlations. As those correlations are normal-ordered ones, they are not hindered by vacuum fluctuations which typically occur in the presence of losses. In addition, as it was demonstrated in a recent quantum-optics experiment, the anomalous quantum correlations are capable of certifying nonclassicality beyond squeezing; see [20]. The reduction of quantum noise effects by the use of squeezed states is limited to narrow phase intervals, in particular for strong squeezing. As strongly squeezed states can be easily prepared in the center-of-mass motion of trapped ions, see [28], this opens new applications of squeezing for phase-noise tolerant applications of trapped ions in quantum technology. Thus, we investigate how anomalous quantum correlations behave in the dynamics of trapped ions driven in the resolved sideband regime and how they can be detected. Moreover, we demonstrate that those correlations can be even prepared when squeezing or sub-Poisson statistics do not persist.

The paper is structured as follows. In section 2 we briefly recapitulate the model under study. Afterwards, in section 3 we analyze in some detail nonclassical phenomena. A detailed consideration of the measurement of the correlation functions under study is provided in section 4. Finally, we give a summary and some conclusions in section 5.

2. The nonlinear Jaynes–Cummings model including detuning

The time-independent version of the nonlinear Jaynes–Cummings model was introduced in [37]. In order to study the influence of time ordering and a time-dependent Hamiltonian in general, we extended the model such that a detuning between the monochromatic driving laser and the electronic transitions can be included [38]. To solve the resulting time-dependent Hamiltonian analytically, the driving laser-field was quantized. That is, the amplitude of the laser, β_0 , was replaced by the corresponding Hilbert-space operator \hat{b} , which obeys the eigenvalue equation

$$\hat{b}|\beta_0\rangle = \beta_0|\beta_0\rangle, \quad (1)$$

where $|\beta_0\rangle$ is a coherent input state of a cavity mode. In the limit of a strong coherent amplitude, $\beta_0 \gg 1$, the classical solutions of the dynamics are recovered [45]. In this section we recapitulate the basic equations and the obtained analytic solutions of the interaction problem. The total Hamiltonian to be studied in the Schrödinger picture, including the quantized

pump field (cavity field), reads as

$$\begin{aligned} \hat{H} &= \hat{H}_0 + \hat{H}_{\text{int}}, \\ \hat{H}_0 &= \hbar\nu\hat{a}^\dagger\hat{a} + \hbar\omega_L\hat{b}^\dagger\hat{b} + \hbar\omega_{21}\hat{A}_{22}, \\ \hat{H}_{\text{int}} &= \hbar\kappa\hat{A}_{21}\hat{b}\hat{f}_k(\hat{a}^\dagger\hat{a}; \eta)\hat{a}^k + \text{H.c.} \end{aligned} \quad (2)$$

The first term of \hat{H}_0 describes the free evolution of the vibrational center-of-mass motion, with the vibrational frequency ν . The second term represents the free evolution of the cavity field, with the laser frequency $\omega_L = \omega_{21} - k\nu + \Delta\omega$. The free evolution of the electronic degrees of freedom of the two-level ion, with the electronic transition frequency $\omega_{21} = \omega_2 - \omega_1$, is given by the third term of \hat{H}_0 . The operators \hat{a}^\dagger (\hat{a}) create (annihilate) the quanta of the vibrational mode whose energy levels are equidistantly separated by ν . The atomic $|j\rangle \rightarrow |i\rangle$ transitions are described by the atomic flip operators $\hat{A}_{ij} = |i\rangle\langle j|$ ($i, j = 1, 2$). In \hat{H}_{int} , κ is the coupling of the vibronic system and

$$\begin{aligned} \hat{f}_k(\hat{n}; \eta) &= \frac{1}{2}e^{i\Delta\phi - \eta^2/2} \sum_{l=0}^{\infty} \frac{(\eta)^{2l+k}}{l!(l+k)!} \hat{a}^l \hat{a}^l + \text{H.c.} \\ &= \frac{1}{2}e^{i\Delta\phi - \eta^2/2} \sum_{n=0}^{\infty} |n\rangle\langle n| \frac{(\eta)^{kn}}{(n+k)!} L_n^{(k)}(\eta^2) + \text{H.c.} \end{aligned} \quad (3)$$

describes the mode structure of the driving laser (standing wave) at the operator-valued position of the ion. $L_n^{(k)}$ denotes the generalized Laguerre polynomials, $|n\rangle$ the motional number states, $\hat{n} = \hat{a}^\dagger\hat{a}$ the corresponding number operator, $\Delta\phi$ defines the position of the trap potential relative to the laser wave, and η is the Lamb–Dicke parameter.

The physical interpretation of the Hamiltonian in equation (2) is as follows: a cavity photon is absorbed (\hat{b}) and the trapped ion is excited (\hat{A}_{21}). The transitions of the vibrational states ($\hat{f}_k(\hat{a}^\dagger\hat{a}; \eta)\hat{a}^k$) occur according to the chosen laser frequency such that only the $|n\rangle \leftrightarrow |n-k\rangle$ transitions are driven. That is, we assume we operate in a limit that the vibrational sidebands can be resolved very well (resolved sideband regime). Note that the electronic de-excitation process is described by the H.c. term.

The dynamics of the Hamiltonian in equation (2) is described by the time-evolution operator [38]

$$\begin{aligned} \hat{U}(t, t_0) &= \sum_{\sigma=\pm} \sum_{m,n=0}^{\infty} e^{-i\omega_{mn}^\sigma(t-t_0)} |\psi_{mn}^\sigma\rangle \langle\psi_{mn}^\sigma| \\ &+ \sum_{n=0}^{\infty} e^{-i\nu n(t-t_0)} |1, 0, n\rangle \langle 1, 0, n| \\ &+ \sum_{m=0}^{\infty} \sum_{q=0}^{k-1} e^{-i[\nu q + \omega_L(m+1)](t-t_0)} |1, m+1, q\rangle \langle 1, m+1, q|. \end{aligned} \quad (4)$$

The eigenstates of the Hamiltonian read as

$$|\psi_{mn}^\pm\rangle = c_{mn}^\pm(|2, m, n\rangle + \alpha_{mn}^\pm|1, m+1, n+k\rangle). \quad (5)$$

In $|i, m, n\rangle$, the $i = 1, 2$ refer to the electronic excitations, m and n are the photon number of the cavity field and the motional excitation of the ion, respectively. Furthermore, one

finds

$$\begin{aligned}
 c_{mn}^{\pm} &= \frac{1}{\sqrt{1 + |\alpha_{mn}^{\pm}|^2}}, \\
 \alpha_{mn}^{\pm} &= \frac{\Delta\omega \pm \sqrt{\Delta\omega^2 + |\Omega_{mn}|^2}}{\Omega_{mn}}, \\
 \omega_{mn}^{\pm} &= \frac{1}{2} \{ \Delta\omega(2m+1) + \nu(2n-2km) + \omega_{21}(2m+2) \\
 &\quad \pm \sqrt{\Delta\omega^2 + |\Omega_{mn}|^2} \}, \\
 \Omega_{mn} &= 2\kappa\sqrt{m+1}f_k(n; \eta)\sqrt{\frac{(n+k)!}{n!}}, \\
 f_k(n; \eta) &= \langle n | \hat{f}_k(\hat{n}; \eta) | n \rangle.
 \end{aligned} \tag{6}$$

Based on these solutions, general properties of the center-of-mass motion can be described.

3. Nonclassicality

During the last decades various criteria to identify nonclassicality of different types were derived. The most elementary conditions are those for squeezing [4–8] and sub-Poisson statistics (Mandel Q parameter) [9–11]. In this section we investigate nonclassical properties and their temporal evolutions in the explicitly time-dependent nonlinear Jaynes–Cummings model. In [38], it was already shown that the vibrational states are clearly nonclassical for the times under study. Here, we discuss this behavior in more detail, especially with respect to the anomalous quantum correlation effects.

3.1. Special nonclassical effects

In the following we denote the nonclassicality criteria by \mathcal{C} . Squeezing is defined through the negativity of the normal-ordered variance of the quadrature operator, $\hat{x}(\varphi; \tau) = e^{i\varphi}\hat{a}(\tau) + e^{-i\varphi}\hat{a}^\dagger(\tau)$, see [46]. Thus, if

$$\langle :[\Delta\hat{x}(\varphi; \tau)]^2: \rangle < 0 \tag{7}$$

for some φ -interval, with $\Delta\hat{x} = \hat{x} - \langle \hat{x} \rangle$, the state is referred to as a quadrature squeezed state. The normal-ordering prescription orders the operators \hat{a} and \hat{a}^\dagger such that all creation operators \hat{a}^\dagger are placed to the left of the annihilation operators \hat{a} . Consequently, we define the criterion for squeezing as

$$\mathcal{C}_{\text{Sq}} := \min_{\varphi \in [0, 2\pi)} \{ \langle :[\Delta\hat{x}(\varphi; \tau)]^2: \rangle \} < 0. \tag{8}$$

That is, if $\mathcal{C}_{\text{Sq}} < 0$ then squeezing occurs at time point τ . Beside the condition in equation (8), we consider the Mandel Q parameter [9–11]:

$$\mathcal{C}_{\text{SP}} := Q(\tau) = \frac{\langle :[\Delta\hat{n}(\tau)]^2: \rangle}{\langle \hat{n}(\tau) \rangle} < 0. \tag{9}$$

In terms of radiation fields a negative Mandel Q parameter certifies a photocounting statistics of sub-Poisson type. Such a statistics does not possess a classical analog and, hence, $\mathcal{C}_{\text{SP}} < 0$ verifies nonclassicality. We also consider an

anomalous quantum-correlation condition, which cannot be fulfilled by classical states [18, 19],

$$\begin{aligned}
 \mathcal{C}_{\text{AC}} &:= \min_{\varphi \in [0, 2\pi)} \{ \langle :[\Delta\hat{n}(\tau)]^2: \rangle \langle :[\Delta\hat{x}(\varphi; \tau)]^2: \rangle \\
 &\quad - | \langle : \Delta\hat{x}(\varphi; \tau) \Delta\hat{n}(\tau) : \rangle |^2 \} < 0.
 \end{aligned} \tag{10}$$

The squeezing condition [equation (8)] depends solely on the normal-ordered variance of the quadrature operator \hat{x} . The sub-Poisson condition [equation (9)] depends on the normal-ordered version of the variance of the number operator \hat{n} . The anomalous quantum-correlation condition in equation (10) contains contributions of both quantities together with their quantum correlations in the last term. Recently, it was shown via homodyne cross-correlation measurements [47] that this condition certifies nonclassicality for radiation fields beyond squeezing [20].

To calculate all needed quantities, we express the inequalities in terms of the creation and annihilation operators. The condition for squeezing [equation (8)] reads as

$$\begin{aligned}
 \langle :[\Delta\hat{x}(\varphi; \tau)]^2: \rangle &= 2 \text{Re} \{ e^{2i\varphi} \langle \hat{a}(\tau)^2 \rangle \} \\
 &\quad - 4 [\text{Re} \{ e^{i\varphi} \langle \hat{a}(\tau) \rangle \}]^2 + 2 \langle \hat{n}(\tau) \rangle.
 \end{aligned} \tag{11}$$

$\text{Re}\{z\}$ denotes the real part of the variable z . The anomalous correlation function in equation (10) may be rewritten as

$$\begin{aligned}
 \langle : \Delta\hat{x}(\varphi; \tau) \Delta\hat{n}(\tau) : \rangle &= 2 \text{Re} \{ e^{i\varphi} \langle \hat{n}(\tau) \hat{a}(\tau) \rangle \} \\
 &\quad - 2 \text{Re} \{ e^{i\varphi} \langle \hat{a}(\tau) \rangle \langle \hat{n}(\tau) \rangle \}
 \end{aligned} \tag{12}$$

and

$$\langle :[\Delta\hat{n}(\tau)]^2: \rangle = \langle : \hat{n}(\tau)^2 : \rangle - \langle \hat{n}(\tau) \rangle^2, \tag{13}$$

with: $\hat{n}(\tau)^2 := \hat{n}(\tau)^2 - \hat{n}(\tau)$. Thus, the sub-Poisson-condition [equation (9)] can be rewritten as

$$\mathcal{C}_{\text{SP}} = \frac{\langle \hat{n}(\tau)^2 \rangle - \langle \hat{n}(\tau) \rangle^2}{\langle \hat{n}(\tau) \rangle} - 1, \tag{14}$$

which equals the commonly used form of the Mandel Q parameter.

Since we consider only single-time expectation values of operators that are initially attributed to the motion of the ion, in general denoted by $\hat{A}(0)$, the expectation values can be calculated via

$$\langle \hat{A}(t) \rangle = \text{Tr} \{ \hat{\rho}_{\text{mot}}(t) \hat{A}(0) \}, \tag{15}$$

with the reduced motional density matrix $\hat{\rho}_{\text{mot}}(t)$. The reduced density matrix of the motional subsystem is obtained by the trace over electronic degrees of freedom and the cavity field,

$$\begin{aligned}
 \hat{\rho}_{\text{mot}}(t, t_0) &= \sum_{i=1,2} \sum_{m=0}^{\infty} \langle i, m | \hat{\rho}(t, t_0) | i, m \rangle \\
 &= \sum_{m=0}^{\infty} \frac{|\beta_0|^{2m} e^{-|\beta_0|^2}}{m!} \sum_{n, n'=0}^{\infty} \rho_{n, n'} \\
 &\quad \times \sum_{\sigma, \sigma'=\pm} e^{i(\omega_{mn'}^{\sigma'} - \omega_{mn}^{\sigma})(t-t_0)} |c_{mn}^{\sigma} c_{mn'}^{\sigma'}|^2 \\
 &\quad \times \{ |n\rangle \langle n'| + \alpha_{mn}^{\sigma} (\alpha_{mn'}^{\sigma'})^* |n+k\rangle \langle n'+k| \}.
 \end{aligned} \tag{16}$$

Here, we introduced $\rho_{n, n'} = \langle n | \hat{\rho}_{\text{mot}}(0) | n' \rangle$ as the motional input state, the cavity field is in a coherent state $|\beta_0\rangle$, and the

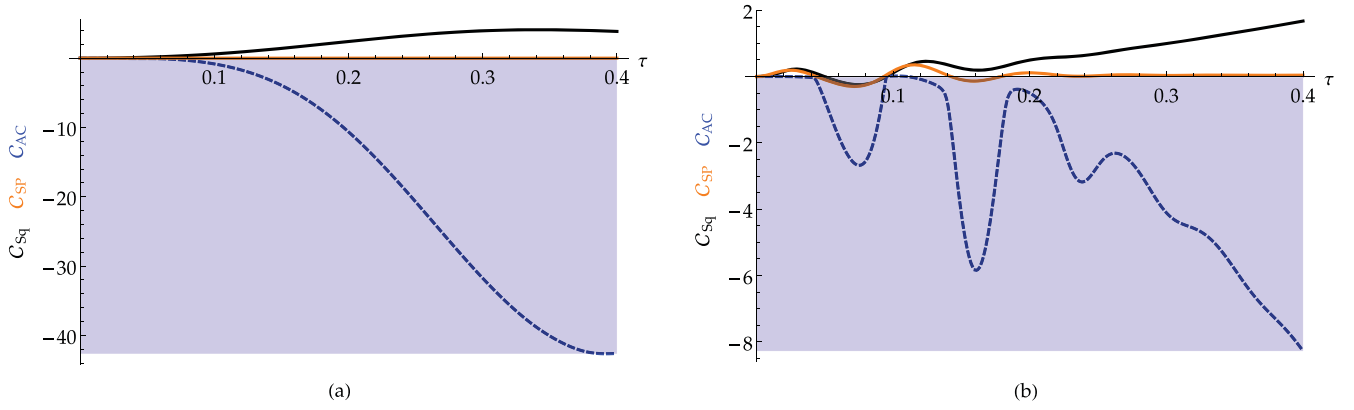


Figure 1. Different nonclassicality criteria are shown as defined in equations (8) (C_{Sq} ; solid black line), (9) (C_{SP} ; solid orange line), and (10) (C_{AC} ; dashed blue line) for excitation to the zeroth sideband $k = 0$ (a) and to the second sideband $k = 2$ (b). Negative values (shaded area) certify nonclassicality. The motional input state is a coherent state $|\alpha_0\rangle$. Note that in the case of C_{Sq} and C_{AC} the phase φ is optimized for each criterion separately. Parameters: $\alpha_0 = \sqrt{8}$, $\eta = 0.3$, $\Delta\omega/|\kappa| = 20$, $\Delta\Phi = 0$, $\nu/|\kappa| = 5000$, and $\beta_0 = 100$.

electronic degree of freedom of the ion is prepared in the excited state as $|2\rangle$.

3.2. Analytical results

We recapitulate: nonclassicality at time τ is certified via $C_x < 0$ for $x = \{ Sq, SP, AC \}$ (squeezing, sub-Poisson statistics, anomalous quantum correlations), according to equations (8)–(10). Let us first consider the case where the ion is driven quasi-resonantly to the zeroth sideband. That is, in our model we choose $k = 0$, which means that we consider the $|1, n\rangle \leftrightarrow |2, n\rangle$ transitions.

According to [48], where the authors considered the semiclassical, $|\beta_0| \gg 1$, case with exact resonance, $\Delta\omega = 0$, the quantum nondemolition measurement of the motional energy of the trapped ion was proposed. This case, extended by a detuning and a quantized pump, is studied in the following with respect to its nonclassical properties. The pump is chosen to be strong such that the dynamics is close to the semiclassical one, as it was treated in [48] for the resonant case.

We consider moderate detuning, $\Delta\omega/|\kappa| = 20$, and a Lamb–Dicke parameter of $\eta = 0.3$. The results are depicted in figure 1(a). Obviously, since $C_{SP} \geq 0$ and $C_{Sq} \geq 0$, neither sub-Poisson statistics nor quadrature squeezing are observed. Nonclassicality is only revealed by the anomalous correlations as defined in equation (10). The same results are found if other values of η or $\Delta\omega$ are considered. On the investigated time scales we can, using the considered nonclassicality criteria, certify nonclassicality criteria only through anomalous correlations.

For the same choice of $\eta = 0.3$ and $\Delta\omega/|\kappa| = 20$, we now consider the excitation to the second vibrational sideband, $k = 2$. The results are given in figure 1(b). Naively, one would expect a significant squeezing contribution as the squeezing operator consists of quadratic contributions of the creation and annihilation operators. Unexpectedly, we only find small regions where the system is nonclassical regarding the squeezing condition [equation (8)] and the sub-Poisson

condition [equation (9)]. Again, the anomalous correlations certify nonclassicality in a very pronounced manner, over nearly the whole considered time range. Additionally, for large times we see that the criteria develop in different directions. This counterintuitive behavior is caused by the nonlinearities, occurring beyond the Lamb–Dicke regime, which have a significant impact on the dynamics. Note that a larger detuning leads to a decrease of the overall strength of the effects.

For convenience, let us visualize the motional state in the corresponding phase-space picture. That is, we need to choose an appropriate phase-space distribution. Here, we use the regularized version of the Glauber–Sudarshan P function. The P function [49, 50] itself can be used to express the density operator of an arbitrary state as a pseudo-mixture of coherent states, namely

$$\hat{\rho}(t) = \int d^2\alpha P(\alpha; t) |\alpha\rangle \langle \alpha|, \quad (17)$$

where $P(\alpha; t)$ can become negative and even strongly singular. A state is referred to as classical state if the corresponding P function has the properties of a classical probability density—i.e. it is non-negative [51, 52]. However, for the most states the P function is not experimentally accessible due to its singularities. Hence, a regularization procedure was introduced in [53] to transform the ordinary P function into a well behaved phase-space representation, P_Ω , of the state under study. This procedure works as follows: since the singularities of P are caused by an unbounded characteristic function Φ , one introduces a suitable filter function Ω_w , with a width w . It is constructed such that the filtered function $\Phi_\Omega = \Omega_w \Phi$ is square-integrable for any quantum state. Since we are mainly interested in the negativities of P , it is important that the filter function must not introduce additional negativities in the filtered P function denoted by P_Ω . Thus, the Fourier transform of Ω_w must be non-negative.

Using the procedure outlined in [38], one may calculate P_Ω directly out of the reduced density matrix in equation (16). A plot of P_Ω is given in figure 2, where we considered the same situation as in figure 1(a) for $|\kappa|t = 0.2$. The depicted state does neither reveal squeezing nor sub-Poisson statistics

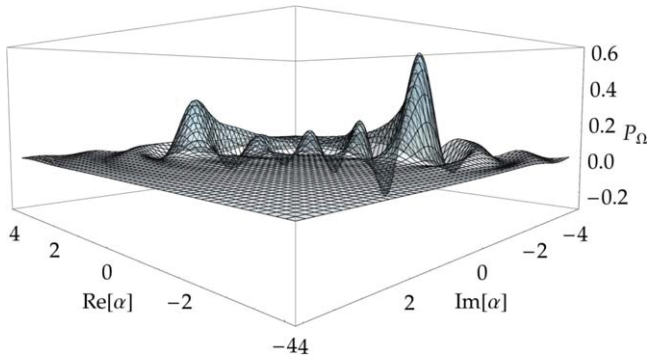


Figure 2. The regularized Glauber–Sudarshan P function, P_Ω , for the excitation to the zeroth sideband at $|\kappa|t = 0.2$. The other parameters are equal to those used in figure 1.

but only anomalous quantum correlations [see figure 1(a)]. The nonclassicality is uncovered by the negative values of P_Ω .

Altogether, we see that for many situations the most commonly used definitions of nonclassicality, such as the negative Mandel Q parameter (sub-Poisson statistics) [equation (9)] and quadrature squeezing [equation (8)], fail to certify nonclassicality in the detuned nonlinear Jaynes–Cummings model. In the scenario $k = 0$, where the zeroth sideband is only excited, the anomalous quantum-correlation condition reveals the nonclassical character of the dynamics. In the $k = 2$ case, the applicability of the criteria, for the purpose to uncover nonclassicality, depends on the choice of η and $\Delta\omega$. However, the anomalous quantum-correlation condition (10) is a powerful tool to certify nonclassicality for nearly the full timescale under study. This underlines the strength of this condition and it encourages one to investigate quantum effects beyond the mostly considered criteria. Especially, the excitation to the zeroth sideband, which only reveals its nonclassical character in terms of anomalous correlations, is a promising scenario to further analyze the physical relevance of such quantum signatures.

4. Measurement

In the following we consider the possible measurement of the correlations studied for the quantized motion of the trapped ion. For radiation fields, the anomalous correlations were measured recently [20]. However, the reconstruction of the motional state of a trapped ion is a sophisticated problem itself [54, 55]. In the following, we are interested in the measurement of the full vibronic quantum state by the technique introduced in [56], for the purpose to detect entanglement of the vibronic degrees of freedom, see the scheme in figure 3.

The strategy is as follows: the weak $|1\rangle \leftrightarrow |2\rangle$ transition is the one whose joint quantum state we are interested in. The electronic state is tested by a strong $|1\rangle \leftrightarrow |3\rangle$ transition via the appearance of resonance fluorescence [57–59]. If the latter is detected, the ion is in the state $|1\rangle$, otherwise in the state $|2\rangle$. The incident laser is tuned to the zeroth sideband, which, in

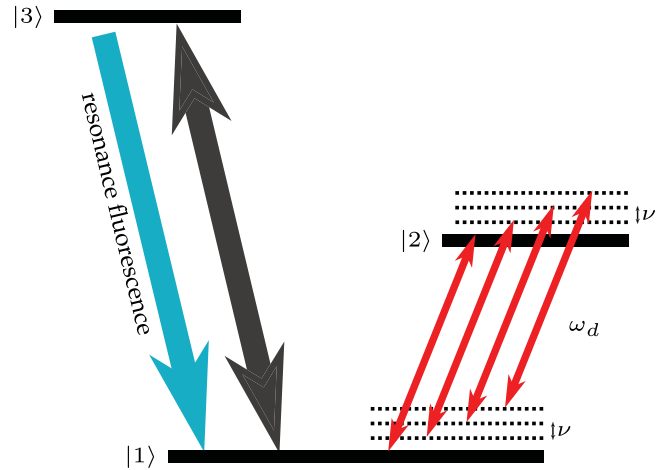


Figure 3. Measurement scheme (reprinted with permission from [56], copyright (1997) by the American Physical Society) to reconstruct the quantum state of a trapped ion whose vibronic states may be entangled. The strong $|1\rangle \leftrightarrow |3\rangle$ transition is used to probe the ion's ground state occupation probability. The weak $|1\rangle \leftrightarrow |2\rangle$ transition leads to an interaction Hamiltonian specified in equation (18). The driving laser (red arrows) is detuned to the zeroth sideband: $\omega_d = \omega_{21}$.

the resolved sideband limit, leads to the interaction Hamiltonian, see [48],

$$\hat{\mathcal{H}}_{\text{int}} = \hbar|\kappa'\langle\hat{f}_0(\hat{n}; \eta)\hat{A}_{12} + \text{H.c.} \quad (18)$$

Here we use the notation $\hat{\mathcal{H}}_{\text{int}}$ to distinguish this Hamiltonian from the previously discussed one in equation (2). The operator-valued function $\hat{f}_0(\hat{n}; \eta)$ is defined in equation (3). The corresponding time-evolution operator is obtained via $\hat{\mathcal{U}}_{\text{int}}(\tau) = \exp\left(-\frac{i}{\hbar}\hat{\mathcal{H}}_{\text{int}}\tau\right)$.

Usually, one focuses on the no-fluorescence events since the motional state is then not disturbed due to recoil effects. The initial *probe cycle* is performed as follows: first, the motional state is coherently displaced by the amplitude α , which can be accomplished via the application of a radio-frequency field. Second, the driving laser with frequency ω_d (figure 3) is switched on for a certain interaction time τ_1 . Afterwards, the electronic state is measured via probing for resonance fluorescence. After such a probe cycle, if no fluorescence is detected, the unnormalized density operator of the ion reads as

$$\hat{\rho}^{(1)}(\tau_1) = |2\rangle\langle 2| \otimes \hat{\rho}_{\text{red}}^{(1)}(\tau_1), \quad (19)$$

with $\hat{\rho}_{\text{red}}^{(1)}(\tau) = \langle 2|\hat{\mathcal{U}}_{\text{int}}(\tau_1)\hat{\rho}(\alpha)\hat{\mathcal{U}}_{\text{int}}^\dagger(\tau_1)|2\rangle$ and $\hat{\rho}(\alpha) = \hat{D}^\dagger(\alpha)\hat{\rho}(0)\hat{D}(\alpha)$, where $\hat{D}(\beta) = \exp(\beta\hat{a}^\dagger - \beta^*\hat{a})$ is the coherent displacement operator. Here, $\hat{\rho}(0)$ denotes the density operator of the vibronic degrees of freedom. This means that the cavity mode is traced out. As long as the coherent amplitude β_0 is sufficiently large—i.e. the dynamics is close to the semiclassical case— $\hat{\rho}(0)$ contains the complete information of the nonclassical properties.

Applying K of those probe cycles, with interaction times τ_1, \dots, τ_K , yields the diagonal elements (still unnormalized)

$$\langle n | \hat{\rho}^{(K)}(\tau_K) | n \rangle = \prod_{q=2}^K \cos^2(|\kappa'| L_n(\eta^2) e^{-\eta^2/2} \tau_q) \langle n | \hat{\rho}^{(1)}(\tau_1) | n \rangle. \quad (20)$$

The probability to obtain such a sequence of cycles, equals the trace of the latter expression. For appropriately chosen interaction times, see the end of section III of [56], this probability can directly be related to the displaced density operator elements $\rho_{ij}^{nm}(\alpha) \equiv \langle i, n | \hat{\rho}(\alpha) | j, n \rangle$ for $i, j = 1, 2$. Using these elements, $\rho_{ij}^{nm}(\alpha)$, one can derive the Wigner-function matrix straightforwardly [56]:

$$W_{ij}(\alpha) = \frac{2}{\pi} \sum_{n=0}^{\infty} (-1)^n \rho_{ij}^{nm}(\alpha). \quad (21)$$

The latter is a unification of the ordinary Wigner function [60], including the electronic degrees of freedom. Hence it was shown that using $W_{ij}(\alpha)$ one can uncover entanglement between the motional and electronic states of the ion which would not be verified by using only the reduced density matrix. However, nowadays we have experimental access to the regularized P function which possesses several advantages over other quasiprobabilities [61, 62]. Remarkably, in [63] a regularized hybrid version of the P function was introduced, unifying the description of continuous- and discrete-variable systems. The definition applies here as well and reads as

$$P_{ij}(\alpha) = \langle \hat{A}_{ji} \otimes : \hat{\delta}(\hat{a} - \alpha) : \rangle, \quad (22)$$

with $\hat{A}_{ji} = |j\rangle \langle i|$. Using this definition, one can define the overall density operator of the system as

$$\hat{\rho} = \sum_{ij} \int d^2\alpha P_{ij}(\alpha) |i\rangle \langle j| \otimes |\alpha\rangle \langle \alpha|. \quad (23)$$

The questions arise how the anomalous moments can be obtained and how $P_{ij}(\alpha)$ can be reconstructed by using the scheme in figure 3.

Let us start with the definition given in equation (21). Applying the inverse Fourier transform yields the characteristic-function matrix of the Wigner-function matrix (indicated by the index W),

$$\Phi_{ij,W}(\beta) = \int d^2\alpha W_{ij}(\alpha) e^{\beta\alpha^* - \beta^*\alpha} = \langle \hat{A}_{ji} \otimes \hat{D}(\beta) \rangle. \quad (24)$$

To transform the symmetric ordered function $\Phi_{ij,W}(\beta)$ into normal order, one may apply the Baker–Campbell–Hausdorff formula to obtain the Fourier transform of the P -function matrix $P_{ij}(\alpha)$,

$$\Phi_{ij}(\beta) = \langle \hat{A}_{ji} \otimes : \hat{D}(\beta) : \rangle = \langle \hat{A}_{ji} \otimes \hat{D}(\beta) \rangle e^{|\beta|^2/2}. \quad (25)$$

As soon as the latter function is derived from $W_{ij}(\alpha)$, one may calculate its trace over the electronic degrees of freedom to obtain the characteristic function of the motional subsystem:

$$\sum_{i=1}^2 \Phi_{ii}(\beta) = \langle : \hat{D}(\beta) : \rangle. \quad (26)$$

Differentiation yields the expectation values needed in equation (10). In principle, all possible combinations of normal-ordered moments can be obtained in this way. For example, in

$$\langle : \Delta \hat{x}(\varphi) \Delta \hat{n}(\tau) : \rangle = \langle : \hat{x}(\varphi) \hat{n} : \rangle - \langle \hat{x}(\varphi) \rangle \langle \hat{n} \rangle \quad (27)$$

one may derive all terms as follows, defining $\beta = |\beta| e^{i\varphi_\beta}$:

$$\begin{aligned} \langle \hat{x}(\varphi) \rangle &= \frac{1}{i} \frac{\partial}{\partial |\beta|} \langle : \hat{D}(\beta) : \rangle \Big|_{|\beta|=0, \varphi_\beta=\varphi+\pi/2}, \\ \langle \hat{n} \rangle &= -\frac{\partial}{\partial \beta} \frac{\partial}{\partial \beta^*} \langle : \hat{D}(\beta) : \rangle \Big|_{|\beta|=0}, \\ \langle : \hat{x}(\varphi) \hat{n} : \rangle &= \frac{-1}{i} \frac{\partial}{\partial \beta} \frac{\partial}{\partial \beta^*} \frac{\partial}{\partial |\beta|} \langle : \hat{D}(\beta) : \rangle \Big|_{|\beta|=0, \varphi_\beta=\varphi+\pi/2}. \end{aligned} \quad (28)$$

Via $\frac{\partial}{\partial |\beta|} = \left(e^{i\varphi_\beta} \frac{\partial}{\partial \beta} + e^{-i\varphi_\beta} \frac{\partial}{\partial \beta^*} \right)$ all moments can be derived with respect to the derivatives of β and β^* .

Furthermore, we may calculate the regularized P -function matrix out of equation (25) via multiplication of an appropriate filter function $\Omega_w(\beta)$ [53, 64] (with a width w). A subsequent Fourier transformation and the usage of equation (24) yields

$$\begin{aligned} P_{ij,\Omega}(\alpha) &= \frac{1}{\pi^2} \int d^2\beta \Omega_w(\beta) e^{\alpha\beta^* - \alpha^*\beta} \Phi_{ij}(\beta) \\ &= \int \frac{d^2\alpha'}{\pi^2} W_{ij}(\alpha') \underbrace{\int d^2\beta \Omega_w(\beta) e^{|\beta|^2/2} e^{\beta^*(\alpha - \alpha') - \beta(\alpha^* - \alpha'^*)}}_{:= \Lambda_\Omega(\alpha, \alpha')}. \end{aligned} \quad (29)$$

Hence, using equation (21) we finally arrive at

$$P_{ij,\Omega}(\alpha) = \frac{2}{\pi^3} \sum_{n=0}^{\infty} (-1)^n \int d^2\alpha' \Lambda_\Omega(\alpha, \alpha') \rho_{ij}^{nm}(\alpha'), \quad (30)$$

where $\rho_{ij}^{nm}(\alpha) \equiv \langle i, n | \hat{\rho}(\alpha) | j, n \rangle$ for $i, j = 1, 2$. Thus, out of the Wigner-function matrix we derive the moments in equation (28) and furthermore, out of the $\rho_{ij}^{nm}(\alpha)$, we may obtain the regularized P -function matrix. The trace $\sum_{i=1}^2 P_{ii,\Omega}(\alpha)$ would yield the regularized P representation including merely the motional subsystem, which we discussed for a special case in figure 2.

Note that in equation (30) one needs to evaluate an integral over the whole α' -plane. One can avoid this integration by using an alternative approach related to the ideas presented in [65, 66]. The *nonclassicality witnesses* for harmonic oscillators, which also apply here, lead to the expression

$$\begin{aligned} P_{ij,\Omega}(\alpha) &= \frac{w^2}{16} \sum_{m=0}^{\infty} \frac{(-w^2/4)^m}{[(m+1)!]^2} \binom{2m+2}{m} \langle \hat{A}_{ji} \otimes : \hat{n}(\alpha)^m : \rangle, \end{aligned} \quad (31)$$

where $\hat{n}(\alpha) = \hat{D}(\alpha) \hat{n} \hat{D}^\dagger(\alpha)$. This result, expressed in terms of normal-ordered displaced-number moments, is obtained via the application of a particular disc-function filter. Inserting the expression

$$\langle \hat{A}_{ji} \otimes : \hat{n}(\alpha)^m : \rangle = \sum_{n=m}^{\infty} \rho_{ij}^{nm}(\alpha) \frac{n!}{(n-m)!} \quad (32)$$

in equation (31), we directly relate the regularized P -function matrix, $P_{ij,\Omega}(\alpha)$, to the elements $\rho_{ij}^{nn}(\alpha)$. Especially, we in this formulation we do not have to evaluate an integral over the complex plane, as in equation (30). We can choose a certain value α and calculate $P_{ij,\Omega}$ at this point in phase-space.

5. Summary and conclusions

In this work we studied nonclassical properties of the recently introduced generalization of the nonlinear Jaynes–Cummings model for the vibronic dynamics of a trapped ion—including a quantized pump field and a small detuning with respect to the vibronic excitation in the resolved sideband regime. We showed that for the excitation of the zeroth and second sideband the so-called anomalous quantum correlations of non-commuting observables certify nonclassicality when established criteria, verifying sub-Poisson number statistics or quadrature squeezing, fail. In particular, in the case of driving the zeroth sideband, the anomalous quantum-correlation condition is the favored one that uncovers the nonclassicality. In addition, we studied the influence of the nonlinearities occurring beyond the Lamb–Dicke regime as well as the detuning from resonance. The great importance of the anomalous quantum correlations in the dynamics under study raises the question whether these phenomena may be useful for practical applications in quantum technologies. In any case, the verification of the nonclassical nature of the system under study through anomalous quantum correlations is of fundamental interest—in particular if standard quantum signatures (e.g. squeezing and sub-Poisson statistics) are negligibly small.

To access the studied quantum signatures in experiments, we studied the possibilities to determine the needed correlations from measured data. For this aim, a measurement technique is suited which was originally proposed for the purpose to verify entanglement within the vibronic quantum system of the trapped ion. We show in detail how the needed moments and correlation functions, including those characterizing the anomalous quantum correlations, are obtained from measured quantities. In the underlying measurement scenario, the Wigner-function matrix was considered as the quantity to be determined. In the present paper we demonstrated how the regularized version of the Glauber–Sudarshan P -function matrix can be obtained from the Wigner-function matrix. This is needed as the desired correlation functions for analyzing the quantum effects of interest are normal-ordered ones. The advantage of normal ordering consists in the fact that these correlations are robust against losses and they are not washed out by vacuum fluctuations which are caused by losses. Based on these techniques, very general quantum effects in the vibronic degrees of freedom of trapped ions may be studied.

ORCID iDs

F Krumm  <https://orcid.org/0000-0002-4606-2894>

References

- [1] Carmichael H J and Walls D F 1976 A quantum-mechanical master equation treatment of the dynamical Stark effect *J. Phys. B* **9** 1199
- [2] Kimble H J and Mandel L 1976 Theory of resonance fluorescence *Phys. Rev. A* **13** 2123
- [3] Kimble H J, Dagenais M and Mandel L 1977 Photon antibunching in resonance fluorescence *Phys. Rev. Lett.* **39** 691
- [4] Walls D F 1983 Squeezed states of light *Nature* **306** 141
- [5] Slusher R E, Hollberg L W, Yurke B, Mertz J C and Valley J F 1985 Observation of squeezed states generated by four-wave mixing in an optical cavity *Phys. Rev. Lett.* **55** 2409
- [6] Wu L-A, Kimble H J, Hall J L and Wu H 1986 Generation of squeezed states by parametric down conversion *Phys. Rev. Lett.* **57** 2520
- [7] Vahlbruch H, Mehmet M, Chelkowski S, Hage B, Franzen A, Lastzka N, Gößler S, Danzmann K and Schnabel R 2008 Observation of squeezed light with 10 db quantum-noise reduction *Phys. Rev. Lett.* **100** 033602
- [8] Vahlbruch H, Mehmet M, Danzmann K and Schnabel R 2016 Detection of 15 dB squeezed states of light and their application for the absolute calibration of photoelectric quantum efficiency *Phys. Rev. Lett.* **117** 110801
- [9] Mandel L 1979 Sub-Poissonian photon statistics in resonance fluorescence *Opt. Lett.* **4** 205
- [10] Short R and Mandel L 1983 Observation of sub-poissonian photon statistics *Phys. Rev. Lett.* **51** 384
- [11] Teich M C and Saleh B E A 1985 Observation of sub-Poisson Franck-Hertz light at 253.7 nm *J. Opt. Soc. Am. B* **2** 275
- [12] Einstein A, Rosen N and Podolsky B 1935 Can quantum-mechanical description of physical reality be considered complete? *Phys. Rev.* **47** 777
- [13] Schrödinger E 1935 Die gegenwärtige situation in der Quantenmechanik *Naturwiss.* **23** 807
- [14] Lewenstein M, Bruß D, Cirac J I, Kraus B, Kus M, Samsonowicz J, Sanpera A and Tarrach R 2000 Separability and distillability in composite quantum systems—a primer *J. Mod. Opt.* **47** 2481
- [15] Bruß D 2002 Characterizing entanglement *J. Math. Phys.* **43** 4237
- [16] Brunner N, Gisin N and Scarani V 2005 Entanglement and non-locality are different resources *New J. Phys.* **7** 88
- [17] Horodecki R, Horodecki P, Horodecki M and Horodecki K 2009 Quantum entanglement *Rev. Mod. Phys.* **81** 865
- [18] Vogel W 2008 Nonclassical correlation properties of radiation fields *Phys. Rev. Lett.* **100** 013605
- [19] Vogel W 1991 Squeezing and anomalous moments in resonance fluorescence *Phys. Rev. Lett.* **67** 2450
- [20] Kühn B, Vogel W, Mraz M, Köhnke S and Hage B 2017 Anomalous quantum correlations of squeezed light *Phys. Rev. Lett.* **118** 153601
- [21] Jaynes E T and Cummings F W 1963 Comparison of quantum and semiclassical radiation theories with application to the beam maser *Proc. IEEE* **51** 89
- [22] Paul H 1963 Induzierte Emission bei starker Einstrahlung *Ann. Phys.* **11** 411
- [23] Haroche S 2013 Nobel lecture: controlling photons in a box and exploring the quantum to classical boundary *Rev. Mod. Phys.* **85** 1083

- [24] Blockley C A, Walls D F and Risken H 1992 Quantum collapses and revivals in a quantized trap *Europhys. Lett.* **17** 509
- [25] Cirac J I, Blatt R, Parkins A S and Zoller P 1994 Quantum collapse and revival in the motion of a single trapped ion *Phys. Rev. A* **49** 1202
- [26] Wineland D J 2013 Nobel lecture: superposition, entanglement, and raising Schrödinger's cat *Rev. Mod. Phys.* **85** 1103
- [27] Cirac J I, Parkins A S, Blatt R and Zoller P 1993 Dark squeezed states of the motion of a trapped ion *Phys. Rev. Lett.* **70** 556
- [28] Meekhof D M, Monroe C, King B E, Itano W M and Wineland D J 1996 Generation of nonclassical motional states of a trapped atom *Phys. Rev. Lett.* **76** 1796
- [29] de Matos Filho R L and Vogel W 1996 Even and odd coherent states of the motion of a trapped ion *Phys. Rev. Lett.* **76** 608
- [30] de Matos Filho R L and Vogel W 1996 Nonlinear coherent states *Phys. Rev. A* **54** 4560
- [31] Gou S-C, Steinbach J and Knight P L 1996 Dark pair coherent states of the motion of a trapped ion *Phys. Rev. A* **54** R1014(R)
- [32] Gou S-C, Steinbach J and Knight P L 1996 Vibrational pair cat states *Phys. Rev. A* **54** 4315
- [33] Gerry C C, Gou S-C and Steinbach J 1997 Generation of motional SU(1,1) intelligent states of a trapped ion *Phys. Rev. A* **55** 630
- [34] Monroe C, Meekhof D M, King B E and Wineland D J 1996 A Schrödinger cat superposition state of an atom *Science* **272** 1131
- [35] Gerry C C 1997 Generation of Schrödinger cats and entangled coherent states in the motion of a trapped ion by a dispersive interaction *Phys. Rev. A* **55** 2478
- [36] Wallentowitz S and Vogel W 1997 Quantum-mechanical counterpart of nonlinear optics *Phys. Rev. A* **55** 4438
- [37] Vogel W and de Matos Filho R L 1995 Nonlinear Jaynes–Cummings dynamics of a trapped ion *Phys. Rev. A* **52** 4214
- [38] Krumm F and Vogel W 2018 Time-dependent nonlinear Jaynes–Cummings dynamics of a trapped ion *Phys. Rev. A* **97** 043806
- [39] Moya-Cessa H and Tombesi P 2000 Filtering number states of the vibrational motion of an ion *Phys. Rev. A* **61** 025401
- [40] Moya-Cessa H, Soto-Eguibar F, Vargas-Martinez J M, Juarez-Amaro R and Zuniga-Segundo A 2012 Ion-laser interactions: the most complete solution *Phys. Rep.* **513** 229
- [41] Pedernales J S, Lizuain I, Felicetti S, Romero G, Lamata L and Solano E 2015 Quantum Rabi model with trapped ions *Sci. Rep.* **5** 15472
- [42] Moya-Cessa H M 2016 Fast quantum Rabi model with trapped ions *Sci. Rep.* **6** 38961
- [43] Cheng X-H, Arrazola I, Pedernales J S, Lamata L, Chen X and Solano E 2018 Nonlinear quantum Rabi model in trapped ions *Phys. Rev. A* **97** 023624
- [44] Casanova J, Puebla R and Moya-Cessa H 2018 Connecting nth order generalised quantum Rabi models: emergence of nonlinear spin-boson coupling via spin rotations *NPJ Quantum Inf.* **4** 47
- [45] Lipfert T, Krumm F, Kolobov M I and Vogel W 2018 Time ordering in the classically driven nonlinear Jaynes–Cummings model *Phys. Rev. A* **98** 06381
- [46] Vogel W and Welsch D-G 2006 *Quantum Optics* 3rd edn (New York: Wiley-VCH) (<https://doi.org/10.1002/3527608524>)
- [47] Vogel W 1995 Homodyne correlation measurements with weak local oscillators *Phys. Rev. A* **51** 4160
- [48] de Matos Filho R L and Vogel W 1996 Quantum nondemolition measurement of the motional energy of a trapped atom *Phys. Rev. Lett.* **76** 4520
- [49] Sudarshan E C G 1963 Equivalence of semiclassical and quantum mechanical descriptions of statistical light beams *Phys. Rev. Lett.* **10** 277
- [50] Glauber R J 1963 Coherent and incoherent states of the radiation field *Phys. Rev.* **131** 2766
- [51] Titulaer U M and Glauber R J 1965 Correlation functions for coherent fields *Phys. Rev.* **140** B676
- [52] Mandel L 1986 Non-classical states of the electromagnetic field *Phys. Scr.* **T12** 34
- [53] Kiesel T and Vogel W 2010 Nonclassicality filters and quasiprobabilities *Phys. Rev. A* **82** 032107
- [54] Wallentowitz S and Vogel W 1995 Reconstruction of the quantum mechanical state of a trapped ion *Phys. Rev. Lett.* **75** 2932
- [55] Wallentowitz S and Vogel W 1996 Motional quantum states of a trapped ion: measurement and its back action *Phys. Rev. A* **54** 3322
- [56] Wallentowitz S, de Matos Filho R L and Vogel W 1997 Determination of entangled quantum states of a trapped atom *Phys. Rev. A* **56** 1205
- [57] Nagourney W, Sandberg J and Dehmelt H 1986 Shelved optical electron amplifier: observation of quantum jumps *Phys. Rev. Lett.* **56** 2797
- [58] Sauter T, Neuhauser W, Blatt R and Toschek P E 1986 Observation of quantum jumps *Phys. Rev. Lett.* **57** 1696
- [59] Bergquist J C, Hulet Randall G, Itano Wayne M and Wineland D J 1986 Observation of quantum jumps in a single atom *Phys. Rev. Lett.* **57** 1699
- [60] Wigner E 1932 On the quantum correction for thermodynamic equilibrium *Phys. Rev.* **40** 749
- [61] Ferraro A and Paris M G A 2012 Nonclassicality criteria from phase-space representations and information-theoretical constraints are maximally inequivalent *Phys. Rev. Lett.* **108** 260403
- [62] Agudelo E, Sperling J and Vogel W 2013 Quasiprobabilities for multipartite quantum correlations of light *Phys. Rev. A* **87** 033811
- [63] Agudelo E, Sperling J, Costanzo L S, Bellini M, Zavatta A and Vogel W 2017 Conditional hybrid nonclassicality *Phys. Rev. Lett.* **119** 120403
- [64] Kühn B and Vogel W 2014 Visualizing nonclassical effects in phase space *Phys. Rev. A* **90** 033821
- [65] Kiesel T and Vogel W 2012 universal nonclassicality witnesses for harmonic oscillators *Phys. Rev. A* **85** 062106
- [66] Kühn B and Vogel W 2016 Unbalanced homodyne correlation measurements *Phys. Rev. Lett.* **116** 163603

Accessing the non-equal-time commutators of a trapped ion

F. Krumm* and W. Vogel

Arbeitsgruppe Theoretische Quantenoptik, Institut für Physik, Universität Rostock, D-18059 Rostock, Germany

(Received 11 October 2018; published 11 June 2019)

The vibronic dynamics of a trapped ion in the resolved-sideband regime can be described by the explicitly time-dependent nonlinear Jaynes-Cummings model. It is shown that the expectation value of the interaction Hamiltonian and its non-equal-time commutator can be determined by measuring the electronic-state evolution. This yields direct insight into the time-ordering contributions to the unitary time evolution. In order to prove extraction of the quantities of interest works for possibly real data, we demonstrate the procedure by means of generated data.

DOI: [10.1103/PhysRevA.99.063816](https://doi.org/10.1103/PhysRevA.99.063816)

I. INTRODUCTION

Starting with the development of quantum mechanics and the introduction of Hilbert-space operators, the noncommutativity of the latter became an issue. It leads to many fascinating physical effects, where the most prominent example is most likely the Heisenberg uncertainty principle [1–3]. Furthermore, noncommutativity plays an important role in quantum field theory [4], quantum many-body systems [5–13], quantum electrodynamics [14–16], the standard model [17], and cosmology [18,19]. Here we consider the problem of non-equal-time commutators from the quantum optics point of view.

A noteworthy achievement in this context is the experimental verification of the bosonic commutation relation, $[\hat{a}, \hat{a}^\dagger] = \hat{1}$. Although this relation is of fundamental relevance for the formulation of quantum mechanics, it was not verified before 2007, in a seminal paper by Bellini and co-authors [20]. Later on, this subject was analyzed in some more detail [21,22]. Elementary commutation rules of such a type are equal-time rules introduced in the procedure of canonical quantization.

This leads to another fundamental subject, namely, the non-equal-time commutation rules, which play an important role in the context of interaction problems including *time ordering*. If the dynamics of an explicitly time-dependent Hamiltonian is formally solved in terms of the standard time-evolution operator, one finds that the latter obeys a time-ordering prescription (cf., e.g., [23–26]). This prescription must not be omitted as it has a crucial impact on the dynamics of the system [27–34]. Paradoxically, despite its key role in basic quantum mechanics, detailed treatments of time-ordering effects are rarely available. A direct verification of the non-equal-time commutators of Hamiltonians has, to our best knowledge, not been studied yet. Of course, the non-equal-time commutators of interest only occur in the case of explicitly time-dependent Hamiltonians. We also stress that the time-dependent commutators are not postulated in the quantization procedure. Instead, they require the solution of

the interaction problem under consideration. Hence, it is very useful to consider an exactly solvable interaction dynamics. As the latter should also not be a trivial example, we consider the nonlinear vibronic interaction of a trapped and laser-driven ion. For a slightly off-resonant driving laser, we are just in the regime of interest.

In this work, we use basic relations of quantum mechanics to show that the measurement of the expectation value of an explicitly time-dependent interaction Hamiltonian yields the expectation value of a partly integrated non-equal-time commutator of this Hamiltonian. If this commutator is nonzero, the system undergoes a time-ordered dynamics. In principle, the latter can be determined for any physical system with an explicitly time-dependent Hamiltonian. For a rigorous treatment of the problem, we focus on the mentioned exactly solvable problem. Note that insight into the non-equal-time commutators is an issue of relevance for the general dynamics of quantum systems. In many cases, when exact solutions are not available, the problem can only be solved numerically. For the trapped-ion dynamics under study, the advantage is that we may obtain the expectation value of the interaction Hamiltonian directly from the measurement of the excited electronic-state occupation probability. The specific steps of the procedure will be demonstrated by the use of generated data.

The paper is structured as follows. In Sec. II we introduce the time evolution in the case of explicitly time-dependent interaction Hamiltonians together with the resulting non-equal-time commutators. The nonlinear explicitly time-dependent Jaynes-Cummings model is introduced in Sec. III, which allows us to study the dynamics of interest on the basis of exact solutions. In Sec. IV we show how one may experimentally determine the interaction Hamiltonian in Fock basis for the case of the laser-driven zeroth motional sideband of the ion. Section V is devoted to the investigation of the relevance of the non-equal-time commutators of the interaction Hamiltonian. A summary and some conclusions are given in Sec. VI.

II. TIME EVOLUTION

We start with some fundamental relations of quantum theory. The properties of a physical system may be compactly

*fabian.krumm@uni-rostock.de

expressed by its Hamiltonian, $\hat{H}_S(t) = \hat{H}_{0,S} + \hat{H}_{\text{int},S}$. The index S denotes the Schrödinger picture, $\hat{H}_{0,S}$ is the free evolution of the system, and $\hat{H}_{\text{int},S}$ is the interaction of different degrees of freedom. In the interaction picture, denoted by the index I , and assuming that the interaction Hamiltonian is in this picture explicitly time dependent, the dynamics of the system is described by the time-evolution operator

$$\hat{U}_I(t) = \mathcal{T} \exp \left(-\frac{i}{\hbar} \int_0^t \hat{H}_{\text{int},I}(\tau) d\tau \right). \quad (1)$$

Throughout this work, the explicit time dependence of the Hamiltonians is presumed. Here, \mathcal{T} denotes the time-ordering prescription which only can be ignored if the interaction Hamiltonian commutes with itself at different times, $[\hat{H}_{\text{int},I}(\tau_1), \hat{H}_{\text{int},I}(\tau_2)] = 0$, $\forall(\tau_1, \tau_2)$ (see, e.g., [23–26]).

We emphasize that throughout this work the time dependence of the Hamiltonian $\hat{H}_{\text{int},I}(\tau)$ refers to the explicit time dependence and not to the (implicit) time dependence of the operators. The latter is directly caused by the time-evolution operator $\hat{U}_I(t)$. In general, the interaction Hamiltonian is proportional to some coupling constant $|\kappa|$ and, hence, we may use a power series expansion

$$\begin{aligned} \hat{U}_I(t) = 1 - \frac{i}{\hbar} \int_0^t d\tau_1 \hat{H}_{\text{int},I}(\tau_1) \\ - \frac{1}{\hbar^2} \int_0^t d\tau_1 \int_0^{\tau_1} d\tau_2 \hat{H}_{\text{int},I}(\tau_1) \hat{H}_{\text{int},I}(\tau_2) + O(|\kappa|^3). \end{aligned} \quad (2)$$

The full time evolution of the interaction Hamiltonian reads as

$$\begin{aligned} \hat{U}_I^\dagger(t) \hat{H}_{\text{int},I}(t) \hat{U}_I(t) \\ = \underbrace{\hat{H}_{\text{int},I}(t)}_{\propto |\kappa|} + \frac{i}{\hbar} \int_0^t d\tau_1 \underbrace{[\hat{H}_{\text{int},I}(\tau_1), \hat{H}_{\text{int},I}(t)]}_{\propto |\kappa|^2} + O(|\kappa|^3). \end{aligned} \quad (3)$$

The terms proportional to $|\kappa|$ and $|\kappa|^2$ yield the interaction Hamiltonian and its partly integrated non-equal-time commutator, respectively. However, especially from the experimental point of view, the determination of the expectation value of solely the interaction Hamiltonian is not a trivial task. In the following, we will consider a realistic model, the explicitly time-dependent nonlinear Jaynes-Cummings Hamiltonian, which describes the vibronic dynamics of a trapped ion in the resolved-sideband regime. We will show that for this model the expectation value of Eq. (3) can be derived from an experimentally accessible observable.

III. NONLINEAR JAYNES-CUMMINGS MODEL

The quantized center-of-mass motion of a trapped ion, in the resolved-sideband limit, can be described by the nonlinear Jaynes-Cummings model [35]. Including a frequency mismatch $\Delta\omega$, which we assume to be small but nonzero, such that the Hamiltonian is explicitly time dependent in the interaction picture. The corresponding k th-order nonlinear interaction Hamiltonian, after a vibrational rotating wave

approximation, reads as

$$\hat{H}_{\text{int},I}(t) = \hbar|\kappa|e^{-i\Delta\omega t + i\theta} \hat{A}_{21} \hat{f}_k(\hat{n}; \eta) \hat{a}^k + \text{H.c.} \quad (4)$$

(see Ref. [36] for a detailed derivation). Here, $\kappa = |\kappa|e^{i\theta}$ is the coupling constant of the ion's electronic and vibrational levels and is proportional to the amplitude of the driving laser. Additionally, \hat{a} and \hat{a}^\dagger are the annihilation and creation operators of the vibrational mode and, in the case of a standing wave, with $\hat{n} = \hat{a}^\dagger \hat{a}$, $\hat{f}_k(\hat{n}; \eta)$ describes the mode structure of the driving laser field at the position of the ion. It is, in Fock basis, defined as follows:

$$\hat{f}_k(\hat{n}; \eta) = \frac{1}{2} e^{i\Delta\phi - \eta^2/2} \sum_{n=0}^{\infty} |n\rangle \langle n| \frac{(i\eta)^k n!}{(n+k)!} L_n^{(k)}(\eta^2) + \text{H.c.}, \quad (5)$$

with $L_n^{(k)}$ denoting the generalized Laguerre polynomials, η is the Lamb-Dicke parameter, and $\Delta\phi$ determines the position of the trap potential relative to the laser wave. The atomic flip operator $\hat{A}_{ij} = |i\rangle \langle j|$ ($i, j = 1, 2$) describes the $|j\rangle \rightarrow |i\rangle$ transition. Furthermore, the classical driving laser with frequency $\omega_L = \omega_{21} - k\nu + \Delta\omega$ is slightly detuned from the k th sideband by $\Delta\omega$, which yields the time dependence of the Hamiltonian in Eq. (4). Here, ν is the trap frequency and $\omega_{21} = \omega_2 - \omega_1$ is the separation of the electronic levels $|1\rangle$ and $|2\rangle$. Finally, the Hamiltonian describing the free evolution reads as

$$\hat{H}_{0,I} = \hbar\nu\hat{n} + \hbar\omega_{21}\hat{A}_{22}. \quad (6)$$

A detailed discussion of the Hamiltonians can be found in Refs. [35,36] or Chap. 13 of [24].

The solution of the corresponding dynamics,

$$\begin{aligned} \hat{U}_I(t) = \sum_{n=0}^{\infty} [a_n(t)|2, n\rangle \langle 2, n| - b_n^*(t)e^{-2i\theta}|1, n+k\rangle \langle 2, n| \\ + b_n(t)e^{2i\theta}|2, n\rangle \langle 1, n+k| \\ + a_n^*(t)|1, n+k\rangle \langle 1, n+k|] + \sum_{q=0}^{k-1} |1, q\rangle \langle 1, q|, \end{aligned} \quad (7)$$

with

$$\begin{aligned} a_n(t) &= e^{-i\Delta\omega t/2} \left[\cos(\Gamma_n t) + \frac{i\Delta\omega}{2\Gamma_n} \sin(\Gamma_n t) \right], \\ b_n(t) &= e^{-i\Delta\omega t/2} \frac{|\kappa|w_n}{i\Gamma_n} \sin(\Gamma_n t), \\ \Gamma_n &= \sqrt{\left(\frac{\Delta\omega}{2}\right)^2 + w_n^2|\kappa|^2}, \\ w_n &= \cos\left(\Delta\phi + \frac{\pi}{2}k\right) \eta^k e^{-\eta^2/2} \sqrt{\frac{n!}{(n+k)!}} L_n^{(k)}(\eta^2) \end{aligned} \quad (8)$$

has been derived in Ref. [37].

Let us consider the time evolution of the occupation probability of the excited electronic state, $\sigma_{22} = \langle \hat{A}_{22} \rangle$. Because of $[\hat{A}_{22}, \hat{H}_{0,I}] = 0$, σ_{22} depends solely on the interaction

Hamiltonian, which yields

$$\dot{\sigma}_{22}(t) = \frac{i}{\hbar} \langle \hat{U}_I^\dagger(t) [\hat{H}_{\text{int},I}(t), \hat{A}_{22}] \hat{U}_I(t) \rangle. \quad (9)$$

Using the Hamiltonian in Eq. (4), we obtain

$$\begin{aligned} \dot{\sigma}_{22}(t) = i|\kappa| \langle -e^{-i\Delta\omega t + i\theta} \hat{A}_{21}(t) \hat{f}_k(\hat{n}(t); \eta) \hat{a}^k(t) \\ + e^{i\Delta\omega t - i\theta} \hat{A}_{12}(t) \hat{a}^{\dagger k}(t) \hat{f}_k(\hat{n}(t); \eta) \rangle. \end{aligned} \quad (10)$$

Comparing this expression with the Hamiltonian (4), for $\Delta\omega \neq 0$ we get

$$\hbar\Delta\omega\dot{\sigma}_{22}(t) \equiv \left\langle \hat{U}_I^\dagger(t) \left(\frac{d}{dt} \hat{H}_{\text{int},I}(t) \right) \hat{U}_I(t) \right\rangle. \quad (11)$$

Note that for $\Delta\omega = 0$, when the Hamiltonian is not explicitly time dependent, both sides of the latter equation vanish and hence they yield no physical insight in the interaction dynamics. Since $\hat{U}_I^\dagger(t) [\frac{d}{dt} \hat{H}_{\text{int},I}(t)] \hat{U}_I(t) = \frac{d}{dt} [\hat{U}_I^\dagger(t) \hat{H}_{\text{int},I}(t) \hat{U}_I(t)]$, we may integrate Eq. (10) to arrive at

$$\begin{aligned} \hbar\Delta\omega[\sigma_{22}(t) - \sigma_{22}(0)] = \langle \hat{U}_I^\dagger(t) \hat{H}_{\text{int},I}(t) \hat{U}_I(t) \rangle \\ - \langle \hat{U}_I^\dagger(0) \hat{H}_{\text{int},I}(0) \hat{U}_I(0) \rangle. \end{aligned} \quad (12)$$

We observe that the measurement of the excited-state occupation probability $\sigma_{22}(t)$, which is achieved via probing an auxiliary transition for resonance fluorescence [38–40], is directly related to the expectation value of the time-dependent interaction Hamiltonian. The consideration of different orders with respect to $|\kappa|$ allows one to determine either the interaction Hamiltonian itself or the corresponding commutator in Eq. (3). Without loss of generality, we set $\theta = 0$ in the following.

In this section, we have briefly recapitulated the detuned nonlinear Jaynes-Cummings model which describes the quantized motion of a trapped ion in the resolved-sideband regime. This model was originally introduced for zero detuning [35] and experimentally proven to properly describe the experimental dynamics of trapped ions [41]. In experiments the extension of the model to include the detuning under study here is a minor issue.

For the case of detuning we have shown that the expectation value of the interaction Hamiltonian can be obtained from the occupation probability $\sigma_{22}(t)$ of the (excited) electronic state. According to Eq. (3), from the latter we can extract the expectation value of the interaction Hamiltonian in the interaction picture ($\propto |\kappa|$) and the corresponding commutator ($\propto |\kappa|^2$). In the next two sections we will demonstrate the procedure step by step by using generated data. The latter are used to visualize the situation for experimental, i.e., fluctuating, data.

IV. DETERMINATION OF THE ZEROth SIDEBAND INTERACTION HAMILTONIAN

In this section we will consider the determination of the interaction Hamiltonian in Fock basis, $\langle \hat{H}_{\text{int},I}(t) \rangle = \text{Tr}_{\text{el}}[\hat{\sigma}(0) \langle n | \hat{H}_{\text{int},I}(t) | n \rangle]$, for $k = 0$ in Eq. (4). Note that this Hamiltonian is diagonal in Fock basis. A remark concerning the case $k > 0$ is given at the end of this section. Here, Tr_{el} is the trace over the electronic degrees of freedom. The

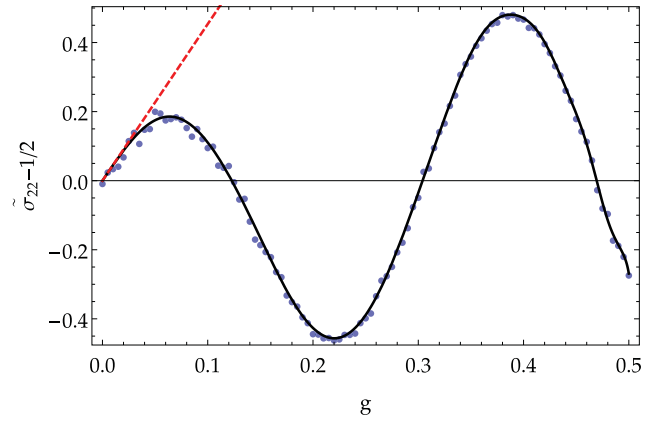


FIG. 1. The generated data (blue dots) of the excited state occupation probability together with a nonlinear curve fit [Eq. (16)] for the excitation to the zeroth sideband, $k = 0$, at $|\kappa'|t = 10$ (solid black line). The motional input state is the ground state $|n = 0\rangle$. The quantity $c_1 g$ is given as the dashed red line. Parameters: $\eta = 0.2$, $\Delta\omega/|\kappa'| = 0.2$, $\Delta\Phi = 0$, and $\nu = 5000$.

generation of vibrational Fock states in an ion trap was already investigated in the 1990s (cf. Refs. [41,42]).

In the following we will use the input density matrix $\hat{\rho}(0) = \hat{\sigma}(0) \otimes \hat{\rho}_{\text{mot}}(0)$, where $\hat{\sigma}(0)$ and $\hat{\rho}_{\text{mot}}(0)$ describe the electronic and the motional input state, respectively. An overview over experimentally possible states of a trapped ion can be found in Ref. [36], and references therein. If the electronic state is initially in a superposition,

$$\hat{\sigma}(0) = (\gamma_1 |1\rangle + \gamma_2 |2\rangle)(\gamma_1^* \langle 1| + \gamma_2^* \langle 2|), \quad (13)$$

with $|\gamma_1|^2 + |\gamma_2|^2 = 1$, and $\hat{\rho}_{\text{mot}} = |n\rangle\langle n|$, one readily derives

$$\langle \hat{U}_I^\dagger(0) \hat{H}_{\text{int},I}(0) \hat{U}_I(0) \rangle = \hbar|\kappa| f_0(n; \eta) (\gamma_1 \gamma_2^* + \gamma_2 \gamma_1^*). \quad (14)$$

Here we defined $f_k(n; \eta) = \langle n | \hat{f}_k(\hat{n}; \eta) | n \rangle$. Hence, if $\arg(\gamma_1) - \arg(\gamma_2) = (2m + 1)\frac{\pi}{2}$ for $m = 0, 1, \dots$, then the expectation value in Eq. (14) becomes zero. Thus, we set $\gamma_1 = e^{i\pi/2}/\sqrt{2}$ and $\gamma_2 = 1/\sqrt{2}$, which leads to $\sigma_{22}(0) = 1/2$. Hence, Eq. (12) simplifies to

$$\langle \hat{U}_I^\dagger(t) \hat{H}_{\text{int},I}(t) \hat{U}_I(t) \rangle = \hbar\Delta\omega[\sigma_{22}(t) - 1/2]. \quad (15)$$

To demonstrate that our approach applies to experimental data, we will generate random numbers which approximate the distribution which σ_{22} obeys.¹ By using this approximated distribution, a sequence of artificial data points is obtained which statistically fluctuate around the exact evolution of σ_{22} . For convenience, we introduce the dimensionless coupling g , i.e., a rescaling, via $|\kappa| \rightarrow g|\kappa'|$ and the dimensionless time $|\kappa'|t$.

A first result of the basic procedure is shown in Fig. 1 for a fixed time. Therein, each value of σ_{22} (blue dots) is obtained from 10^3 random numbers, to mimic the distribution of σ_{22} for a fixed n for the motional input state $|n\rangle\langle n|$. They are fitted by

¹For the generation of random numbers from a given distribution the *Mathematica* inbuilt method `RandomVariate` was used.

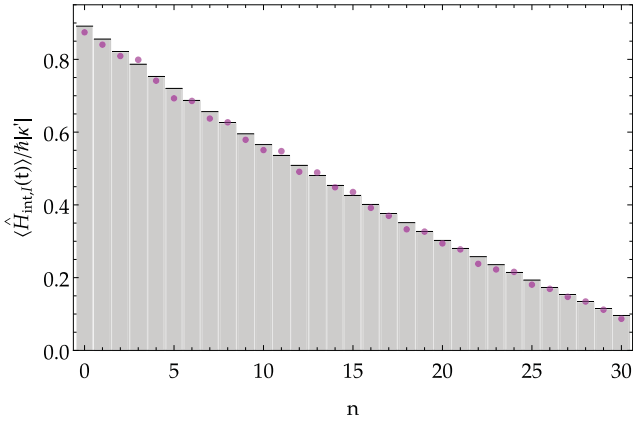


FIG. 2. Generated data (magenta dots) obtained by the technique in Fig. 1, for motional Fock states $|n\rangle$ at $|\kappa'|t = 10$. The other parameters are the same as in Fig. 1. The gray bars represent the analytical results according to Eq. (17).

the polynomial

$$\tilde{\sigma}_{22} - \frac{1}{2} = \sum_{l \geq 0} c_{2l+1} g^{2l+1}. \quad (16)$$

In the fit function only odd orders of g appear, due to the structure of the Hamiltonian (4)—in this case due to the algebra of the atomic flip operators—and our choice of the electronic input state. The parameter c_1 leads to the desired Hamiltonian [cf. Eq. (3)] and is visualized in Fig. 1 via the dashed red line. It is obvious that especially at $g \ll 1$ a meticulous resolution of the data is important. Here we note that in experiments the dependence on the coupling strength g , as considered in Fig. 1, can be well controlled through the amplitude of the laser driving the trapped ion. For details on this dependence, we refer to Sec. 13.3 of Ref. [24].

Repeating this procedure for various Fock input states $|n\rangle$ yields the interaction Hamiltonian in Fock-space representation (see Fig. 2). Here we increased the number of random events to 5×10^3 . The theoretical prediction (gray bars) of the expectation value of the interaction Hamiltonian in the Fock state $|n\rangle$ is easily calculated to be

$$\langle \hat{H}_{\text{int},I}(t) \rangle = \hbar |\kappa| f_0(n; \eta) (\gamma_1 \gamma_2^* e^{-i\Delta\omega t} + \gamma_2 \gamma_1^* e^{i\Delta\omega t}). \quad (17)$$

On this basis we easily obtain, for the case under study, the expectation value for an arbitrary motional quantum state $[\hat{\rho}_{\text{mot}}(0)]$ as

$$\begin{aligned} \text{Tr}[\hat{\rho}_{\text{mot}}(0) \otimes \hat{\sigma}(0) \hat{H}_{\text{int},I}(t)] &= \hbar |\kappa| (\gamma_1 \gamma_2^* e^{-i\Delta\omega t} + \text{c.c.}) \\ &\times \sum_{n=0}^{\infty} P_n f_0(n; \eta), \end{aligned} \quad (18)$$

in which $\hat{\sigma}(0)$ is given in Eq. (13) and P_n is the number statistics of the motional quantum state under consideration. The depicted results, which were derived from the generated data, are close to the analytical results. In certain situations the extraction of the expectation value of the interaction Hamiltonian could also serve as a consistency check before investigating the non-equal-time commutators, which will be considered in the next section. Hamiltonians which are not

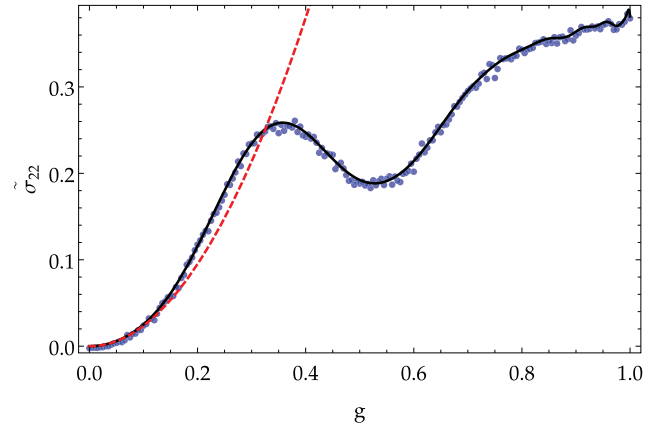


FIG. 3. The generated data (blue dots) of the excited state occupation probability together with a nonlinear curve fit $\tilde{\sigma}_{22}$ [Eq. (20)] for the excitation to the second sideband, $k = 2$, are shown for $|\kappa'|t = 40$ (solid black line). The quantity $c_2 g^2$ is given as the dashed red line. Parameters: $\alpha_0 = \sqrt{12}$, $\eta = 0.2$, $\Delta\omega/|\kappa'| = 0.2$, $\Delta\Phi = 0$, and $\nu = 5000$.

diagonal in the Fock basis can be accessed via its determination in the coherent state basis. The subsequent integration over the Glauber-Sudarshan P function yields the expectation values of the more general interaction Hamiltonians (for $k \neq 0$) in Eq. (4) (see, e.g., Ref. [24]).

V. ACCESSING THE COMMUTATOR

For this task we use $\hat{\sigma}(0) = |1\rangle\langle 1|$. Hence, the ion is initially in the electronic ground state, so that $\sigma_{22}(0) = 0$. From Eq. (12) we get

$$\langle \hat{U}_I^\dagger(t) \hat{H}_{\text{int},I}(t) \hat{U}_I(t) \rangle = \hbar \Delta\omega \sigma_{22}(t). \quad (19)$$

Furthermore, we assume that the vibrational input state is a coherent state $|\alpha_0\rangle$. Details concerning the preparation of coherent motional states can be found, for example, in Ref. [41].

In Fig. 3 we outline the basic procedure, where the statistics is approximated by using 10^4 random numbers for each data point; for explanations see the discussion following Eq. (15). The generated data are now fitted by the function

$$\tilde{\sigma}_{22} = \sum_{l \geq 1} c_{2l} g^{2l}. \quad (20)$$

For similar reasons as in Eq. (16) now only even orders of g appear. According to Eq. (3), the parameter c_2 yields the desired time-integrated commutator in Eq. (3). The parameter c_2 is visualized in Fig. 3 by the dashed red line and describes the quadratic contribution which represents the sought commutator.

To finally obtain the time evolution of the commutator one has to repeat the measurement for all times. The result is depicted in Fig. 4 for 2×10^4 random numbers per data point and time. For each point in time we repeat the step which is depicted in Fig. 3. Afterward we fit the data and extract the quadratic slope. The commutator of interest, i.e., the theoretical prediction, can be analytically derived and

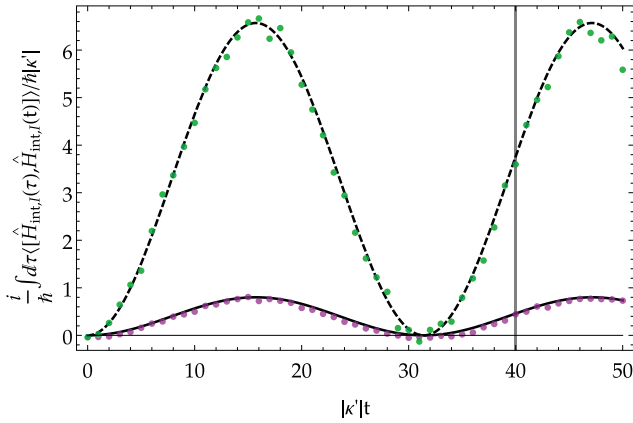


FIG. 4. The generated data together with the theoretical predictions of the expectation value of the time-integrated commutator (black lines) from Eq. (21). The data correspond to the scenarios $k = 2$ (magenta dots) and $k = 0$ (green dots). The gray line at $|\kappa'|t = 40$ marks the situation depicted in Fig. 3 for the $k = 2$ case. The other parameters are the same as in Fig. 3.

reads as

$$\begin{aligned} & \frac{i}{\hbar} \int_0^t d\tau \langle 1, \alpha_0 | [\hat{H}_{\text{int},I}(\tau_1), \hat{H}_{\text{int},I}(t)] | 1, \alpha_0 \rangle \\ &= \frac{2|\kappa|^2 \hbar}{\Delta\omega} (1 - \cos \Delta\omega t) \sum_{n=0}^{\infty} |f_k(n; \eta)|^2 \frac{|\alpha_0|^{2(n+k)}}{n!} e^{-|\alpha_0|^2}, \end{aligned} \quad (21)$$

which is a harmonic oscillation in time. This result is given as the black lines in Fig. 4.

The magenta and green dots correspond to the excitation to the second ($k = 2$) and the zeroth ($k = 0$) sideband, respectively. The results derived from the generated data resemble the theoretical results sufficiently well. It is noteworthy that, for an explicitly time-dependent Hamiltonian, to certify clear experimental evidence of the relevance of the non-equal-time commutators of the interaction Hamiltonian for the system dynamics, it is sufficient to demonstrate statistically significant nonzero contributions in Fig. 4. Here we show that such a certification is, by the techniques proposed here, rather easy to do.

VI. SUMMARY AND CONCLUSIONS

To our best knowledge, presently no proposal of a method for the experimental verification of the non-equal-time commutators of interaction Hamiltonians does exist. A reason for this is, that usually it is preferred to operate a certain dynamics under perfect resonance conditions. However, the general situation with an explicitly time-dependent interaction needs to be fully understood. The present paper aims to contribute significantly to this fundamental issue. For this purpose, we derived analytical expressions for measurable quantities, which render it possible to experimentally access the quantities of interest.

We have shown that, for the vibronic dynamics of a laser-driven trapped ion in the resolved-sideband regime, the measurement of the electronic-state occupation probability yields the temporal evolution of the expectation value of the interaction Hamiltonian. From this value one can derive both the expectation value of the interaction Hamiltonian in the interaction picture and the partly integrated non-equal-time commutator of the interaction Hamiltonian. Statistically generated data points are only used to demonstrate that the proposed methods will work under realistic experimental conditions. The obtained results well approximate the analytically derived ones. Thus, the detuned nonlinear Jaynes-Cummings Hamiltonian under study is appropriate to access the fundamentals of explicitly time-dependent temporal evolutions of quantum systems.

For the determination of the Hamiltonian we have considered an input motional Fock state and obtained the interaction Hamiltonian in the Fock basis for the quasiresonant excitation of the zeroth motional sideband. In addition, the non-equal-time commutator, which explicitly accounts for time-ordering corrections, has been investigated. For an initially prepared motional coherent state, the evolution of the partly time-integrated commutator can be determined. This allows one to directly visualize in experiments the noncommutativity of the interaction Hamiltonian at different times. Our approach paves the way to study the explicitly time-dependent dynamics also for other quantum systems of interest. However, this requires the reformulation of the corresponding measurement principles for the systems to be studied, which is beyond the scope of the present paper.

[1] W. Heisenberg, Über den anschaulichen Inhalt der quantentheoretischen Kinematik und Mechanik, *Z. Phys.* **43**, 172 (1927).
 [2] E. H. Kennard, Zur Quantenmechanik einfacher Bewegungstypen, *Z. Phys.* **44**, 326 (1927).
 [3] P. Busch, T. Heinonen, and P. Lahti, Heisenberg's uncertainty principle, *Phys. Rep.* **452**, 155 (2007).
 [4] M. R. Douglas and N. A. Nekrasov, Noncommutative field theory, *Rev. Mod. Phys.* **73**, 977 (2001).
 [5] S. Khan, B. Chakraborty, and F. G. Scholtz, Role of twisted statistics in the noncommutative degenerate electron gas, *Phys. Rev. D* **78**, 025024 (2008).
 [6] C. Duval and P. A. Horvathy, The exotic Galilei group and the "Peierls substitution", *Phys. Lett. B* **479**, 284 (2000).

[7] V. P. Nair and A. P. Polychronakos, Quantum mechanics on the noncommutative plane and sphere, *Phys. Lett. B* **505**, 267 (2001).
 [8] R. Banerjee, A novel approach to noncommutativity in planar quantum mechanics, *Mod. Phys. Lett. A* **17**, 631 (2002).
 [9] B. Chakraborty, S. Gangopadhyay, and A. Saha, Quantum mechanical systems interacting with different polarizations of gravitational waves in noncommutative phase space, *Phys. Rev. D* **70**, 107707 (2004).
 [10] F. G. Scholtz, B. Chakraborty, S. Gangopadhyay, and A. G. Hazra, Dual families of noncommutative quantum systems, *Phys. Rev. D* **71**, 085005 (2005).

- [11] K. Li and S. Dulat, The Aharonov–Bohm effect in non-commutative quantum mechanics, *Eur. Phys. J. C* **46**, 825 (2006).
- [12] R. V. Mendes, Some consequences of a non-commutative space-time structure, *Eur. Phys. J. C* **42**, 445 (2005).
- [13] F. S. Bemca and H. O. Girotti, The noncommutative degenerate electron gas, *J. Phys. A: Math. Gen.* **38**, L539 (2005).
- [14] M. Chaichian, M. M. Sheikh-Jabbari, and A. Tureanu, Hydrogen Atom Spectrum and the Lamb Shift in Noncommutative QED, *Phys. Rev. Lett.* **86**, 2716 (2001).
- [15] N. Chair and M. M. Sheikh-Jabbari, Pair production by a constant external field in noncommutative QED, *Phys. Lett. B* **504**, 141 (2001).
- [16] Y. Liao and C. Dehne, Some phenomenological consequences of the time-ordered perturbation theory of QED on non-commutative spacetime, *Eur. Phys. J. C* **29**, 125 (2003).
- [17] T. Ohl and J. Reuter, Testing the noncommutative standard model at a future photon collider, *Phys. Rev. D* **70**, 076007 (2004).
- [18] H. García-Compeán, O. Obregón, and C. Ramírez, Noncommutative Quantum Cosmology, *Phys. Rev. Lett.* **88**, 161301 (2002).
- [19] S. Alexander, R. Brandenberger, and J. Magueijo, Noncommutative inflation, *Phys. Rev. D* **67**, 081301(R) (2003).
- [20] V. Parigi, A. Zavatta, M. Kim, and M. Bellini, Probing quantum commutation rules by addition and subtraction of single photons to/from a light field, *Science* **317**, 1890 (2007).
- [21] M. S. Kim, H. Jeong, A. Zavatta, V. Parigi, and M. Bellini, Scheme for Proving the Bosonic Commutation Relation Using Single-Photon Interference, *Phys. Rev. Lett.* **101**, 260401 (2008).
- [22] A. Zavatta, V. Parigi, M. S. Kim, H. Jeong, and M. Bellini, Experimental Demonstration of the Bosonic Commutation Relation via Superpositions of Quantum Operations on Thermal Light Fields, *Phys. Rev. Lett.* **103**, 140406 (2009).
- [23] W. P. Schleich, *Quantum Optics in Phase Space* (Wiley-VCH, Berlin, 2001).
- [24] W. Vogel and D.-G. Welsch, *Quantum Optics*, 3rd ed. (Wiley-VCH, New York, 2006).
- [25] G. S. Agarwal, *Quantum Optics* (Cambridge University Press, Cambridge, 2013).
- [26] G. Grynberg, A. Aspect, and C. Fabre, *Introduction to Quantum Optics* (Cambridge University Press, Cambridge, 2010).
- [27] L. Knöll, W. Vogel, and D.-G. Welsch, Action of passive, lossless optical systems in quantum optics, *Phys. Rev. A* **36**, 3803 (1987).
- [28] J. D. Cresser, Intensity correlations of frequency-filtered light fields, *J. Phys. B* **20**, 4915 (1987).
- [29] L. Knöll, W. Vogel, and D.-G. Welsch, Spectral properties of light in quantum optics, *Phys. Rev. A* **42**, 503 (1990).
- [30] A. Christ, B. Brecht, W. Mauerner, and C. Silberhorn, Theory of quantum frequency conversion and type-II parametric down-conversion in the high-gain regime, *New J. Phys.* **15**, 053038 (2013).
- [31] N. Quesada and J. E. Sipe, Effects of time ordering in quantum nonlinear optics, *Phys. Rev. A* **90**, 063840 (2014).
- [32] N. Quesada and J. E. Sipe, Time-Ordering Effects in the Generation of Entangled Photons Using Nonlinear Optical Processes, *Phys. Rev. Lett.* **114**, 093903 (2015).
- [33] N. Quesada and J. E. Sipe, High efficiency in mode-selective frequency conversion, *Opt. Lett.* **41**, 364 (2016).
- [34] F. Krumm, J. Sperling, and W. Vogel, Multi-time correlation functions in nonclassical stochastic processes, *Phys. Rev. A* **93**, 063843 (2016).
- [35] W. Vogel and R. L. de Matos Filho, Nonlinear Jaynes-Cummings dynamics of a trapped ion, *Phys. Rev. A* **52**, 4214 (1995).
- [36] F. Krumm and W. Vogel, Time-dependent nonlinear Jaynes-Cummings dynamics of a trapped ion, *Phys. Rev. A* **97**, 043806 (2018).
- [37] T. Lipfert, F. Krumm, M. I. Kolobov, and W. Vogel, Quantum effects of operator time ordering in the nonlinear Jaynes-Cummings model, *Phys. Rev. A* **98**, 063817 (2018).
- [38] W. Nagourney, J. Sandberg, and H. Dehmelt, Shelved Optical Electron Amplifier: Observation of Quantum Jumps, *Phys. Rev. Lett.* **56**, 2797 (1986).
- [39] Th. Sauter, W. Neuhauser, R. Blatt, and P. E. Toschek, Observation of Quantum Jumps, *Phys. Rev. Lett.* **57**, 1696 (1986).
- [40] J. C. Bergquist, Randall G. Hulet, Wayne M. Itano, and D. J. Wineland, Observation of Quantum Jumps in a Single Atom, *Phys. Rev. Lett.* **57**, 1699 (1986).
- [41] D. M. Meekhof, C. Monroe, B. E. King, W. M. Itano, and D. J. Wineland, Generation of Nonclassical Motional States of a Trapped Atom, *Phys. Rev. Lett.* **76**, 1796 (1996).
- [42] R. L. de Matos Filho and W. Vogel, Quantum Nondemolition Measurement of the Motional Energy of a Trapped Atom, *Phys. Rev. Lett.* **76**, 4520 (1996).

Acknowledgments

Ich möchte mich zunächst bei Prof. Werner Vogel bedanken, der mir die Anfertigung der Dissertation in seiner Arbeitsgruppe ermöglicht hat und mir während dieser Zeit stets mit Rat und Tat zur Seite stand. Außerdem bedanke ich mich bei Dr. Jan Sperling, der mich bereits während der Bachelor- und Masterarbeit betreut hat und auch während meiner Promotionszeit stets ein offenes Ohr hatte. Selbstverständlich bedanke ich mich auch bei der übrigen Arbeitsgruppe (Sergej Ryl, Stefan Gerke, Benjamin Kühn, Martin Bohmann, Elizabeth Agudelo, Dmytro Vasylyev, Andrii Semenov und Jelena Boldt) für eine angenehme Zeit in Rostock.

Darüber hinaus gebührt mein Dank den mutigen Gegenlesern dieser Arbeit: Martin Bohmann, Karsten Sperlich, Friederike Tomm und (mal wieder) Jan Sperling. Durch letztere konnten in dieser Arbeit 78 bzw. 75 Kommata korrekt gesetzt werden.

Weiterhin bedanke ich mich natürlich bei meiner Familie (Wolf, Urs, Maximilijörn, Ganeshas wuchtiger Fruchtzweig, 2mm Trimmerdinger), meinen Freunden (allen halt) und meiner Lebensabschnittsgefährtin Marlena, wobei insbesondere letztere meine Sorgen und Nöte, mal mehr, mal weniger freiwillig, teilen und ertragen durfte. Grüße auch an Artemis und Purzel.

Ferner danke ich Riot Games, der Valve Corporation, Stunlock Studios und der Trotzenburg für willkommene Ablenkung während meiner Promotionszeit.

Zuletzt danke ich Frau Vivian Breitsprecher des Dekanats der MNF für Ihre Hinweise zur Formulierung einer ordnungsgemäßen Danksagung.

Selbstständigkeitserklärung

Hiermit erkläre ich an Eides statt, dass ich die hier vorliegende Dissertation selbstständig und ohne fremde Hilfe verfasst habe, bis auf die in der Bibliographie angegebenen Quellen keine weiteren Quellen benutzt habe und die den Quellen wörtlich oder inhaltlich entnommene Stellen als solche kenntlich gemacht habe.

Rostock,